



Metabolomic Profiling of the Effects of Melittin and Cisplatin on Ovarian Cancer Cells using High Resolution Mass Spectrometry

A Thesis Submitted in Fulfilment of the Requirements for the Degree of
Doctor of Philosophy in the Strathclyde Institute of Pharmacy and
Biomedical Sciences at the University of Strathclyde

A thesis presented by

Sanad M. Z. Alonezi

2017

Declaration

‘This thesis is the result of the author’s original research. It has been composed by the author and has not been previously submitted for examination which has led to the award of a degree.’

‘The copyright of this thesis belongs to the author under the terms of the United Kingdom Copyright Acts as qualified by University of Strathclyde Regulation 3.50. Due acknowledgement must always be made of the use of any material contained in, or derived from, this thesis.’

Signed: _____

Date: _____

Acknowledgements

First and foremost, I would like to express my sincerest gratitude to Allah (God) for providing me the blessings to complete this work. I would like also to express my sincere appreciation and immense gratitude to my supervisor, Dr. David G Watson, for his continued support, patience, moral uplifting and guidance throughout this study. I really appreciated your support. My thanks also extend to my second supervisor, Dr. Valerie A. Ferro, for her kind words of encouragement during the various phases of developing this work. I would like also to thank my academic assessor, Dr. Paul Coats who reviewed my research progress through mini-vivas.

Furthermore, the project team is extremely grateful to Jonans Tusiimire, Louise Young, and Carol Clements for their support and interest throughout the entire project. My cordial thanks to the entire research team in David's lab for their support during my study. I am also more than thankful to all people who helped me in completing this work. Without their earnest and keen involvement, my objectives would not have been achieved. Particular thanks are owed to Dr. Mohammad Alwashih, Dr. Khalid Alharbi, Dr. Ibtisam Kaziri and Mohammad Al Rofaidi for their kind help.

I would also like to thank my parents for whose continual encouragement and cordial assistance were of great value in accomplishing this work. I am grateful to my wife and my daughter for their patience, support and love. Also, my thanks go to all my family members and friends for their supports.

Finally, I would to thank the government of Saudi Arabia for sponsoring my PhD study.

Table of Contents

Declaration.....	i
Acknowledgements	ii
List of Tables	viii
List of Figures.....	ix
List of Abbreviations	xiii
Papers Published and Posters Presented	xv
Abstract.....	xvi
1 Introduction.....	2
1.1 Metabolomics.....	2
1.2 Metabolomics approaches in biomarker identification: targeted and untargeted	4
1.3 Analytical techniques.....	6
1.3.1 LC-MS	7
1.3.2 Nuclear magnetic resonance (NMR) spectroscopy.....	12
1.3.3 GC-MS	13
1.4 Principles of HILIC separation	16
1.4.1 Mobile phases	17
1.4.2 Stationary phases.....	17
1.4.2.1 Silica gel.....	17
1.4.2.2 Zwitterionic phases	18
1.4.3 Factors that determine retention times in HILIC	20
1.5 Metabolomic data extraction and statistical analyses	21
1.6 Metabolomics in ovarian cancer	25
1.6.1 Ovarian cancer	25
1.6.2 Pathophysiology.....	27
1.6.3 Stages of ovarian cancer	27
1.6.4 Samples used in the metabolomics-based ovarian cancer research	28
1.6.4.1 Blood.....	28
1.6.4.2 Urine	29
1.6.4.3 Tissues.....	30
1.6.4.4 Cell cultures	31
1.7 Ovarian cancer treatment	35
1.7.1 Current chemotherapy.....	35
1.7.2 Need for novel alternative cytotoxic agents.....	38

1.8	Melittin: A potential anticancer therapy	39
1.8.1	Chemistry of melittin	39
1.8.2	Anticancer properties of melittin	40
1.9	Research objectives.....	42
2	Materials and Methods.....	44
2.1	Chemicals and solvents.....	44
2.2	Cell culture methods	44
2.2.1	Cell lines and cultures	44
2.2.2	Determination of IC ₅₀ values for melittin and cisplatin	45
2.2.3	Calculation of Combination Index (CI) for melittin-cisplatin	45
2.3	Chromatographic conditions for columns.....	46
2.3.1	Chromatographic conditions for ZIC-pHILIC column	46
2.3.2	Chromatographic conditions for ZIC-HILIC column	46
2.3.3	Chromatographic conditions for Silica gel column	47
2.4	Liquid chromatography–mass spectrometry (LC-MS) conditions	47
2.4.1	Accela HPLC-ESI-Exactive Orbitrap	47
2.4.2	Finnigan HPLC-ESI-Exactive Orbitrap	48
2.5	Data extraction and analysis	48
2.5.1	LC-MS data processing by MZmine software	48
2.5.2	Data bases used for identification of metabolites	50
2.5.3	Statistical software’s used for identification of metabolites	51
2.6	Optimisation of Phenotype Microarray experiment parameters	53
2.6.1	Phenotype MicroArrays Experiment Design	55
2.6.2	Calculation of Redox Dye Reduction	57
2.7	Caspase activity Assay.....	57
3	Metabolomic Profiling of the Effects of Melittin on Cisplatin Resistant and Cisplatin Sensitive Ovarian Cancer Cells Using Mass Spectrometry and Biolog Microarray Technology.....	59
3.1	Abstract.....	59
3.2	Introduction.....	60
3.3	Materials and Methods.....	65
3.3.1	Cell lines and cultures	65
3.3.2	Cell viability assay against melittin	65
3.3.3	Determination of IC ₅₀	65
3.3.4	Determination of effect of melittin on cell metabolomes	66

3.3.5	Chromatographic conditions for columns	66
3.3.6	Liquid Chromatography–Mass Spectrometry (LC-MS) conditions.....	67
3.3.7	Data extraction and analysis	67
3.3.8	Phenotype Microarray experiment.....	67
3.3.1	Calculation of redox dye reduction.....	69
3.3.2	LDH assay.....	69
3.3.3	Caspase assay activity	70
3.4	Results.....	70
3.4.1	Melittin sensitivity of the ovarian cancer cells	70
3.4.2	Phenotypic MicroArray (PM) assay of untreated and melittin treated A2780 and A2780CR cells	71
3.4.3	Effect of melittin on the metabolomes of both cell lines	75
3.4.4	Assessment of necrotic and apoptotic cell death in A2780 and A2780CR cells	81
3.5	Discussion.....	84
3.6	Conclusions.....	89
4	LCMS and Phenotype Microarray Profiling of Ovarian Cancer Cells after Exposure to Cisplatin	91
4.1	Abstract.....	91
4.2	Introduction.....	92
4.3	Materials and Methods.....	96
4.3.1	Cell lines and cultures	96
4.3.2	Cell viability assay against cisplatin	96
4.3.3	Determination of IC ₅₀	97
4.3.4	Determination of effect of cisplatin on cell metabolomes	97
4.3.5	Chromatographic conditions for column	98
4.3.6	Liquid Chromatography–Mass Spectrometry (LC-MS) conditions.....	98
4.3.7	Data extraction and analysis	98
4.3.8	Phenotype MicroArrays analysis	98
4.3.9	Calculation of redox dye reduction.....	100
4.3.10	Caspase activity assay	100
4.4	Results.....	100
4.4.1	Cisplatin cytotoxicity	100
4.4.2	Phenotypic MicroArray (PM) assay of cisplatin treated A2780 and A2780CR cells	101
4.4.3	Metabolic profile of cisplatin treated cells.....	104

4.4.4	Assessment of apoptotic cell death in A2780 and A2780CR cells	111
4.5	Discussion	113
4.6	Conclusions	120
5	Comparative Metabolomic Profiling of the Synergistic Effects of Melittin in Combination with Cisplatin on Ovarian Cancer Cells Using Mass Spectrometry	122
5.1	Abstract	122
5.2	Introduction	123
5.3	Materials and Methods	126
5.3.1	Cell lines and cultures	126
5.3.2	Cell viability assay	126
5.3.3	Calculation of Combination Index (CI)	127
5.3.4	Determination of effect of melittin in combination with cisplatin on cell metabolomes	127
5.3.5	Chromatographic conditions for column	128
5.3.6	Liquid Chromatography–Mass Spectrometry (LC-MS) conditions	129
5.3.7	Data extraction and analysis	129
5.4	Results	129
5.4.1	The cytotoxicity of melittin in combination with cisplatin	129
5.4.2	The combination index (CI)	131
5.4.3	Metabolome analysis	134
5.5	Discussion	141
5.6	Conclusions	151
6	Lipidomic Analysis of the Effects of Melittin on Ovarian Cancer Cells Using Mass Spectrometry	153
6.1	Abstract	153
6.2	Introduction	154
6.3	Materials and Methods	157
6.3.1	Cell lines and cultures	157
6.3.2	Cell viability assay against melittin	157
6.3.3	Determination of IC ₅₀	157
6.3.4	Determination of effect of melittin on cell lipids metabolism	158
6.3.5	Chromatographic conditions for column	158
6.3.6	Liquid Chromatography–Mass Spectrometry (LC-MS) conditions	158
6.3.7	Data extraction and analysis	159
6.4	Results	159
6.5	Discussion	176

6.6	Conclusions.....	181
7	General discussion and Future Works.....	183
8	Appendix.....	193
9	References.....	204

List of Tables

Table 1.1. A summary of common analytical techniques used in metabolomics	16
Table 1.2. Currently available zwitterionic phases and their functional groups.	19
Table 1.3. Summary of representative current metabolomics on ovarian cancer.	34
Table 1.4. Mechanisms of Ovarian Cancer Drug Resistance.....	38
Table 2.1. MZMine 2.10 procedure and settings	49
Table 3.1. Statistical differentiating metabolites.....	79
Table 4.1. Comparison of the substrate dependant readings that vary between the sensitive and resistant cells	102
Table 4.2. Statistical differentiating metabolites showing the differential response of the sensitive and resistant cells to cisplatin treatment.....	109
Table 5.1. Statistical differentiating of melittin in combination with cisplatin at 5 $\mu\text{g}/\text{mL}$ Melittin + 2 $\mu\text{g}/\text{mL}$ Cisplatin on metabolites of A2780 and at 2 $\mu\text{g}/\text{mL}$ Melittin + 10 $\mu\text{g}/\text{mL}$ Cisplatin on A2780CR.....	139
Table 6.1. Differences in the lipids between A2780 cells and A2780CR cells before and after melittin treatment.	164

List of Figures

Figure 1.1. Overall metabolomics structure with lipids as part of metabolomics.....	4
Figure 1.2. An outline of a ‘typical metabolomics study’ for identification of the metabolite biomarkers. (LC-MS, liquid chromatography-mass spectrometry; NMR, nuclear magnetic resonance spectroscopy) (Maguire, 2014).	5
Figure 1.3. A schematic diagram to illustrate the components of an HPLC system...	8
Figure 1.4. A schematic diagram to show the main components of a mass spectrometer.	10
Figure 1.5. A schematic diagram representing the Orbitrap Mass Spectrometer.	11
Figure 1.6. The different types of silanols in silica gel.	18
Figure 1.7. Chemical structure of platinum compounds (A) Cisplatin; (B) Carboplatin	36
Figure 1.8. Chemical structure of taxane compounds (A) Paclitaxel; (B) Docetaxel	37
Figure 1.9. Structure of melittin, the main component in bee venom.....	40
Figure 2.1. Layout of chemicals in the wells on the PM-M1 microplate.....	56
Figure 3.1. Effect of melittin on the viability of the ovarian cancer cells A2780 and A2780CR. Cell viability was determined following treatment with varying doses of melittin for 24 h ($IC_{50}= 6.8\pm 0.4 \mu\text{g/mL}$ A2780; $IC_{50}= 4.5\pm 0.4 \mu\text{g/mL}$ A2780CR)...	71
Figure 3.2. Comparison of substrate metabolism in A2780 and A2780CR cells. Dye reduction levels measured following 24 h incubation of cells.	73
Figure 3.3. Comparison of substrate metabolism in A2780 cells following melittin exposure. Dye reduction levels measured following 24 h incubation of cells with melittin at IC_{50} ($6.8 \mu\text{g/mL}$) concentration. C= untreated controls; T= melittin treated.	74
Figure 3.4. Comparison of substrate metabolism in A2780CR cells following melittin exposure. Dye reduction levels measured following 24 h incubation of cells with melittin at IC_{50} ($4.5 \mu\text{g/mL}$) concentration. C= untreated controls; T= melittin treated.	74
Figure 3.5. (A) PCA vs (B) OPLS-DA of ovarian cancer cells of A2780 and A2780CR treated with melittin. The groups: MS circles: A2780-treated cells; C circles: untreated A2780 cells; MR circles: A2780CR-treated cells; CR circles: untreated A2780CR	

cells. QC circles: Quality control samples.	76
Figure 3.6. Hierarchical clustering analysis (HCA) of 20 ovarian cancer cell samples. It shows two main groups and four subgroups. The groups: CR, control of cisplatin resistance cell lines; MR: A2780CR after treatment with melittin; C, control of cisplatin sensitive cell lines; MS, A2780 after treatment with melittin.	77
Figure 3.7. OPLS-DA score plot of (A) A2780CR cell lines before and after treatment with melittin; (B) A2780 cell lines before and after treatment with melittin.....	77
Figure 3.8. Lactate dehydrogenase (LDH) assay. Effect of melittin on leakage of lactate dehydrogenase (LDH) from A2780 and A2780CR cell lines.	82
Figure 3.9. Effect of Melittin on caspase-3 activity in A2780 and A2780CR cells..	83
Figure 4.1. Cell viability was determined following treatment with cisplatin for 24 h (A) $IC_{50}= 10.8\pm 0.9 \mu\text{g/mL}$ A2780CR; (B) $IC_{50}= 4.9\pm 0.6 \mu\text{g/mL}$ A2780.	101
Figure 4.2. Comparison of substrate metabolism in A2780 cells following cisplatin exposure. Dye reduction rates calculated following 24 h incubation of cells with cisplatin at IC_{50} ($4.9 \mu\text{g/mL}$) concentration.	103
Figure 4.3. Comparison of substrate metabolism in A2780CR cells following cisplatin exposure. Dye reduction rates calculated following 24 h incubation of cells with cisplatin at IC_{50} ($10.8 \mu\text{g/mL}$) concentration.	103
Figure 4.4. (A) PCA vs (B) OPLS-DA. PCA and OPLS-DA scores plot generated from PCA and OPLS-DA using LC-MS normalized data of cells after exposure to cisplatin and controls of A2780 and A2780CR cell lines. The groups: CR, control of cisplatin resistance cell lines; TCR: A2780CR after treatment with cisplatin; C, control of cisplatin sensitive cell lines; TCS, A2780 after treatment with cisplatin.	107
Figure 4.5. Hierarchical clustering analysis (HCA) of 20 ovarian cancer cell samples. It shows two main groups and four subgroups. The groups: CR, control of cisplatin resistance cell lines; TCR: A2780CR after treatment with cisplatin; C, control of cisplatin sensitive cell lines; TCS, A2780 after treatment with cisplatin.	108
Figure 4.6. OPLS-DA score plot of (A) A2780 cell lines before and after treatment with cisplatin; (B) A2780CR cell lines before and after treatment with cisplatin...	108
Figure 4.7. Effect of Cisplatin on caspase-3 activity in A2780 and A2780CR cells.	112
Figure 5.1. Examination of cell viability after treatment with either cisplatin or	

melittin alone with various concentrations on (A) A2780 cell line and (B) A2780CR cell line..... 130

Figure 5.2. Effects of melittin in combination with cisplatin on (A) cell viability of A2780 cell lines and (B) Combination index. (A) The A2780 cells were treated with various concentrations of melittin+cisplatin for 24 hours. Bar graphs represent mean \pm SD values. (B) Combination index (CI) analysis was generated using the method of Chou and Talalay to determine the extent of synergy if any for melittin + cisplatin on A2780 cell lines..... 132

Figure 5.3. Effect of melittin in combination with cisplatin on (A) cell viability of A2780CR cell lines and (B) Combination index. (A) The A2780CR cells were treated with various concentrations of melittin+cisplatin for 24 hours. Bar graphs represent mean \pm SD values. (B) Combination index (CI) analysis was generated using the method of Chou and Talalay to determine the extent of synergy if any for melittin +cisplatin on A2780CR cell lines. 133

Figure 5.4. (A) PCA vs (B) OPLS-DA. PCA and OPLS-DA scores plot generated from PCA and OPLS-DA using LC-MS normalized data of cells after exposure to combination (Melittin+Cisplatin) and controls of A2780 and A2780CR cell lines. A2780-treated cells at 5 μ g/mL Melittin + 2 μ g/mL Cisplatin (SOS); untreated A2780 cells (C); A2780CR -treated cells 2 μ g/mL Melittin + 10 μ g/mL Cisplatin (SOR); untreated A2780CR (CR); Quality control (QC) samples (P). 137

Figure 5.5. Hierarchical clustering analysis (HCA) of 20 ovarian cancer cell samples. It shows two main groups and four subgroups. The groups: CR, control of cisplatin resistance cell lines; SOR: A2780CR after treatment with melittin+cisplatin; C, control of cisplatin sensitive cell lines; SOS, A2780 after treatment with melittin+cisplatin. 138

Figure 5.6. OPLS-DA score plot of (A) A2780 cell lines before and after treatment with melittin+cisplatin; (B) A2780CR cell lines before and after treatment with melittin+cisplatin. 138

Figure 6.1. (A) PCA vs (B) OPLS-DA. PCA and OPLS-DA scores plot generated from PCA and OPLS-DA using LC-MS normalized data of cells after exposure to melittin and controls of A2780 and A2780CR cell lines. LMS circles: A2780-treated cells; LCS circles: untreated A2780 cells; LMR circles: A2780CR –treated cells; LCR

circles: untreated A2780CR. P circles: Quality control (QC) samples.....	162
Figure 6.2. Hierarchical clustering analysis (HCA) of 16 ovarian cancer cell samples. It shows two main groups and four subgroups. The groups: LCR, control of cisplatin resistance cell lines; LMR: A2780CR after treatment with melittin; LCS, control of cisplatin sensitive cell lines; LCS, A2780 after treatment with melittin.....	163
Figure 6.3. OPLS-DA score plot of (A) A2780CR cell lines before and after treatment with melittin; (B) A2780 cell lines before and after treatment with melittin.....	163
Figure 6.4. Heat Map showing the relative abundance of phosphocholine lipids in A2780 (S), A2780CR (R) and melittin treated (LMS and LMR) cells. Red $< 2 \times 10^5$, Yellow $> 1 \times 10^6$, Green $> 1 \times 10^7$	168
Figure 6.5. Heat Map showing the relative abundance of various types of lipid in A2780 (S), A2780CR (R) and melittin treated (LMS and LMR) cells. Red $< 2 \times 10^5$, Yellow $> 1 \times 10^6$, Green $> 1 \times 10^7$	169
Figure 6.6. MS ² spectra of (A) LysoPC 16:0 and (B) LysoPC 18:0 lipid at 35 V following application of a source fragmentation energy of 35 V.	172
Figure 6.7. MS ² spectra of 18:1/18:1 PC lipid at 35 V following application of a source fragmentation energy of 35 V.	173
Figure 6.8. Fragmentation of PC lipids in positive ion mode resulting in m/z 184 due to the phosphocholine head group.	173
Figure 6.9. MS ² spectra of PC ether lipids 36:6 and 36:5 indicate that they are acylated with 20:5 and 20:4 chains respectively.	174
Figure 6.10. Source induced dissociation spectrum of lactosylceramide (d18:1/16:0) lipid at 35 V.....	175
Figure 6.11. MS ² spectra of 18:0/20:4 PE lipid.	176

List of Abbreviations

APCI	Atmospheric Pressure Chemical Ionization
ATP	Adenosine Triphosphate
BOT	Benign Ovarian Tumor
CE	Capillary Electrophoresis
CI	Chemical Ionization
CV-ANOVA	Cross Validated ANOVA
DIMS	Direct Infusion Mass Spectrometry
EGF	Epidermal Growth Factor
EI	Electron Impact
EOC	Epithelial Ovarian Cancer
ESI	Electrospray Ionisation
ESI-MS	Electrospray Ionisation-Mass Spectrometry
FAD	Flavin Adenine Dinucleotide
FDR	False Discovery Rate
FFAs	Free Fatty Acids
FT-ICR	Fourier Transform Ion Cyclotron Resonance
FT-IR	Fourier Transform Infrared
GC	Gas Chromatography
GC-MS	Gas Chromatography-Mass Spectrometry
GSH	Glutathione
GTP	Guanosine Triphosphate
HCA	Hierarchical Cluster Analysis
HCD	High-Energy C-trap Dissociation
HILIC	Hydrophilic Interaction Liquid Chromatography
HPLC	High Performance Liquid Chromatography
IT	Ion Traps
KEGG	Kyoto Encyclopedia of Genes and Genomes
LC	Liquid Chromatography
LC-MS	liquid chromatography-mass spectrometry
LDH	Lactate Dehydrogenase

m/z	Mass to Charge Ratio
MS	Mass Spectrometer
MS/MS	Tandem Mass Spectrometry
NAD ⁺	Nicotinamide Adenine Dinucleotide (oxidised)
NADH	Nicotinamide Adenine Dinucleotide (reduced)
NMR	Nuclear Magnetic Resonance
NP	Normal Phase
OLMPT	Ovarian Low Malignant Potential Tumour
OPLS-DA	Orthogonal Partial Least Squares Discriminant Analysis
PBS	Phosphate Buffered Saline
PC	Phosphocholines
PCA	Principal Component Analysis
PE	Phosphoethanolamines
PLA ₂	Phospholipase A ₂
PLS-DA	Partial Least Squares Discriminant Analysis
Q	Quadrupoles
QC	Quality control
ROC	Receiver Operating Characteristic
RP	Reversed Phase
RT	Retention Time
SIMCA	Soft-Independent Modelling of Class Analogy
TCA cycle	Tricarboxylic Acid cycle
TOF	Time of Flight
UPLC-MS	Ultra-Performance Liquid Chromatograph- Mass Spectrometer
VEGF	Vascular Endothelial Growth Factor
VIP	Variable Importance in the Projection
ZIC	Zwitterionic

Papers Published and Posters Presented

Published works

- Alonezi, S., Tusiimire, J., Wallace, J., Dufton, M., Parkinson, J., Young, L., Clements, C., Park, J., Jeon, J., Ferro, V. and Watson, D. **2016**. Metabolomic Profiling of the Effects of Melittin on Cisplatin Resistant and Cisplatin Sensitive Ovarian Cancer Cells Using Mass Spectrometry and Biolog Microarray Technology. *Metabolites*, 6, 35.
- Sanad Alonezi, Mohammed Al Washih, Carol J. Clements, Louise C. Young, Valerie A. Ferro and David G. Watson. **2017**. Liquid chromatography mass spectrometry (LCMS) and Phenotype Microarray Profiling of Ovarian Cancer Cells after Exposure to Cisplatin. *Current Metabolomics*. In press.
- Alonezi, S., Tusiimire, J., Wallace, J., Dufton, M., Parkinson, J., Young, L., Clements, C., Park, J., Jeon, J., Ferro, V. and Watson, D. **2017**. Metabolomic Profiling of the Synergistic Effects of Melittin in Combination with Cisplatin on Ovarian Cancer Cells. *Metabolites*, 7, 14.

Posters presented

- Sanad Alonezi, Jonans Tusiimire, Mark Dufton, Valerie A. Ferro and David G. Watson. The metabolomic effects of melittin on ovarian cancer cells using high resolution mass spectrometry. Scottish Metabolomics Network Inaugural Meeting; **2015**; Edinburgh, UK.
- Sanad Alonezi, Jonans Tusiimire, Mark Dufton, Valerie Ferro and David G. Watson. Metabolomic profiling of the effects of melittin on cisplatin resistant and cisplatin sensitive ovarian cancer cells. Metabomeeting; **2015**, Robinson's College, Cambridge, UK.
- Sanad Alonezi and David Watson. The effects of cisplatin on the metabolome of sensitive and resistant ovarian cancer cells. Scottish Metabolomics Network Meeting; **2016**; Inverness, UK.

Abstract

Over the last few years, metabolomics has come to play an increasingly important part in many fields of research, notably medical studies. However, there is a dearth of research on metabolomics in the area of ovarian cancer and the increase in anti-cancer (platinum) drug resistance. Thus further studies on the modes of anticancer action and the mechanisms of resistance of ovarian cancer cells at the metabolome level are needed. The aim of this study was to characterise the metabolic profiles of two human ovarian cancer cell lines, A2780 (cisplatin-sensitive) and A2780CR (cisplatin-resistant), in response to their exposure to melittin, cisplatin and melittin-cisplatin combination therapy. It has been suggested that melittin may have potential as an anti-cancer therapy; combining cisplatin and melittin may increase response and tolerability in cancer treatment, as well as reducing drug resistance.

The A2780 and A2780CR cell lines were treated with sub-lethal doses of melittin, cisplatin and melittin-cisplatin combination therapy for 24 hours before extraction and global metabolite analysis of cell lysates by LC-MS using a HPLC system. Phenotype MicroArray™ experiments were also applied in order to test carbon substrate utilisation or sensitivity in both cell lines after exposure to melittin and cisplatin. Data extraction was carried out with MZmine 2.10 with metabolite searching against an in-house database. The data were analysed using univariate and multivariate methods.

The changes induced by melittin in the cisplatin-sensitive cells mainly resulted in reduced levels of amino acids in the proline/glutamine/arginine pathway, as well as to decreased levels of carnitines, polyamines, ATP and NAD⁺. It was necessary to evaluate the effect of a melittin on lipid activities of ovarian cancer cell lines. In order to do so, an LC coupled to an Orbitrap Exactive mass spectrometer using an ACE silica gel column was employed. The two cell lines had distinct lipid compositions, with the A2780CR cells having lower levels of several ether lipids than the A2780 cells. The changes induced by melittin in both cell lines mainly led to a decrease the level of PC and PE. Lipids were significantly altered in both A2780 and A2780CR cells. The observed effect was much more marked in the cisplatin-sensitive cells, suggesting that the sensitive cells undergo much more extensive membrane re-modelling in response

to melittin in comparison with the resistant cells. Regarding the metabolic effects of cisplatin on A2780 cells, these mainly resulted decreased levels of acetylcarnitine, phosphocreatine, arginine, proline and glutathione disulfide, as well as to increased levels of tryptophan and methionine. A number of metabolites were differently affected between the A2780 and A2780CR cells following cisplatin treatment, with A2780CR cells presenting increased levels of lysine, and decreased levels of N-acetylglutamate, oxoglutarate and 2-oxobutanoate compared to sensitive cells. However, when the combination treatment was applied, there were significant changes in both cell lines, mainly resulting in a reduction of levels of citrate cycle, oxidative phosphorylation, purine, pyrimidine and arginine/proline pathways. The combination of melittin with cisplatin has a synergistic effect when targeting these pathways. The melittin-cisplatin combination had stronger effect on A2780 cell lines than it had on those of A2780CR.

Overall, this study suggests that melittin may have some potential as an adjuvant therapy in cancer treatment. A global metabolomics approach can be a useful tool for evaluating the pharmacological effects of anti-cancer compounds or synergetic sensitisers using mass spectrometry.

Chapter 1

General Introduction

1 Introduction

1.1 Metabolomics

Due to rapid technological advances in the biological sciences in recent few years, a new era of research has begun, including the relatively new field of systems biology. Proteomics, genomics and transcriptomics are all part of a group of emerging technologies of which metabolomics is an important member. Metabolomics facilitates the analysis of bioactive molecules and their constitution, whether in urine, tissues, or even cells (Dettmer et al., 2007). Oliver and colleagues coined the name “metabolomics” in the late 1990s for an area of study concerned mainly with identifying and quantifying metabolites within an organism, such as organic acids, amino acids, nucleotide precursors and lipids, the totality of which makes up the organism’s metabolome. The metabolome comprises all metabolites, which themselves emerge within a biological system as end products of metabolic pathways (Oliver et al., 1998). This globalisation of metabolic profiling took place some considerable time after the first identification and quantification of metabolites which was carried out on a targeted basis. Previously analysis had been carried out with techniques ranging from thin layer chromatography to gas chromatography targeted at selected metabolites or metabolite pathways.

The definitions of metabolomics and metabonomics are similar, both being concerned with using the techniques of analytical chemistry, together with statistical analysis, to examine how the passage of time, perturbation and/or disease can alter a metabolome. However, the term “metabolomics” is found in the literature more often and will be

used here. Lipidomics is a related concept that has come into play more recently to refer to the identification and quantification of all lipids in a sample (Han and Gross, 2003).

A complete understanding of an organism's metabolome in different disease states can enable the identification of key biomarkers for diagnosis and therapeutic evaluation of various disease states, including cancer (Vermeersch and Styczynski, 2013; Dettmer et al., 2007). The past few years have witnessed a surge in the amount of cancer-related metabolomics research seeking to understand such phenomena as chemotherapeutic resistance, altered survival rates, and prognosis. The technology is powerful enough to detect hundreds of metabolites in cells (Frezza et al., 2011), tissues (Zhang et al., 2016b) and biofluids (Zhang and Watson, 2015). Figure 1.1 illustrates the different "omics" technologies and the different biological entities each of them deals with. It can be seen that metabolomics assesses the effects of the other technologies by assessing the metabolic outcomes at cellular level.

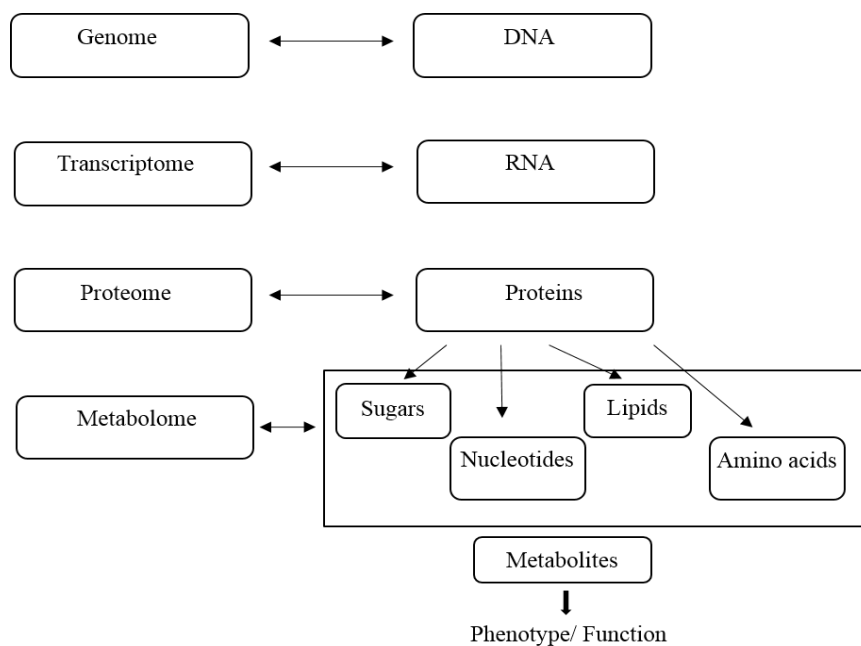


Figure 1.1. Overall metabolomics structure with lipids as part of metabolomics.

1.2 Metabolomics approaches in biomarker identification: targeted and untargeted

The various methods employed in metabolomics can be divided into targeted and untargeted techniques (Dettmer et al., 2007). Targeted analysis means that the former deals with a particular metabolite or a small group of related metabolites within the same or closely related pathways of interest (Dudley et al., 2010). On the other hand, untargeted metabolomics, also known as global metabolomics, simultaneously assesses as many metabolites as possible and compared their proportions within a given metabolome without any bias (Krastanov, 2010). For this reason, untargeted metabolomics datasets can be extremely complex but based on their relatively semi-quantitative estimates of various compounds, some of which are unknown, the data yielded can be employed in the formulation of hypotheses (Krastanov, 2010), which can be further tested in a targeted approach.

Apart from biomarker identification, metabolomics can also be employed in other aspects of cancer research for metabolic profiling and fingerprinting. Metabolic profiling deals with the analysis of a specific group of metabolites in a given metabolic pathway in order to create visual maps for enhancing understanding of the possible biological interactions between different pathways or systems. On the other hand, metabolic fingerprinting deals with the analysis of significant metabolites within a sample for subsequent classification based on the metabolites and for the purpose of identifying any class-defining differentially expressed metabolites (Di Gangi et al., 2014).

During any metabolomics study, the number and type of the metabolites targeted for investigation dictate the appropriate experimental design that is required, with regard to various aspects including sample preparation, choice of instrumentation, and the data analysis approaches employed. The flowchart below (Figure 1.2) illustrates the ‘typical’ workflow of a metabolomics experiment (Maguire, 2014).

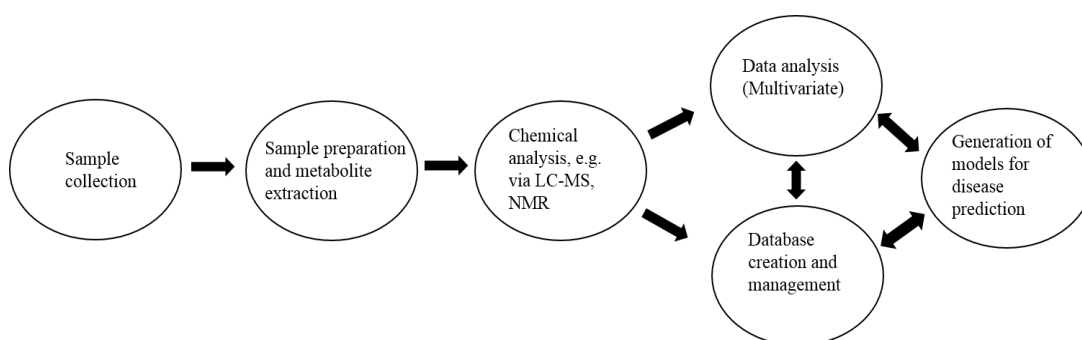


Figure 1.2. An outline of a ‘typical metabolomics study’ for identification of the metabolite biomarkers. (LC-MS, liquid chromatography-mass spectrometry; NMR, nuclear magnetic resonance spectroscopy) (Maguire, 2014).

1.3 Analytical techniques

Metabolites are a diverse group of chemical compounds whose analysis can be performed by employing the same techniques as those used in routine chemical analyses (Dunn and Ellis, 2005). These analytical techniques can be applied to identify and quantify the metabolic changes occurring in cancer tissue or cell extracts following treatment with selected chemotherapeutic agents, and to compare them with those of other treatments or negative controls. The most commonly used techniques in metabolomics include liquid chromatography (LC), gas chromatography (GC), and capillary electrophoresis (CE), coupled with a suitable detectors such as a mass spectrometer (MS) (Katajamaa and Orešič, 2007) and nuclear magnetic resonance (NMR) spectroscopy. Coupling a mass spectrometer to each of these separation techniques enables the detection of hundreds of molecules in a given sample simultaneously (Budczies et al., 2012; Dettmer et al., 2007). The need for comprehensive analysis of highly chemically diverse samples during metabolomics means that complementary techniques are necessary (Boccard et al., 2010; Atherton et al., 2006). Previous metabolomics studies have employed an extensive number of analytical techniques such as Fourier transform infrared (FT-IR) spectroscopy (Sayqal et al., 2016), NMR spectroscopy (Ubhi et al., 2012; Serkova et al., 2005), direct infusion mass spectrometry (DIMS) (Kaderbhai et al., 2003), and liquid or gas chromatography interfaced to the mass spectrometry platforms (LC-MS or GC-MS) respectively (Takahashi et al., 2011; Johnson et al., 2003). In choosing which instrument to employ, factors such as equipment costs, sensitivity, selectivity, mass accuracy and speed of the analysis are taken into consideration.

1.3.1 LC-MS

Chromatography is a technique of physical separation of compounds in a mixture in which analytes distribute themselves between a mobile phase and a stationary phase (Watson, 2012). These two phases act together to achieve separation of the components in a mixture based on the strength of interaction of the analytes and the two phases. Depending on the stationary and mobile phases used, liquid chromatography can be categorised as reversed phase (RP), normal phase (NP), and hydrophilic interaction liquid chromatography (HILIC), which are the three commonly used techniques in pharmaceutical analysis. The columns used are usually silica-based or monolithic and they can be derivatised with different ligands to make them suitable for either of the RP, NP or HILIC chromatographic separations. Generally, RP-HPLC is the commonest of the three techniques and utilises a hydrophobic stationary phase (for example, a C18) and a mobile phase gradient starting from high aqueous content to high organic content (Harris, 2010).

The LC-MS technique consists of a high performance liquid chromatography (HPLC) system interfaced to a mass spectrometer (MS). The modern HPLC system consists of a solvent reservoir, an online degasser, a pump, an autosampler, a column compartment, and a suitable detection system (Figure 1.3). For good separation of a given set of analytes in a mixture, the HPLC column should have an appropriate stationary phase, and the mobile phase should have a suitable modifier or buffer. There are various detectors which can be employed on the HPLC and these include UV, Diode Array Detectors, Evaporative Light Scattering Detector (ELSD), and Mass Spectrometer (MS) (Harris, 2010). The UV-based detectors have the disadvantage of

not being able to detect compounds that do not have chromophores, such as amino acids, but the use of a mass spectrometer with the HPLC offers a powerful analytical tool in pharmaceutical analysis. This is due to the benefit of the chromatographic resolution of the HPLC combined with the high sensitivity and high mass resolution from the MS (Watson, 2012).

Although reversed phase chromatography is the most popular type in pharmaceutical analysis, both in industry and quality control laboratories, it is much less popular in metabolomics profiling studies due to the fact that it does not retain metabolites, such as sugars and most amino acids (Rojo et al., 2012). Instead, metabolomics analysis employs stationary phases capable of separation in HILIC mode since these are designed to retain polar compounds that constitute most metabolomics samples. The principles of the separation of analytes in HILIC will be discussed in section 1.4.

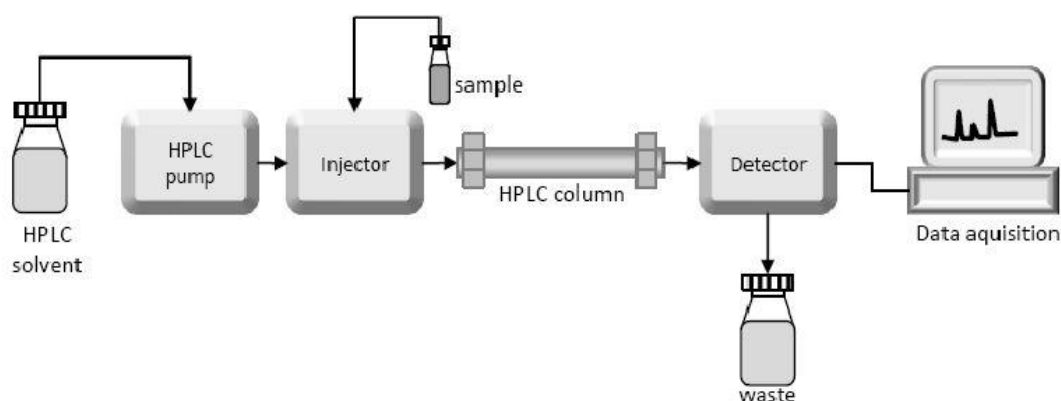


Figure 1.3. A schematic diagram to illustrate the components of an HPLC system.

The role of the mass spectrometer as a detector in LC-MS is to measure the mass-to-charge ratio (m/z) of the analytes present in a sample. Mass spectrometry is the technique of choice in metabolomics studies and as such, it is the most commonly used tool (Katajamaa and Orešič, 2007). The MS is superior to other common methods of detection such as UV, ELSD, fluorimetry, and NMR due to the combination of its high sensitivity, selectivity, resolution, and ability to give compound specific accurate mass data depending on the instrument used.

The MS has three main components: an ionisation chamber, a mass analyser, and a detector (Figure 1.4). The ion source is used to produce gas phase ions from the sample. The ionisation processes used in MS vary in their techniques and they include those which operate under vacuum such as electron impact (EI) and chemical ionisation (CI), and those which operate at atmospheric pressure such as electrospray ionisation (ESI) and atmospheric pressure chemical ionisation (APCI) (Kraj et al., 2008; Watson and Sparkman, 2007). The ions produced by the ion source are accelerated through a region of electric and magnetic fields so that only those ions with m/z in a given range can reach the analyser and be detected. The current MS systems were made to be suitable for application to metabolomics by the addition of soft ionisation techniques such as APCI or ESI which form mainly molecular ions without fragmentation, allowing the compounds to be identified based on their databases, constructed specifically using accurate mass data of the common metabolites (Watson and Sparkman, 2007; Kraj et al., 2008).

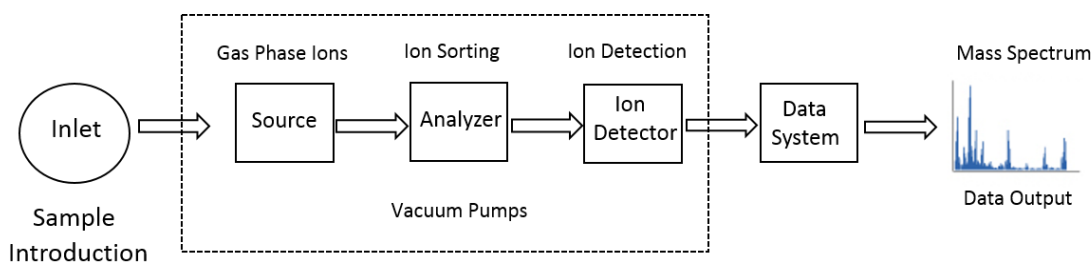


Figure 1.4. A schematic diagram to show the main components of a mass spectrometer.

The second main component of a MS instrument is the analyser, where the ions are separated based on their mass-to-charge (m/z) ratios. There are different mass analysers which are currently used in MS systems to separate the ions in time or space; these include quadrupoles (Q), ion traps (IT), time-of-flight (TOF), Fourier transform ion cyclotron resonance (FT-ICR), and the Orbitrap analyser (Hu et al., 2005). The main differences between these mass analysers arise from their resolving power, mass accuracy, sensitivity, dynamic range and fragmentation capabilities for MS^n studies. Recent developments have led to hybrid mass systems that combine the strengths of various mass analysers so that a single mass spectrometer can have various capabilities based on the ion separation techniques being encompassed in the hybrid system. Examples of such hybridised mass analysers include triple-Q, Q-IT, TOF-TOF, Q-TOF, IT-Orbitraps, LTQ-Orbitraps and Q-Exactives (Michalski et al., 2011).

The third part of a MS is the detector. In this region, the mass-to-charge ratios (m/z) of the detected ions and their abundances are measured. In the Orbitrap, for example, detection is based on image current of the ions in the mass analyser (Makarov and Scigelova, 2010). The conversion of the image current into the mass spectrum utilises

mathematical algorithms such as Fourier transformation (FT) which is also employed in other FT instruments such as FT-ICR (Michalski et al., 2012).

An ideal MS system should be able to detect very low concentrations of a given analyte in a sample, achieve high mass resolution between very closely related masses, give high mass accuracy, and have a high dynamic scan range. These attributes can all be found in some modern mass spectrometers such as the Orbitraps (Hu et al., 2005) (Figure 1.5). Additionally, mass spectrometers allow the analyst to tailor the conditions of the analysis to the specific analytes in the sample, which improves the robustness of the detection method. Generally, LC/MS systems have better sensitivity in the analysis of metabolites than GC-MS, without need for prior derivatisation. The capabilities of LC-MS can be expanded through MS-MS studies and high-energy C-trap dissociation (HCD) on the Orbitrap to enhance parent ion characterisation and to elucidate the structures of fragments resulting from analyte breakdown (Kamleh et al., 2009; Holčapek et al., 2012).

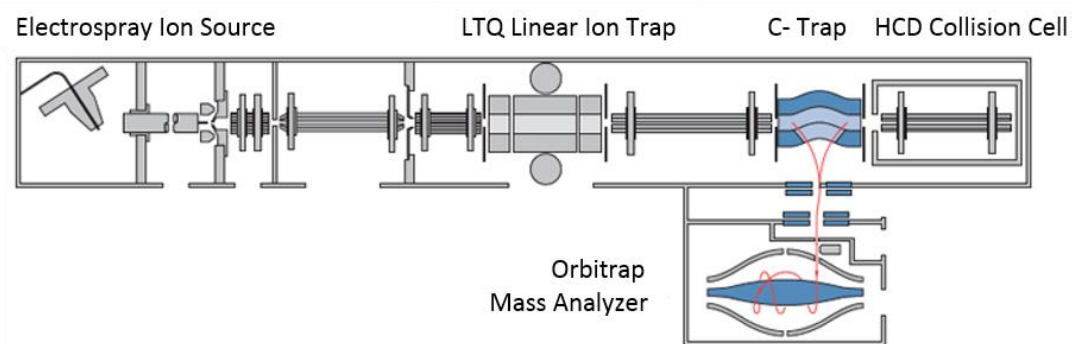


Figure 1.5. A schematic diagram representing the Orbitrap Mass Spectrometer.

1.3.2 Nuclear magnetic resonance (NMR) spectroscopy

NMR is a universal technique that can detect any organic compound in a sample. For this reason, it is one of the techniques that has found wide application in metabolomics studies (Simmler et al., 2014). It is non-destructive by nature, which allows the sample to be fully recovered. This enables the sample to be subjected to further analysis by other complementary techniques such as LC-MS. However, the application of NMR is limited by its lack of separation of analytes prior to data acquisition, leading to overlapping spectra in cases of mixed analytes which can be very difficult to analyse, and it has a relatively lower sensitivity compared to the MS technique. Because of these two limitations it is most useful for the screening of abundant established marker compounds rather than biomarker discovery. It is also useful for the detection of atypical outlying samples within a sample set. The technique is most useful during structure elucidation studies for targeted metabolomics and it is also directly quantitative without the need for a standard provided with instrument is calibrated (Simmler et al., 2014).

The use of NMR in metabolomics profiling has been reported previously by many researchers (Tiziani et al., 2009; Xi et al., 2008; Young et al., 2013). As with data generated by LC-MS techniques, NMR data generated for each sample is multi-dimensional and contains variables such as chemical shifts, splitting patterns, signal strength (area under curve), coupling constants and multiplicity. Since multivariate classification obtained from data analysis techniques such as PCA depends on the variance present in the data, there is a need to minimise variance contributions from random technical procedures such as sample preparation and sample analysis. This

ensures that there is maximisation of the contribution from wanted biological variance between individual classes, which improves grouping and separation (Parsons et al., 2007).

1.3.3 GC-MS

Gas chromatography– mass spectrometry (GC-MS) is a combined analytical system. Gas chromatography (GC) uses an inert gas as mobile phase, hence its name. The most commonly used gases in GC include nitrogen, helium, and hydrogen. The use of a gas as the mobile phase is the key difference between the GC and LC, as the latter uses a liquid mobile phase. The columns used in modern GC systems are long capillary columns which contain stationary phases coated internally. The stationary phase coatings vary in their polarity; polar ones include carbowax phases while methyl silicone phases are less polar. There is a range of commercial GC columns available whose stationary phases vary in terms of their polarity and suitability for analysis of different analytes. Samples can be injected in split or splitless mode depending on their concentration; the split mode is used with concentrated samples. However, splitless mode is preferable for samples containing very low levels of the metabolites being analysed (Watson, 2012). The main compartments of the GC such as column and injection port are maintained at high temperatures in an oven maintained to keep analytes in the gas phase. The temperature gradient of the column compartment is employed to modify retention times of the analytes. Apart from temperature, retention times depend also on the molecular weight and polarity of the compound, which in turn affect its volatility.

A GC-MS system consists of a GC with a MS as the detector. Different types of mass spectrometers can be interfaced to the GC but since analytes entering the MS are in gas phase, only MS ion sources that are capable of dealing with gas-phase analytes are employed. These ion sources include chemical ionisation (CI) and electron impact (EI) ionisation. The latter uses high collisional energy (70eV) with fast moving electrons to ionise analytes, resulting in extensive fragmentation of the compound, which can facilitate identification procedures. GC-MS can be carried out with quadrupole and time-of-flight (TOF) mass analysers. GC-quadrupole systems have a high dynamic range and sensitivity but their mass accuracy and scan speed are quite low. On the other hand, GC-TOF/MS has higher mass resolution and mass accuracy (Bedair and Sumner, 2008).

GC-MS is one of the preferred techniques applied in metabolomics research because it combines the high separation efficiency (chromatographic resolution) of a capillary GC column and the high sensitivity and robustness of the mass spectrometer (Kopka, 2006). The availability of GC-MS spectral libraries also makes the task of metabolite identification easier. Compared to LC-MS, GC-MS has a limited application because of the need for the samples to be volatile and thermally stable. For some non-volatile analytes such as fatty acids, volatility can be achieved by derivatisation; for instance fatty acids can be derivatised through methylation to form esters which are volatile (Schauer et al., 2005; Kopka, 2006). Another common method for derivatisation is by oxime/silylation derivatisation. Silylation introduces a trimethylsilyl (TMS) group onto the non-volatile compound resulting into volatility and the method can be applied to alcohols, amides, amino acids and thiols (Roessner et al., 2000; Dunn et al., 2005).

TMS derivatives are less polar than the parent metabolites and have less dipole-dipole interactions which increase their volatility, which is suitable for analysis by GC-MS (Dunn et al., 2005). It should be noted that the derivatisation process can be time-consuming and the additional sample preparation might introduce extra technical errors into the experiment, thus increasing the total variability in the samples. In the case of thermal stability, except for small molecular weight hydrocarbons, short chain alcohol and esters, most metabolites are affected by the high temperatures employed in GC-MS, which can be as high as 350°C (Bedair and Sumner, 2008). An overview of the more common advantages and disadvantages of analytical techniques is given in Table 1.1.

Table 1.1. A summary of common analytical techniques used in metabolomics

Analytical technique	Advantages	Disadvantages
NMR	<ul style="list-style-type: none">• Robust and reproducible• Minimal sample preparation required• Sample analysis is fast and robust• Non-destructive	<ul style="list-style-type: none">• Low analytical sensitivity• More than one peak per compound in most cases, meaning spectra are often complex• Does not analyse fats and lipids well• NMR spectrometers can take up a lot of space
GC-MS	<ul style="list-style-type: none">• High analytical sensitivity• Robust and reproducible technique• Large dynamic range• Compound identification is facilitated by large, well-established mass spectral libraries	<ul style="list-style-type: none">• Sample analysis can be slow• The similarity of isomers can make it difficult to identify compounds• Many metabolites are non-volatile and must be derivatized prior to analysis• Many large molecules (e.g. proteins) cannot be measured
LC-MS	<ul style="list-style-type: none">• High analytical sensitivity• Robust technique• Large dynamic range• No derivatization required (usually)	<ul style="list-style-type: none">• Analysis can be slow• Reproducibility issues and matrix effects can hinder compound identification• There are very few commercial libraries

1.4 Principles of HILIC separation

Hydrophilic interaction liquid chromatography (HILIC) is a technique which combines the mobile phases used in reversed phase with stationary phases used in normal phase (Tang et al., 2014). The emergence of HILIC as a technique of choice in metabolomics was due to the lack of retention for highly polar compounds on reversed phase columns. In this case, HILIC can be employed as an alternative to RP to achieve sufficient retention for these polar analytes. Both RP and HILIC columns are silica based but unlike the former, HILIC stationary phases are hydrophilic. For this reason,

HILIC stationary phases have higher retention for polar analytes and lower retention for nonpolar ones, which is an orthogonal effect to that observed in RP (Jandera, 2011). HILIC is employed extensively in the metabolomics field due to the fact that many hydrophilic metabolites such as carbohydrates cannot be sufficiently retained in a RP column and often elute close to the column hold-up volume.

1.4.1 Mobile phases

HILIC uses the same mobile phases as those employed with reversed phase (Buszewski and Noga, 2012). These include water and an organic solvent such as acetonitrile. The elution is a gradient mobile phase, which starts at a high organic solvent concentration and low water to achieve sufficient retention of analytes on the column and then proceeds with gradually increasing water content. Analyte retention in HILIC can be modified by the use of buffer salts such as ammonium carbonate, ammonium formate, ammonium acetate, and ammonium chloride. The counter ions in the buffer can modify retention of analytes by competing for the sites of interaction on the stationary phase, which leads to faster elution. Alternatively, the counter ions can increase the thickness of the aqueous layer on the HILIC surface, which increases retention of the polar analytes (Jandera, 2008).

1.4.2 Stationary phases

1.4.2.1 Silica gel

HILIC stationary phases include bare silica (silica gel) consisting of silanol groups (Si-OH) bonded to the silica atoms of the particles. These silanols vary in their acidic activity depending on the environment of the silica atoms to which they are attached.

The most common groups are isolated, geminal and vicinal, as shown in Figure 1.6. The surface of silica gel is polar due to the silanols present. Thus, the stationary phase can be used in HILIC since water can form a coating on the gel to facilitate the separations. In addition to partitioning in the water layer formed, some analytes can form hydrogen bonds with silanols and there is possibility for ion exchange interactions with the more acidic silanols depending on the pH of the mobile phase (Moldoveanu and David, 2016; Jandera, 2011).

Silica is the most suitable sorbent for lipid fractionation, as these analytes are first recovered in non-polar solvents. Hence, polar compounds such as phospholipids are more strongly adsorbed by the silica sorbent than by neutral lipids such as sterols and triglycerides (Cazes, 2005).

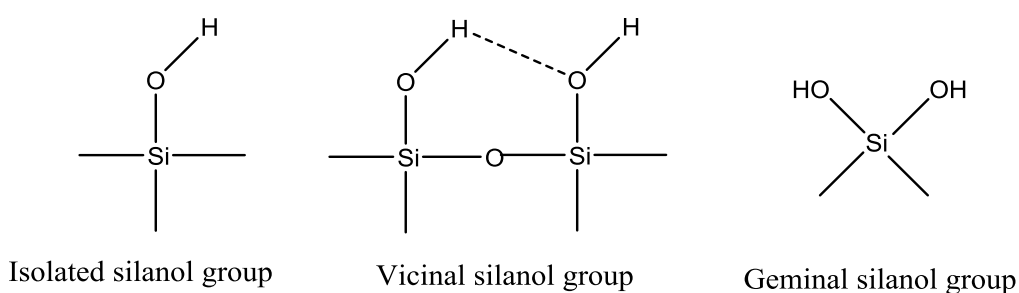


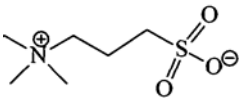
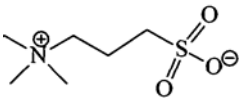
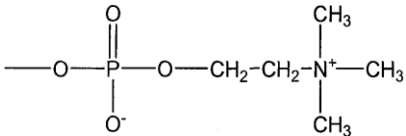
Figure 1.6. The different types of silanols in silica gel.

1.4.2.2 Zwitterionic phases

Zwitterionic stationary phases are some of the latest HILIC stationary phases which are based on the sulfobetaine or phosphorylcholine functional groups (Table 1.2). Both ZIC-HILIC and ZIC-pHILIC have a sulfobetaine functional group but the latter

possesses polymeric particles instead of silica. On the other hand, ZIC-cHILIC has a phosphorylcholine functional group bonded to silica particles. These columns are currently available and have shown reproducible efficiency at separating metabolites in various metabolomics samples. As such, they offer the best results in comparative studies for metabolomic applications (Jandera, 2011).

Table 1.2. Currently available zwitterionic phases and their functional groups.

Column	Functional group	Particle	Structure
ZIC-HILIC	Sulfobetaine	Silica	
ZIC-pHILIC	Sulfobetaine	Polymer	
ZIC-cHILIC	Phosphorylcholine	Silica	

In the case of zwitterionic columns, due to the charges on the sulfobetaine and phosphorylcholine groups, the possibilities for interaction include partitioning in the stationary aqueous layer formed on the phase, anion and cation exchange, and some minor non-polar interactions with the carbon backbone (Rojo et al., 2012). Thus separation of the analytes is generally similar to that in HILIC in general but electrostatic and ion exchange interactions play a more crucial part. Electrostatic forces can be repulsive if the analyte charge is similar to the column charge, which leads to less retention, or can be attractive where the analyte can be bound by the oppositely charged stationary phase leading to increased retention (Jandera, 2008). Other HILIC-type stationary phases include silica-derived neutral stationary phases

such as amide, cyanopropyl, diol, aminopropyl (weakly basic), and silicon hydride.

1.4.3 Factors that determine retention times in HILIC

The separations in HILIC are governed by various factors, of which the main ones include temperature, mobile phase composition, buffer pH, and ionic strength. To begin with, the effect of temperature used depends on the type HILIC stationary phase. An increase in temperature increases the solubility and diffusibility of analytes, which might give better peaks. In addition, in zwitterionic HILIC stationary phases it has been observed that the thickness of the solvating aqueous layer decreases as the temperature increases (Guo and Gaiki, 2005). This reduces the retentivity of the column, which causes the analytes to elute faster. Secondly, the nature of solvents used in the mobile phase can also affect retention in HILIC separations. Protic solvents such as methanol, ethanol, and isopropanol can displace water from the polar sites on the stationary phase due to their ability to form hydrogen bonds. This makes the stationary phase surface less hydrophilic and therefore less retentive for polar analytes (Wade et al., 2007). On the other hand, aprotic solvents such as acetonitrile do not displace water from the polar sites on the stationary phase and therefore increase the retention of polar analytes (Li and Huang, 2004). Thirdly, buffer pH has an effect on retention times in HILIC especially for ionisable analytes. When the pH leads to ionisation of analytes, there is an increase in polarity which increases retention times in HILIC. However, if the pH suppresses ionisation, the retention times will decrease since the compounds become less polar. Thus, the general rule is that retention times increase with an increase in pH for acidic compounds due to ionisation (Guo and Gaiki, 2005), but they decrease with an increase in pH for weakly basic compounds due to the suppression

of ionisation (Watson, 2012). It should be noted that as well as affecting the ionisation of the analytes, buffer pH can also modify the ionisation of the stationary phases, thus modifying other interactions such as ion exchanges, which changes the retention times. Finally, the ionic strength of the mobile phase can also modify retention times of analytes by changing the thickness of the water layer on the stationary phase or by acting as competing ions for oppositely charged ionic sites on the surface of the stationary phase. Increased ionic strength increases the water layer thickness which increases retention times in HILIC, while binding to charged sites on the stationary phase decreases retention times for similarly charged analytes. The latter also minimises repulsion for oppositely charged analytes, which can result in decreased retention (Bawazeer et al., 2012; Santali et al., 2014).

1.5 Metabolomic data extraction and statistical analyses

Metabolomics samples, when analysed, produce an enormous amount of data of a very complex nature that cannot be easily interpreted until statistical software has been used to analyse it. Processing the data in this way allows all relevant information about the analytes that were found in the sample to be extracted while, at the same time, making subsequent data analysis and interpretation easier by minimising background noise.

Metabolomics data therefore cannot be properly analysed or interpreted without data processing as an essential step. Data usually passes through two distinct steps: data processing, followed by data analysis. In data processing, the raw data is transformed into a format that the subsequent data analysis will find easy to use. Then, in data analysis, the processed data is analysed and interpreted; multivariate analysis will typically be used including, for example, the clustering of metabolic profiles and the

identification of significant differences between different groups of samples (Ferrara and Sebedio, 2014).

Software packages and web-based tools are constantly under development to improve the processing of metabolomics data. Software for this purpose is widely available, including non-commercial open source software like MZmatch and MZmine, which allow for peak detection; filtering; normalisation; and identification using both local and online databases. MZmine was published in 2005 and was first written to process mass spectrometry-based profile data (Katajamaa et al., 2006). It has since been used for a variety of metabolomic analyses (Macintyre et al., 2014; Alonezi et al., 2016). The same is true of MZmatch (Stipetic et al., 2016; Trochine et al., 2014), which is the underlying platform that software like IDEOM is based on (Creek et al., 2012). There is also commercially available software such as SIEVE, developed by Thermo Fisher Scientific, whose main functions are peak extraction; peak alignment; and peak tabulation according to peak intensity. When identified peaks are tabulated, each selected peak receives a unique ID signifying a particular metabolite. Also given in relation to each set of metabolites are statistics like p-values (for the differences between treated and control samples). Important differences in peak intensities between two groups of samples, and their visual display in a plot, are made easier by this software (Zhu et al., 2009).

The next step is for database searches to be carried out to identify metabolites found in the samples. The basis of this search is the predicted atomic composition, or the accurate mass data of the metabolites. It follows that the reliability of the identification thrown up by the database search depends both on the instrument, and on the method

used to analyse the data. There is a range of public databases currently available, but those most commonly used are MassBank, Human Metabolome Database, KEGG, LipidMaps and Metlin (Dettmer et al., 2007; Horai et al., 2010). Metabolomic profiling requires that these databases be used for the identification of unknown metabolites so that biologically relevant information about the data may be obtained.

Analytical techniques used may include GC-MS, LC-MS and NMR, and data processing begins with data acquisition from the analytical instrument (Cui et al., 2008; Kuhn et al., 2008). As an example, data produced by LC-MS analysis collected by XCalibur software needs to be pre-processed before carrying out multivariate statistical analysis (MVA) or using chemometric tools. Multivariate statistical analysis methods as currently deployed include the unsupervised technique, principal component analysis (PCA); as well as two supervised techniques, OPLS-DA (orthogonal partial least square discriminant analysis) and PLS-DA (partial least square discriminant analysis). PCA provides for the identification and grouping of samples whose metabolic profile is similar, and is frequently the first step when investigating data variability and clustering trends using chemometric analysis. Supervised techniques demand a priori knowledge of sample classification, and so allow identification of the metabolites discriminating the groups. Construction of models requiring further validation is also permitted by supervised techniques; an example would be a cross-validation procedure where samples were excluded and their classification predicted. What happens in practice is often a combination of these methods (Ferrara and Sebedio, 2014).

The two stages of internal validation followed by external validation can be the means by which model validation is performed. It is also possible to perform internal validation of OPLS-DA models by using ROC (receiver operating characteristic) analysis and testing permutation (Pasikanti et al., 2010; Xia et al., 2013). The permutation test compares how closely the fit of (R^2 and Q^2) in the original model matches the fit of a number of OPLS-DA models constructed using the data matrix with random permutation of the order of the Y observations while keeping the X matrix intact (Mahadevan et al., 2008; Wiklund et al., 2007). In addition, the robustness of the model can be verified with ROC analysis based on predicted Y values that have been cross-validated (predicted Y values being predicted class values). Trade-offs in sensitivity and specificity for each model can be summarised with trapezoidal rule calculations on the area under the ROC curve (AUROCC) (Pasikanti et al., 2010). A good indication of the sensitivity and specificity achievable in predicting unknown samples can be provided by ROC analysis (AUC= 0.9–1.0 excellent; 0.8–0.9 good; 0.7–0.8 fair; 0.6–0.7 poor; 0.5–0.6 fail) (Xia et al., 2013).

The conclusion regarding the validity of each model can be strengthened by external validation after internal validation strategies have confirmed it. External validation involves predicting the classification of remaining samples after a training set has been constructed from a randomly selected subset of observations. Chemometric analysis should take place only after the selection of sets for training and testing in order to avoid any bias from data pre-processing and pre-treatment in the unknown sample prediction. It is possible to make external validation an iterative process, performed by selecting at random a variety of combinations of training and test sets for estimating the model's predictive ability. There are inbuilt features for performing internal and

external validation in most software packages (SIMCA-P or MetaboAnalyst). When internal and external validation strategies have confirmed the validity of each model, the statistical significance of potential marker metabolites in control and treatment groups may be further verified by such univariate tests as ANOVA and the T test (Chan et al., 2012). Because the metabolome data sets contain so many variables, the level of significance should be determined to ensure fewer false positives. False positives may also be reduced by Bonferroni correction and false discovery rate (FDR) correction methods. Bonferroni -based comparison procedures are highly conservative, tending to increase the number of wrong rejections of true hypotheses as the number of hypotheses being simultaneously tested increases. FDR-based comparison procedures are becoming more common in metabolomics because they are often more appropriate than Bonferroni methods for identifying actually significant results (Tsugawa and Bamba, 2014; Pike, 2011).

1.6 Metabolomics in ovarian cancer

1.6.1 Ovarian cancer

Cancer is a destructive disease that changes in metabolic activity of a cell and the surrounding milieu. Cancer cells have different metabolic properties compared to normal cells. The growth of cancers is associated with various metabolic changes, at cellular level, which can be used as biomarkers for diagnosis, prognosis, and evaluation of anticancer therapies (Vermeersch and Styczynski, 2013). For instance, unlike normal cells, cancer cells are more dependent on aerobic glycolysis (Warburg effect), fatty acid synthesis, and glutaminolysis for proliferation (Vander Heiden et al., 2009). Thus, evaluation of the concentrations of specific metabolites in a cell can

provide insights into its metabolic state relative to the physiological norm. The metabolic profile of cancer cells can also provide an understanding of the process of carcinogenesis and the mechanism of chemoresistance leading to the development of better diagnostic and therapeutic tools (Poisson et al., 2015).

Ovarian cancer is the fifth most common cancer among women after breast, bowel, lung and uterine cancers respectively. Worldwide, more than 230,000 women are diagnosed with ovarian cancer each year, and this disease is responsible for an estimated annual mortality of 140,000 people (Wang and Lippard, 2005). This makes it one of the commonest and most fatal cancers of the female reproductive system. According to the National Health Service (NHS 2015, Ovarian Cancer), ovarian cancer is diagnosed in approximately 7,000 women each year in the United Kingdom (NHS, 2015). In the United States, there will be an estimated 22,280 cases of ovarian cancer diagnosed in 2016, which will result in approximately 14,240 deaths (Howlader et al., 2016). Ovarian cancer has the lowest five-year survival rate among gynaecologic cancers at 46.2%. The disease most commonly affects women over 50 years of age who have been through the menopause but it can potentially come at any age (Howlader et al., 2016). Ovarian cancer typically remains asymptomatic in its early stages, and over 70% of patients present with advanced stage disease. The symptoms are quite similar to those of other conditions such as irritable bowel syndrome (IBS) and pre-menstrual syndrome (PMS), thus making it difficult to diagnose, but early symptoms include persistent bloating, difficulty eating, urinary urgency/frequency and pelvic/abdominal pain (Goff et al., 2007).

1.6.2 Pathophysiology

Ovarian cancer is a term that refers to several of the neoplastic growths that affect the ovary epithelium and associated organs, including the fallopian tube. Ovarian cancer develops from different cell types within the ovary. The most common form of the cancer is known as epithelial ovarian cancer (EOC) but other types include ovarian low malignant potential tumour (OLMPT) as well as germ cell and sex cord-stromal tumours. The risk of developing ovarian cancer is high in women who experience many ovulation cycles over their life time because the constant rupturing of the ovary to release the ovum at each cycle might increase the likelihood of development of the cancer (Bast et al., 2009; Furuya, 2012). Additionally, family history also plays a significant role. In fact, more than 15% of all ovarian cancers are genetically related. Inherited mutations affecting the BRCA1 and BRCA2 genes have been shown to greatly increase the woman's lifetime chances of developing ovarian cancer up to 54% (Toss et al., 2015). Other gene lesions responsible for increase predisposition to ovarian cancer have also been described (Furuya, 2012; Toss et al., 2015). For this reason, women diagnosed with ovarian cancer are normally requested to undergo testing for these mutations in order to enable their families be monitored for various cancers that might be associated with these mutations.

1.6.3 Stages of ovarian cancer

The stage of ovarian cancer depends on the extent to which the disease has metastasised at the time of the diagnosis. In stage 1, the disease is limited to one or both ovaries while in stage 2 it is limited to the pelvic region. Once the disease has spread outside the pelvis but still limited to the abdomen, or lymph nodes, without

liver involvement, it is a stage 3. The final stage 4 involves metastasis to the liver and other sites outside the abdomen. The staging of ovarian cancer is normally done surgically but stage 4 or advanced cases of stage 3 are often proven with a biopsy before initiating chemotherapy prior to surgery (Cancerresearchuk, 2016).

1.6.4 Samples used in the metabolomics-based ovarian cancer research

The application of metabolomics in the diagnosis of malignancies such as ovarian cancer has been previously conducted through analysis of plasma (Fan et al., 2012), urine (Slupsky et al., 2010), and tumour tissues (Fong et al., 2011).

1.6.4.1 Blood

In clinical settings, it is important that the most appropriate samples be taken for analysis in order to obtain the most optimal performance for the assay. Blood is one of the most readily assessable biofluids and analyses of its metabolite profile can be conducted on its plasma or serum (Wedge et al., 2011). For instance, an NMR-based metabolomics assay was employed in the metabolic fingerprinting of ovarian cancer using serum samples from patients as test samples and normal healthy women as controls (Odunsi et al., 2005). In this study, it was demonstrated that ovarian cancer is associated with significant increases in levels of glucose, 3-hydroxybutyrate, alanine, and valine metabolites (Odunsi et al., 2005). In addition, Fan et al. (2012) identified eight metabolites associated with epithelial ovarian cancer which could be used as its novel biomarkers. In their study, the researchers employed an ultra-performance liquid chromatograph (UPLC) system coupled to a quadrupole time-of-flight (QTOF) mass spectrometer to analyse plasma samples from both patients and normal controls (Fan

et al., 2012). In another study utilising UPLC-MS, the six biomarkers responsible for metabolic discrimination between epithelial ovarian cancer and benign ovarian tumor were identified from plasma samples in which four of the biomarkers (L-tryptophan, lysophosphocholines (32:3), and 2-piperidinone) were significantly lower in the cancer patients than in those with the benign tumour (Zhang et al., 2012b). Other metabolites that have been identified as specific biomarkers for epithelial ovarian cancer in plasma are piperine, 3-indolepropionic acid, 5-hydroxyindoleacetaldehyde, and hydroxyphenyllactate (Ke et al., 2015), as well as kynurenine, bilirubin, and lysophosphoethanolamine (18:2) (Zhang et al., 2015). Thus, through analysis of metabolite profiles in blood, it could be possible to distinguish between epithelial ovarian cancer, benign ovarian tumour, and uterine fibroid.

1.6.4.2 Urine

Other than blood, urine is an ideal sample which can be studied during metabolomics investigations because it can be readily obtained and is less complex than most other body fluids. The use of urine as a test sample in the establishment of biomarkers for ovarian carcinomas has been employed in a number of previous studies. For instance, Woo et al. (2009) identified potential urinary biomarkers of ovarian cancer based on analysis of samples from patients and normal controls. This led to the identification of three known biomarkers 1-methyladenosine, 3-methyluridine, and androstenedione which were significantly raised in the patients (Woo et al., 2009). Other studies have employed NMR spectroscopy on urine samples to screen for ovarian and breast cancer biomarkers by comparing samples from patients and normal controls (Slupsky et al., 2010). Metabolic strategies have also been employed in assessing the differences in

hydrophilic and hydrophobic urinary metabolites of healthy women and those suffering from benign and malignant ovarian tumours. These metabolites were analysed by HILIC and reversed phase HPLC interfaced to the mass spectrometry and five of them were identified as being specific to ovarian cancer. In addition, ten of the metabolites were considered to be commonly related to ovarian tumors both benign and malignant (Chen et al., 2012). Urine has also been employed in the evaluation of potential biomarkers in EOC where samples were collected from preoperative EOC, benign ovarian tumor (BOT) and healthy patients and analysed by LC-MS on an ultra-performance liquid chromatograph interfaced to a quadrupole time-of-flight mass spectrometer (UPLC-QTOF/MS). The affected pathways in EOC patients included those of nucleotide (pseudouridine, N4-acetylcytidine), histidine (L-histidine, imidazol-5-yl-pyruvate), tryptophan (3-indolelactic acid), and mucin (3'-sialyllactose and 3-sialyl-N-acetyllactosamine) metabolism (Zhang et al., 2012a). Therefore, urine metabolomics analysis has a high probability of biomarker discovery for ovarian cancer.

1.6.4.3 Tissues

Tissue samples have also been used in metabolomic profiling of cancers. A previous study by Denkert et al. (2006) compared the metabolic profile of invasive ovarian carcinomas and borderline tumours using a gas chromatograph interfaced to a time-of-flight mass spectrometer (GC-TOF MS). The study identified 51 significant metabolites as being quantitatively different between the two conditions (Denkert et al., 2006). It has been generally recognised that adenosine monophosphate (AMP)-activated protein kinase (AMPK) plays a key role in cellular energy metabolism

regulation. The expression of AMPK in ovarian carcinoma specimens was investigated in tissue specimens from ovarian carcinomas, borderline tumours and normal ovaries. Employing the GC/TOF-MS in the metabolomics, it was revealed that significantly higher levels of glucose were present in AMPK-negative carcinomas, as were several of the carbohydrate metabolites (Buckendahl et al., 2011). Fong et al. (2011) also compared the metabolic profile of EOC and metastatic ovarian cancer (MOC) compared to normal tissues using GC-MS and tandem MS. The study identified about 95 metabolites which were significantly different between all the three ovarian groups, among which were fatty acids and carnitine metabolites such as carnitine, acetylcarnitine and butyrylcarnitine which were significantly raised in both diseased tissue types (Fong et al., 2011).

In terms of evaluating the efficacy of drug combinations in the treatment of ovarian tumours, metabolomics-based approaches have already been shown to be quite reliable. For instance, Katragadda et al. (2013) demonstrated the feasibility of this metabolomics application using paclitaxel/tanespimycin-loaded micelles in mice bearing xenografts from human ovarian tumours using ¹H-NMR-based metabolomics. It was observed that there was a decrease in levels of glucose, lactate and alanine, which were associated with simultaneous increases in the levels of glutamine, glutamate, aspartate, choline, creatine and acetate (Katragadda et al., 2013).

1.6.4.4 Cell cultures

Cell cultures offer a robust means of conducting metabolomics-based testing in many applications and offer many advantages to alternative methods for cell line testing. It

is anticipated that the recent development of more robust metabolomics platforms will greatly enhance the applications of cell cultures in the evaluation of mechanisms of drug actions both *in vitro* and *in vivo* thus aiding the speed of their development as novel therapeutic agents (Čuperlović-Culf et al., 2010). There are a number of previous studies in which cell cultures were employed to identify metabolic differences of varying treatments. For instance, the metabolic effects of gossypol, a natural phenol derivative obtained from cotton plants, were investigated in the ovarian cancer cell line SKOV3. Treatment was shown to result in oxidative stress-related cell death and the analysis of metabolic effects showed that gossypol decreases cellular levels of glutathione, a natural antioxidant, as well as those of the amino acid aspartate and flavin adenine dinucleotide (FAD) (Wang et al., 2013). Other recent metabolomics studies involving the use of cell cultures include the study by Purwaha et al. employing tandem MS for high-throughput quantitation of proteinogenic amino acids, amino acid derivatives (e.g. ornithine, citrulline, sarcosine, taurine, hypotaurine, and cystine), and polyamines (e.g. putrescine, spermidine, and spermine) in the human ovarian cancer cell line (OVCAR-8) (Purwaha et al., 2014). On the other hand, Vermeersch et al., employed 2D GC-MS in the investigation of the metabolic effects of docetaxel, an ovarian cancer chemotherapeutic agent, using ovarian cancer cells (OVCAR-3) and the isogenic ovarian cancer stem cells (OCSCs), which led to the observation that the drug induced significant metabolic changes on OVCAR-3 but not OCSCs cells (Vermeersch et al., 2014).

The use of cell cultures has been demonstrated to be applicable in both targeted and untargeted metabolite profiling approaches. For instance, Tolstikov et al., employed

HILIC-LC-MS and GC-MS in the analysis of the metabolomic effects of inhibition of the enzyme nicotinamide phosphoribosyltransferase (NAMPT) on human cancer cells. These researchers treated the ovarian cancer A2780 and colorectal cancer HCT-116 cell lines with FK866, a small molecule inhibitor of NAMPT, in the presence and absence of nicotinic acid. The most significant effects were observed in the metabolism of amino acids, purines and pyrimidines as well as metabolic alterations in glycolysis, the Krebs cycle or tricarboxylic acid cycle (TCA), and the pentose phosphate pathway (Tolstikov et al., 2014). The use of untargeted metabolomic profiling has been studied in cell cultures to distinguish between ovarian and colon cancer cell lines based on analysis by UPLC-MS and GC-MS. The study identified 67 metabolites that could be used to discriminate colon from ovarian cancer. The metabolic signatures observed in this study revealed significantly elevated levels of TCA cycle and lipid metabolites in the ovarian cancer cell lines, as well as increased levels of β -oxidation and urea cycle activation in colon cancer (Halama et al., 2015). In another study, Poisson et al. (2015) conducted a global metabolic analysis of platinum-sensitive A2780 ovarian cancer cell line and its platinum-resistant C200 derivative using UPLC-MS and GC-MS. The study identified 179 metabolites were significantly different between A2780 and C200 cells, the most significantly affected pathways were those of cysteine and methionine metabolism (Poisson et al., 2015). A summary of key studies in literature which have been recently published on metabolomics of ovarian cancer is shown in Table 1.3.

Table 1.3. Summary of representative current metabolomics on ovarian cancer.

Biological materials	Approach	Treatment	Reference
Serum	NMR	None	Odunsi et al., 2005
Plasma	UPLC/QTOF/MS	None	Fan et al., 2012
	UPLC/MS	None	Zhang et al., 2012
	UPLC/MS	None	Ke et al., 2015
	UPLC/MS	None	Zhang et al., 2015
Urine	GC-MS & LC-MS	None	Woo et al., 2009
	NMR	None	Slupsky et al., 2010
	LC-MS	None	Chen et al., 2012
	UPLC-QTOF/MS	None	Zhang et al., 2012
Tumor tissues (HO)	GC/TOF-MS	None	Denkert et al., 2006
	GC/TOF-MS	None	Buckendahl et al., 2011
	GC-MS & LC/MS/MS	None	Fong et al., 2011
Mouse tumor cells	NMR	Paclitaxel/ Tanespimycin	Katragadda et al., 2013
Cell cultures			
SKOV3	LC/MS/MS	Gossypol	Wang et al., 2013
OVCAR-8	LC/MS/MS	L-asparaginase	Purwaha et al., 2014
OVCAR-3 & OCSCs	GCxGC-MS	Docetaxel	Vermeersch et al., 2014
A2780	HILIC-LC-MS & GC-MS	FK866	Tolstikov et al., 2014
OVCAR3 & SKOV3	UPLC/MS & GC-MS	None	Halama et al., 2015
A2780 (PS) & C200 (PR)	UPLC/MS & GC-MS	None	Poisson et al., 2015

HO (human ovaries); **PS** (platinum sensitive); **PR** (platinum resistance)

1.7 Ovarian cancer treatment

1.7.1 Current chemotherapy agents

Chemotherapy has a generally good success rate with ovarian cancers, many of which respond well to standard primary treatment with surgery. The usual ovarian cancer treatment combines chemotherapy with optimal cytoreductive surgery; the chemotherapeutic agents will normally be such platinum agents as carboplatin or cisplatin and such taxane compounds as docetaxel or paclitaxel (Ozols, 2006; Bookman, 2005; Poisson et al., 2015).

Platinum compounds continue to be the most important among the cytotoxic agents used to treat ovarian cancer. The efficacy of carboplatin and cisplatin (figure 1.7) has been found to be similar, though there may be more side effects with cisplatin; among those side effects may be nephrotoxicity, neurotoxicity and emetogenesis (Wang and Lippard, 2005; Bookman, 2005). DNA strands are cross-linked by the platinum compound, and a number of cellular processes mediating the cytotoxicity of platinum drugs are activated by these platinum-DNA adducts. The platinum compounds cause damage to DNA which sets off multiple signalling pathways; cell cycle arrest, cell death, or cell survival result (Wang and Lippard, 2005). Two modes of cell death (apoptosis and necrosis) have been shown to be induced by cisplatin, the mode being determined, as with other genotoxic drugs, by the amount of cisplatin exposure (Gonzalez et al., 2001). A high cisplatin dose will induce necrosis within a few hours, while it will take several days of cisplatin exposure at low dosage to induce apoptosis (Lieberthal et al., 1996). The mechanism of cisplatin cytotoxicity is further elaborated in Chapter 4.

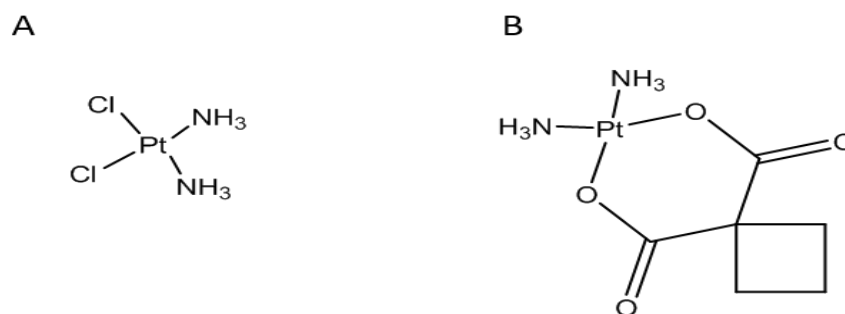


Figure 1.7. Chemical structure of platinum compounds (A) Cisplatin; (B) Carboplatin

Taxane compounds can be a diterpenoid or taxoid. A diterpenoid is produced naturally and has a C-20 carbon skeleton derived biogenetically from geranylgeraniol pyrophosphate. Extracted from the bark of the Pacific yew, Paclitaxel is a well-established natural anti-cancer agent in widespread clinical use (Nguyen, 2008). Its chemical structure, published for the first time in 1971, is shown in Figure 1.8 A (Wani et al., 1971). In 1992, the United States Food and Drug Administration approved taxol for treatment of refractory (platinum-resistant) ovarian cancer (Wall and Wani, 1995). Paclitaxel is one of the most important recently available ovarian cancer drugs. The mechanisms through which paclitaxel and cisplatin act are different. Paclitaxel binds to the cytoskeleton and microtubules, brings stability to the polymeric form, and prevents disassembly of the microtubule. As with analogues of cisplatin, there has been development of a number of taxanes and one of these – docetaxel – has been successful as a substitute for paclitaxel (Figure 1.8 B), from which it has a different toxicity profile (Bookman, 2005). While there is a better than 80% response rate for ovarian cancer cases treated according to the standard regimen, advanced cases show a 70% relapse rate within five years (Markman et al., 2004; Heintz et al., 2006).

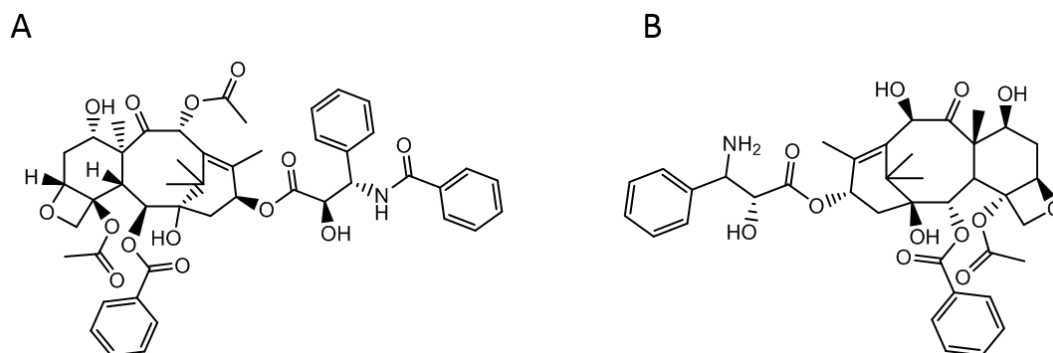


Figure 1.8. Chemical structure of taxane compounds (A) Paclitaxel; (B) Docetaxel

Although platinum and taxane-based chemotherapies are currently the first line treatments for ovarian cancer, relapse occurs in 70% of patients (Poisson et al., 2015). Table 1.3 summarises the ways ovarian cancer resists drugs. Cancer cells may develop more than one drug resistance mechanism (Chan and Fong, 2007). As an example, let us take resistance to paclitaxel. A gradual increase in dosage of the drug is likely to lead to resistance through P-glycoprotein or protein expression, while resistance to single high dose treatments is likely to be β -tubulin mutation (Agarwal and Kaye, 2003; Chan and Fong, 2007). Patients resistant to both platinum and taxane are likely to receive other agents such as gemcitabine, liposomal doxorubicin, ectoposide or topotecan as treatment. Response rates to those drugs are 10-25% overall (Agarwal and Kaye, 2003).

Table 1.4. Mechanisms of Ovarian Cancer Drug Resistance.

Drug Resistance	Molecular Mechanism
<i>Cisplatin and other platinum compounds</i>	
• Increased drug efflux	Activation of transporters MRPs and MVP/LRP
• Activation of detoxification system	Drug inactivation by thiols glutathione and metallothioneins
• Increased repair of DNA damage	Activation of NER (nucleotide excision repair)
• Increased tolerance of DNA damage	Defect in MMR (mismatch repair) by silencing of Hmlh1
• Evasion of apoptosis	Activation of anti-apoptotic pathways (BCL-2)
• Loss of tumour suppressor function	Mutations in p53
• Altered gene expression	Activation of HER-2/NEU, NFkB, PI3K/Akt and Ras/MARK signalling pathways
<i>Paclitaxel and other taxanes</i>	
• Increased drug efflux	Activation of transporters P-glycoprotein (MDR1)
• Alteration of drug targets	Mutation in β -tubulin
• Evasion of apoptosis	Activation of anti-apoptotic pathways (BCL-2)
• Altered gene expression	Activation of HER-2/NEU and NFkB signalling pathways

This table is taken from (Chan and Fong, 2007)

1.7.2 Need for novel alternative cytotoxic agents

Platinum and taxane agents are effective and well tolerated in treating newly-diagnosed cases of ovarian cancer, but the search continues both for new targets and for innovative ways of treating old targets. Drug development is particularly targeted on DNA damage, repair and replication. Trabectedin is an antineoplastic agent that was first isolated from the tunicate *Ecteinascidia turbinata* and is now being

synthetically manufactured. It has demonstrated clinical benefit in recurrent ovarian cancer patients, binding covalently to DNA (minor groove) and bending it towards the major groove as well as disrupting transcription and causing G2-M apoptosis and cell cycle arrest. It was approved in 2009 for use with pegylated liposomal doxorubicin to treat relapsed, platinum-sensitive ovarian cancer and is very active in recurrent platinum-sensitive ovarian cancer (Monk et al., 2010; Colombo, 2014).

Another agent examined in Phase III studies is pemetrexed, which blocks purine and pyrimidine nucleotide formation, so inhibiting DNA formation and interrupting the replication of malignant cells (Chen et al., 1999). Combined with cisplatin, it is used to treat mesothelioma; on its own, it is active in recurring platinum-resistant ovarian cancer, dose selection and use of vitamin supplements to manage haematologic toxicity (Vogelzang et al., 2003).

While molecular-targeted biology is the subject of strong interest, cytotoxic chemotherapy continues to be central to advanced-stage cancer treatment, making necessary better targeting with better and more specific drug delivery.

1.8 Melittin: A potential anticancer therapy

1.8.1 Chemistry of melittin

Melittin (Figure 1.9) is an amphipathic peptide that contains 26 amino acid residues and is the principal component of crude bee venom. The linear amino acid sequence of Gly-Ile-Gly-Ala-Val-Leu-Lys-Val-Leu-Thr-Thr-Gly-Leu-Pro-Ala-Leu-Ile-Ser-Trp-Ile-Lys-Arg-Lys-Arg-Gln-GlnNH₂ gives the peptide a chemical formula of

$C_{131}H_{229}N_{39}O_{31}$ (Terwilliger and Eisenberg, 1982). The particular arrangement of the amino acids in melittin causes the peptide to exhibit amphipathic properties. The mostly hydrophobic, nonpolar and neutral amino acids are positioned near the N-terminus, forming the first 20 amino acid residues, while the basic and hydrophilic residues (lysine, arginine and glutamine) are located near the C-terminus (last 6 amino acids). The proportion of melittin in crude bee venom samples varies between about 40 to 60% by dry weight (Chen and Lariviere, 2010; Terwilliger and Eisenberg, 1982).

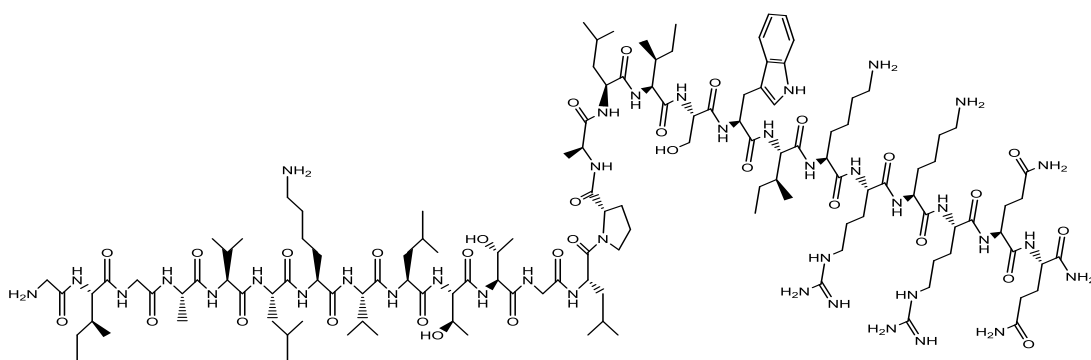


Figure 1.9. Structure of melittin, the main component in bee venom

1.8.2 Anticancer properties of melittin

The search continues for new anti-cancer therapy to combat the raised incidence of morbidity and mortality due to drug resistance, and particularly in the treatment of ovarian cancer where treatment effectiveness is low in comparison with colorectal and breast cancer. Resistance to taxanes and platinum compounds needs to be overcome (Chan and Fong, 2007), and melittin has been identified as a potentially powerful drug, having demonstrated a number of anticancer results in cell lines including gastric (Mahmoodzadeh et al., 2013; Mahmoodzadeh et al., 2015), breast (Jo et al., 2012;

Jeong et al., 2014), ovarian (Jo et al., 2012; Liu et al., 2013), liver (Qian et al., 2015; Wu et al., 2015), prostate (Jo et al., 2012), cervical (Jo et al., 2012), and lung (Oh et al., 2014) cancers.

Melittin's pore-forming activity may be connected to its effectiveness as an anti-cancer agent. The ability of cancer cells to develop drug resistance is thought to be greatly reduced when the drug is one that perforates the cell's membranes (Gajski and Garaj-Vrhovac, 2013). It is also likely, thanks to a mechanism of action completely unlike that of conventional anti-cancer agents, that combining melittin with cisplatin or some other standard chemotherapy agent could boost its effectiveness through a synergistic effect on cancer cells. An effect of this sort would allow the reduction of the amount of one or other agent while maintaining a sufficient level of efficacy, and this would reduce the likelihood of either drug's toxicity (Hui et al., 2001).

Observations so far indicate that the way melittin acts on cancer cells is different from the activity of agents based on platinum. If the difference in molecular action is reflected at cellular level and can be seen in differences in metabolite profiles, synergy between the agents should be possible, perhaps with no cross-resistance. Identifying metabolite differences between platinum-sensitive and resistant cancer cells after they have been treated with melittin would make possible an understanding of melittin's metabolic effects on the cells and how it relates to the cells' chemosensitivity to platinum. The mechanism of melittin cytotoxicity is further elaborated in Chapter 3.

1.9 Research objectives

The overall aim of this study was to investigate the metabolic profiles of two human ovarian cancer cell lines A2780 (cisplatin-sensitive) and A2780CR (cisplatin-resistant) in response to their exposure to melittin or cisplatin or combination melittin/cisplatin by using LC/MS. Changes identified in the metabolome can generate hypotheses and hence enhance biochemical knowledge which might be exploited in treatment. Observed changes in metabolites can potentially indicate novel adaptation mechanisms or could support postulated adaptation mechanisms, for which there is little evidence at time of writing. The following objectives were used to achieve the main aims of the study:

- I. To identify metabolite variations that differentiate between A2780 and A2780CR cancer cell lines.
- II. To characterise the metabolomic effects induced by melittin in A2780 and A2780CR ovarian cancer cells.
- III. To study the metabolomic effects of cisplatin on A2780 and A2780CR ovarian cancer cells.
- IV. To investigate the combination effects between melittin and cisplatin on the metabolome of A2780 and A2780CR ovarian cancer cells.
- V. Carry out lipidomic analysis of the effects of melittin treatment on A2780 and A2780CR ovarian cancer cells by using LC/MS and LC/MS/MS.
- VI. To assess the utility of the biolog phenotype microarray technology in examining the utilisation of carbon sources by A2780 and A2780CR ovarian cancer cells.

Chapter 2

Materials and Methods

2 Materials and Methods

2.1 Chemicals and solvents

The melittin used in this study was purified from bee venom (supplied by Beesen Co. Ltd, Dae Jeon, Korea) by reversed phase liquid chromatography (Tusiimire et al., 2015) and reconstituted in sterile water to form a stock solution of 1 mg/mL. A stock solution of melittin in water was prepared and used fresh. Cisplatin was purchased from Tocris Bioscience (Bristol, UK) and was dissolved in sterile water with gentle warming according to manufacturer's instructions.

HPLC grade acetonitrile, methanol, and isopropanol were purchased from Sigma-Aldrich (Poole, UK). AnalaR grade formic acid (98%) was obtained from Fisher Scientific, UK. A Direct Q-3 water purification system (Millipore, Walford, UK) was used to produce the HPLC water that was in all of the analyses. Ammonium carbonate, ammonium formate, ammonium hydroxide solution (30-33%) and all the analytical standards used to evaluate the column or develop the methods were purchased from Sigma-Aldrich, UK.

2.2 Cell culture methods

2.2.1 Cell lines and cultures

The cisplatin-sensitive (A2780) and resistant (A2780CR) human ovarian carcinoma cells were obtained from ECACC (Porton Down, Salisbury, UK) and maintained at 75×10^4 cells/mL in RPMI 1640 medium (Lonza, Verviers, Belgium) supplemented with 1% (v/v) L-glutamine (Invitrogen, Paisley, UK), 100 IU/mL/100 μ g/mL

penicillin/streptomycin (Invitrogen, Paisley, UK), and 10% (v/v) foetal bovine serum (FBS) (Life Technologies, Carlsbad, CA). In addition, the cultures for the A2780CR cells contained 1µm cisplatin in the first three passages. Sub-confluent cultures were split by trypsinisation every 4-5 days and maintained at 37°C in a humidified atmosphere saturated with 5% CO₂. The cell morphology of A2780 and A2780CR cell lines were observed using phase-contrast microscopy (Figure S2.1, appendix).

2.2.2 Determination of IC₅₀ values for melittin and cisplatin

GraphPad Prism for Windows (version 5.00, GraphPad Software, San Diego, California, USA) was employed to produce dose-response curves by performing nonlinear regression analysis of the cell viability data. The mean inhibitory concentration (IC₅₀) values were calculated from at least three measurements of independent experiments (n=3).

2.2.3 Calculation of Combination Index (CI) for melittin-cisplatin

The specific interaction between melittin and cisplatin on A2780 and A2780CR cancer cell lines was evaluated by the combination index (CI) analysis. Drug combination synergy was performed using CompuSyn software (Chou and Martin, 2005). *CI* values, *Fa-CI* plot (plot representing *CI* versus *Fa*, the fraction affected by a particular dose) were calculated by CompuSyn program (Compusyn Inc, Paramus, NJ, USA). All experiments were repeated at least three times.

2.3 Chromatographic conditions for columns

2.3.1 Chromatographic conditions for ZIC-pHILIC column

A ZIC-pHILIC column (150 x 4.6 mm, 5 µm particle size, HiChrom, Reading U.K.) was used to study the effects of melittin, cisplatin and melittin-cisplatin combination on cisplatin resistant and cisplatin sensitive ovarian cancer cell metabolomes. The mobile phase for ZIC-pHILIC consisted of 20 mM ammonium carbonate in water purified by Direct-Q 3 Ultrapure water purification system at pH 9.2 (solvent A) and acetonitrile (solvent B) at a flow rate of 300 µL/min . The elution gradient was an A:B ratio of 20:80 at 0 min, 80:20 at 30 min, 92:8 at 35 min and finally 20:80 at 45 min as described previously (Watson et al., 2013). Samples were kept in a vial tray which was set at constant temperature of 4°C to avoid any possible degradation of samples. All mobile phase solutions were freshly prepared and were stored at room temperature for up to 48 hours.

2.3.2 Chromatographic conditions for ZIC-HILIC column

A ZIC-HILIC column (150 x 4.6 mm, 5 µm particle size), supplied by Hichrom Ltd (Reading, UK) was used to study the effects of melittin on cisplatin resistant and cisplatin sensitive ovarian cancer cell metabolomes. Since chromatographic separation of polyamines is poor on a ZIC-pHILIC column (Zhang et al., 2014), the ZIC-HILIC column was employed for the determination of putrescine and spermidine in the samples. The mobile phase was 0.1% (v/v) formic acid in water (A) and 0.1% (v/v) formic acid in acetonitrile (B) with a gradient of A:B 50:50 at 0 min, 95:5 from 20-30 min, and 50:50 from 31-36 min. The flow rate and the injection volume were 300 µL/min and 10 µL, respectively.

2.3.3 Chromatographic conditions for Silica gel column

An ACE silica gel column (150 x 4.6 mm, 3 μ m, Hichrom Reading UK) was used to study the effects of melittin on cisplatin resistant and cisplatin sensitive ovarian cancer cell lipid metabolism. The mobile phase for ACE silica gel column consisted of (A) 20% isopropyl alcohol (IPA) in acetonitrile (ACN) (v/v) and (B) 20% IPA in 0.02M ammonium formate (v/v). The flow rate was 300 μ L/min and gradient was as follows: 0–1 min 8% B, 5 min 9% B, 10 min 20% B, 16 min 25% B, 23 min 35% B, 26–40 min 8% B as described previously (Zheng et al., 2010).

2.4 Liquid chromatography–mass spectrometry (LC-MS) conditions

2.4.1 Accela HPLC-ESI-Exactive Orbitrap

Liquid chromatographic separation was carried out on an Accela HPLC system interfaced to an Exactive Orbitrap mass spectrometer (Thermo Fisher Scientific, Bremen, Germany). The nitrogen sheath and auxiliary gas flow rates were maintained at 50 and 17 mL/min. The electrospray ionisation (ESI) interface was operated in a positive/negative dual polarity mode. The spray voltage was 4.5 kV for positive mode and 4.0 kV for negative mode, while the ion transfer capillary temperature was 275°C. Full scan data was obtained in the mass-to-charge ratio (m/z) range of 75 to 1200 for both ionisation modes with settings of AGC target and resolution as Balanced (1E6) and High (50,000) respectively. Mass calibration was performed for both positive and negative ESI polarities before the analysis using the standard Thermo Calmix solution (Thermo Fisher Scientific, Bremen, Germany) with additional coverage of the lower mass range with signals at m/z 83.0604 ($2\times\text{ACN}+\text{H}$) for the positive and m/z 91.0037 ($2\times\text{HCOO}^-$) for the negative modes respectively. The resulting data were recorded

using the XCalibur 2.1.0 software package (Thermo Fisher Scientific, Bremen, Germany).

2.4.2 Finnigan HPLC-ESI-Exactive Orbitrap

MS² analysis of lipids was carried out on an LTQ Orbitrap using the ACE silica gel column. Instrument settings were as for the Exactive instrument except that the instrument was operated in negative ion mode alone. The PC lipids of interest were analysed in negative ion mode by setting the source collision energy to 35V to remove formic acid and methyl from the formic acid adducts of the molecular ions (Zheng et al., 2010) and then carrying of MS² with a collision energy of 35V using the LTQ ion trap as the detector.

2.5 Data extraction and analysis

2.5.1 LC-MS data processing by MZmine software

Data extraction for each of the samples was carried out by MZmine-2.10 software (Pluskal et al., 2010) (mzmine.github.io/) using identical parameters for peak detection, deconvolution, deisotoping, alignment, filtering, gap filling and identification in order to make multiple data files comparable (Zhang et al., 2013). The raw data files (Thermo-Xcalibur format) were initially split into a single ESI positive and negative data set, and also converted into mzML format by using ProteoWizard. The procedure and the settings of each step used in MZmine-2.10 are described in the Table 2.1.

Table 2.1. MZMine 2.10 procedure and settings

Methods	Setting 1	Setting 2
Peak detection	Mass detection	Mass detector: Centroid
		Noise level: 1000
		MS level: 1
	Chromatogram builder	Minimum time span (min): 0.2
		Minimum height: 3000
		m/z tolerance: 0.001
	Chromatogram Deconvolution	Algorithm: Local minimum search
		Chromatographic threshold: 1%
		Search minimum in RT range (min): 0.4
		Minimum relative height: 5%
Minimum absolute height: 30000		
Min ratio of peak top/edge: 5		
Peak duration range (min): 0.3-5		
Deisotope	m/z tolerance: 0.001	
	Retention time tolerance: 0.1 absolute (min)	
	Maximum charge: 2	
Alignment	Join aligner	Representative isotope: Most intense
		m/z tolerance: 0.001
		Weight for m/z: 20
		Retention time tolerance: 5 relative%
Filtering	Peak list rows filter	Weight for RT: 10
		Minimum peaks in a row: 45
		Minimum peaks in an isotope pattern: 1
		Retention time: 3-35
Gap filling	Same Rt and m/z range gap filler	Peak duration range: 0.2-5
		m/z tolerance: 0.001

Table 2.1. (Contd.)

Methods	Setting 1	Setting 2
Identification	Adduct search	RT tolerance: 0.2 absolute (min)
		Adducts: Na, K, NH ₄ for ESI positive mode and formate for ESI negative mode and ACN+H for both modes
		m/z tolerance: 0.001
	Complex search	Max relative adduct peak height: 30%
		Ionization method: M+H for ESI positive mode and M-H for negative mode
		Retention time tolerance: 0.2 absolute (min)
		m/z tolerance: 0.001
		Max complex peak height: 50%

2.5.2 Data bases used for identification of metabolites

The extracted ions, with their corresponding m/z values and retention times, were pasted into an Excel macro of the most common metabolites prepared in-house to facilitate identification, and a library search was also carried out against accurate mass data of the metabolites in the Human Metabolome, KEGG, Lipid Maps and Metlin databases.

The databases used for identification of metabolites:

- KEGG Kyoto Encyclopedia of Genes and Genomes
(<http://www.genome.jp/kegg/>)
- HMDB Human Metabolome Data Base (<http://www.hmdb.ca/>)
- METLIN Metabolomics Database (<https://metlin.scripps.edu/>)
- LIPID MAPS (<http://www.lipidmaps.org/>)

The lists of the metabolites obtained from these searches were then carefully evaluated manually by considering the quality of their peaks and their retention time match with to the standard metabolite mixtures run in the same sequence.

2.5.3 Statistical software's used for identification of metabolites

Statistical analyses were performed using both univariate and multivariate approaches. The *p*-values from univariate analysis were adjusted using the FDR control and differences in the levels (or peak areas) of the metabolites between treated and control cells were considered significant at $p < 0.05$. MetaboAnalyst's (www.metaboanalyst.ca), a web-based metabolomic data processing tool, was used for supports fold-change analysis, and t-tests (Xia et al., 2015).

SIMCA-P software version 14.0 (Umetrics, Crewe, UK) was used for multivariate analysis of the metabolite data. Prior to multivariate analysis, data were \log_2 -transformed and then Pareto scaled where the responses for each variable were centred by subtracting its mean value and then dividing by the square root of its standard deviation (van den Berg et al., 2006; Yang et al., 2015b; Lau et al., 2015). PCA was initially used for data visualization and to explore how variables clustered based on their metabolic composition regardless of their grouping (Kirwan et al., 2012; Ivosev et al., 2008). Then, OPLS-DA was applied to discrimination between groups while neglecting the systemic variation (Kirwan et al., 2012). OPLS-DA models were validated based on multiple correlation coefficient (R^2) and cross-validated R^2 (Q^2) in cross-validation and permutation test. The R^2 represents the percentage of variation explained by the model while Q^2 indicates the percentage of variation in response to

cross validation (Kirwan et al., 2012). Model validity was also assessed using cross validated ANOVA (CV-ANOVA) which corresponds to H_0 hypothesis of equal cross validated predictive residual of the supervised model in comparison with the variation around the mean (Eriksson et al., 2008). The significance of the biomarkers was ranked using the variable importance in projection (VIP) score (VIP predictive >1 , VIP orthogonal <1) from the OPLS-DA model. VIP was employed to assess the contribution of each variable in the observed metabolomics change to a given model compared to the rest of variables (Eriksson et al., 2013; Chong and Jun, 2005). A permutations test was also applied to supervised models to evaluate whether the specific grouping of the observations in the two designated classes is significantly better than any other random grouping in two arbitrary classes (Triba et al., 2015; Zhang et al., 2016b), and in Simca P, this is carried out by repeatedly leaving out 1/7th of the data and refitting the model, all the Q^2 values for the refitted models should be lower than the original Q^2 value. The criteria for validity for OPLS-DA models tested via cross-validation are that all blue Q^2 -values to the left are lower than the original points to the right or the blue regression line of the Q^2 -points intersects the vertical axis (on the left) at, or below zero. When all green R^2 -values to the left are lower than the original point to the right, this is also an indication for the validity of the original model although this is not essential for the model to be valid. The AUCROC was used to indicate the accuracy of a test for correctly identifying a disorder, that is, treated samples from controls, with an AUC = 1 indicating a perfect test (Xia et al., 2013). The p-values of the biomarkers were evaluated for their significance applying the false discovery rate statistic (FDR).

2.6 Optimisation of Phenotype Microarray experiment parameters

The cells were tested by using the standard protocol for metabolic phenotype microarray (PM) assays as recommended by the manufacturer. In order to select the proper dye mix, an optimization experiment was performed to determine which of the two dyes (MA or MB) available for phenotype microarrays was more appropriate for A2780 and A2780CR ovarian cancer cells. Specifically, the procedure used was as follows:

- i. A2780 and A2780CR cells were cultured in a 75 cm² culture flask containing 10 mL RPMI-1640 medium lacking phenol red but containing 5% FBS, L-glutamine and Pen/Strep.
- ii. The medium was removed from the culture flask and saved it in a 15 mL sterile conical tube. The remaining medium was aspirated and discarded from the culture flask. The adherent cells washed twice with 10 mL of Dulbecco's Phosphate-Buffered Saline (D-PBS) (Gibco) and any remaining D-PBS was aspirated and discarded.
- iii. The cells are detached by adding 2 mL of a 0.25 % Trypsin-EDTA (Gibco) and incubated at 37° C for 3 minutes.
- iv. Then, 3 mL of culture medium taken from the 15 mL conical tube was added to quench the detachment reaction and the cell suspension mixed by gently pipetting up and down several times to disperse the cells.
- v. The cells harvested by transferring the cell suspension to the 15 mL conical tube containing the culture medium and centrifuged at 350 x g for 5 minutes. After centrifugation, the medium aspirated and 10 ml of D-PBS was added.

After that, the cell pellet suspended in the D-PBS by pipetting up and down several times, then centrifuged again at 350 x g for 5 minutes.

- vi. After the second centrifugation, the medium aspirated and 10 mL of pre-warmed MC-0 was added. The cell pellet in the MC-0 Assay Medium was suspended by pipetting up and down several times. The MC-0 medium was composed of IF-M1 (Biolog, USA) medium supplemented with 5.3% dialyzed fetal bovine serum (dFBS) (Gibco), 1.1% of 100x Pen/Strep solution (Gibco), and 0.16% of 200 mM glutamine (final concentration 0.3 mM).
- vii. The cell number was determined and cell viability was assessed by trypan blue staining (Sigma-Aldrich, Germany).
- viii. The cells suspended in enough MC-0 Assay Medium to fill the selected number of PM panels and to achieve a density of 4×10^5 cells/mL.
- ix. After that, 50 μ L/well of the cell suspension was added to the PM-M1 plates (Biolog, USA) so that each well has 20,000 cells.
- x. Then, the PM plates incubated at 37° C in a humidified atmosphere with 95% Air-5% CO₂ for 42 hours, after which the Biolog Redox Dye Mix was added to all wells (10 μ L/well to the plate). The plate was sealed with tape to prevent off-gassing of CO₂.
- xi. The plates were incubated for additional 6 h with Biolog Redox Dye Mix MA and 6 hr with Biolog Redox Dye Mix MB (Biolog, USA).
- xii. Tetrazolium reduction was determined with a Microplate Reader (SpectraMax M3, Molecular Devices, Sunnyvale, CA). The endpoint read was performed at 590 nm with subtraction of a 750 nm reference reading (A₅₉₀₋₇₅₀) which corrects for any background light scattering.

The results confirmed that MA dye was metabolised more rapidly and generated a higher absorbance compared to MB dye in a given time period. Therefore, MA dye was used in subsequent experiments.

2.6.1 Phenotype MicroArrays Experiment Design

PM plates used in this study were PM-M1 (precoated with carbon sources). Figure 2.1. shows the layout of the carbon sources in the PM-M1 microplate. Complete medium MC-0 was used for both A2780 and A2780CR cells inoculated into PM-M1. A2780 and A2780CR cells at a concentration of 2×10^4 cells/well ($50 \mu\text{L}$ /well) were seeded on two sets of microplates. The first one was used as the control set, where non-treated A2780 and A2780CR were cultured. A2780 and A2780CR seeded in the second set of plates were exposed to melittin or cisplatin. Both sets of PMs containing A2780 and A2780CR were first incubated for 24 h to allow cells to catabolise all nutrients in medium MC-0. The treated cells set was subsequently inoculated with $25 \mu\text{L}$ of melittin or cisplatin/well of three PM-M1 plates at IC_{50} concentration, while $25 \mu\text{L}$ of MC-0 medium was added to each well in the control set of three PM-M1 plates. After additional 18 h of incubation, $15 \mu\text{L}$ of MA dye was added to each well and the plates were incubated for additional 6 h and the absorbance was measured as before.

PM-M1 MicroPlate™ - Carbon and Energy Sources

A1 Negative Control	A2 Negative Control	A3 Negative Control	A4 α -Cyclodextrin	A5 Dextrin	A6 Glycogen	A7 Maltitol	A8 Maltotriose	A9 D-Maltose	A10 D-Trehalose	A11 D-Cellobiose	A12 β -Gentiobiose
B1 D-Glucose-6-Phosphate	B2 α -D-Glucose-1-Phosphate	B3 L-Glucose	B4 α -D-Glucose	B5 α -D-Glucose	B6 α -D-Glucose	B7 3-O-Methyl-D-Glucose	B8 α -Methyl-D-Glucoside	B9 β -Methyl-D-Glucoside	B10 D-Salicin	B11 D-Sorbitol	B12 N-Acetyl-D-Glucosamine
C1 D-Glucosaminic Acid	C2 D-Glucuronic Acid	C3 Chondroitin-6-Sulfate	C4 Mannan	C5 D-Mannose	C6 α -Methyl-D-Mannoside	C7 D-Mannitol	C8 N-Acetyl- β -D-Mannosamine	C9 D-Melezitose	C10 Sucrose	C11 Palatinose	C12 D-Turanose
D1 D-Tagatose	D2 L-Sorbose	D3 L-Rhamnose	D4 L-Fucose	D5 D-Fucose	D6 D-Fructose-6-Phosphate	D7 D-Fructose	D8 Stachyose	D9 D-Raffinose	D10 D-Lactitol	D11 Lactulose	D12 α -D-Lactose
E1 Melibionic Acid	E2 D-Melibiose	E3 D-Galactose	E4 α -Methyl-D-Galactoside	E5 β -Methyl-D-Galactoside	E6 N-Acetyl-Neuraminic Acid	E7 Pectin	E8 Sedoheptulosan	E9 Thymidine	E10 Uridine	E11 Adenosine	E12 Inosine
F1 Adonitol	F2 L-Arabinose	F3 D-Arabinose	F4 β -Methyl-D-Xylopyranoside	F5 Xylitol	F6 Myo-Inositol	F7 Meso-Erythritol	F8 Propylene glycol	F9 Ethanolamine	F10 D,L- α -Glycerol-Phosphate	F11 Glycerol	F12 Citric Acid
G1 Tricarballic Acid	G2 D,L-Lactic Acid	G3 Methyl D-lactate	G4 Methyl pyruvate	G5 Pyruvic Acid	G6 α -Keto-Glutaric Acid	G7 Succinamic Acid	G8 Succinic Acid	G9 Mono-Methyl Succinate	G10 L-Malic Acid	G11 D-Malic Acid	G12 Meso-Tartaric Acid
H1 Acetoacetic Acid (a)	H2 γ -Amino-N-Butyric Acid	H3 α -Keto-Butyric Acid	H4 α -Hydroxy-Butyric Acid	H5 D,L- β -Hydroxy-Butyric Acid	H6 γ -Hydroxy-Butyric Acid	H7 Butyric Acid	H8 2,3-Butanediol	H9 3-Hydroxy-2-Butanone	H10 Propionic Acid	H11 Acetic Acid	H12 Hexanoic Acid

Figure 2.1. Layout of chemicals in the wells on the PM-M1 microplate.

2.6.2 Calculation of Redox Dye Reduction

Dye reduction was calculated from A590-A750 values measured from microplate wells after 6 h from addition of MA dye. Plots of A590-A750 values versus metabolic substrates were used. Paired t tests from univariate analysis were adjusted using the Bonferroni correction and differences in the levels (absorbance) of the metabolic substrates between treated and control cells were considered significant at $p < 0.05$.

2.7 Caspase activity Assay

Fluorometric assays of caspase activity were carried out by using the substrate Ac-DEVD-AMC (BD Pharmingen, San Diego, CA, USA) for caspase-3. Both A2780 and A2780CR cells were seeded at 1×10^4 cells/well in Costar 96-well black plates and incubated at 37°C and 5% CO_2 in a humidified atmosphere for 24 h. Then, the cells were treated for 6 and 24 h with different concentrations of Melittin or Cisplatin to measure caspase-3 activity. Staurosporine (Sigma-Aldrich, Dorset, UK) was used to induce apoptosis at concentration $10 \mu\text{M}$. The control cells were treated with media alone. The caspase-3 assay buffer was prepared as described previously (Carrasco et al., 2003). The caspase-3 assay buffer ($3\times$) was added to each well and incubated at 37°C in 5% CO_2 for 1 h. Fluorescence was measured at 360 nm (excitation) and at 460 nm (emission) by using Spectramax M3 microplate reader. The average fluorescence values of the background were subtracted from the fluorescence values of experimental wells. Statistical analysis was done by using one-way ANOVA followed by Bonferroni's Multiple Comparison test.

Chapter 3

Metabolomic Profiling of the Effects of Melittin on Cisplatin Resistant and Cisplatin Sensitive Ovarian Cancer Cells Using Mass Spectrometry and Biolog Microarray Technology

3 Metabolomic Profiling of the Effects of Melittin on Cisplatin Resistant and Cisplatin Sensitive Ovarian Cancer Cells Using Mass Spectrometry and Biolog Microarray Technology

3.1 Abstract

In the present study, LC-MS was employed to characterise the metabolic profiles of two human ovarian cancer cell lines A2780 (cisplatin-sensitive) and A2780CR (cisplatin-resistant) in response to their exposure to melittin, a cytotoxic peptide from bee venom. In addition, the metabolomics data were supported by application of Biolog microarray technology to examine the utilisation of carbon sources by the two cell lines. Data extraction with MZmine 2.10 and database searching were applied to provide metabolite lists. PCA and OPLS-DA gave clear separation between the cisplatin-sensitive and resistant strains and their respective controls. The cisplatin-resistant cells were slightly more sensitive to melittin than the sensitive cells with IC_{50} values of 4.5 ± 0.4 and 6.8 ± 0.4 $\mu\text{g/mL}$ respectively, although the latter cell line exhibited the greatest metabolic perturbation upon treatment. The changes induced by melittin in the cisplatin-sensitive cells led mostly to reduced levels of amino acids in the proline/glutamine/arginine pathway, as well as to decreased levels of carnitines, polyamines, adenosine triphosphate (ATP) and nicotinamide adenine dinucleotide (NAD^+). The effects on energy metabolism were supported by the data from the Biolog assays. Overall, this study suggests that melittin might have some potential as an adjuvant therapy in cancer treatment.

3.2 Introduction

Various metabolic changes at the cellular level are associated with the growth of cancers. These changes can be used as biomarkers for diagnosis, prognosis and evaluation of anticancer therapies (Vermeersch and Styczynski, 2013). For example, in contrast to normal cells, for proliferation, cancer cells have greater dependence on aerobic glycolysis, fatty acid synthesis, and glutaminolysis (Vander Heiden et al., 2009). Hence, evaluation of the concentrations of particular metabolites in a cell can offer insights into its metabolic state in comparison to the physiological norm. The metabolic profile of cancer cells can also enhance the understanding of the process of carcinogenesis and the mechanism of chemoresistance, thus contributing to the development of better diagnostic and therapeutic tools (Poisson et al., 2015).

Although most ovarian cancers remain sensitive to chemotherapies such as platinum and taxane groups, there is growing resistance against them which reduces the time to disease progression following the initial treatment, and minimises their efficacy upon further treatment during relapse (Matsuo et al., 2010). The anticancer activity of platinum arises from its ability to form irreparable intra-strand DNA crosslinks/adducts which lead to cell apoptosis (Zwelling and Kohn, 1978), as well as induction of oxidative and endoplasmic reticulum stress (Siddik, 2003; Galluzzi et al., 2012; Mandic et al., 2003). On the other hand, platinum resistance in cancer results from various adaptive mechanisms including reduced cellular uptake, increased DNA repair and tolerance (Rabik and Dolan, 2007), and inactivation by glutathione (Byun et al., 2005; Rabik and Dolan, 2007). It has been previously reported that platinum-sensitive (A2780) and resistant (C200) ovarian cancer cell lines have distinct

metabolic profiles in various interdependent pathways (Poisson et al., 2015).

Melittin, is the main component of honey bee venom and has demonstrated a variety of biological and pharmacological applications (Jeong et al., 2014; Kohno et al., 2014). It has natural anti-bacterial, anti-viral, and anti-inflammatory properties (Jeong et al., 2014; Kohno et al., 2014). Melittin has also been shown to have diverse anticancer effects in several different cancer cell lines, including ovarian cancer (Jo et al., 2012; Liu et al., 2013). The mechanisms by which melittin, an amphipathic haemolytic peptide, exerts its potential anticancer effects include inhibition of cell proliferation (Jeong et al., 2014; Liu et al., 2013), induction of apoptosis (Mahmoodzadeh et al., 2013; Mahmoodzadeh et al., 2015; Jeong et al., 2014; Gajski and Garaj-Vrhovac, 2013), and direct necrosis (Mahmoodzadeh et al., 2013; Mahmoodzadeh et al., 2015). The mechanism of apoptosis appears to be related to the activation of the caspase-dependent pathway (Mahmoodzadeh et al., 2015; Jo et al., 2012; Gajski and Garaj-Vrhovac, 2013). On the other hand, necrosis arises from damage to the cell membranes through necrotic cytotoxicity, as has been observed in rat thymocytes, murine skeletal muscle cells, gastrointestinal (GI) tumour cells, erythrocytes, lymphocytes, lymphoblastoid cells, rat primary alveolar cells, and intestinal Caco-2 cells (Mahmoodzadeh et al., 2015; Gajski and Garaj-Vrhovac, 2013). Melittin can also cause cell cycle arrest leading to inhibition of cell proliferation and growth. It can contribute to inhibition of angiogenesis through its ability to suppress epidermal growth factor (EGF)-induced vascular endothelial growth factor (VEGF) secretion and inhibit the creation of new blood vessels by influencing hypoxia-inducible factor (HIF)-1 α (Tang et al., 2014). Previous studies on ovarian cancer cells have shown that

melittin inhibits their growth through induction of apoptosis mediated via inhibition of signal transducer and activator of transcription 3 (STAT3) and activation of Janus kinase 2 (JAK2), both of which are critical during angiogenesis (Jo et al., 2012). Melittin can also prevent EGF-induced cell invasion through its inhibition of the PI3K/Akt/mTOR signaling pathway, but this is primarily related to breast cancer cells (Jeong et al., 2014). In hepatocellular carcinoma, melittin appears to inhibit cell proliferation through its influence on methyl-CpG binding protein 2 (MeCP2), which is a critical element in tumour growth and development (Wu et al., 2015). As a consequence, melittin induces a delay in G0/G1 cell cycle progression, which it is able to accomplish without causing apoptosis (Wu et al., 2015). Based on these observations, it is apparent that melittin affects cancer cells in a variety of ways that are different from those induced by platinum-based agents. This difference in molecular action could be reflected at cellular level in terms of differences in the metabolite profiles, and would suggest an opportunity for synergy between the two agents and a possible lack of cross-resistance. By determining the metabolite differences between platinum-sensitive and resistant cancer cells after treatment with melittin, it could be possible to understand the latter's metabolic effects on these cells in relation to their platinum chemosensitivity.

Metabolomics is a growing and powerful technology capable of detecting several of metabolites (Zhang et al., 2013; Zhang and Watson, 2015; Zhang et al., 2016b; Frezza et al., 2011). With recent advances in both instrumental and computational metabolomics technologies, it is now possible to gain deeper understanding of the metabolic processes occurring within cancer cells, including how they exploit the

process of glycolysis. Cancer cells are known to rely on higher rates of glycolysis, an observation that is known as the “Warburg effect”. With metabolomic profiling, it is possible to relate the “Warburg effect” to the production of amino acids, nucleotides, and lipids necessary for tumour proliferation and vascularisation (Beger, 2013). Some researchers have suggested that metabolic profiling can be an invaluable tool in the evaluation of drug targets and analysis of malignant phenotypes, including the diagnosis of cancer (Griffin and Shockcor, 2004). For instance, by comparing the metabolite profile of cancer cell lines such as ovarian cancer cells pre- and post-treatment, it is possible to identify relevant metabolic changes that relate to specific treatments, which not only helps in determining the efficacy of the treatment, but is also essential in elucidating its pharmacodynamics and identifying the essential biomarkers involved. Thus, metabolomic analysis of lysates from cell cultures has many potential applications and advantages over conventional methods of analytical biochemistry and cell line testing. It is anticipated that as more robust platforms for metabolomics of cell cultures become available, this will facilitate greater understanding of drug actions both *in vitro* and *in vivo*, as well as aiding the rapid incorporation of drug leads into novel therapeutic agents (Čuperlović-Culf et al., 2010).

Phenotype Microarrays (PMs) use a patented redox chemistry, employing cell respiration as a universal reporter. These assays potentially provide a natural fit to support data obtained from metabolomics screens. The redox assay provides for both amplification and precise quantitation of phenotypes. Redox dye mixes contain a water-soluble nontoxic tetrazolium reagent that can be used with virtually any type of

animal cell line or primary cell (Bochner et al., 2011). The dyes used in Biolog™ assays measure output of NADH production from various catabolic pathways present in the cells being tested. If cell growth is supported by the medium in an assay well, the actively metabolizing cells reduce the tetrazolium dye. Reduction of the dye results in colour formation in the well, and the phenotype is considered “positive.” If metabolism is hampered or growth is poor, then the phenotype is “weakly positive” or “negative,” and little or no colour is formed in the well. This colorimetric redox assay allows examination of the effect of treatment on the metabolic rate produced by different substrates and thus is an excellent technique to combine with examination of metabolic output via metabolomics screens.

The current study sought to examine the metabolic effects of melittin on cisplatin-resistant (A2780CR) and cisplatin-sensitive (A2780) human ovarian cancer cell lines via mass spectrometry-based metabolic profiling in combination with Biolog microarray assays. Each of the cell lines was separately treated with sub-lethal doses of melittin for 24 hours before extraction and global metabolite analysis of cell lysates by LC-MS using a high performance liquid chromatography (HPLC) system coupled to an Orbitrap Exactive mass spectrometer using a ZIC-pHILIC column. The resulting data were extracted by MZMine and subsequently analysed by univariate and multivariate approaches with SIMCA-P.

3.3 Materials and Methods

3.3.1 Cell lines and cultures

As detailed in section 2.2.1, Chapter 2.

3.3.2 Cell viability assay against melittin

Cell viability was assessed by an Alamar® Blue (AB) cell viability reagent (Thermo Fisher Scientific, Loughborough, UK). Both A2780 and A2780CR cells were seeded at 1×10^4 cells/well in 96-well plates (Corning®, Sigma-Aldrich) and incubated at 37°C and 5% CO₂ in a humidified atmosphere for 24 h. After 24 hour incubation period, the cells were treated with various concentrations of melittin ranging from 0.5 to 14 µg/mL in 100 µL of medium, and re-incubated at 37°C and 5% CO₂ for a further 24 h. Triton X at 1% (v/v) and cell culture media were used as positive and negative controls, respectively. After this, AB was added at a final concentration of 10% (v/v) and the resultant mixture was incubated for a further 4 h at 37°C and 5% CO₂. Then, the plates were read at an excitation wavelength of 560 nm and the emission at 590 nm was recorded on a SpectraMax M3 microplate reader (Molecular Devices, Sunnyvale, CA). Background-corrected fluorescence readings were converted to cell viability data for each test well by expressing them as percentages relative to the mean negative control value.

3.3.3 Determination of IC₅₀

As detailed in section 2.2.2, Chapter 2.

3.3.4 Determination of effect of melittin on cell metabolomes

The A2780 and A2780CR cell lines were separately treated with melittin at concentrations of 6.8 and 4.5 $\mu\text{g/mL}$ respectively for 24 h (n=5). The cells were seeded at 75×10^4 cells/mL in T-25 cell culture flasks and incubated for 1 doubling time (48 h) before treatment with the melittin and incubation for an additional 24 h. After the treatment, the medium was removed and the cells were washed twice with 3 mL of phosphate-buffered saline (PBS) at 37°C before lysis. Cell lysates were prepared by extraction with ice cold methanol:acetonitrile:water (50:30:20) (1 mL per 2×10^6 cells). The cells were scraped and cell lysates mixed on a Thermo mixer at 1440 rotations per minute (r.p.m.) for 12 min at 4°C, before being centrifuged at 13500 r.p.m. for 15 min at 0°C. The supernatants were collected and transferred into HPLC vials for LC-MS analysis. During the analysis, the temperature of the autosampler was maintained at 4°C. Mixtures of authentic standard metabolites, prepared as previously described (Zhang et al., 2014), and the pooled quality control (QC) sample, were injected in each analysis run in order to facilitate identification and to evaluate the stability and reproducibility of the analytical method, respectively. The pooled QC sample was obtained by taking equal aliquots from all the samples and placing them into the same HPLC vial.

3.3.5 Chromatographic conditions for columns

A ZIC-pHILIC and ZIC-HILIC columns were used to study the effects of melittin on cisplatin resistant and cisplatin sensitive ovarian cancer cell metabolomes. As detailed in sections 2.3.1 and 2.3.2, Chapter 2.

3.3.6 Liquid Chromatography–Mass Spectrometry (LC-MS) conditions

As detailed in section 2.4.1, Chapter 2.

3.3.7 Data extraction and analysis

As detailed in section 2.5, Chapter 2.

3.3.8 Phenotype Microarray experiment

(1) A2780 and A2780CR cells were cultured in a 75 cm² culture flask containing 10 mL RPMI-1640 medium lacking phenol red but containing 5% (v/v) FBS, L-glutamine and Pen/Strep (Gibco™ by Life Technologies, Paisley, UK).

(2) The medium was removed from the culture flask and saved in a 15 mL sterile conical tube. The remaining medium was aspirated and discarded from the culture flask. The adherent cells were washed twice with 10 mL of Dulbecco's Phosphate-Buffered Saline (D-PBS) (Gibco, Paisley, UK) and any remaining D-PBS was aspirated and discarded.

(3) The cells were then detached by adding 2 mL of 0.25 % (v/v) Trypsin-EDTA (Gibco, Paisley, UK) and incubated at 37 °C for 3 min.

(4) Then, 3 mL of culture medium was taken from the 15 mL conical tube was added to quench the detachment reaction and the cell suspension mixed by gently pipetting up and down several times to disperse the cells.

(5) The cells were harvested by transferring the cell suspension to the 15 mL conical tube containing the culture medium and centrifuged at 350× g for 5 min. After centrifugation, the medium was aspirated and 10 mL of D-PBS was added. After that, the cell pellet was suspended in the D-PBS by pipetting up and down several times,

then centrifuged again at $350\times g$ for 5 min.

(6) After the second centrifugation, the medium was aspirated and 10 mL of pre-warmed MC-0 was added. The cell pellet in the MC-0 Assay Medium was suspended by pipetting up and down several times. The MC-0 medium was composed of IF-M1 (Technopath Distribution, Tipperary, Ireland) medium supplemented with 5.3% (v/v) dialysed foetal bovine serum (dFBS) (Gibco™by Life Technologies, Paisley, UK), 1.1% of 100× Pen/Strep solution (Gibco™by Life Technologies, Paisley, UK), and 0.16% (v/v) of 200mM glutamine (final concentration 0.3 mM).

(7) The cell number was determined and cell viability was assessed by trypan blue dye exclusion (Sigma-Aldrich, Dorset, UK).

(8) The cells were suspended in enough MC-0 Assay Medium to fill the selected number of PM panels and to achieve a density of 4×10^5 cells/mL.

(9) After that, 50 μ L/well of the cell suspension was added on two sets of PM-M1 plates (Technopath Distribution, Tipperary, Ireland) so that each well had 20,000 cells. The first one was used as the control set, where untreated A2780 and A2780CR were cultured. A2780 and A2780CR seeded in the second set of plates were exposed to melittin. Both sets of PMs containing A2780 and A2780CR were first incubated for 24 h to allow cells to catabolise all nutrients in medium MC-0. The treated cells set was subsequently inoculated with 25 μ L of Melittin/well of three PM-M1 plates at IC_{50} concentration, while 25 μ L of MC-0 medium was added to each well in the control set of three PM-M1 plates.

(10) Then, the PM plates were incubated at 37 °C in a humidified atmosphere with 95% Air-5% CO₂ for 18 h, after which the Biolog Redox Dye MixMA was added to all wells (15 μ L/well to the plate). The plate was sealed with tape to prevent off-

gassing of CO₂.

(11) The plates were incubated for an additional 6 h with Biolog Redox Dye Mix MA (Technopath Distribution, Tipperary, Ireland).

(12) Tetrazolium reduction was determined with a microplate reader (SpectraMax M3, Molecular Devices, Sunnyvale, CA, USA). The endpoint read was performed at 590 nm with subtraction of a 750 nm reference reading (A590-750) which corrects for any background light scattering.

3.3.1 Calculation of redox dye reduction

As detailed in section 2.6.2, Chapter 2.

3.3.2 LDH assay

The cytotoxicity of the melittin was determined by the lactate dehydrogenase (LDH) release assay on A2780 and A2780CR cells. LDH release in the medium is due to the loss of membrane integrity due to necrosis. Briefly, A2780 and A2780CR cells were seeded at 1×10^4 cells/well in 96-well plates and incubated at 37°C and 5% CO₂ in a humidified atmosphere for 24 h. The cells were treated with different concentrations of the melittin for 24 hours. The cells were lysed with Triton X-100 lysing solution (2% Triton X-100) to induce maximal cell lysis. Then, the supernatant (50 µL) of the treated cells was transferred into 96-well flat-bottom plates, and 50 µL of the LDH reaction mix (Lactate Dehydrogenase Activity Assay Kit, MAK066, Sigma–Aldrich) was added for 30 minutes. Finally, the intensity of orange color in the samples indicating the LDH activity was measured at 490 nm using an LDH cytotoxicity kit. LDH release increased in a dose-dependent manner

in melittin treated A2780 and A2780CR cells compared with untreated cells. Values for treated cells were expressed as the percentage compared with the total quantity of LDH release (Podder et al., 2013; Moghimi et al., 2005). Background LDH release induced by media alone was subtracted from the experimental values. The values are represented as the means \pm SD of three separated experiments.

Percent Cytotoxicity = $100 \times (\text{Experimental} - \text{Culture Medium Background}) / (\text{Maximum LDH Release} - \text{Culture Medium Background})$

*Experimental: The treated or control cells.

*Maximum LDH Release Control: The Lysis Solution-treated cells.

3.3.3 Caspase assay activity

As detailed in section 2.7, Chapter 2.

3.4 Results

3.4.1 Melittin sensitivity of the ovarian cancer cells

Melittin exhibited toxicity against both A2780CR and A2780 cells, with IC₅₀ values of 4.5 and 6.8 $\mu\text{g/mL}$, respectively (Figure 3.1). Thus, the cisplatin-resistant A2780CR cells were more sensitive to melittin than the cisplatin-sensitive A2780 cells and exhibited a response curve suggestive of a dose-response relationship (Figure 3.1).

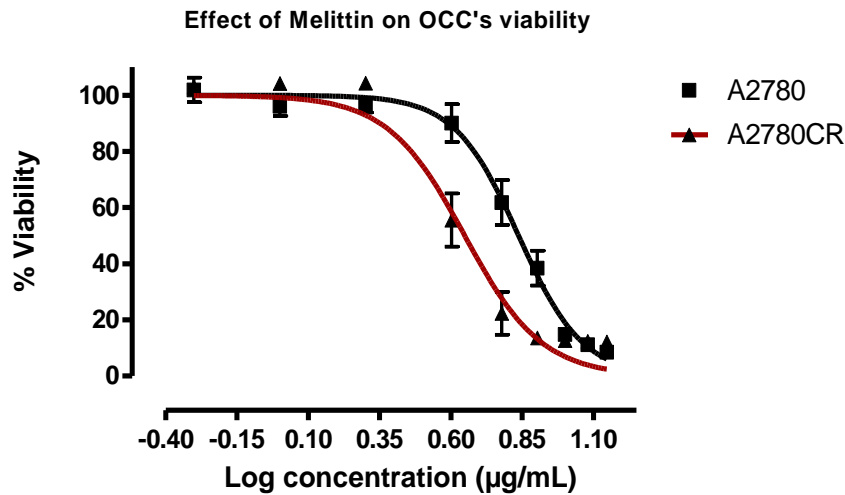


Figure 3.1. Effect of melittin on the viability of the ovarian cancer cells A2780 and A2780CR. Cell viability was determined following treatment with varying doses of melittin for 24 h ($IC_{50} = 6.8 \pm 0.4 \mu\text{g/mL}$ A2780; $IC_{50} = 4.5 \pm 0.4 \mu\text{g/mL}$ A2780CR).

3.4.2 Phenotypic MicroArray (PM) assay of untreated and melittin treated A2780 and A2780CR cells

The cells were tested by using standard protocols for metabolic phenotype microarray-mammalian (PM-M) cell assays (Biolog, Hayward, CA). Figure S3.1 in an appendix chapter shows the colours which developed in the plates after inoculation with A2780 and A2780CR cells in the presence and absence of melittin. Figure 3.2 indicates the extent of utilisation of the different carbon sources by the resistant and sensitive cells. A number of the carbon sources were used by both cell lines. However, many of the substrates in the microarray plate do not appear to be useful as carbon sources. There were clear phenotypic differences although it is not clear which pathways are affected. The A2780CR cells would appear to have a slightly more active glycolytic pathway as judged by the rate of utilisation of glucose and fructose phosphates but on the other hand glucose and pyruvate utilisation were higher in the A2780 cell line. Inosine also

appears to be a very favourable carbon source and is used by the A2780CR cells to a greater extent than by the A2780 cells. Neither Krebs cycle intermediates nor short chain fatty acids appear to be useful as carbon sources underlining the dependence of both cell lines on glycolysis, which is generally the case in cancer cell lines (Vander Heiden et al., 2009).

Treatment of the cells with melittin produced a very different effect on the sensitive cells in comparison with the resistant cells. In the resistant cells carbon metabolism was not that strongly affected and the cells continued to produce NADH, but in the sensitive cells there was a huge reduction in carbon metabolism (Figures 3.3 and 3.4). This suggests that there may be differences in the mechanisms by which the two cell lines respond to melittin, which could lead to different mechanisms of cell death induced by the treatment.

Phenotype MicroArrays PM-M1
Carbon and Energy Substrate Changes in A2780 and A2780CR

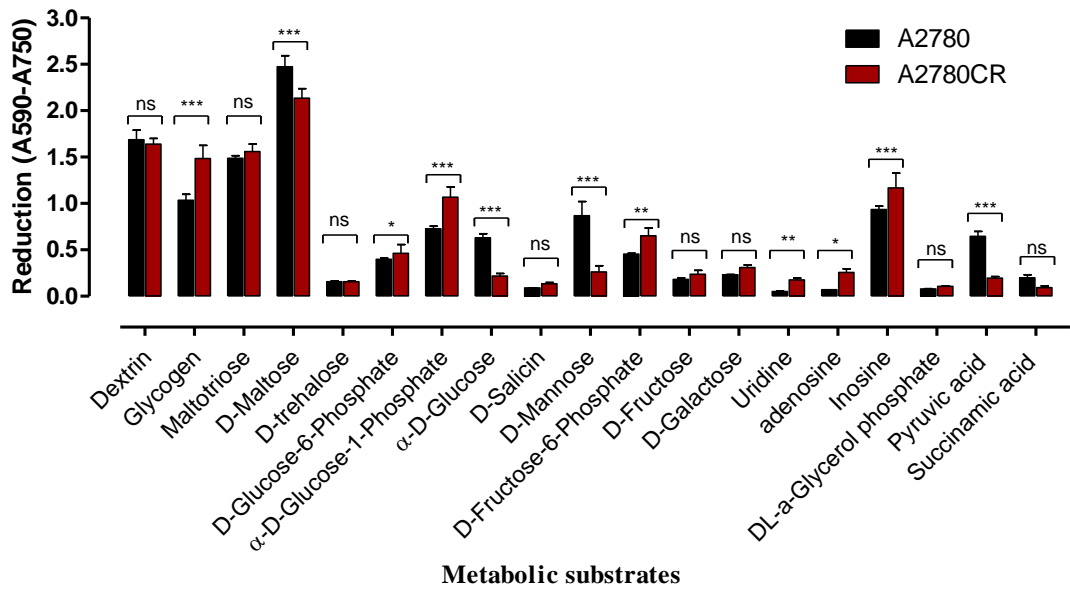


Figure 3.2. Comparison of substrate metabolism in A2780 and A2780CR cells. Dye reduction levels measured following 24 h incubation of cells.

Phenotype MicroArrays PM-M1
Carbon and Energy Substrate Changes in A2780 before and after treated with melittin

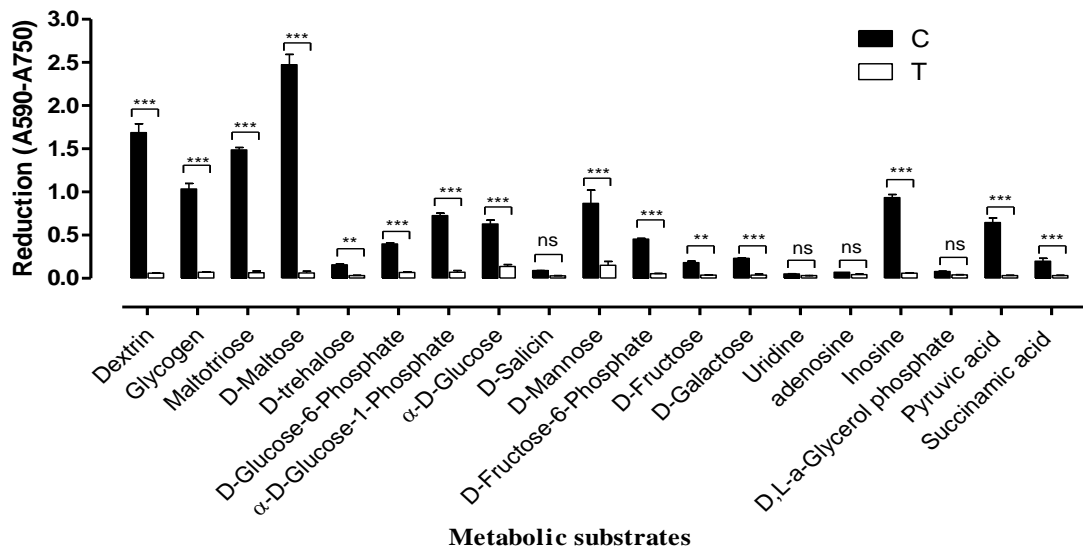


Figure 3.3. Comparison of substrate metabolism in A2780 cells following melittin exposure. Dye reduction levels measured following 24 h incubation of cells with melittin at IC₅₀ (6.8 µg/mL) concentration. C= untreated controls; T= melittin treated.

Phenotype MicroArrays PM-M1
Carbon and Energy Substrate Changes in A2780CR before and after treated with melittin

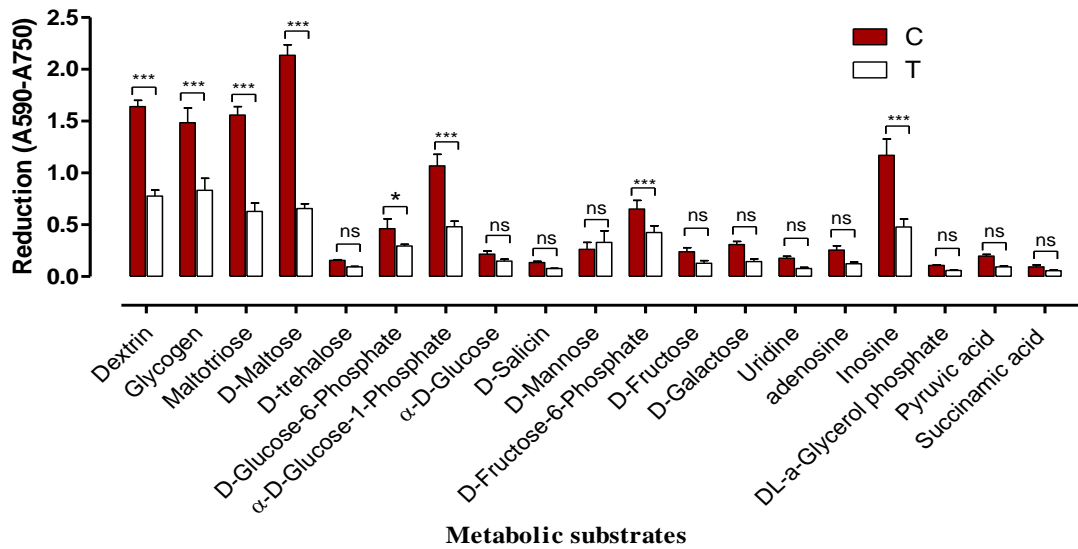


Figure 3.4. Comparison of substrate metabolism in A2780CR cells following melittin exposure. Dye reduction levels measured following 24 h incubation of cells with melittin at IC₅₀ (4.5 µg/mL) concentration. C= untreated controls; T= melittin treated.

3.4.3 Effect of melittin on the metabolomes of both cell lines

In order to gain a better understanding of the mechanism of melittin toxicity in the two cell lines, differences in the levels of metabolites induced by treatment with melittin at concentrations corresponding to IC_{50} with respect to each cell line were assessed. The multivariate analysis techniques used in this study included PCA and OPLS-DA. A clear separation of melittin-treated A2780 and A2780CR cells, and their respective untreated controls, was achieved indicating unique metabolite profiles for the treated and control cells on a PCA scores plot (Figure 3.5 A). PCA is used as the first step in chemometric analysis to visualise grouping trends. The model parameters and validation of the plot suggested a good model (2 components, R^2X (cum) = 0.814; Q^2 (cum) = 0.757). Figure 3.5 A is also shown the clustered QC samples in the PCA scores plot indicated that the LC/MS system is stable throughout the entire analytical run. The OPLS-DA model parameters and validation of the plot suggested that the models are robust and not the results of statistical over-fitting (R^2X (cum) = 0.843, R^2Y (cum) = 1, Q^2 (cum) = 0.948), three components), and the CV-ANOVA for this model was $3.22E-015$ (Figure 3.5 B). The HCA groupings of the metabolomics data showed distinct separation between the cell lines themselves as well as between the control and treated samples of each cell line (Figure 3.6).

Significantly changed metabolites distinguishing melittin-treated samples (A2780) from control are summarised in Table 3.1. Based on that, a new OPLS-DA model was built (Figure 3.7A). The OPLS-DA model parameters and validation of the plot suggested a strong model (R^2X (cum) = 0.993, R^2Y (cum) = 1, Q^2 (cum) = 0.992), two components), and the CV-ANOVA for this model was $1.72E-5$. The validity of

the ROC and permutation test were also applied (Figure S3.2, appendix). The AUC for a ROC classification is regarded as excellent when $AUC > 0.9$. The OPLS-DA model classified the treated and untreated A2780 cells into two groups, and the AUC of the ROC for the groups were excellent to perfect classification.

There was also a very clear separation of the treated versus untreated A2780CR cells obtained by using OPLS-DA model (Figure 3.7B). The model parameters and validation of the plot suggested a strong model (2 components, R^2X (cum) = 1, R^2Y (cum) = 1, Q^2 (cum) = 0.975, CV-ANOVA= 0.00034). Furthermore, the validity of the ROC and permutation test showed the constructed OPLS-DA model was positive and valid (Figure S3.3, appendix).

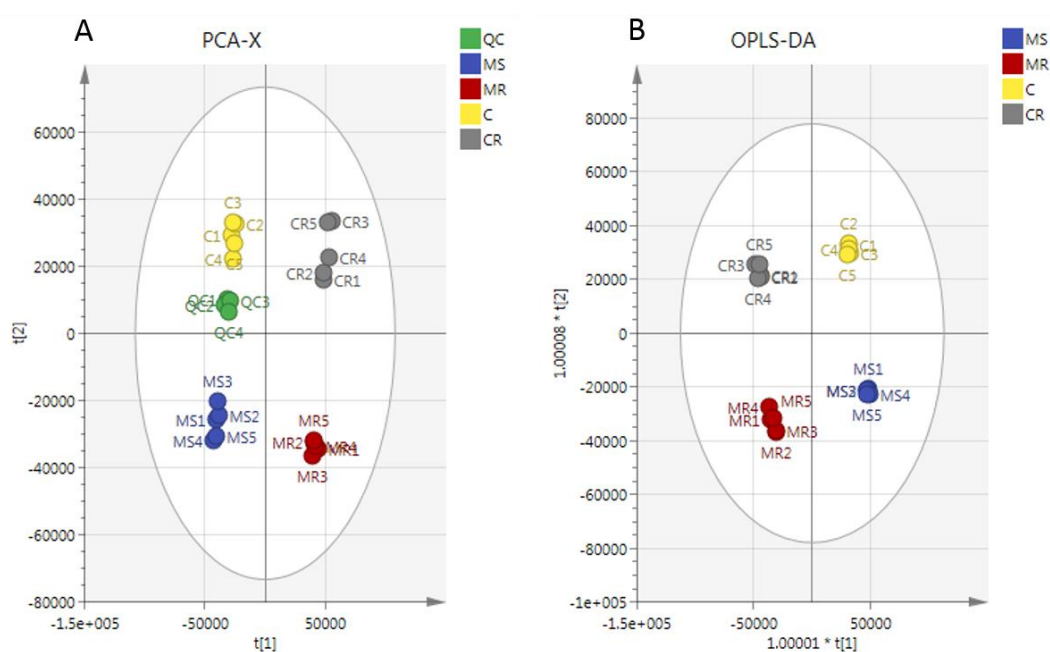


Figure 3.5. (A) PCA vs (B) OPLS-DA of ovarian cancer cells of A2780 and A2780CR treated with melittin. The groups: MS circles: A2780-treated cells; C circles: untreated A2780 cells; MR circles: A2780CR-treated cells; CR circles: untreated A2780CR cells. QC circles: Quality control samples.

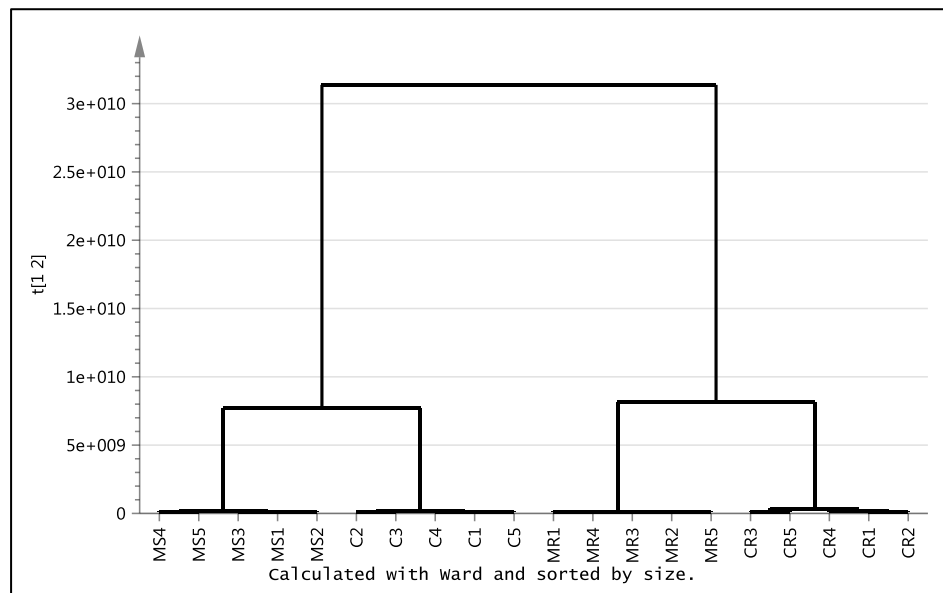


Figure 3.6. Hierarchical clustering analysis (HCA) of 20 ovarian cancer cell samples. It shows two main groups and four subgroups. The groups: CR, control of cisplatin resistance cell lines; MR: A2780CR after treatment with melittin; C, control of cisplatin sensitive cell lines; MS, A2780 after treatment with melittin.

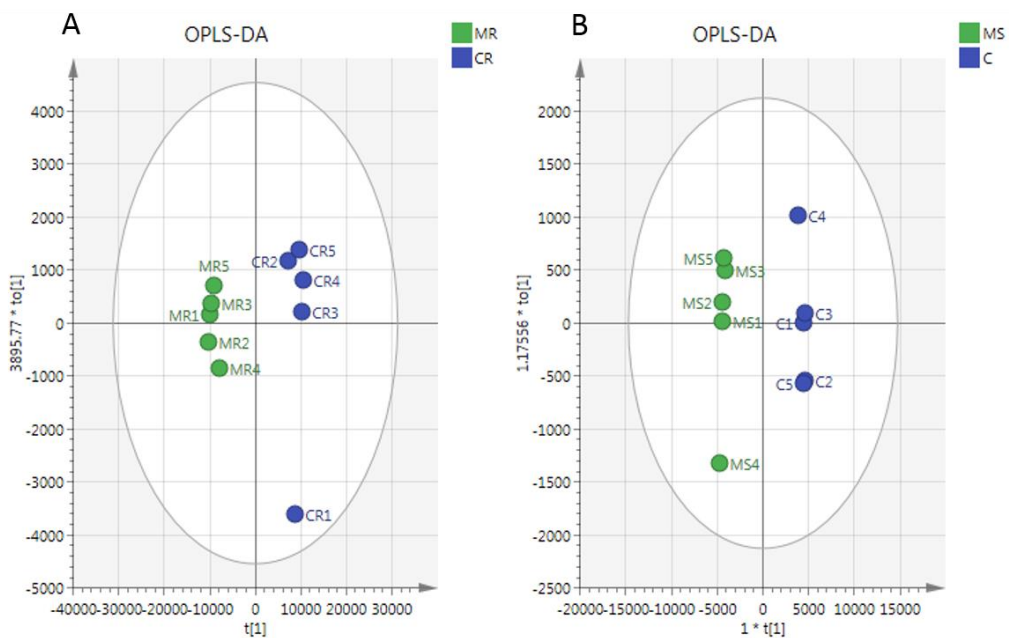


Figure 3.7. OPLS-DA score plot of (A) A2780CR cell lines before and after treatment with melittin; (B) A2780 cell lines before and after treatment with melittin.

Table 3.1 shows the metabolic differences between the sensitive and resistant cell lines. The low levels of ATP in the A2780 cells reflected the Biolog data suggesting that these cells have reduced rates of glycolysis/TCA cycle activity in comparison with the resistant cells. Several metabolites in the TCA cycle differed between the sensitive and resistant cells including citrate, 2-oxoglutarate, and malate. None of the TCA cycle intermediates supplied in the Biolog array were utilised by the cell lines as carbon sources, this might reflect the permeability of the cells for these substrates. However, pyruvate was used as a carbon source and presumably enters the Krebs cycle. Treatment with melittin further reduced the levels of ATP in the A2780 cells whereas melittin had little effect on the ATP levels in the A2780CR cells. There were marked differences in levels of some carnitines between the sensitive and resistant cells with the sensitive cells having much higher levels of butyryl carnitine. However, there was no evidence from the Biolog data that short chain fatty acids were utilised as carbon sources.

The most marked differences between the sensitive and resistant cells were in the polyamine pathway where 14 metabolites in the pathway were altered in the sensitive cells in comparison with the resistant cells. The polyamines spermidine, putrescine and N-acetylputrescine were markedly higher in the sensitive cells and, correspondingly, many of their precursors, especially arginine, were down regulated. Melittin treatment decreased the levels of polyamines in the sensitive cells and the levels of arginine present in the cells were reduced almost to zero.

Table 3.1. Statistical differentiating metabolites.

m/z	RT	Metabolites	S/R		MS/MR		MR/R		MS/S	
			P-value	Ratio	P-value	Ratio	P-value	Ratio	P-value	Ratio
Proline/glutamate/arginine/polyamine metabolism										
116.071	12.8	*Proline	<0.01	0.837	<0.001	0.409	ns	1.056	<0.001	0.516
128.035	10.3	*1-Pyrroline-3-hydroxy-5-carboxylate	<0.05	0.839	<0.001	0.364	ns	1.114	<0.001	0.453
130.051	14.4	*Glutamate-5-semialdehyde	ns	0.944	<0.001	0.607	ns	1.065	<0.001	0.658
131.083	11.4	*Ornithine	<0.001	4.774	<0.001	3.573	ns	1.001	<0.001	0.749
132.030	15.2	*Aspartate	ns	1.091	<0.001	1.229	ns	1.055	<0.01	1.159
146.046	10.8	Glutamate	<0.001	0.608	<0.001	0.113	ns	0.999	<0.001	0.187
147.076	14.9	*Glutamine	<0.001	0.299	<0.001	0.503	<0.001	1.204	<0.001	1.906
173.104	24.6	*Arginine	<0.001	0.155	<0.001	0.004	ns	1.023	<0.05	0.026
188.057	14.4	*N-Acetyl-L-glutamate	<0.001	0.637	<0.001	0.146	<0.001	1.348	<0.001	0.313
89.107	15.4	**Putrescine	<0.001	2.339	<0.001	1.490	ns	1.051	<0.001	0.670
131.118	8.2	**N-Acetylputrescine	<0.001	5.175	<0.001	1.603	ns	1.021	<0.001	0.316
146.165	26.2	**Spermidine	<0.001	2.354	ns	1.150	ns	1.127	<0.001	0.550
150.058	11.4	*Methionine	<0.001	0.422	<0.001	0.669	<0.01	1.127	<0.001	1.594
298.096	6.4	*5'-Methylthioadenosine	0.003	1.92	ns	0.830	ns	0.839	<0.001	0.361
TCA cycle/glycolysis										
133.014	16.4	*Malate	<0.001	0.647	<0.001	0.238	<0.001	1.129	<0.001	0.418
145.014	15.9	*2-Oxoglutarate	ns	0.972	<0.001	0.173	<0.001	1.217	<0.001	0.221
191.020	18.4	*Citrate	<0.001	2.207	<0.001	0.534	ns	1.098	<0.001	0.265
508.003	16.6	*ATP	<0.001	0.267	<0.001	0.118	ns	0.963	<0.001	0.415

Table 3.1. (Contd.)

m/z	RT	Metabolites	S/R		MS/MR		MR/R		MS/S	
			P-value	Ratio	P-value	Ratio	P-value	Ratio	P-value	Ratio
Carnitine metabolism/fatty acid metabolism										
162.112	13.3	*Carnitine	<0.001	0.253	<0.001	0.164	ns	1.065	<0.001	0.676
204.123	11.0	*Acetylcarnitine	<0.001	0.273	<0.001	0.050	ns	1.016	<0.001	0.190
232.154	8.7	Butanoylcarnitine	<0.001	14.083	ns	1.992	ns	0.903	<0.001	0.131
664.117	14.3	*NAD+	<0.001	0.487	<0.001	0.135	<0.001	1.228	<0.001	0.336
Miscellaneous										
104.106	19.6	*Choline	<0.001	0.019	<0.001	0.231	<0.001	1.423	<0.001	7.270
166.086	10.0	*Phenylalanine	<0.001	0.381	<0.05	0.873	<0.01	1.157	<0.001	2.358
118.086	12.4	*Valine	<0.001	1.148	<0.01	2.257	<0.01	1.148	<0.001	2.257
120.065	14.3	*Threonine	<0.001	0.610	ns	0.948	<0.05	1.140	<0.001	1.704
88.040	14.7	*Alanine	ns	0.965	<0.001	0.385	ns	1.098	<0.001	0.442
179.056	17.1	*Hexose	<0.001	0.564	<0.001	0.364	<0.01	0.931	<0.001	0.605
195.051	13.7	*Gluconic acid	<0.001	0.559	<0.001	0.103	<0.001	0.837	<0.001	0.154
258.110	14.4	*Glycerophosphocholine	<0.001	0.020	<0.001	0.031	<0.001	1.529	<0.001	2.342

RT:min; MR: melittin treated A2780CR; R: control A2780CR; MS: melittin treated A2780; S: control A2780; ns: non-significant. * Retention time matches standard on pHILIC column. ** Retention time matches standard on ZIC-HILIC column.

3.4.4 Assessment of necrotic and apoptotic cell death in A2780 and A2780CR cells

LDH (lactate dehydrogenase) release in the medium is an enzymatic indicator that illustrates the breakdown of membrane integrity, necrosis of a cell. A2780 and A2780CR cancer cells were incubated with increasing concentrations of melittin for 24 h and intracellular LDH release increased as a result of the breakdown of the cell or plasma membrane. The results suggest that compared to control cells (untreated cells), melittin produced an increase in LDH leakage when incubated with ovarian cancer cells at levels $\geq 6 \mu\text{g/mL}$ (Figure 3.8); the amount of LDH released appeared to be concentration-dependent in A2780, but not in A2780CR, cells. However, in comparison to staurosporine, melittin did not induce high levels of caspase activity particularly at 6 h (Figure 3.9). This suggests that the mechanism of cell death promoted by melittin was via necrosis rather than apoptosis.

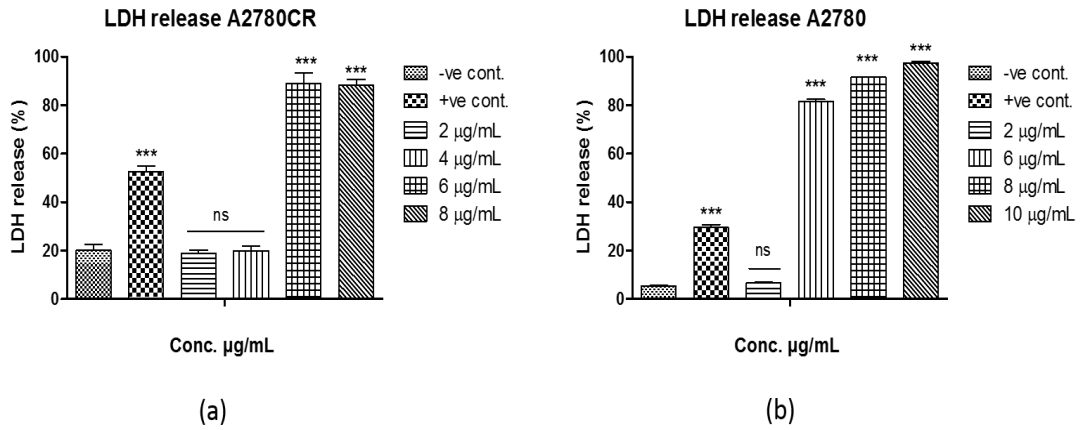


Figure 3.8. Lactate dehydrogenase (LDH) assay. Effect of melittin on leakage of lactate dehydrogenase (LDH) from A2780 and A2780CR cell lines.

The cells were incubated with melittin at different concentrations for 24 h. LDH activity was measured at 490 nm using an LDH cytotoxicity kit. Data were expressed as the mean \pm SD of three independent experiments. Significant difference in LDH activity of melittin compared to untreated cells was tested by one-way ANOVA followed by Bonferroni's Multiple Comparison test to determine the differences between the experimental groups. Differences were considered significant at $p < 0.001$ (***) and ns: no significance. **(a)** LDH release A2780CR; **(b)** LDH release A2780.

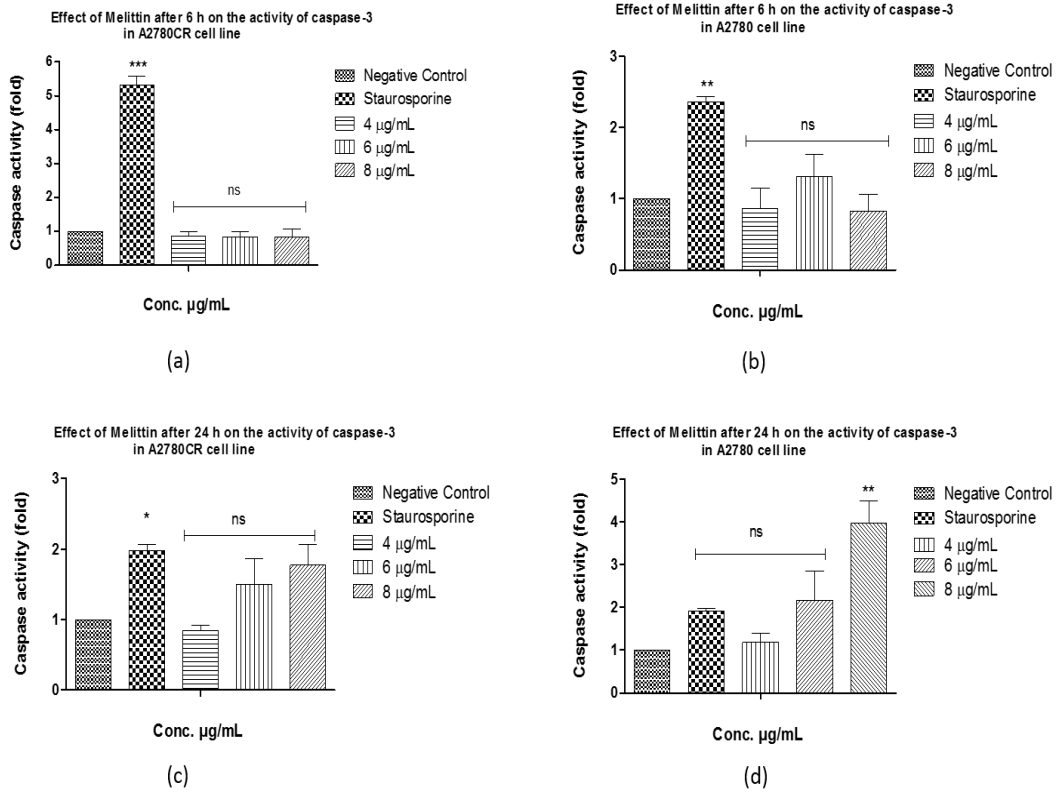


Figure 3.9. Effect of Melittin on caspase-3 activity in A2780 and A2780CR cells.

(a) Effect of melittin after 6 h on the activity of caspase-3 in A2780CR cell line; (b) Effect of melittin after 6 h on the activity of caspase-3 in A2780 cell line; (c) Effect of melittin after 24 h on the activity of caspase-3 in A2780CR cell line; (d) Effect of melittin after 24 h on the activity of caspase-3 in A2780 cell line.

3.5 Discussion

In this study, untargeted metabolomics was performed in order to determine the effects of melittin on the metabolic output of A2780 and A2780CR ovarian cancer cell lines. The altered metabolites in both cells encompassed several pathways including those of amino acid, energy, and carbohydrate metabolism. In a previous study it was found that docetaxel, the chemotherapeutic agent used for treatment of ovarian cancer, caused significant metabolic changes in amino acid and carbohydrate metabolism in ovarian cancer cells (OVCAR-3) (Vermeersch et al., 2014). In addition, recent metabolomics based studies in ovarian cancer cells have demonstrated that gossypol, which is a phenolic aldehyde extracted from cotton plant, decreases cellular levels of glutathione (GSH), aspartic acid, and flavin adenine dinucleotide (FAD) (Wang et al., 2013). Thus, the results obtained with melittin in this study add to the growing body of evidence regarding the utility of metabolomics as a tool for evaluating metabolic alterations in cancer cells induced by various agents. However, while there have been some previous metabolomic studies on the comparison between platinum-sensitive and resistant ovarian cancer cell lines (Poisson et al., 2015), and between effects of nicotinamide phosphoribosyltransferase on ovarian and colorectal cancers (Sasada et al., 2013), this is the first metabolomics-based study to evaluate the effects of melittin on human ovarian cancer cell lines as a potential anticancer therapeutic agent.

The overall impression is that the cisplatin-sensitive cells exhibit a much stronger metabolic response to melittin treatment than the resistant cells, possibly indicating a greater capacity of the former cell line to neutralise the effects of melittin given its higher IC₅₀ value against this cell line. In particular, the levels of several amino acids

including proline, pyrroline-3-hydroxy-5-carboxylate, glutamate, glutamate-5-semialdehyde, N-acetyl-L-glutamate, and arginine were all markedly decreased in A2780 cells following melittin exposure. In a previous study by Poisson et al. (2015) to compare the metabolic profiles of untreated cisplatin-resistant and sensitive cell lines (Poisson et al., 2015), arginine was found to be significantly higher in the latter. In contrast, our study shows that arginine was higher in the resistant compared to sensitive cell lines both pre- and post-treatment with melittin. However, it should be noted that the Poisson et al. study compared the sensitive A2780 cells with C200, a different cisplatin resistant cell line from the one used in the current study. Thus, our findings suggest that the A2780CR cell line contains more arginine than both the cisplatin sensitive A2780 and cisplatin-resistant C200 cell lines and, unlike in A2780 cells where it is lowered, the arginine level in A2780CR cells is unperturbed by treatment with melittin. In correspondence to lower levels of intermediates in the arginine pathway, ornithine, putrescine, N-acetylputrescine and spermidine were all upregulated suggesting that the levels of arginine and its precursors are lower in the A2780 cells since they are being directed towards polyamine biosynthesis. The lower level of methionine in these cells correlates with an increased requirement for it in the biosynthesis of spermidine. High levels of polyamines have been linked to high rates of cell proliferation. Treatment of the sensitive cells with melittin results in an almost complete depletion of arginine within the cells and further lowering of arginine precursors. The lack of arginine as a precursor appears to result in a fall in the level of ornithine and polyamines within the cells although the levels still remain higher than those in the resistant cells and methionine is higher after treatment suggesting that the requirement for it in spermidine biosynthesis is reduced because of the depletion of

spermidine. Polyamine metabolism in the resistant cells remains unaffected by melittin. Polyamines are known to act to stabilise membranes through interaction with phospholipid head groups (Schuber, 1989). It has been speculated that polyamines stabilize membrane flow, which involves fusion between the plasma membrane and Golgi derived vesicles (Moinard et al., 2005; Morré et al., 1979). The resistant cells contain higher levels of arginine and lower levels of polyamines suggesting a slower rate of biosynthesis of polyamines from arginine in these cells. Treatment of the resistant cells with melittin does not affect the levels of either the polyamines or arginine to any great extent. If the hypothesis regarding the role of polyamines in stabilizing membrane flow is true, then it is possible that the lower levels of polyamines might result in reduced capability in these cells to repair membrane damage caused by melittin. In addition there is a link between polyamine depletion and the inhibition of apoptotic cell death (Seiler and Raul, 2005). This further underlines possible differences in the mechanism of cell death between these two cell lines.

The A2780 cells have lower levels of ATP both before and after melittin treatment in comparison with the A2780CR cells. The Biolog data also indicates lower levels of glycolysis in the A2780 cells in comparison with the A2780CR cells. Since ATP generation in cancer cells is primarily from glycolysis as opposed to oxidative phosphorylation, even under normoxic conditions (Uetaki et al., 2015), the observed effect implies that glycolysis may be a potential target for melittin as an anticancer agent. The strong dependence of cancer cells on glycolysis could be the basis for melittin's selective toxicity against them (Kohno et al., 2014; Mahmoodzadeh et al.,

2013; Mahmoodzadeh et al., 2015; Jo et al., 2012; Liu et al., 2013; Qian et al., 2015; Wu et al., 2015). On the other hand, levels of ATP in A2780CR cells were higher than in A2780 at the outset and were not greatly affected by melittin treatment. The Biolog data also suggested a smaller effect of melittin on ATP production A2780CR cells since the production of NADH by the cells was much less affected by melittin treatment than in the case of the A2780 cells. ATP levels have been linked to the capability of cells to undergo apoptotic as opposed to necrotic cell death and this suggests that the A2780CR cells may be undergoing apoptotic cell death in response to melittin whereas the A2780 cells may be undergoing necrotic cell death. However, the effect of melittin on caspase levels does not support this. In our study, we found that melittin inhibited glycolysis in A2780 cells by reducing the level of NAD⁺, but this biomarker was increased in A2780CR cells. Cancer cells require increased NAD⁺ biosynthesis to support anabolic metabolism, to sustain signalling processes including sirtuin activity and ADP-ribosylation, and to maintain a redox balance. Accordingly, inhibitors of nicotinamide phosphoribosyltransferase (NamPT), the enzyme that catalyses the rate-limiting step in NAD⁺ biosynthesis, have been shown to possess moderate anti-tumour activity in monotherapy both *in vitro* and *in vivo* (Moore and Boothman, 2014). The peptide toxin ricin was found to promote apoptosis by decreasing both ATP and NAD levels in U937 cells (Komatsu et al., 2000) although it was proposed that necrotic mechanisms might also be operating.

Levels of choline, methionine, phenylalanine, valine and threonine observed were raised in both cell lines when treated with melittin and they were significantly higher in A2780 cells. These findings resemble those from a previous study in which the

levels of phenylalanine and methionine were elevated in A2780 and HCT-116 (colorectal cancer) cell lines following treatment with FK866, a small molecule inhibitor of NamPT (Tolstikov et al., 2014). However, the levels of metabolic intermediates of the TCA cycle, such as citrate, 2-oxoglutarate, and malate were decreased in A2780 cells by melittin, but they were increased in A2780CR. Some recent studies have demonstrated higher levels of TCA cycle intermediates (including succinate, fumarate, and malate) observed in tissue samples from ovarian carcinoma without treatment (Ben Sellem et al., 2011; Denkert et al., 2006; Halama et al., 2015) and our study shows as well that there are significant differences in citrate and malate levels in the untreated cells (negative controls) in which malate is decreased and citrate is increased in A2780 relative to A2780CR cells respectively. However, the previously mentioned study by Poisson et al. did not find significant differences in TCA cycle metabolites between untreated platinum-sensitive (A2780) and resistant (C200) cells (Poisson et al., 2015), suggesting that the A2780CR cell line has relatively specific distinctions in its metabolome. Some acyl carnitines were also found to respond to melittin treatment in A2780, but not in A2780CR cells. The dose-dependent decreases in L-carnitine, acetylcarnitine and butanoylcarnitine levels in A2780 cells after melittin exposure might be explained based on cell-specific alteration of metabolic pathways. Carnitine serves an important role in the regulation of energy production from fatty acids at the cellular level. It is involved in the transport of long-chain fatty acids across the inner mitochondrial membrane, as well as facilitating chain-shortened acyl group transportation from the peroxisomes, where they are produced, to the mitochondria for further energy metabolism (Zammit et al., 2009).

3.6 Conclusions

In conclusion, this study shows that the cisplatin sensitive A2780 cells contain relatively higher levels of polyamines, which might result in increased membrane stability and repair and thus resistance to the lytic action of melittin in comparison with the cisplatin resistant A2780CR cells. After exposure to melittin, the levels of most of the significantly altered metabolites, particularly amino acids and TCA cycle intermediates, were lower in A2780 compared to A2780CR cells, suggesting different metabolic responses in the two cell lines. Given that melittin interacts with cell membranes, the observed effects might suggest that the membranes are less adaptable in the cisplatin resistant cells compared to the sensitive ones. The effects of melittin on the cell lipid profile will be discussed in chapter 6.

Chapter 4

Liquid chromatography mass spectrometry (LCMS) and Phenotype Microarray Profiling of Ovarian Cancer Cells after Exposure to Cisplatin

4 LCMS and Phenotype Microarray Profiling of Ovarian Cancer Cells after Exposure to Cisplatin

4.1 Abstract

Despite cisplatin's effectiveness against ovarian cancer, these cancer cells have shown the ability to resist chemotherapy – a resistance that represents a major obstacle to current therapeutic strategies. The objective of the study was to determine whether or not cellular resistance could be linked to changes in metabolites. LC-MS hydrophilic interaction chromatography was used to analyze the intracellular metabolomic profile of ovarian cancer cell line A2780 and the cisplatin resistant cell line A2780CR, before and following treatment with cisplatin at inhibitory concentration (IC_{50}) concentrations. Phenotype MicroArray™ (PM) experiments were also applied in order to test carbon substrate utilisation or sensitivity in both cell lines after exposure to cisplatin. Data extraction was carried out with MZmine 2.10 with metabolite searching against an in-house database. The data were analyzed using univariate and multivariate PCA and OPLS-DA methods. There was clear discrimination between the controls and the cisplatin treated samples on the basis of PCA and OPLS-DA. The cisplatin-sensitive cells were as expected more sensitive to cisplatin than the resistant cells with IC_{50} values of 4.9 and 10.8 $\mu\text{g/mL}$, respectively. The results demonstrated that the intracellular metabolomic changes induced by cisplatin in the cisplatin-sensitive cells led to reduced levels of acetylcarnitine, phosphocreatine, arginine, proline and glutathione disulfide (GSSG) as well as to increased levels of tryptophan and methionine. While PM experiments showed lowered glucose metabolism in the sensitive cells following treatment which was reflected in decreased levels of ATP. Overall the metabolic changes induced in A2780CR cells by cisplatin were much

fewer than those induced in A2780 cells. The sensitive cells had a much quicker onset of apoptosis than the resistant cells as judged by measurement of caspase 3. Increased resistance to oxidative stress in the resistant cells was consistent with higher levels of proline, due to less induction of proline dehydrogenase, and elevated levels of glutathione (GSH) and GSSG following cisplatin treatment.

4.2 Introduction

One of the key components of chemotherapy treatment of cancer is through the use of cytotoxic drugs. Platinum containing drugs are among the most active antitumor drugs known, and have been used as a first-line chemotherapy treatment of numerous solid tumors, including ovarian cancer. One of the most effective broad spectrum cytotoxic agents in the treatment of ovarian cancer is cisplatin (*cis* diaminedichloroplatinum), which is also commonly used in the treatment of other cancers including breast, testicular, and lung cancers (Martín, 2001; Eckstein, 2011). The cytotoxicity of cisplatin is related to its interaction with DNA, prompting the formation of DNA adducts; these adducts impair replication of cancer cells and contribute to cell death, or apoptosis (Zwelling and Kohn, 1979). The damage to DNA caused by platinum compounds affects multiple signalling pathways, causing cell cycle arrest, cell survival, or cell death.

Several other proposed mechanisms of cisplatin cytotoxicity include mitochondrial damage, decreased ATPase activity, and altered cellular transport mechanisms. Mitochondria have been implicated in cell death, based on their interaction with nuclear DNA (Zamzami and Kroemer, 2001). Furthermore, mitochondria are thought

to be a major target of cisplatin, meaning that mitochondrial DNA is likely to experience significant cisplatin-related damage which can in turn lead to mitochondrial loss of energy production and a decrease in ATPase activity (Murata et al., 1989; Olivero et al., 1997). Additionally, cisplatin is known to induce oxidative stress and endoplasmic reticulum stress; however, the extent to which these pathways contribute to cell death has not yet been established (Mandic et al., 2003; Galluzzi et al., 2012).

Despite cisplatin's effectiveness against ovarian cancer, these cancer cells have shown the ability to resist chemotherapy – a resistance that represents a major obstacle to current therapeutic strategies. Several mechanisms of platinum compound resistance have been proposed, including diminished drug accumulation, improved drug efflux, drug inactivation, enhanced DNA repair ability, and enhanced expression of anti-apoptotic genes or other survival genes in the cancers (Eckstein, 2011; Parker et al., 1991). A number of studies have reported the cytotoxic effects of cisplatin in sensitive and resistant ovarian cancer cells through apoptosis or necrosis (Huang et al., 2016; Yang et al., 2015a). One study in particular has demonstrated that cisplatin may induce autophagy in ovarian cancer cell lines; the induced level of autophagy was higher in resistant cells (A2780CR) when compared with the level in A2780 cells (Bao et al., 2015). An improved understanding of the molecular basis of cisplatin resistance has the potential to facilitate the development of new anti-tumour strategies that can sensitize unresponsive or resistant ovarian cancers to cisplatin-based chemotherapy. Owing to the fact that all chemotherapeutic drugs are metabolically processed, it can be proposed that metabolism plays a significant role in the chemoresponse of tumours.

Cell death, whether by apoptosis or necrosis, requires energy from the cell as well as regulation by various metabolic enzymes. Targeting metabolic enzymes from key metabolic pathways, including glycolysis (Yamaguchi et al., 2011), fatty acid synthesis (Menendez et al., 2004), and glucose transport (Cao et al., 2007), has been shown to boost the cytotoxicity of several chemotherapeutic and radiotherapeutic agents. Furthermore, cisplatin treatment has recently been implicated in the inducement of intracellular metabolic changes (von Stechow et al., 2013). Therefore, one can postulate that chemoresistant tumour cells may have specifically altered metabolism when compared to chemosensitive tumour cells, a difference which could be detected by the comparison of the cell metabolites.

To that end, metabolomics in this context – that is, the profiling of metabolites in biofluids, cells, and tissues – can be routinely utilised as a tool for biomarker discovery. It is now feasible to expand metabolomic analyses to understand the systems-level effects of metabolites, owing to innovative developments in informatics and analytical technologies, as well as the integration of orthogonal biological approaches. Cisplatin interrupts certain metabolic pathways including energy, amino acid, and lipid metabolism (Zhang et al., 2016a), interruptions which can yield a variety of metabolic evidence of effect. Metabolomic analysis of the cytotoxic effects of cisplatin has already been conducted, focusing on examining the effects on the kidneys through urine samples and identifying an assortment of metabolomic fingerprints and potential biomarkers (Bae et al., 2011; Portilla et al., 2006; Wen et al., 2011).

A number of metabolomic-based studies have reported the effects of cisplatin in different cell lines including those of ovary cells (Nevedomskaya et al., 2015) as well as cervical cells (Doherty et al., 2014), lung cells (Duarte et al., 2013), pluripotent stem cells (von Stechow et al., 2013), colorectal cells (Tomita et al., 2014), medulloblastoma (Pan et al., 2013), and liver cells (Liu et al., 2014). Exposure of lung cells to cisplatin revealed a variety of metabolites that have been identified as potential biomarkers including increases in lipids (particularly unsaturated triglycerides) and nucleotide sugars (particularly uridine diphosphate *N*-acetylglucosamine) (Duarte et al., 2013). With regard to ovarian cancer cells (OCCs), the level of ecto-5'-nucleotidase mRNA (NT5E) was raised following treatment with platinum compounds; the increasing level of NT5E could be the result of acquired platinum resistance in OCCs. This suggests that the efficacy of chemotherapeutic treatment with platinum could be improved through the inhibition of NT5E; it also suggests that NT5E expression may be useful as a prognostic and predictive clinical biomarker for ovarian cancer (Nevedomskaya et al., 2015).

As a continuation to the previous studies on the metabolomics analysis of metabolomics differences between cisplatin sensitive and cisplatin resistant ovarian cancer cells (Alonezi et al., 2016), the current study aimed to examine metabolic effects of cisplatin as a conventional therapy on A2780 and A2780CR human ovarian cancer cell lines. Metabolic profiling of these cell lines after treatment with IC_{50} concentrations of cisplatin was performed by LC-MS based metabolomics approach using a ZIC-pHILIC column. Phenotype MicroArray™ testing was also used in combination with MS to characterize cells after exposure to cisplatin.

Understanding the mechanism of collateral sensitivity or resistance to cisplatin could lead to biomarker discovery for platinum effects in patients with ovarian cancer.

4.3 Materials and Methods

4.3.1 Cell lines and cultures

As detailed in section 2.2.1, Chapter 2.

4.3.2 Cell viability assay against cisplatin

Cell viability was assessed by an Alamar® Blue (AB) cell viability reagent (Thermo Fisher Scientific, Loughborough, UK). Both A2780 and A2780CR cells were seeded at 1×10^4 cells/well in 96-well plates (Corning®, Sigma-Aldrich) and incubated at 37°C and 5% CO₂ in a humidified atmosphere for 24 h. After this incubation period, the cells were treated with various concentrations of cisplatin ranging from 0.5 to 15 µg/mL for A2780 and 1.5-188 µg/mL for A2780CR in 100 µL of medium, and re-incubated at 37°C and 5% CO₂ for a further 24 h. Triton X-100 at the concentration of 1% (v/v) and cell culture media were used as positive and negative controls, respectively. After this, AB was added at a final concentration of 10% (v/v) and the resultant mixture was incubated for a further 4 h at 37°C and 5% CO₂. Then, the plates were read at an excitation wavelength of 560 nm and the emission at 590 nm was measured using a SpectraMax M3 microplate reader (Molecular Devices, Sunnyvale, CA). Background-corrected fluorescence readings were converted to cell viability data for each test well by expressing them as percentages relative to the mean negative control value.

4.3.3 Determination of IC₅₀

As detailed in section 2.2.2, Chapter 2.

4.3.4 Determination of effect of cisplatin on cell metabolomes

The A2780 cell line was treated with cisplatin at the IC₅₀ concentration of 4.9 µg/mL for 24 h (n=5) and the A2780CR was treated with cisplatin at the IC₅₀ concentration of 10.8 µg/mL respectively for 24 h (n=5). The cells were seeded at 75×10⁴ cells/mL in T-25 cell culture flasks and incubated for 1 doubling time (48 h) before treatment with the cisplatin and incubation for an additional 24 h. After the treatment, the medium was removed and the cells were washed twice with 3 mL of phosphate-buffered saline (PBS) at 37°C before lysis. Cell lysates were prepared by extraction with ice cold methanol: acetonitrile: water (50:30:20) (1 mL per 2×10⁶ cells). The cells were scraped and cell lysates mixed on a Thermo mixer at 1440 rotations per minute (r.p.m.) for 12 min at 4°C, before being centrifuged at 13500 r.p.m. for 15 min at 0°C. The supernatants were collected and transferred into HPLC vials for LC-MS analysis. During the analysis, the temperature of the autosampler was maintained at 4 °C. Mixtures of standard metabolites (Sigma-Aldrich, Dorset, UK) and the pooled quality control (QC) sample were injected in each analysis run in order to facilitate identification and to evaluate the stability and reproducibility of the analytical method. The pooled QC sample was obtained by taking equal aliquots from all the samples and placing them into the same HPLC vial.

4.3.5 Chromatographic conditions for column

A ZIC-pHILIC column was used to study the effects of cisplatin on cisplatin resistant and cisplatin sensitive ovarian cancer cell metabolomes. As detailed in section 2.3.1, Chapter 2.

4.3.6 Liquid Chromatography–Mass Spectrometry (LC-MS) conditions

As detailed in section 2.4.1, Chapter 2.

4.3.7 Data extraction and analysis

As detailed in section 2.5, Chapter 2.

4.3.8 Phenotype MicroArrays analysis

Both cell lines were cultured in a 75 cm² culture flask containing 10 mL RPMI-1640 medium lacking phenol red but containing 5% (v/v) FBS, L-glutamine and Pen/Strep (Gibco, Paisley UK). The medium was removed from the culture flask and saved in a 15 mL sterile conical tube. The adherent cells were washed twice with 10 mL of Dulbecco's Phosphate-Buffered Saline (D-PBS) (Gibco, Paisley UK). The cells were then detached by adding 2 mL of 0.25 % (v/v) Trypsin-EDTA (Gibco, Paisley, UK) and incubated at 37° C for 3 min. Then, 3 mL of culture medium was taken from the 15 mL conical tube was added to quench the detachment reaction and the cell suspension mixed by gently pipetting to disperse the cells. The cells were harvested by transferring the cell suspension to the 15 mL conical tube containing the culture medium and centrifuged at 350 x g for 5 min. Then, the medium was aspirated and 10 mL of D-PBS was added. After that, the cell pellet was suspended in the D-PBS by

pipetting, then centrifuged again at 350 x g for 5 min. After the second centrifugation, the medium was aspirated and 10 mL of pre-warmed MC-0 was added. The cell pellet in the MC-0 assay medium was suspended by pipetting. The MC-0 medium was composed of IF-M1 (Technopath Distribution, Tipperary, Ireland) medium supplemented with 5.3% (v/v) dialysed foetal bovine serum (dFBS) (Gibco, Paisley, UK), 1.1% of 100x Pen/Strep solution (Gibco, Paisley, UK), and 0.16% (v/v) of 200 mM glutamine (final concentration 0.3 mM). The cell number was determined and cell viability was assessed by trypan blue dye exclusion (Sigma-Aldrich, Germany). The cells were suspended in enough MC-0 assay medium to fill the selected number of PM panels and to achieve a density of 4×10^5 cells/mL. After that, 50 μ L/well of the cell suspension was added on two sets of PM-M1 plates (Technopath Distribution, Tipperary, Ireland) so that each well had 20,000 cells. The first one was used as the control set, where untreated A2780 and A2780CR cells were cultured. A2780 and A2780CR cells seeded in the second set of plates were exposed to cisplatin. Both sets of PMs containing A2780 and A2780CR were first incubated for 24 h to allow cells to catabolise all nutrients in medium MC-0. The treated cell set was subsequently inoculated with 25 μ L of cisplatin /well of three PM-M1 plates at IC₅₀ concentration, while 25 μ L of MC-0 medium was added to each well in the control set of three PM-M1 plates. Then, the PM plates were incubated at 37° C in a humidified atmosphere with 95% Air-5% CO₂ for 18 hours, after which the Biolog Redox Dye Mix MA was added to all wells (15 μ L/well to the plate). The plate was sealed with tape to prevent off-gassing of CO₂. The plates were incubated for an additional 6 h with Biolog Redox Dye Mix MA (Technopath Distribution, Tipperary, Ireland). Tetrazolium reduction was determined with a microplate reader (SpectraMax M3, Molecular Devices,

Sunnyvale, CA). The endpoint read was performed at 590 nm with subtraction of a 750 nm reference reading (A590-750) which corrects for any background light scattering.

4.3.9 Calculation of redox dye reduction

As detailed in section 2.6.2, Chapter 2.

4.3.10 Caspase activity assay

As detailed in section 2.7, Chapter 2.

4.4 Results

4.4.1 Cisplatin cytotoxicity

The cytotoxicity of cisplatin against A2780 and A2780CR cells was determined using an *in vitro* alamar blue assay. The A2780 and A2780CR cells were treated with increasing concentrations of cisplatin for 24 h at 0.5-15 $\mu\text{g}/\text{mL}$ and 1.5-188 $\mu\text{g}/\text{mL}$, respectively. The percentage of surviving cells decreased in a dose-dependent manner for both the A2780 and A2780CR cells. However, the A2780CR cells were more resistant to cisplatin than were A2780 cells. The 24 h half maximal inhibitory concentrations (IC_{50}) of cisplatin in A2780CR and A2780 cells, were 10.8 and 4.9 $\mu\text{g}/\text{mL}$, respectively (Figure 4.1).

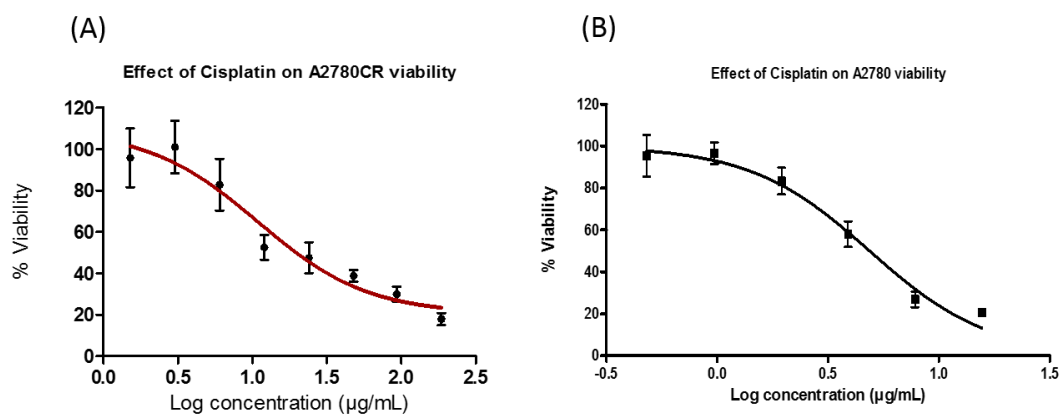


Figure 4.1. Cell viability was determined following treatment with cisplatin for 24 h (A) $IC_{50} = 10.8 \pm 0.9 \mu\text{g/mL}$ A2780CR; (B) $IC_{50} = 4.9 \pm 0.6 \mu\text{g/mL}$ A2780.

4.4.2 Phenotypic MicroArray (PM) assay of cisplatin treated A2780 and A2780CR cells

The cells were tested using standard protocols for metabolic phenotype microarray-mammalian (PM-M) cell assays (Biolog, Hayward, CA). Treatment of the cells with cisplatin produced a similar effect on the sensitive cells in comparison with the resistant cells with exception of D-maltose and α -D-glucose. The metabolism of carbohydrate carbon sources by the cells were quantitatively, but not qualitatively different, as shown by the fact that the carbohydrate metabolism wells were purple rather than yellow colour (Figure S4.1). Reduction of the dye was observed in colour formation in the wells containing the following substrates: dextrin, glycogen, D-trehalose, maltotriose, D-maltose, D-mannose, α -D-glucose-1-phosphate, α -D-glucose, D-glucose-6-phosphate, inosine, D-fructose, D-galactose, uridine, adenosine, D, L- α -glycerol phosphate, pyruvic acid, α -keto-glutaric acid, and succinamic acid. The metabolism of the sensitive cells appeared to be slightly more rapid than that of the resistant cells with pyruvate, glucose and maltose being used more rapidly in the

sensitive cells. Treatment of the cells with cisplatin caused glucose metabolism to fall in the sensitive cell line, but to increase to a non-significant degree in the resistant line (Table 4.1). In A2780 cells, there was also a reduction in metabolism of maltotriose, D-maltose, α -D-glucose-1-phosphate, and inosine (Figure 4.2) following treatment with cisplatin. The metabolism of pyruvate was lower in A2780CR cells while galactose and ketoglutaric acid were metabolised more rapidly by these cells and all three substrates were metabolised at a significantly lower rate in the treated A2780CR cells.

Table 4.1. Comparison of the substrate dependant readings that vary between the sensitive and resistant cells

Substrate Metabolism	S/R		TCR/R		TCS/S	
	P-value	Ratio	P-value	Ratio	P-value	Ratio
Dextrin	0.014	0.854	0.047	0.739	0.046	0.731
Glycogen	0.001	0.725	0.223	0.864	0.123	0.892
Maltotriose	0.483	0.921	0.023	0.715	0.050	0.673
D-Maltose	0.000	1.418	0.171	0.839	0.000	0.751
D-trehalose	0.000	0.649	0.005	0.733	0.003	0.805
D-Glucose-6-Phosphate	0.000	0.455	0.000	0.734	0.089	0.832
α -D-Glucose-1-Phosphate	0.004	0.531	0.002	0.743	0.001	0.765
α -D-Glucose	0.048	1.330	0.052	1.803	0.000	0.346
D-Salicin	0.006	0.704	0.001	0.575	0.010	0.787
D-Mannose	0.013	0.517	0.744	1.065	0.119	0.555
D-Fructose-6-Phosphate	0.004	0.639	0.067	0.713	0.293	1.543
D-Fructose	0.257	0.914	0.014	0.637	0.017	0.441
D-Galactose	0.006	0.623	0.017	0.487	0.000	0.635
Uridine	0.000	0.560	0.001	0.593	0.199	0.884
Adenosine	0.009	0.365	0.763	0.949	0.413	1.053
Inosine	0.374	0.968	0.005	0.486	0.000	0.624
D,L-a-Glycerol phosphate	0.041	0.876	0.581	0.947	0.834	1.009
Pyruvic acid	0.000	5.617	0.000	0.519	0.647	0.970
α -keto glutaric acid	0.026	0.790	0.007	0.666	0.111	0.888
Succinamic acid	0.086	1.600	0.001	0.705	0.014	0.500

TCR: cisplatin treated A2780CR; R: control A2780CR; TCS: cisplatin treated A2780; S: control A2780

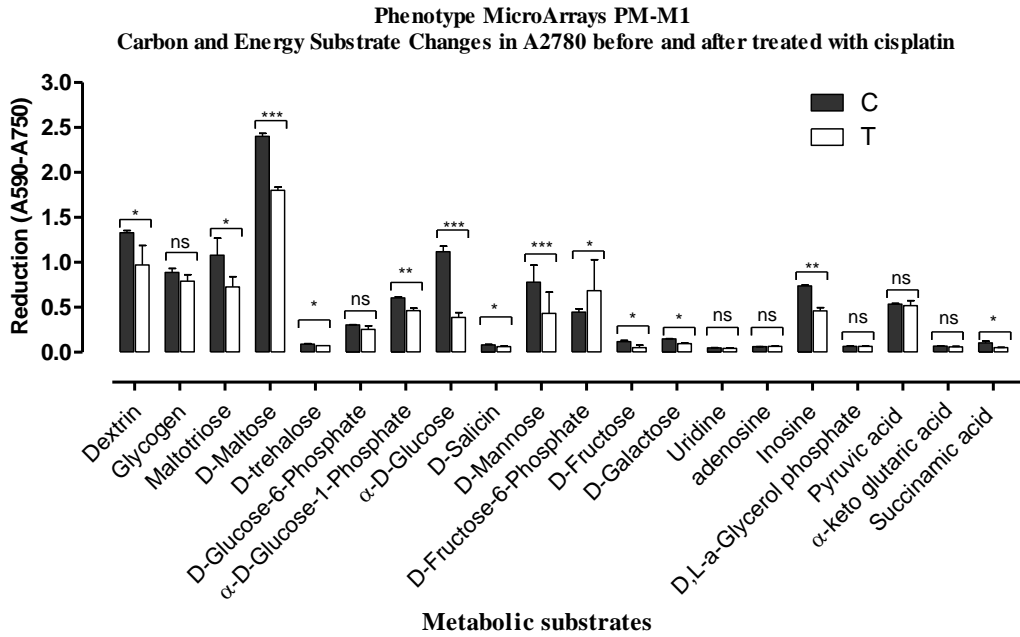


Figure 4.2. Comparison of substrate metabolism in A2780 cells following cisplatin exposure. Dye reduction rates calculated following 24 h incubation of cells with cisplatin at IC_{50} (4.9 μ g/mL) concentration.

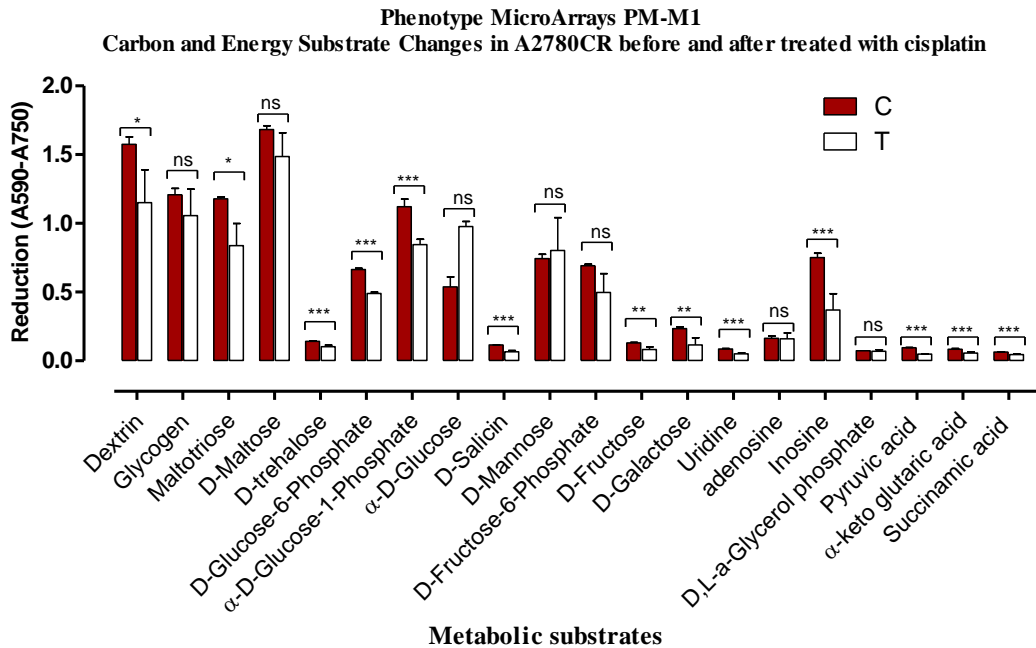


Figure 4.3. Comparison of substrate metabolism in A2780CR cells following cisplatin exposure. Dye reduction rates calculated following 24 h incubation of cells with cisplatin at IC_{50} (10.8 μ g/mL) concentration.

4.4.3 Metabolic profile of cisplatin treated cells

As the current study aim was to focus on changes of intracellular metabolites in relation to cisplatin metabolism, LC/MS based metabolomics was performed to determine the important metabolites changes in A2780 and A2780CR in response to exposure to cisplatin at IC_{50} concentrations for 24 h. Multivariate and univariate analysis were used for the analysis of the HILIC-LC-MS-generated data.

Metabolites were identified at metabolomics standards initiative levels 2 or 3 according to either exact mass (<3 ppm deviation) or exact mass plus retention time matching that of a standard (Sumner et al., 2007). Univariate and multivariate analyses were applied to the data obtained from the samples (n=20). For univariate and multivariate analysis of candidate specific biomarkers in OCCs after exposure to cisplatin, the FDR was used to reduce the probability of false positive results. Following testing of their significance using FDR statistics all the marker metabolites with P values <0.05 were deemed to be significant. The results revealed that following exposure to cisplatin the levels of many metabolites were clearly altered in both A2780 and A2780CR cell lines. Multivariate analysis such as the descriptive PCA and OPLS-DA, were also used to extract meaningful information (Wiklund et al., 2008; Chan et al., 2012). From the PCA and OPLS-DA score plots (Figure 4.4), it can be seen that cisplatin induced metabolic perturbations in both cell lines. PCA was used as the first step in chemometric analysis to investigate inherent data variability and clustering trends. The ovarian cancer cell samples originating from the treated and untreated cells clustered in different areas in the plots. The OPLS-DA model parameters and validation of the plot suggested a strong model ($R^2X (cum) = 0.934$, $R^2Y (cum) = 1$,

$Q2 (cum) = 0.978$, three components), and the CV-ANOVA for this model was $3.14E-25$. OPLS-DA plot, which is a supervised multivariate analysis technique, was used to identify the metabolites that discriminated the groups. Hierarchical clustering analysis of metabolomics data showed distinct separation between the control and treated samples (Figure 4.5). The metabolites that were differentially regulated between the cisplatin-treated and control samples were mainly involved in amino acid, carbohydrate, energy and nucleotide metabolism pathways. Lipid metabolism was not selected for study since the method used in the current study was not optimal for the analysis of lipid metabolites and effects of melittin on lipids will be considered in chapter 6.

The separation between treated and control cells would be expected, since cell death might account for a lot of the changes. Thus the main interest was in the differential effects of cisplatin on the sensitive and resistant cells. The most affected metabolites due to cisplatin treatment in A2780 cell line compared to the other pathways were highly ranked in arginine and proline metabolism pathways (including L-glutamate 5-semialdehyde, phosphocreatine, N2-(D-1-Carboxyethyl)-L-arginine, L-arginine, L-proline, and 5'-methylthioadenosine). In addition, there were other important differences in metabolic pathways between the treated and untreated cells such as oxidative phosphorylation and TCA cycle. Significantly changed metabolites distinguishing cisplatin-treated samples (A2780) from control are summarised in Table 4.2. Based on that, a new OPLS-DA model was built (Figure 4.6A). The OPLS-DA model parameters and validation of the plot suggested a strong model ($R2X (cum) = 0.955$, $R2Y (cum) = 1$, $Q2 (cum) = 0.996$, two components), and the CV-ANOVA

for this model was $8.53E-6$. The validity of the ROC and permutation test were also applied (Figure S4.2, appendix). The OPLS-DA model classified the treated and untreated A2780 cells into two groups: TCS and C. The AUC of the ROC for the groups were excellent to perfect classification.

There was a very clear separation of the treated versus untreated A2780CR cells obtained by using OPLS-DA model (Figure 4.6B). The model parameters and validation of the plot suggested a strong model (2 components, R^2X (cum) = 0.962, R^2Y (cum) = 1, Q^2 (cum) = 0.990, CV-ANOVA = $3.28E-5$). Furthermore, the validity of the ROC and permutation test showed the constructed OPLS-DA model was positive and valid (Figure S4.3, appendix). By combining the multivariate and univariate statistical analyses, significantly changed metabolites distinguishing cisplatin-treated A2780CR samples from controls were obtained and are summarised in Table 4.2. The metabolomics differences between untreated sensitive and resistant cells were reported in chapter 3. The metabolites were mainly involved in amino acid, carbohydrate, and energy metabolism pathways. These metabolites include seventeen amino acids (proline, glutamate-5-semialdehyde, N-acetyl-L-glutamate, N₂-(D-1-carboxyethyl)-L-arginine, glutamate, glutamine, L-serine, 2-oxobutanoate, L-threonine, L-lysine, L-tryptophan, O-acetylcarnitine, creatine, choline, acetylcholine, hydroxyglutarate, and asparagine), five carbohydrate metabolites (2-oxoglutarate, (S)-malate, citrate, gluconic acid, N-acetylneuraminic acid), one nucleotide (GTP), and four energy metabolites (NADH, ADP, ATP, NAD⁺) and the metabolites outlined above are suggested as metabolite biomarkers for the effects of cisplatin treatment on A2780CR cells. Serine is currently of great interest in cancer biology since it is utilised

in the one carbon metabolism used for DNA repair. The levels of serine are markedly increased in both the treated sensitive and resistant cells and this would be consistent with the requirement for DNA repair resulting from cisplatin-induced damage.

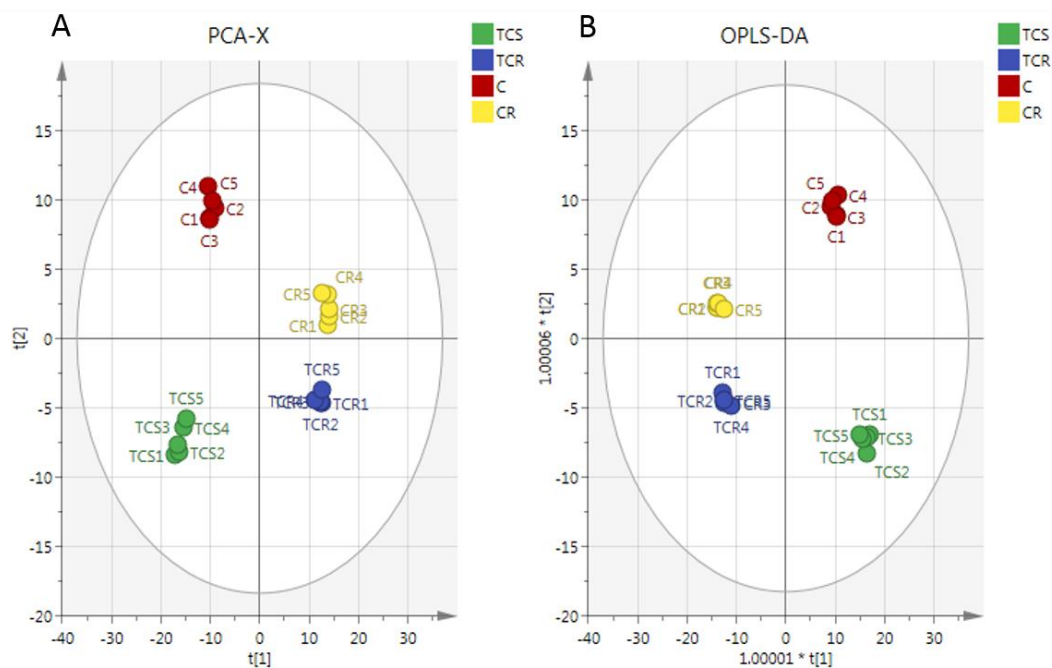


Figure 4.4. (A) PCA vs (B) OPLS-DA. PCA and OPLS-DA scores plot generated from PCA and OPLS-DA using LC-MS normalized data of cells after exposure to cisplatin and controls of A2780 and A2780CR cell lines. The groups: CR, control of cisplatin resistance cell lines; TCR: A2780CR after treatment with cisplatin; C, control of cisplatin sensitive cell lines; TCS, A2780 after treatment with cisplatin.

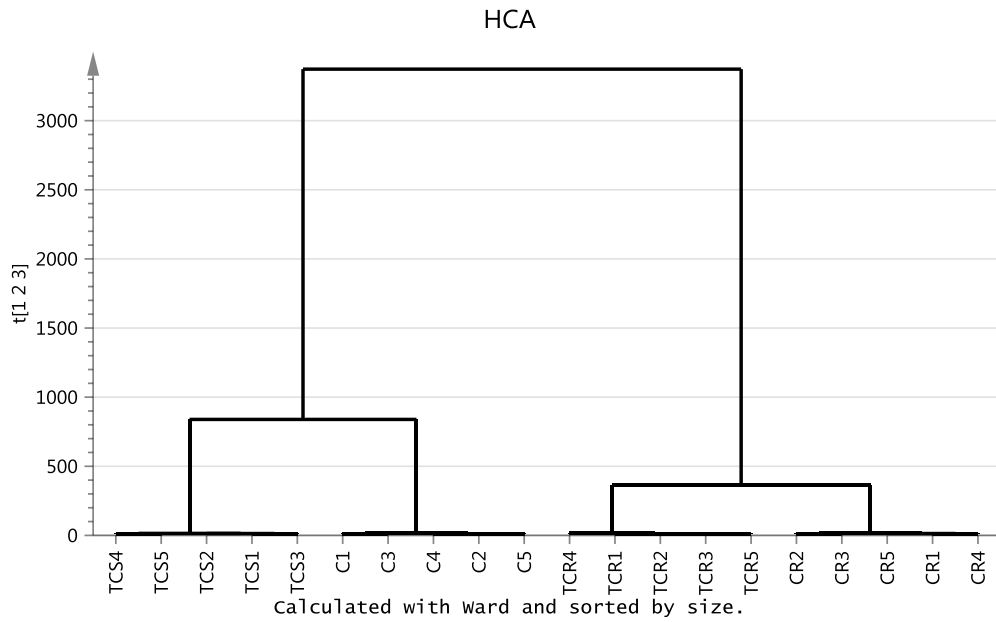


Figure 4.5. Hierarchical clustering analysis (HCA) of 20 ovarian cancer cell samples. It shows two main groups and four subgroups. The groups: CR, control of cisplatin resistance cell lines; TCR: A2780CR after treatment with cisplatin; C, control of cisplatin sensitive cell lines; TCS, A2780 after treatment with cisplatin.

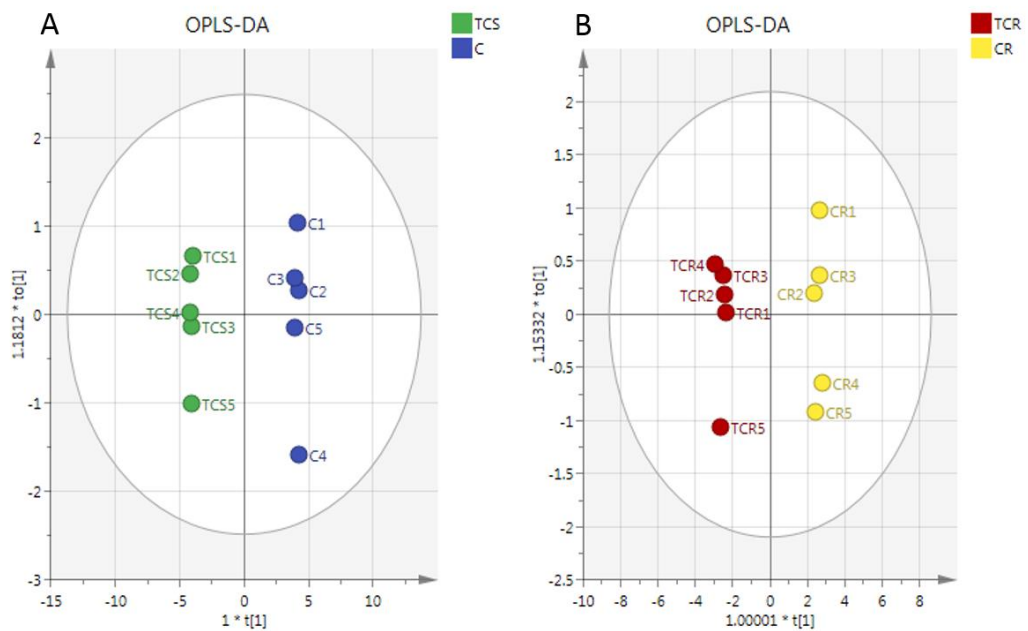


Figure 4.6. OPLS-DA score plot of (A) A2780 cell lines before and after treatment with cisplatin; (B) A2780CR cell lines before and after treatment with cisplatin.

Table 4.2. Statistical differentiating metabolites showing the differential response of the sensitive and resistant cells to cisplatin treatment.

m/z	RT	Metabolites	TCR/R		TCS/S	
			p-value	IC ₅₀	p-value	IC ₅₀
Proline/glutamate/arginine/polyamine metabolism						
+116.071	12.8	*Proline ^{1,2}	<0.01	0.821	<0.001	0.374
-128.035	10.0	L-1-Pyrroline-3-hydroxy-5-carboxylate	<0.01	0.809	<0.01	0.808
-210.029	15.4	*Phosphocreatine ¹	ns	0.953	<0.001	0.387
-130.051	14.4	Glutamate-5-semialdehyde ^{1,2}	<0.01	0.874	<0.001	0.437
+298.096	6.4	*5'-Methylthioadenosine ¹	ns	1.307	<0.001	0.608
+399.144	15.9	*S-Adenosyl-L-methionine	ns	1.436	<0.001	0.687
-173.104	24.6	*Arginine ¹	ns	1.319	<0.001	0.531
-188.057	14.4	*N-Acetyl-L-glutamate ^{1,2}	<0.001	0.54	<0.001	0.701
247.140	14.1	N2-(D-1-Carboxyethyl)-L-arginine ^{1,2}	<0.001	0.513	<0.001	0.225
-146.046	10.5	*Glutamate ^{1,2}	<0.001	0.636	<0.001	0.314
+147.076	14.9	*Glutamine ^{1,2}	<0.01	1.177	<0.001	1.576
+176.102	15.8	*L-citrulline ¹	ns	0.915	<0.01	0.570
TCA cycle/glycolysis						
-133.014	16.4	*Malate ^{1,2}	<0.001	0.589	<0.001	0.663
-145.014	15.9	*2-Oxoglutarate ^{1,2}	<0.001	0.447	<0.01	0.802
-191.020	18.4	*Citrate ^{1,2}	<0.001	0.771	<0.001	0.425
+508.003	16.6	*ATP ^{1,2}	<0.001	0.780	<0.001	0.538
Oxidative phosphorylation						
+666.132	13.4	*NADH ^{1,2}	<0.001	0.475	<0.001	0.208
-426.023	15.3	*ADP ^{1,2}	<0.01	0.659	<0.001	0.520
+664.116	14.2	*NAD ⁺ ^{1,2}	<0.01	0.780	<0.001	0.260
Glycine, serine and threonine metabolism						
+106.050	15.6	*L-Serine ^{1,2}	<0.001	2.345	<0.001	2.299
+101.024	15.8	2-Oxobutanoate ^{1,2}	<0.001	0.437	<0.01	0.689
-118.051	14.1	*L-Threonine ¹	ns	1.243	<0.001	1.439
+132.077	14.6	*Creatine ^{1,2}	<0.01	0.827	<0.001	0.702

Table 4.2. (Contd.)

m/z	RT	Metabolites	TCR/R		TCS/S	
			p-value	IC ₅₀	p-value	IC ₅₀
Miscellaneous						
+104.106	19.6	Choline ^{1,2}	<0.001	1.536	<0.001	1.943
+146.118	13.2	Acetyl choline ^{1,2}	<0.001	0.786	<0.001	0.435
+189.160	21.3	*N6,N6,N6-Trimethyl-L-lysine ¹	ns	1.322	<0.001	0.636
+147.113	23.6	*L-Lysine ²	<0.01	2.114	ns	1.159
+181.072	13.7	*D-Sorbitol ¹	ns	1.095	<0.001	0.831
-151.026	11.3	*Xanthine ¹	ns	0.953	<0.01	0.808
+150.058	11.2	*L-Methionine ¹	ns	1.081	<0.001	1.872
-611.146	17.7	*Glutathione disulfide ¹	ns	1.307	<0.001	0.323
+308.091	14.5	*Glutathione ²	<0.001	1.300	ns	1.007
+132.102	11.1	*L-Leucine ¹	ns	1.092	<0.001	0.676
+521.984	19.7	*GTP ^{1,2}	<0.05	0.868	<0.001	0.549
+205.097	11.4	*L-Tryptophan ^{1,2}	ns	1.271	<0.001	5.741
-147.030	15.4	2-Hydroxyglutarate ^{1,2}	<0.001	0.869	<0.001	0.806
-195.051	13.7	*Gluconic acid ^{1,2}	<0.001	0.528	<0.001	0.353
-308.099	13.3	N-Acetylneuramate ^{1,2}	<0.001	0.544	<0.01	0.677
+156.077	17.9	*L-Histidine ¹	ns	1.204	<0.001	0.223
+204.123	10.8	*O-Acetylcarnitine ^{1,2}	<0.001	0.639	<0.001	0.377
-131.046	15.0	*L-Asparagine ^{1,2}	<0.001	0.653	<0.001	0.580

RT:min; TCR: cisplatin treated A2780CR; R: control A2780CR; TCS: cisplatin treated A2780; S:control A2780; ns: non-significant; IC₅₀: half maximal inhibitory concentrations. ¹ A2780 cells (VIP predictive >1, VIP orthogonal <1, $p<0.05$); ² A2780CR cells (VIP predictive >1, VIP orthogonal <1, $p<0.05$). * Matched to retention time of standard. + positive ion detection – negative ion detection. The differences between the untreated sensitive and resistant cells were reported in Chapter 3.

4.4.4 Assessment of apoptotic cell death in A2780 and A2780CR cells

Caspases are known to be activated during apoptosis induction. In order to understand the differential activation of caspases between the ovarian cancer cell lines, caspase 3 was studied (Figure 4.7). A significant increase in the activity of caspase 3 was detected in A2780 cells at either 6 or 24 h after cisplatin treatment. In contrast, no significant increase in the activities of caspase 3 was detected in A2780CR cells after cisplatin treatment for 6 h, but there was an increase in activity of caspase 3 at 24 h. The ability to detect activated caspase-3 in A2780 cells following cisplatin treatment at different concentrations suggested that cisplatin exhibited dose-dependent cytotoxic effects against ovarian cancer cells by inducing apoptosis as a specific feature.

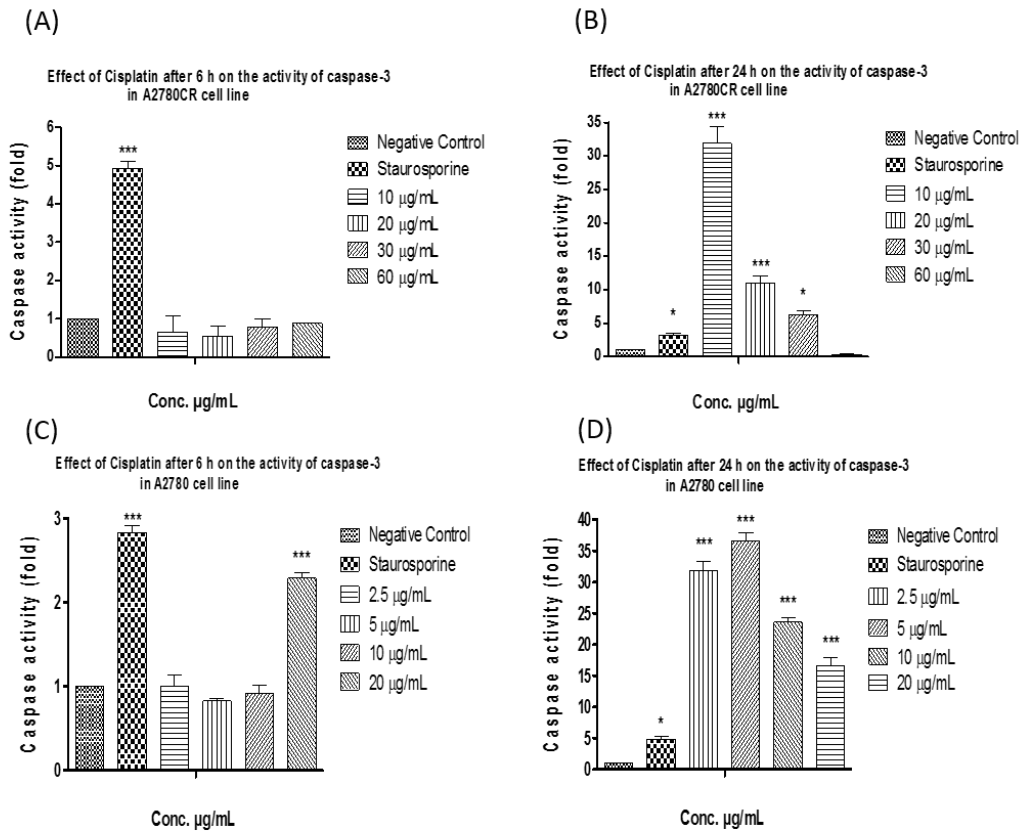


Figure 4.7. Effect of Cisplatin on caspase-3 activity in A2780 and A2780CR cells.

Effect of cisplatin on the activity of caspase-3 (a) after 6 h in A2780CR; (b) after 24 h in A2780CR; (c) after 6 h in A2780; (d) after 24 h in A2780.

4.5 Discussion

In this study, the *in vitro* effects of cisplatin on the metabolomic profiles of OCCs was examined. The intracellular metabolites of A2780 cells sensitive and A2780CR resistant to cisplatin treatment showed differential changes following cisplatin treatment at IC_{50} concentrations within 24 h. The overall impression is that the cisplatin-sensitive cells exhibited a much stronger metabolic response to cisplatin treatment than the resistant cells because the resistant cells may have developed a mechanism that inactivates the drug or transports the drug across the cell membrane. The pathways most affected in both cell lines by cisplatin treatment were those involved in amino acid metabolism, but pathways involved in carbohydrate, energy and nucleotide metabolism were also altered. Among these amino acids, arginine, proline and glycine, serine and threonine were markedly altered in A2780 and A2780CR cells following cisplatin treatment. In a previous study it was found that cisplatin caused significant metabolic changes in methionine degradation pathways (including transmethylation, transsulfuration/glutathione synthesis), as well as in polyamine synthesis and catabolism, urea cycle, proline/arginine metabolism, and nucleotide metabolism in pluripotent stem cells (von Stechow et al., 2013). In addition, recent metabolomics based studies in OCCs have demonstrated that docetaxel caused significant metabolic changes in amino acid and carbohydrate metabolism in OCCs (Vermeersch et al., 2014). However, while there have been some previous metabolomic studies on the comparison between effects of cisplatin on squamous cancer cell lines (SCC11)-sensitive and resistant to cisplatin (SCC11M) (Huang et al., 2012), and the effects of cisplatin on cervical cells (Doherty et al., 2014), and lung cells (Duarte et al., 2013), this is the first metabolomics-based study to evaluate the

effects of cisplatin on human ovarian cancer cell lines.

Effects of cisplatin on amino acid metabolism pathways

The major pathway affected in the A2780 cell line related to cisplatin treatment was the arginine and proline pathway whereas cisplatin had little effect on this pathway in the A2780CR cells. The arginine and proline pathway metabolites arginine, proline, glutamate 5-semialdehyde, phosphocreatine, N2-(D-1-carboxyethyl)-L-arginine, and 5'-methylthioadenosine were altered in A2780 cells, whereas only N-acetyl-L-glutamate and N2-(D-1-carboxyethyl)-L-arginine were altered in A2780CR.

A previous study by von Stechow et al. compared the metabolic profiles of pluripotent stem cells treated with cisplatin at 4 and 8 h (von Stechow et al., 2013), and found proline was raised in both experiments. In contrast, our study showed that the proline was significantly decreased in both the sensitive and resistant cells. However, it should be noted that the von Stechow et al. compared the effect of cisplatin at a concentration of 5 μM (1.5 $\mu\text{g/mL}$) on pluripotent stem cells for 4 h and 8 h. The production of proline is highly dependent on cell type and developmental stage of the cell (Guoyao and Morris, 1998). Proline oxidase, localized on inner mitochondrial membranes, is encoded by a p53-induced gene and metabolically participates in p53-induced apoptosis (Liu et al., 2005). Proline oxidase causes cytochrome c release from mitochondria and the activation of caspases 9 and 3, indicating proline oxidase-induced apoptosis was through the mitochondrial or intrinsic apoptotic pathway (Hu et al., 2001; Maxwell and Rivera, 2003). The more marked increase in the metabolism of proline by the A2780 cells is consistent with the more rapid onset of apoptosis in

these cells following cisplatin treatment in comparison with the resistant cells.

The level of arginine was also markedly reduced in A2780 cells, but its reduction was non-significant in A2780CR cells following cisplatin exposure. Treatment of the sensitive cells with cisplatin resulted in a decrease of arginine within the cells and further lowering of arginine precursors. These findings resemble those from a previous study in which the level of arginine was reduced in pluripotent stem cells, treated with cisplatin (von Stechow et al., 2013). Moreover, our previous study showed that the level of arginine was reduced in A2780 cells following melittin exposure (Alonezi et al., 2016). Previous studies showed that arginine deprivation enhances apoptosis in different cell lines including human lymphoblastic cell lines (Gong et al., 2000), mesothelioma cells (Szlosarek et al., 2006), and melanoma cell lines (Feun et al., 2008). An increase mitochondrial membrane permeability is a rate-limiting step of cell death (Vieira et al., 2000). The anticancer activity of platinum arises from its ability to form irreparable intra-strand DNA crosslinks/adducts which lead to cell apoptosis (Zwelling and Kohn, 1978). In the present work, we have monitored cisplatin-induced apoptosis of A2780 and A2780CR cells by measuring activation of caspase-3. For example, cisplatin-induced (20 $\mu\text{g}/\text{mL}$) increases in caspase 3 activity were time-dependent because activity increased 2.5 and 15 fold in A2780 cells after 6 and 24 h, respectively. However, there was no apoptotic effect of cisplatin on A2780CR after 6 h and caspase-3 was only increased after 24 h. Singh et al. reported that caspase-3 was active in the A2780 cell line at cisplatin concentrations of 10 μM (3 $\mu\text{g}/\text{mL}$) but it was not active in A2780CR (Singh et al., 2013). However, it should be noted that their study examined the caspase-3 activity in both cell lines at low concentrations of

cisplatin. A previous study showed that an increase in caspase 3 activity was found to be concentration- and time-dependent in renal cells treated with cisplatin. Cisplatin-induced apoptosis was found to be concentration and time-dependent with concentrations of 100 μM or less inducing apoptosis, and those higher than 200 μM inducing oncosis (Cummings and Schnellmann, 2002). Thus whether the mechanism of cell death is due to apoptosis or oncosis is dependent on the concentration and length of exposure of cells to cisplatin (Lieberthal et al., 1996; Lau, 1999).

A previous study by Huang et al. (2012) compared the metabolic profile effects of cisplatin treatment on sensitive cells (SCC11) and resistant cells (SCC11M) (Huang et al., 2012); glutamine was found to be upregulated in sensitive cells compared with resistant cells, while our study shows that the glutamine was also increased in sensitive cells compared with resistant cells. They also found that 5-methylthioadenosine and glutamate were decreased in SCC11 in comparison to SCC11M cells (Huang et al., 2012). These findings resemble to our results in which the level of citrulline, S-adenosylmethionine, 5-methylthioadenosine and glutamate were also decreased to a greater extent in cisplatin sensitive cells compared with resistant cells. The A2780 cells have lower levels of creatine and creatine phosphate after cisplatin treatment in comparison with the A2780CR cells. Arginine is necessary for the synthesis of creatine and can also be used for synthesis of citrulline and glutamate. It should be noted that the lack of arginine appears to result in a fall in the level of citrulline and glutamate within the cells. It is important to note that the pathways linking arginine, glutamate, and proline are bidirectional. Thus, the net utilisation or production of these amino acids is highly dependent on cell type and developmental stage (Guoyao and

Morris, 1998). Arginine, proline, and glutamate are all interconvertible provided that glutamine is available as a precursor of carbamoyl phosphate. This metabolism is the basis for synthesis of nitrogen-containing compounds such as urea, putrescine, agmatine, creatine and even nitric oxide and is furthermore crucial for pyrimidine synthesis (Morris, 2004). Cisplatin promoted higher levels of some amino acids in resistant cells in comparison to sensitive cells. In particular, the level of N-acetyl-L-glutamate was markedly decreased in A2780CR cells following cisplatin exposure. The level of N-acetyl-L-glutamate was slightly decreased in A2780 cells in comparison with A2780CR cells. However, there was an increase in level of lysine in A2780CR promoted by cisplatin, but cisplatin did not affect the level of lysine metabolism in A2780.

Cisplatin decreased the level of glutathione disulfide (GSSG) in A2780 cells compared with resistant cells and in addition, the levels of reduced glutathione (GSH) were significantly elevated in resistant cells. GSH depletion ultimately may be a result of the accompanying GSSG deficiency (Dröge et al., 1994). A previous study showed that the levels of GSH were lower in cisplatin sensitive cells (SCC-11) compared with resistant cells (SCC-11M) after treatment with cisplatin (Huang et al., 2012). Cisplatin was also found to significantly lower total cellular glutathione in cervical cell lines (KB-3-1) (Doherty et al., 2014). Other studies have also reported a significant decrease in GSH upon drug treatment for other cells such as leukemia cells (Rainaldi et al., 2008), breast cancer (Bayet-Robert et al., 2010) and prostate cancer (Lodi and Ronen, 2011). GSH depletion is a contributing factor for cisplatin sensitivity in cancer cells (Byun et al., 2005). Glutathione or metallothioneins are cysteine-rich peptides, capable

of detoxifying the highly reactive aquo-complexes. Cisplatin resistance in ovarian cancer was reported to be directly proportional to increased intracellular glutathione (Lukyanova, 2010). Therefore, the current results suggest that oxidative damage is a major factor in the response of A2780 cells to cisplatin, but not in A2780CR cells. These data also suggest that the glutathione metabolic pathways are likely to be altered in A2780 cells compared with A2780CR cells. The higher levels of GSH and GSSG in the A2780CR cells suggest a more active role for GSH in these cells in comparison with A2780 cells.

Effects of cisplatin on nucleotide metabolism

Other than amino acid-related changes, consistent variations were observed for nucleotides which included guanosine triphosphate (GTP) and xanthine. These metabolites are derived from the purine pathway and they were altered in the sensitive cells in comparison with the resistant cells following treatment. Cisplatin has been reported to inhibit mitochondrial function and overall cellular energetics in renal cells (Brady et al., 1990; Kruidering et al., 1997). The GTP levels were lowered in both the sensitive and resistant cells, but were lowered to a greater extent in the sensitive cells. This observation is supported by recent studies that report a decrease in cellular GTP levels during treatment with anticancer agents and ischemic-induced apoptosis (Vitale et al., 1997; Cummings and Schnellmann, 2002; Dagher, 2000). It is also important to note that the effect of cisplatin on nucleotide sugars is likely to be cell-dependent (Duarte et al., 2013).

Effects of cisplatin on carbohydrate and energy metabolism

There are some significant differences in the carbohydrate composition between sensitive and resistant cells after treatment with cisplatin. The A2780 cells have lower levels of gluconic acid after cisplatin treatment. However, malate, 2-oxoglutarate, N-acetylneuraminate were found to be lower in resistant cells after cisplatin treatment in comparison with the sensitive cells. Levels of sorbitol were slightly decreased in the sensitive cells when treated with cisplatin and it was non-significant in resistant cells. A previous study shows that sorbitol was found to be increased in human lung cell samples at 48 h of cisplatin exposure, but the difference to control cells did not reach statistical significance (Duarte et al., 2013).

From the phenotype array experiment it is clear that glucose utilisation falls in the sensitive cells in comparison with the resistant cells following cisplatin treatment. Thus lower levels of ATP and NADH in the treated sensitive cells are consistent with lower rates of glucose metabolism. The two Krebs cycle metabolites oxoglutarate and malate are decreased more in the treated resistant cells in comparison with the treated sensitive cells and this might indicate greater flux through the TCA cycle. The levels of NAD⁺ are markedly lower in the cisplatin treated sensitive cells. This is consistent with the role of NAD⁺ depletion in promoting apoptosis (Scovassi and Poirier, 1999). The depletion of NAD⁺ in sensitive cells is also promoted by the depletion of ATP which is required for the re-synthesis of NAD⁺.

4.6 Conclusions

In this study, the *in vitro* effects of cisplatin on the metabolomic profiles of OCCs was examined. The intracellular metabolites of A2780 cells sensitive and A2780CR showed differential changes following cisplatin treatment at IC₅₀ concentrations within 24 h. The cisplatin-sensitive cells exhibit a much stronger metabolic response to cisplatin treatment than the resistant cells because the resistant cells may have developed a mechanism that inactivates the drug or transport of the drug across the cell wall. Cisplatin was found to induce pronounced effects on the metabolome of A2780 and A2780CR cells, producing alterations mainly in amino acid metabolism, carbohydrate, and oxidative phosphorylation. Significant decreases in arginine and proline metabolism pathway such as L-glutamate 5-semialdehyde, phosphocreatine, N₂-(D-1-carboxyethyl)-L-arginine, L-arginine, 5'-methylthioadenosine, and L-proline in A2780 and N-acetyl-L-glutamate and N₂-(D-1-carboxyethyl)-L-arginine in A2780CR cells, upon drug exposure. However, the strong effect of cisplatin on A2780CR was found in the TCA cycle/glycolysis pathway. Levels of malate, 2-oxoglutarate, and N-acetylneuraminate were found to be lower in resistant cells after cisplatin treatment in comparison with the sensitive cells. Many of the changes in the treated cells are consistent with a higher level of oxidative stress in the cisplatin sensitive cells.

Chapter 5

Comparative Metabolomic Profiling of the Synergistic Effects of Melittin in Combination with Cisplatin on Ovarian Cancer Cells Using Mass Spectrometry

5 Comparative Metabolomic Profiling of the Synergistic Effects of Melittin in Combination with Cisplatin on Ovarian Cancer Cells Using Mass Spectrometry

5.1 Abstract

Melittin has been proposed as to have potential for anticancer therapy, the addition of cisplatin to melittin may increase the response in cancer treatment via synergy and thus tolerability and decrease drug resistance. Cisplatin has been used for ovarian cancer treatment alone. However, evaluation of the effectiveness of different concentrations of melittin and cisplatin in procedural operation regarding changes in metabolomics was not yet studied. Thus this study was designed to compare the metabolomic effects of melittin in combination with cisplatin in A2780 and A2780CR ovarian cancer cells. Liquid chromatography (LC) coupled with mass spectrometry (MS) was applied to identify the key differential metabolites in A2780 (combination treatment 5 µg/mL Melittin + 2 µg/mL Cisplatin) and A2780CR (combination treatment 2 µg/mL Melittin + 10 µg/mL Cisplatin). Mzmine software in combination with a database search was used to convert MS out-put in order to perform pathway analysis. PCA and OPLS-DA multivariate data analysis models were produced using SIMCA-P software. All models displayed good separation between experimental groups, high-quality goodness of fit (R^2) and high-quality goodness of prediction (Q^2). The combination treatment induced significant changes in both cell lines led mostly to reduced levels of TCA cycle metabolites, oxidative phosphorylation, purine and pyrimidine metabolites and the arginine/proline pathway. The combination of melittin with cisplatin that targets these pathways has a synergistic effect. The melittin-cisplatin combination had stronger effect on A2780 cell lines in comparison with A2780CR. Overall, this study suggests

that a global metabolomics approach can be a useful tool for evaluating the pharmacological effects of anti-cancer compounds or synergetic sensitizers using mass spectrometry.

5.2 Introduction

What has emerged thus far is that bee venom, particularly the components melittin and phospholipase A₂, has potential anti-cancer and protective effects and is therefore an effective agent with regard to treating ovarian cancer, and that cisplatin, a commonly-used chemotherapy agent, produces certain measurable metabolic effects on cisplatin-resistant and cisplatin-sensitive ovarian cancer cells. This prompts the question as to what the combined effects of melittin, or bee venom and/or phospholipase A₂, and cisplatin would be, as well as what metabolomic investigations would reveal about the combined effects of those two agents.

Combination therapy has long been studied in the treatment of cancer, including ovarian cancer (Takakura et al., 2010). It is a logical approach, focusing on increasing response and tolerability to treatment while also decreasing resistance (Pinto et al., 2011). Unfortunately, it can be difficult to assess whether a particular combination will behave in a synergistic, additive, or antagonist fashion when used on a particular cancer patient. The only known way of determining their effectiveness is to identify specific measures, such as response rate, survival, or time to progression, and assess if or whether the new combination is able to achieve a significant increase (Pinto et al., 2011). Combination therapy is essentially cooperative: each agent involved should have non-overlapping toxicities, different mechanisms of action with minimal cross-

resistance, and individually proven in treatment by itself (Pinto et al., 2011).

Several cancers, including ovarian cancer, have demonstrated resistance or reduced sensitivity to cisplatin treatment, as well as causing significant health problems, such as nephrotoxicity, and prone to fostering relapse (Fontaine et al., 2015; Kim et al., 2013; Kim et al., 2015). Ideally, cisplatin in combination with a drug that diminishes the negative effects while enhancing the therapeutic effects would (1) decrease resistance or sensitivity while (2) offering protection against and/or mitigation of negative effects. For example, cisplatin (or carboplatin) in combination with taxans is now regarded as a novel standard of chemotherapeutic treatment in ovarian cancer, where the taxans enhance the tumour's radiosensitivity. Cisplatin and the adenovirus OBP-301 have been shown to work synergistically (Takakura et al., 2010).

Cisplatin shares cytotoxic synergy with bee venom. Bee venom makes sense as a complement to the cisplatin: it has protective effects in many areas of the body such as the blood and nerves (Chvetzoff et al., 1998); is able to inhibit cell growth in tumours (Choi et al., 2014); and has even been examined and used in complementary treatments that are necessitated by the effects of chemotherapy, such as allodynia (Lim et al., 2013) and neuropathy (Yoon et al., 2012). Cisplatin in combination with bee venom has been successfully used against human cervical and laryngeal carcinoma cells, including their drug-resistant sublines (Gajski et al., 2014) and human glioblastoma (Gajski et al., 2015).

Several studies have found that phospholipase A₂, another component of bee venom,

not only mitigates the negative impact of cisplatin on kidneys (Lee and Bae, 2016) but also boosts Treg numbers in the spleen and enhancing Treg traffic to the kidneys following cisplatin exposure; this is important, as Tregs play a significant role in many mechanisms, including inflammation and autoimmunity suppression (Lee and Bae, 2016; Kim et al., 2013; Kinsey and Okusa, 2014). A significant bonus in this dynamic is that bee venom has no impact on the anti-cancer properties of the cisplatin (Kim et al., 2013), meaning it in no way diminishes the effect of the cisplatin treatment. This is critical; a combinatory agent which diminishes any positive effects of the primary treatment undermines its effectiveness overall.

The effects that cisplatin and honey bee venom together have on ovarian cancer cells emerge from the synergistic relationship between the two agents (Alizadehnohi et al., 2012). Alizadehnohi et al. (2012) report that separately and together, the two agents induce apoptosis in human ovarian cancer cells; bee venom appears to enhance the cytotoxic impact of cisplatin. It also appears that melittin provokes responses in cisplatin-sensitive cells which led to decreasing levels of amino acids which in turn affect the energy metabolism of the tumour (Alonezi et al., 2016).

In order to understand these effects and the metabolic changes that the cisplatin-melittin combination has on ovarian cancer cells, metabolomic investigations can be undertaken. Metabolomics in the context of oncology usefully focus on diagnosis and prognosis, as well as evaluating the effectiveness of therapy (Palmnas and Vogel, 2013; Spratlin et al., 2009). One study employing nuclear magnetic resonance (¹H-NMR) spectroscopy to accurately separate serum metabolic profiles of three groups of

women: women with ovarian cancer, normal premenopausal women, and women with a benign ovarian disease (Odunsi et al., 2005). A Biolog Microassay and liquid chromatography-mass spectrometry (LC-MS) of individuals with cisplatin-resistant and sensitive ovarian cancer revealed that melittin affected the lipid composition of cells – an affect measurable by metabolomic tests (Alonezi et al., 2016). NMR spectroscopy has been used to produce and examine metabolic profiles in other cancers such as liver cancer (Zheng et al., 2015). In essence, the effects of the cytotoxic mechanisms of both cisplatin and melittin, together and separate, cause changes in cells which can be identified and measured through metabolomic tests, namely LC-MS, NMR, and certain assays.

The current study aimed to examine of metabolic effects of melittin in combination with cisplatin on A2780 and A2780CR human ovarian cancer cell lines. The effects of the cytotoxic mechanisms of both cisplatin and melittin on ovarian cancer cells was performed by LC/MS based metabolomics approach using a ZIC-pHILIC column. PCA and OPLS-DA multivariate data analysis models were performed using SIMCA-P software.

5.3 Materials and Methods

5.3.1 Cell lines and cultures

As detailed in section 2.2.1, Chapter 2.

5.3.2 Cell viability assay

Cell viability was assessed by an Alamar® Blue (AB) cell viability reagent (Thermo

Fisher Scientific, Loughborough, UK). Both A2780 and A2780CR cells were seeded at 1×10^4 cells/well in 96-well plates (Corning®, Sigma-Aldrich) and incubated at 37°C and 5% CO₂ in a humidified atmosphere for 24 h. To test the synergistic anti-proliferation effect, experiments were performed with A2780 and A2780CR cell lines by using the combination of melittin with cisplatin at various concentrations in medium, to assess possible synergistic/additive effects. Both A2780 and A2780CR cells were seeded at 1×10^4 cells/well in 96-well plates (Corning®, Sigma-Aldrich) and incubated at 37°C and 5% CO₂ in a humidified atmosphere for 24 h. For A2780 cell line, 3, 4, 5, and 6 µg/mL of melittin was combined with 2 µg/mL of cisplatin and 3, 4, and 5 µg/mL of cisplatin was combined with 3 µg/mL of melittin. For A2780CR cell line, 2, 3, 4 and 5 µg/mL of melittin was combined with 10 µg/mL of cisplatin and 20 and 30 µg/mL of cisplatin was combined with 2 µg/mL of melittin. Twenty hours after drug treatment, AB was added at a final concentration of 10% (v/v) and the resultant mixture was incubated for a further 4 h at 37°C and 5% CO₂. Then, the plates were read at an excitation wavelength of 560 nm and the emission at 590 nm was recorded on a SpectraMax M3 microplate reader (Molecular Devices, Sunnyvale, CA). All experiments were performed in triplicate.

5.3.3 Calculation of Combination Index (CI)

As detailed in section 2.2.3, Chapter 2.

5.3.4 Determination of effect of melittin in combination with cisplatin on cell metabolomes

The A2780 cell lines was treated with the combination of melittin and cisplatin at

concentrations of 5 and 2 $\mu\text{g}/\text{mL}$ respectively for 24 h (n=5). The A2780CR cells were treated with the combination of melittin and cisplatin at concentrations of 2 and 10 $\mu\text{g}/\text{mL}$ respectively for 24 h (n=5). The cells were seeded at 75×10^4 cells/mL in T-25 cell culture flasks and incubated for 1 doubling time (48 h) before treatment with the combinations and incubation for an additional 24 h. After the treatment, the medium was removed and the cells were washed twice with 3 mL of phosphate-buffered saline (PBS) at 37°C before lysis. Cell lysates were prepared by extraction with ice cold methanol: acetonitrile: water (50:30:20) (1 mL per 2×10^6 cells). The cells were scraped and cell lysates mixed on a Thermo mixer at 1440 rotations per minute (r.p.m.) for 12 min at 4°C , before being centrifuged at 13500 r.p.m. for 15 min at 0°C . The supernatants were collected and transferred into HPLC vials for LC-MS analysis. During the analysis, the temperature of the autosampler was maintained at 4°C . Mixtures of standard metabolites (Sigma-Aldrich, Dorset, UK) and the pooled quality control (QC) sample were injected in each analysis run in order to facilitate identification and to evaluate the stability and reproducibility of the analytical method. The pooled QC sample was obtained by taking equal aliquots from all the samples and placing them into the same HPLC vial.

5.3.5 Chromatographic conditions for column

A ZIC-pHILIC column was used to study the effects of cisplatin in combination with melittin on cisplatin resistant and cisplatin sensitive ovarian cancer cell metabolomes. As detailed in section 2.3.1, Chapter 2.

5.3.6 Liquid Chromatography–Mass Spectrometry (LC-MS) conditions

As detailed in section 2.4.1, Chapter 2.

5.3.7 Data extraction and analysis

As detailed in section 2.5, Chapter 2.

5.4 Results

5.4.1 The cytotoxicity of melittin in combination with cisplatin

The viabilities of the cisplatin-sensitive and cisplatin-resistant ovarian cancer cells (A2780 and A2780CR, respectively) treated with melittin or cisplatin were compared. Both single treatments exerted a concentration-dependent cytotoxic effect on A2780 and A2780CR cells (Figure 5.1). The cisplatin mediated growth inhibition of the sensitive cell line (A2780) was significantly greater than that of the melittin over the concentration range from 1 µg/mL to 8 µg/mL (Figure 5.1A; $P < 0.05$). However, the A2780CR cells were more resistant to cisplatin than were A2780 cells (Figure 5.1B). The 24 h half maximal inhibitory concentrations (IC_{50}) of cisplatin in A2780CR and A2780 cells, were 10.8 and 4.9 µg/mL, respectively (as previously described in chapter 4). Melittin exhibited toxicity against both A2780CR and A2780 cells, with IC_{50} values of 4.5 and 6.8 µg/mL, respectively (as previously described in chapter 3). The cytotoxicity of melittin in combination with cisplatin against A2780 and A2780CR cells was studied by using the alamar blue assay. The A2780 and A2780CR cells were treated for 24 h at various concentrations of melittin in combination with cisplatin. The percentage of surviving cells decreased in a dose-dependent manner in both the A2780 and A2780CR cells. The cytotoxic effects of melittin in combination with cisplatin on

A2780 and A2780CR cell lines are shown in figures 5.2A and 5.3A, respectively.

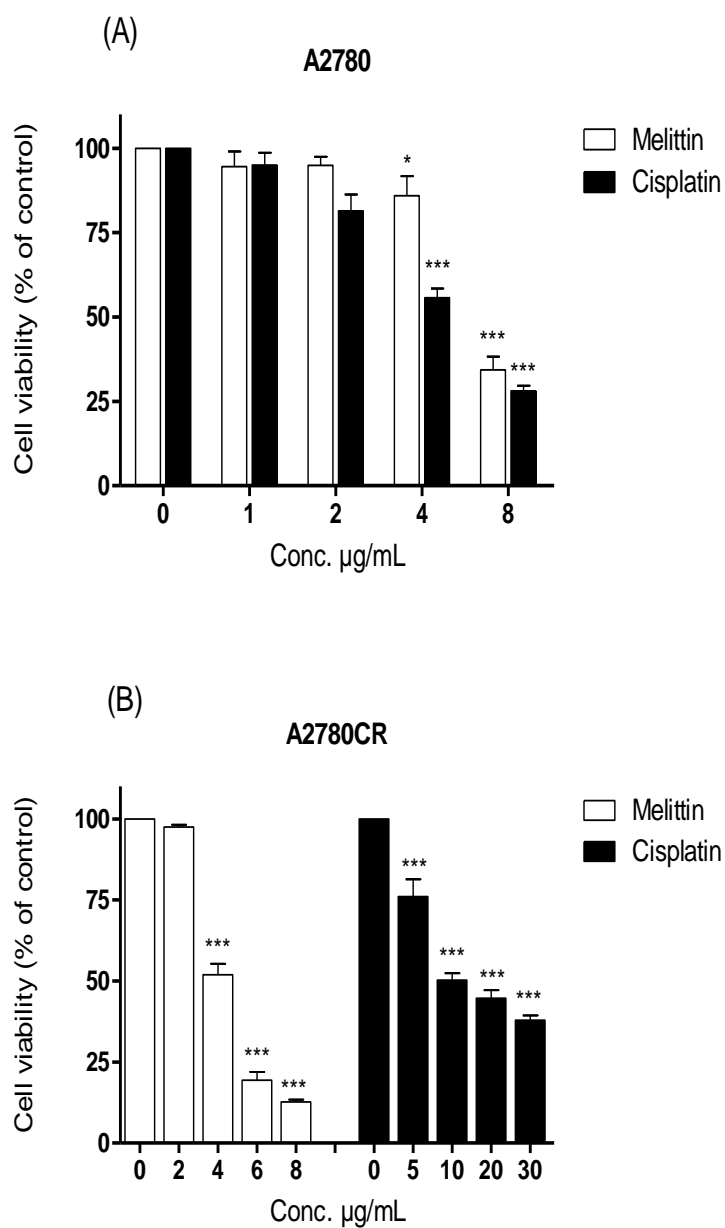


Figure 5.1. Examination of cell viability after treatment with either cisplatin or melittin alone with various concentrations on (A) A2780 cell line and (B) A2780CR cell line. * Significantly different from zero concentration at <0.05 ; *** Significant at <0.001 .

5.4.2 The combination index (CI)

In order to qualitatively evaluate whether the combination of melittin with cisplatin might cause synergistic cytotoxic effects, the value of CI, a commonly used evaluation index, was calculated. It has been proposed that CI values be interpreted as follows: <0.1 very strong synergism, 0.1-0.3 strong synergism, 0.3-0.7 synergism, 0.7-0.9 moderate to slight synergism, 0.9-1.1 nearly additive, 1.1-1.45 slight to moderate antagonism, 1.45-3.3 antagonism, and >3.3 strong to very strong antagonism (Patrick Reynolds and Maurer, 2005).

The combination index (CI) analyses showed that increased cytotoxic activity was observed in A2780 with the melittin+cisplatin combination at concentrations of 5+2 (CI= 0.647) and 6+2 (CI= 0.512) $\mu\text{g/mL}$ and with the cisplatin+melittin combination at concentrations of 4+3 (CI= 0.789) and 5+3 (CI= 0.711) $\mu\text{g/mL}$ and was due to synergy. However, the calculated CI was found to be > 1 in A2780 with the melittin+cisplatin combination at concentrations of 3+2 (CI= 2.812) and 4+2 (CI= 1.259) $\mu\text{g/mL}$ and thus could represent an antagonism effect (Figure 2B). The melittin/cisplatin combinations had CI between 0.7-0.9, indicating a moderate to slight synergism relationship in A2780CR at 2+10 (CI=0.888) and 5+10 (CI=0.741) $\mu\text{g/mL}$, as shown in figure 3B. CI value of melittin+cisplatin was 0.985 at concentrations 3+10 $\mu\text{g/mL}$ and 0.921 at concentrations 4+10 $\mu\text{g/mL}$ used to treat A2780CR, indicating a nearly additive effect. However, the calculated CI was found > 1 in A2780CR with the cisplatin+melittin combination at concentrations of 20+2 and 30+2 $\mu\text{g/mL}$ and thus could represent an antagonism effect.

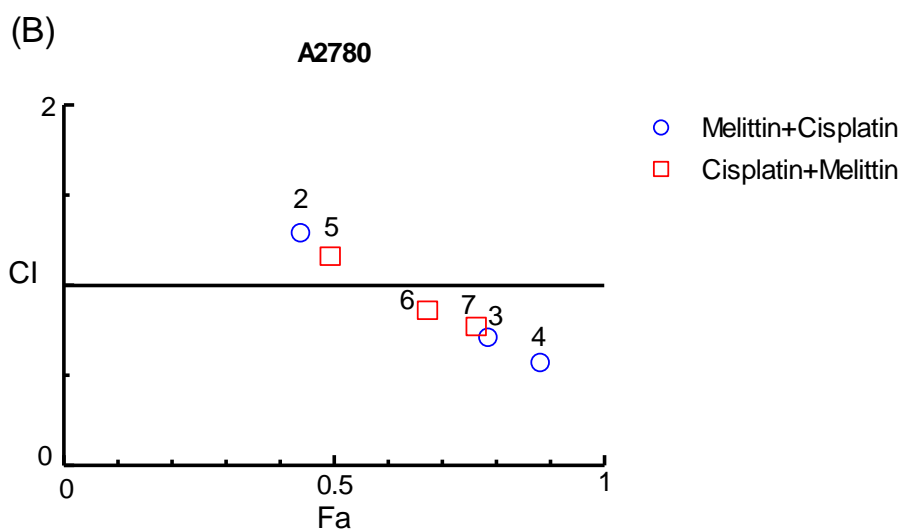
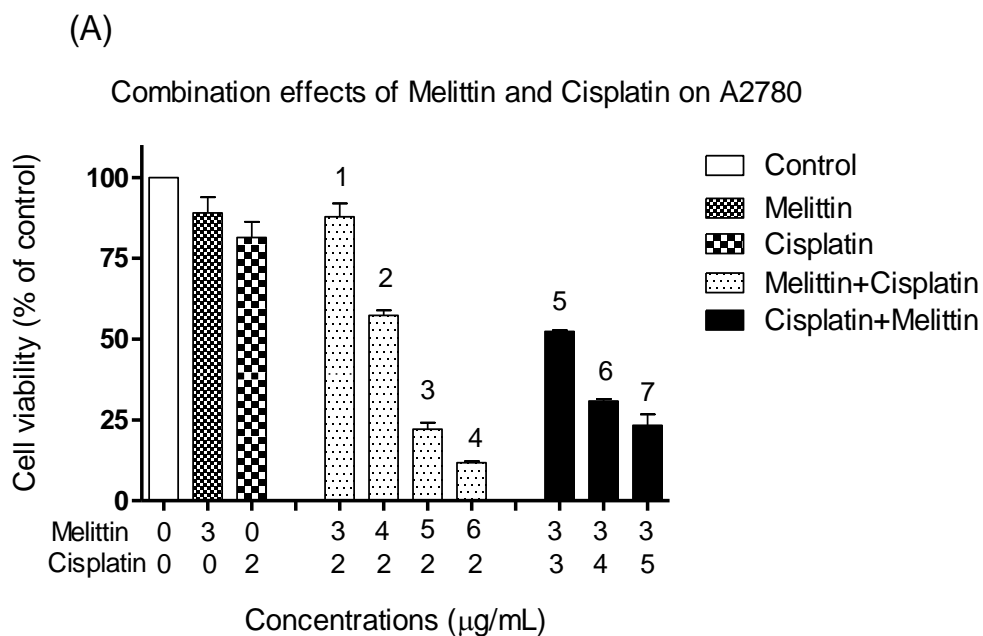


Figure 5.2. Effects of melittin in combination with cisplatin on (A) cell viability of A2780 cell lines and (B) Combination index. (A) The A2780 cells were treated with various concentrations of melittin+cisplatin for 24 hours. Bar graphs represent mean \pm SD values. (B) Combination index (CI) analysis was generated using the method of Chou and Talalay to determine the extent of synergy if any for melittin + cisplatin on A2780 cell lines.

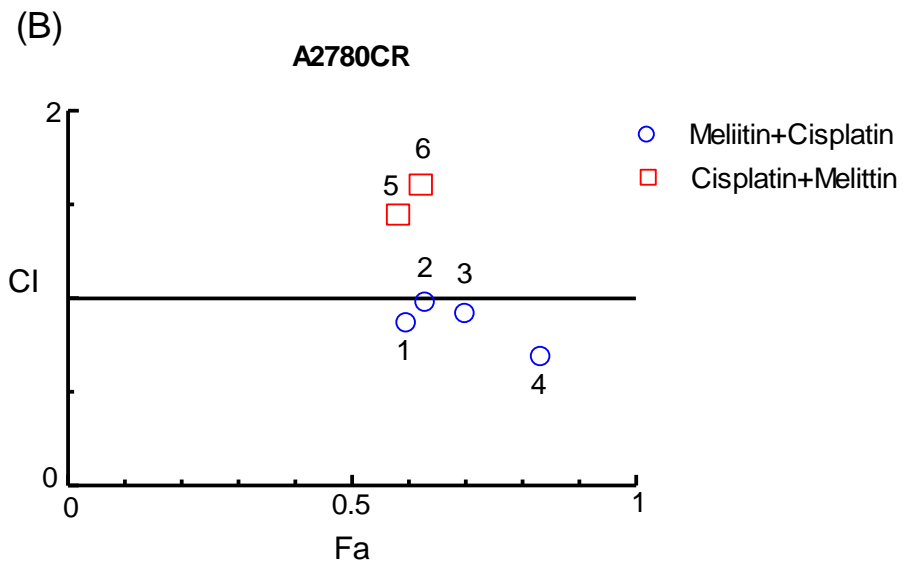
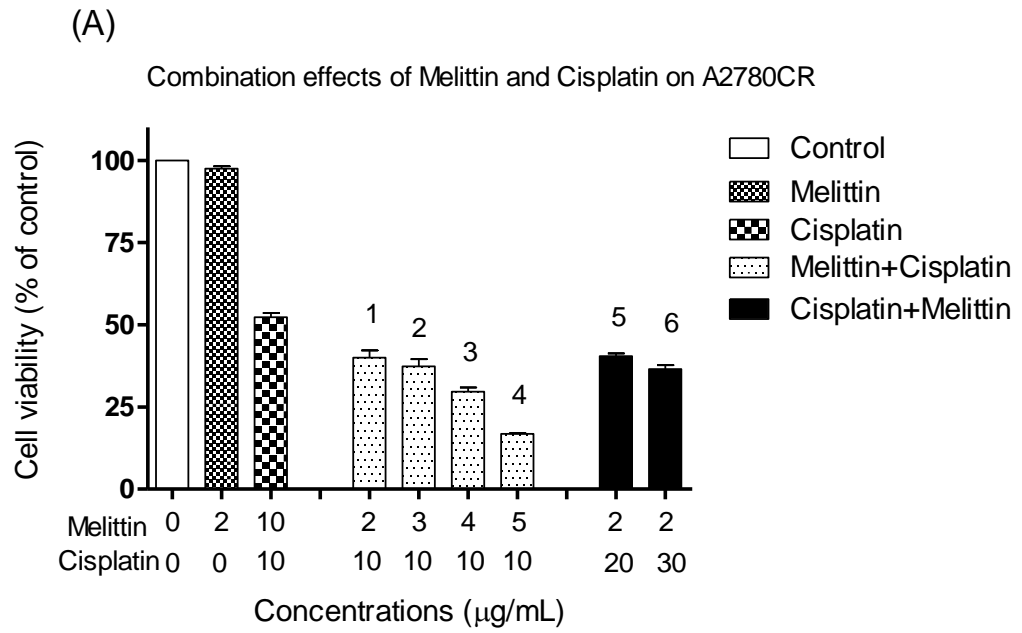


Figure 5.3. Effect of melittin in combination with cisplatin on (A) cell viability of A2780CR cell lines and (B) Combination index. (A) The A2780CR cells were treated with various concentrations of melittin+cisplatin for 24 hours. Bar graphs represent mean \pm SD values. (B) Combination index (CI) analysis was generated using the method of Chou and Talalay to determine the extent of synergy if any for melittin +cisplatin on A2780CR cell lines.

5.4.3 Metabolome analysis

The metabolic effects of melittin in combination with cisplatin on ovarian cancer cells were assessed using an LCMS based metabolic approach. Univariate and multivariate statistical analyses were used to examine the effect of combination 1 (5 $\mu\text{g}/\text{mL}$ of Melittin + 2 $\mu\text{g}/\text{mL}$ Cisplatin) and combination 2 (2 $\mu\text{g}/\text{mL}$ of Melittin + 10 $\mu\text{g}/\text{mL}$ Cisplatin) on A2780 and A2780CR cells, respectively.

A clear separation of A2780 and A2780CR cells was achieved indicating unique metabolite profiles for the treated and control cells on the PCA and OPLSDA scores plots at both combinations (Figure 5.4 A and B, respectively). Pooled quality control (QC) samples were injected in the analysis run in order to quantify the precision of the measurements (Figure 5.4 A). The PCA model parameters and validation of the plot suggested a good model (4 components, R^2X (cum) = 0.918; Q^2 (cum) = 0.856). There was also a very clear separation of A2780 and A2780CR cells obtained by using OPLS-DA for classifying the treated and control samples. The OPLS-DA model parameters and validation of the plot suggested a strong model (R^2X (cum) 0.916, R^2Y (cum) 1, Q^2 (cum) 0.975), three components), and the CV-ANOVA for this model was $1.28\text{E-}24$. Hierarchical clustering analysis of metabolomics data showed distinct separation between the control and treated samples (Figure 5.5).

There was a very clear separation of the treated versus untreated A2780 cells obtained by using OPLS-DA model based on the significant metabolites (Figure 5.6 A). The model parameters and validation of the plot suggested a strong model (2 components, R^2X (cum) = 0.965, R^2Y (cum) = 1, Q^2 (cum) = 0.996, CV-ANOVA= $2.62\text{E-}6$, two

components). To test the validity a ROC and permutation test were also applied (Figure S5.1, appendix). The AUC for a ROC classification is regarded as excellent when $AUC > 0.9$. The OPLS-DA model classified the treated and untreated A2780 cells into two groups, and the AUC of the ROC for the groups were in the excellent to perfect classification.

In case of the A2780CR cells, OPLS-DA models were also generated by comparing control and treated samples based on the significant metabolites (Figure 5.6 B). However, a clear separation was also found between the treated and untreated samples and the CV-ANOVA for this model was $8.42E-6$ (R^2X (cum) = 0.966, R^2Y (cum) = 1, Q^2 (cum) = 0.994, two components). Furthermore, the validity of the ROC and permutation test showed the constructed OPLS-DA model was valid (Figure S5.2, appendix).

For univariate statistical analysis of candidate specific biomarkers in OCC's after exposure to the combinations, the false discovery rate (FDR) was used to reduce the probability of false positive results. Changes in various classes of metabolites, especially mitochondrial Krebs cycle, energy metabolism, nucleotide and amino acids metabolism. A list of the metabolites is shown in Table 5.1.

The major impression is that the combination of melittin and cisplatin has radically changed the metabolites affected in comparison with the effects of each agent alone which were described in chapters 3 and 4.

It can be observed that there is a strong reduction the levels of metabolites involved in Krebs cycle and energy metabolism. Several metabolites in the TCA cycle were decreased in sensitive and resistant cells after treatment with the combinations including citrate, 2-oxoglutarate, malate and phosphoenolpyruvate. Treatment with the combinations also reduced the levels of ATP in both cell lines. It should be noted that combination 1 had stronger effect on the ATP levels in the A2780 cells than combination 2 in the A2780CR cells. There were also marked decreases in levels of pentose phosphate pathway metabolites in both cell lines after treatment. Moreover, there were important differences in purine and pyrimidine composition between the two cell lines after treatment with the combinations.

The most affected metabolites due to the combination treatment in both cell lines compared to the other pathways were involved in amino acid metabolism. In A2780 cells, the metabolite of valine methyloxobutanoic acid increased, while there were decreases in many amino acids related to arginine and proline metabolism. In A2780CR cells, a significant increase was observed in the levels of S-adenosyl-L-methionine, 5'-methylthioadenosine, L-lysine, and L-serine.

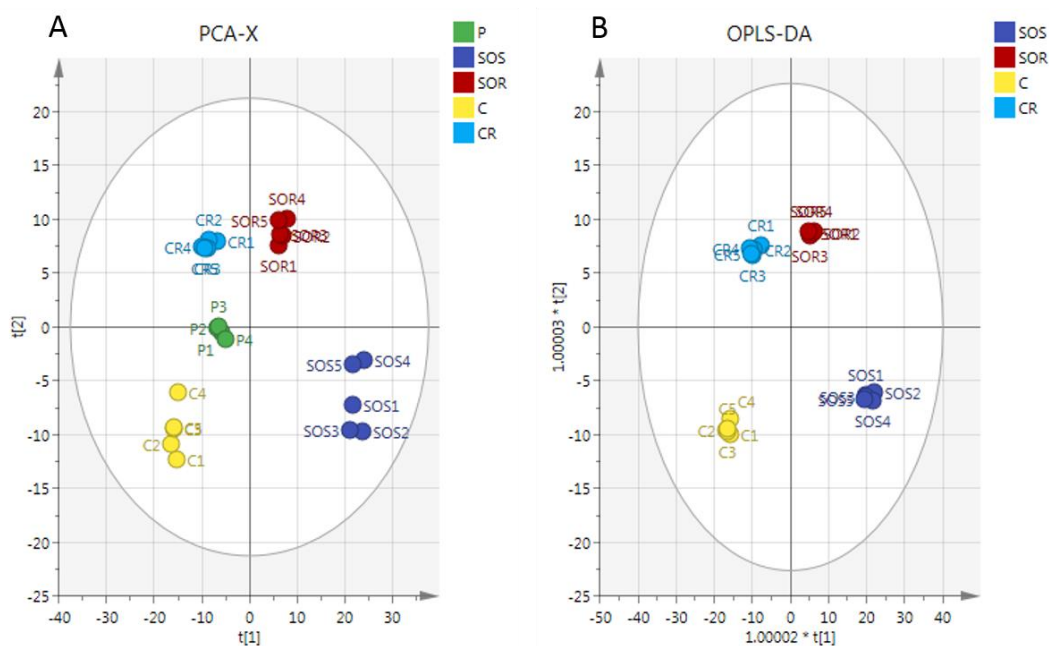


Figure 5.4. (A) PCA vs (B) OPLS-DA. PCA and OPLS-DA scores plot generated from PCA and OPLS-DA using LC-MS normalized data of cells after exposure to combination (Melittin+Cisplatin) and controls of A2780 and A2780CR cell lines. A2780-treated cells at 5 $\mu\text{g}/\text{mL}$ Melittin + 2 $\mu\text{g}/\text{mL}$ Cisplatin (SOS); untreated A2780 cells (C); A2780CR -treated cells 2 $\mu\text{g}/\text{mL}$ Melittin + 10 $\mu\text{g}/\text{mL}$ Cisplatin (SOR); untreated A2780CR (CR); Quality control (QC) samples (P).

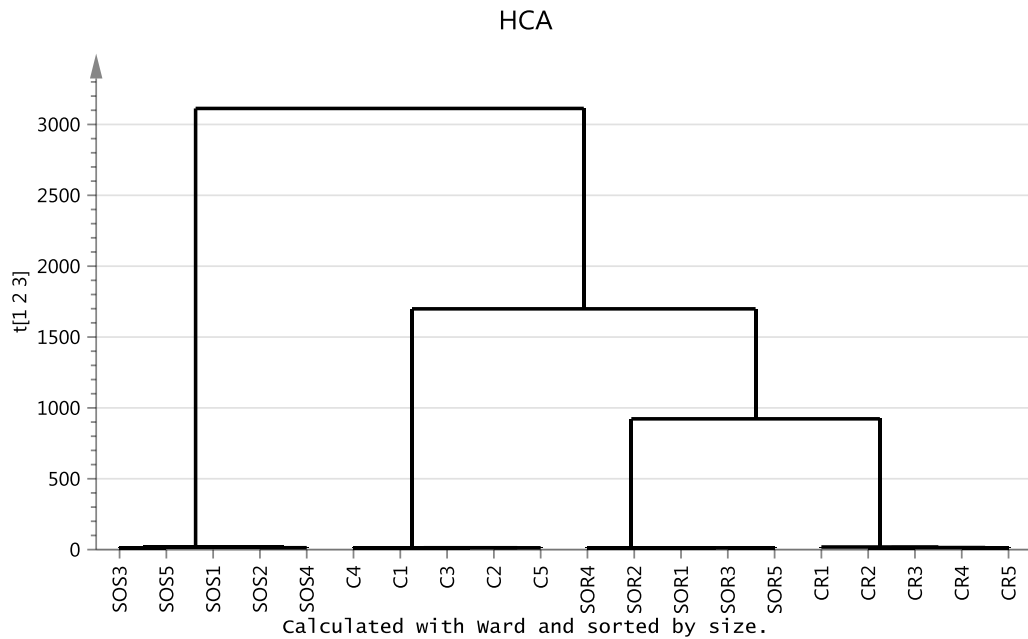


Figure 5.5. Hierarchical clustering analysis (HCA) of 20 ovarian cancer cell samples. It shows two main groups and four subgroups. The groups: CR, control of cisplatin resistance cell lines; SOR: A2780CR after treatment with melittin+cisplatin; C, control of cisplatin sensitive cell lines; SOS, A2780 after treatment with melittin+cisplatin.

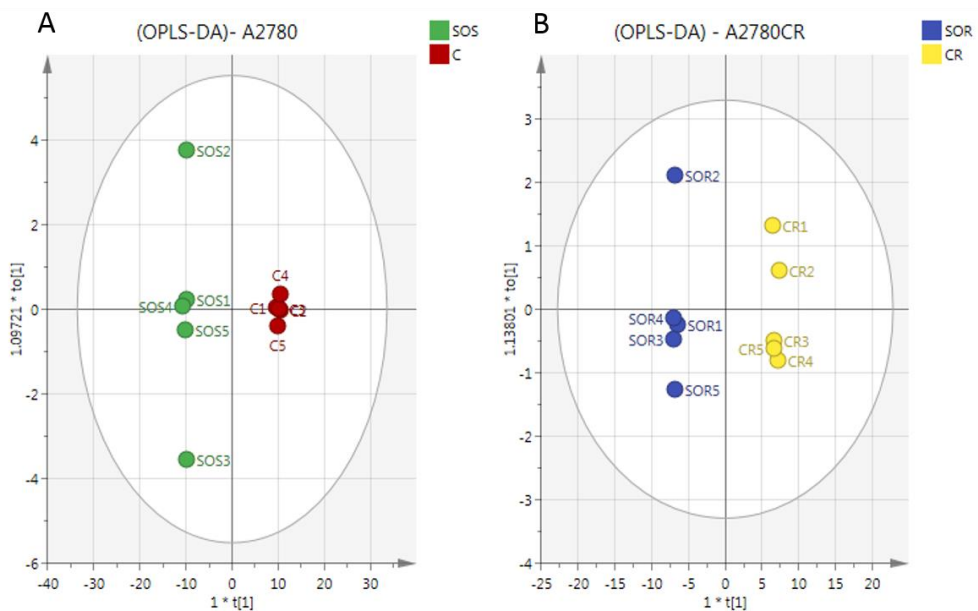


Figure 5.6. OPLS-DA score plot of (A) A2780 cell lines before and after treatment with melittin+cisplatin; (B) A2780CR cell lines before and after treatment with melittin+cisplatin.

Table 5.1. Statistical differentiating of melittin in combination with cisplatin at 5 µg/mL Melittin + 2 µg/mL Cisplatin on metabolites of A2780 and at 2 µg/mL Melittin + 10 µg/mL Cisplatin on A2780CR.

m/z	RT min	Metabolites	SR/CR		SS/C	
			p-value	Ratio	p-value	Ratio
Citrate cycle (TCA cycle)/glycolysis						
338.989	18.1	*D-Fructose 1,6-bisphosphate	<0.001	0.278	<0.001	0.246
115.004	16.0	*Fumarate	<0.001	0.227	<0.01	0.402
133.014	16.1	*(S)-Malate	<0.001	0.218	<0.001	0.062
145.014	15.7	*2-Oxoglutarate	<0.001	0.324	<0.001	0.048
191.02	18.1	*Citrate	<0.001	0.588	<0.001	0.172
173.009	17.9	*cis-Aconitate	<0.001	0.490	<0.001	0.072
166.975	17.5	*Phosphoenolpyruvate	<0.001	0.344	<0.05	0.082
Oxidative phosphorylation						
664.116	14.2	NAD+	<0.001	0.294	<0.001	0.067
508.003	16.2	ATP	<0.001	0.362	<0.001	0.073
Glycine/Serine/ Cysteine and Glutathione metabolism						
241.031	16.3	*L-Cystine	ns	1.739	ns	1.832
427.095	17.1	S-glutathionyl-L-cysteine	ns	0.750	<0.001	0.218
152.002	14.6	3-Sulfinyl-L-alanine	ns	0.706	<0.001	0.139
308.091	14.5	*Glutathione	<0.001	0.562	<0.001	0.092
179.048	14.4	L- Cysteinylglycine (Cys-Gly)	<0.001	0.521	<0.001	0.067
223.074	17.1	L-Cystathionine	<0.001	0.438	<0.001	0.004
76.0394	15.7	*Glycine	ns	1.050	<0.001	0.142
116.035	10.8	L-2-Amino-3-oxobutanoic acid	<0.001	0.319	<0.001	0.317
106.050	15.8	*L-Serine	<0.001	7.112	<0.001	0.420
Pentose phosphate pathway						
195.051	13.7	*D-Gluconic acid	<0.001	0.147	<0.001	0.093
308.978	16.5	D-Ribose 1,5-bisphosphate	<0.001	0.259	<0.001	0.124
149.046	11.9	*D-Ribose	<0.001	0.222	<0.001	0.285
229.012	15.8	*D-Ribose 5-phosphate	<0.001	0.545	<0.001	0.131
Lysine biosynthesis						
170.046	14.3	2,3,4,5-Tetrahydrodipicolinate	<0.001	0.245	<0.001	0.112
147.113	24.3	*L-Lysine	<0.001	1.966	ns	0.724
162.112	13.3	*L-Carnitine	<0.001	0.508	<0.001	0.135
243.074	17.2	5-Phosphonooxy-L-lysine	<0.001	0.303	<0.001	0.006
128.071	15.5	2,3,4,5-Tetrahydropyridine-2-carboxylate	<0.001	0.433	<0.001	0.271

Table 5.1. (Contd.)

m/z	RT	Metabolites	SR/CR		SS/C	
			p-value	Ratio	p-value	Ratio
Purine metabolism						
137.046	10.2	*Hypoxanthine	<0.001	16.99	<0.01	7.87
152.056	12.4	*Guanine	<0.001	13.19	<0.01	102.21
348.07	13.8	*AMP	<0.001	0.372	<0.001	0.190
428.036	15.0	*ADP	<0.001	0.376	<0.001	0.163
442.018	17.8	GDP	<0.001	0.509	ns	0.104
521.984	18.9	*GTP	<0.001	0.442	<0.001	0.079
426.013	16.9	Adenylyl sulfate	<0.001	0.271	<0.01	0.014
Pyrimidine metabolism						
155.01	10.3	*Orotate	<0.001	0.218	<0.001	0.050
129.066	14.8	5,6-Dihydrothymine	<0.001	0.326	<0.001	0.120
480.982	15.8	dTTP	<0.001	0.337	<0.001	0.347
175.036	16.8	N-Carbamoyl-L-aspartate	<0.001	0.036	<0.001	0.017
115.05	14.7	5,6-Dihydrouracil	<0.001	0.383	<0.001	0.079
402.995	16.4	*UDP	<0.001	0.485	<0.001	0.035
484.975	17.6	*UTP	<0.001	0.465	<0.001	0.059
323.029	15.2	*UMP	ns	1.195	<0.001	0.282
Arginine/ Proline/ Glutamate/Methionine metabolism						
188.057	14.3	N-Acetyl-L-glutamate	<0.001	0.241	<0.001	0.029
176.103	15.8	*L-Citrulline	<0.001	0.521	<0.001	0.189
173.104	25.8	*L-Arginine	ns	1.161	<0.001	0.379
130.051	14.5	L-Glutamate 5semialdehyde	<0.001	0.538	<0.001	0.235
116.071	12.8	*L-Proline	<0.001	0.568	<0.001	0.228
399.144	16.3	S-Adenosyl-L-methionine	<0.001	2.005	<0.001	0.115
298.096	6.4	*5'-Methylthioadenosine	<0.05	2.016	<0.001	0.158
146.093	15.1	*4-Guanidinobutanoate	<0.001	0.325	<0.001	0.055
291.129	16.8	N-(L-Arginino) succinate	<0.001	0.260	<0.001	0.010
247.14	14.2	N2-(D-1-Carboxyethyl)-L-arginine	<0.001	0.170	<0.001	0.010
174.087	15.3	5-Guanidino-2 oxopentanoate	<0.001	0.680	<0.001	0.058
132.077	14.7	*Creatine	<0.001	0.403	<0.001	0.075
210.029	15.2	*Phosphocreatine	<0.001	0.422	<0.001	0.051

Table 5.1. (Contd.)

m/z	RT	Metabolites	SR/CR		SS/C	
			p-value	Ratio	p-value	Ratio
Miscellaneous						
110.027	14.9	Hypotaurine	<0.001	0.139	<0.001	0.009
115.04	8.2	3-Methyl-2-oxobutanoic acid	<0.001	0.191	<0.05	5.604
166.053	13.4	L-Methionine S-oxide	<0.01	0.470	<0.001	0.250
218.067	13.9	O-Succinyl-L-homoserine	<0.001	0.082	<0.001	0.011
181.051	9.0	3-(4-Hydroxyphenyl)lactate	<0.001	0.656	<0.001	0.087
204.123	11.1	*O-Acetylcarnitine	<0.001	0.137	<0.001	0.021
176.056	10.3	4-Hydroxy-4-methylglutamate	ns	1.911	<0.001	0.022
159.076	15.8	4-Methylene-L-glutamine	<0.001	0.607	ns	0.258
175.025	14.4	*Ascorbate	<0.001	0.067	<0.001	0.024
165.041	13.0	L-Arabinonate	<0.001	0.372	<0.001	0.166
179.056	17.1	Hexose	<0.05	0.670	<0.05	0.334

RT: min; SR: combination 2 treated A2780CR; CR: control A2780CR; SS: combination 1 treated A2780; C: control A2780; ns: non-significant. * Retention time matches standard.

5.5 Discussion

Cisplatin is one of the most effective anticancer drugs currently used for treating many types of cancer, however, it comes with serious side effects. Combination therapy has been the standard of care, especially in cancer treatment, since it is a rationale strategy to increase response and tolerability and to decrease resistance (Pinto et al., 2011).

The present study aimed to determine whether melittin, a cytotoxic peptide from bee venom, possesses an inhibitory effect in combination with cisplatin on both A2780 and A2780CR cells or whether it has a synergistic effect with cisplatin. Analysis of cytotoxicity by the alamar blue assay confirmed the cytotoxic effects of melittin in combination with cisplatin at various concentrations. Recent studies have reported that

components of bee venom may exert an anti-tumor effect on human ovarian cancer and that it has the potential for enhancing the cytotoxic effect of the antitumor agent cisplatin (Alizadehnohi et al., 2012). Different melittin/cisplatin mechanisms could interact to either reduce or increase anticancer efficacy, thus producing three possible effects: 1) Additive, when the combined effect is equal to the sum of individual effects; 2) Antagonist, when the effect of one or both compounds is less when they are applied together than when individually applied; 3) Synergism, when the effect of combined substances is greater than the sum of the individual effects (Chou and Talalay, 1983). Combination index analysis of the melittin in combination with cisplatin showed that on A2780 cells the combinations had a synergistic effect at high concentrations of melittin and cisplatin. In contrast, the combination of melittin and cisplatin can be cytotoxic to A2780 at concentrations of 3+2 and 4+2 $\mu\text{g/mL}$ (melittin+cisplatin). Synergistic effects were observed in A2780CR cells when the melittin was combined with cisplatin at 2+10 and 5+10 $\mu\text{g/mL}$, while with a fixed concentration of melittin and variable concentrations of cisplatin in combination antagonist effects were observed. Suggesting that melittin somehow inhibited the effect of cisplatin on A2780CR cells. Using the median effect equation of Chou and the combination index equation of Chou and Talalay, quantitation of synergism or antagonism at different concentrations and the selection the best pair of drugs to combine for potentially maximal antitumor efficacy (Chou and Talalay, 1984; Chou et al., 1994). This method of analysis has been useful in identifying combinations of anticancer agents (Chang et al., 1985; Bible and Kaufmann, 1997).

In the current study, untargeted metabolomics was performed in order to compare the

metabolic profile of the metabolic composition of A2780 and A2780CR cells treated with melittin-cisplatin combination using LC-MS based metabolomics approach, with OPLS-DA models displaying good separation between the experimental groups, high-quality goodness of fit (R^2), and high-quality goodness of prediction (Q^2). With respect to ovarian cancer cells (OCC's), several previous metabolomics studies have analyzed the metabolic responses of OCC's to various compounds (Wang et al., 2013; Vermeersch et al., 2014; Tolstikov et al., 2014). Additionally, there have been some previous metabolomic studies on the comparison between effects of cisplatin on squamous cancer cell lines -sensitive and resistant to cisplatin (Huang et al., 2012), and the effects of docetaxel on ovarian cancer stem cells (Vermeersch et al., 2014). Alonezi et al., employed a metabolomics approach to assess the effects of melittin monotherapy on the ovarian cancer cell lines that revealed significant changes in amino acid and carbohydrate metabolism in ovarian cancer cells (Alonezi et al., 2016). Although Alonezi et al. study demonstrated profound the metabolic changes in ovarian cancer cells after melittin monotherapy, there has been no metabolomic study to date that has comparatively profiled the metabolite composition of OCC's treated by a combination of melittin and cisplatin. A previous study suggested that combination therapy is more effective than monotherapy on cancer cells such as hepatocellular carcinoma (Zheng et al., 2015).

The metabolomics analysis demonstrated that distinct metabolic profiles can be detected for the effects of the combinations of melittin and cisplatin on the A2780 and A2780CR cells. The intracellular metabolites of A2780 cells showed differential changes following combination 1 treatment. In addition, the intracellular metabolites

of A2780CR cells showed differential changes following combination 2 treatment. It should be noted that these concentrations were chosen based on cytotoxicity assay and CI value for synergy to allow detection of a combination effect rather than to achieve maximal anticancer effect. The most altered metabolites in A2780 and A2780CR cells could be categorized under amino acid, energy, carbohydrate and nucleotide metabolism. Most of the altered metabolites participate in more than one pathway in significant ways and the change in that one metabolite could have a resonating effect for other pathways.

There was a very clear effect of the combination treatment on the purine and pyrimidine pathways. This was different from the metabolic shifts observed for melittin and cisplatin alone suggesting the combination has quite a different effect on the cells. There was a very large increase in levels of the adenine metabolite hypoxanthine, and guanine in both cell lines. This possibly indicates that the combination of melittin with cisplatin is promoting adduct formation with DNA in comparison with the treatment with cisplatin alone discussed in chapter 4. The adducts formed with cisplatin are mainly intra-strand crosslinks joining two guanine residues and to lesser extent intra-strand links between guanine and adenine (Chaney et al., 2005). DNA is repaired by excision of damaged bases and this would correlate with hugely increased levels of guanine and hypoxanthine although this presumes that the cisplatin adduct somehow breaks down during the excision. The levels of purine metabolites AMP, ADP and GTP were decreased in both cell lines by the combination treatment. In a previous study it was found that FK866, a small molecule inhibitor of NAMPT, caused significant metabolic changes in purine metabolism in ovarian cancer

and colorectal cancer cells (Tolstikov et al., 2014). Moreover, Zhou et al. study in hepatocellular carcinoma (HepG2 cells) showed that high-dose sorafenib treatment affects purine metabolism with significant decreases in GTP levels after sorafenib treatment (Zhou and Luo, 2013). Although Zhou et al. study demonstrated profound dose-dependent metabolic changes in HepG2 cells after sorafenib monotherapy, they showed that everolimus in combination with first-line sorafenib therapy results in more pronounced metabolic changes to pyruvate, amino acid, methane, glyoxylate and dicarboxylate, and glycolysis or gluconeogenesis in hepatocellular carcinoma cells (Zheng et al., 2015). Other than purine metabolite changes, consistent variations were observed for pyrimidine metabolism. The levels of pyrimidine metabolites such as orotate, dihydrothymine, dihydrouracil and UTP were reduced in both cell lines after exposure to the melittin-cisplatin combinations. The reason for the decrease in pyrimidine metabolites is not clear. Normally DNA damage might be associated with increased levels of dihydrothymine which is produced by excision of damaged thymine residues from DNA.

The many altered metabolites belonged to amino acid metabolism pathways. Most of the metabolites were grouped under the arginine and proline pathways were reduced in sensitive cells after the combination treatments; while arginine metabolite was non-significantly altered in resistant cells. Similarly, our previous study examined the effect of melittin on A2780 and A2780CR cells which showed that the level of arginine was downregulated in cisplatin sensitive cells compared with resistant cells (Alonezi et al., 2016). The results presented in chapters 3 and 4 showed that the A2780 cell line contained lower levels of arginine than A2780CR. A number of studies reported that

arginine deficiency enhances apoptosis in different cell lines include human lymphoblastic cell lines (Gong et al., 2000), mesothelioma cells (Szlosarek et al., 2006), and melanoma cell lines (Feun et al., 2008). Some human cancers, such as melanoma and hepatocellular carcinoma (Ensor et al., 2002), do not express arginosuccinase synthase and therefore are unable to synthesize arginine from citrulline (Lind, 2004). A recent study observed that ovarian carcinoma SKOV3 cells under arginine deprivation showed increased sensitivity to treatment with paclitaxel, a chemotherapy drug used to treat cancers, at low doses. In this context, it is to be noted that paclitaxel is a disruptor of the cytoskeleton and negatively impacts on the autophagosome-lysosome fusion step (Shuvayeva et al., 2014). A previous study suggested that combinational treatment based on arginine deprivation and an autophagy inhibitor (for example chloroquine, a known nontoxic antimalarial drug) can potentially be applied as a second line treatment for a subset of ovarian carcinomas deficient in argininosuccinate synthetase (Shuvayeva et al., 2014). It was also observed that the development of chemoresistance to platinum compounds in ovarian carcinomas leads to collateral appearance of arginine auxotrophy due to the downregulation of argininosuccinate synthetase (Nicholson et al., 2009). The exact mechanism whereby deficiency arginine biosynthesis confers resistance remains unclear.

There was a strong effect of the combination treatment on cellular cysteine and glutathione metabolism; S-glutathionyl-L-cysteine, 3-sulfino-L-alanine, glutathione, L-cysteinylglycine (Cys-Gly), and L-cystathionine were all lower in cisplatin sensitive cells compared with resistant cells after treated with the combinations. However, L-

cysteine was increased in both cell lines but it was non-significant. Cysteine metabolism is one of the downstream metabolic tributaries of the glutathione pathway (Poisson et al., 2015). In a previous study it was found that the level of glutathione was higher in resistant cells (A2780-CP20) than in sensitive cells (A2780) (Mohell et al., 2015). This finding resemble to our results in which the level of glutathione was higher in resistant cells than sensitive cells. Two of the main reasons for platinum resistance in ovarian cancer cells are the p53 mutation and drug-induced increases in intracellular glutathione concentration. A study by Mohell et al. showed that methylene quinuclidinone (MQ), in addition to binding to cysteine residues in p53, also binds to the cysteine in glutathione, a tripeptide formed by glutamic acid, cysteine and glycine, decreasing intracellular free glutathione levels in ovarian cancer cells (Mohell et al., 2015). Therefore, it is possible that the combinations binds to free cysteine and thereby inhibits glutathione synthesis in OCC's. The previously mentioned study by Mohell et al. observed that combination effects of APR-246 (which is a prodrug that is converted to the active compound MQ) with doxorubicin were cause DNA damage response, including activation of the p53 pathway leading to apoptosis (Mohell et al., 2015). Moreover, recent metabolomics based studies in ovarian cancer cells have demonstrated that gossypol decreases cellular levels of GSH and induces apoptosis through oxidative stress (Wang et al., 2013). Similarly, in our study we found that the level of glutathione was decreased following the combinations treatment in sensitive and resistant cells. It should be noted that the stronger effect was on A2780 cells that could be because they contain lower levels of glutathione. Furthermore, it could be possible that combination effects of melittin with cisplatin caused a DNA damage response, including activation of the p53 pathway leading to apoptosis.

L-cysteine is a product of glycine, threonine, and serine metabolism. Increased serine biosynthesis is one of many metabolic changes that have been reported in cancer cells (Davis et al., 1970; Snell, 1984), and serine is a central node for the biosynthesis of many molecules such as glycine and cysteine (Locasale, 2013). High levels of serine in cancer cells have been linked to increase rates of cell proliferation (Mattaini et al., 2016). The level of serine was increased in resistant cells following the combination treatment. In contrast, treatment of the sensitive cells where treatment with the combination resulted in a decrease of serine within the cells and a further lowering of the nonessential amino acid glycine. Glycine is incorporated directly into purine nucleotide bases and into glutathione (GSH). The conversion of serine to glycine, catalysed by serine hydroxymethyltransferase (SHMT), donates a one-carbon unit to tetrahydrofolate to produce 5, 10-methylenetetrahydrofolate (CH₂-THF). CH₂-THF is used in thymidine synthesis and is a precursor of other folate species that contribute to purine synthesis (Mattaini et al., 2016). The difference in ovarian cancer cells could be reflected at cellular level in terms of differences in the metabolite profiles. Serine is required for a number of biosynthetic and signalling pathways, including the production of phospholipids such as sphingolipids and phosphatidylserine. Serine is necessary for the production of sphingolipids via the synthesis of sphingosine, and serine is a precursor for phospholipids (Mattaini et al., 2016). Previous studies have shown that serine biosynthesis appears to be part of an adaptive response to oxidative stress (Maddocks et al., 2013). The tumour suppressor p53 is emerging as an important regulator of cellular metabolism. P53 is a key player in the cellular response to stress in the form of numerous challenges, including DNA damage, hypoxia, and oncogene activation (Vousden and Prives, 2009). Cells lacking p53 fail to respond to serine

starvation due to oxidative stress, which would normally lead to reduced viability and severely impaired proliferation (Amelio et al., 2014).

The level of ATP was found reduced in both cell lines after the combinations treatment. The sensitive cells have lower levels of ATP after treatment in comparison with the resistant cells. ATP was found more reduced in both cell lines when they treated with the combinations compared with the results discussed in chapter 3. Since glycolysis provides ATP and energy in most cell types, but cancer cells extensively use glycolysis to sustain anabolism, which is necessary for tumour growth (Amelio et al., 2014). We found that the combinations inhibited glycolysis in both cell lines as indicated by lower levels of fructose biphosphate and phosphoenolpyruvate. In addition several TCA cycle intermediates were lowered. Cell death can be executed by different mechanisms, including apoptosis, autophagy, necrosis, or combinations of these processes. Although different cell death mechanisms are unique in their molecular signalling cascades, one molecule is involved in the processes that mediates all types of cell death; adenosine-5'-triphosphate (ATP). During late-stage apoptosis, ATP levels sharply drop, mostly because of the loss of mitochondrial function and consumption by ATP-dependent proteases. In autophagy, a rescue process of self-degradation to compensate for energy paucity is also featured with ATP insufficiency prior to cell death (Lemasters et al., 2002; Skulachev, 2006). During necrosis, depletion of ATP precedes mitochondrial permeability changes (Vanlangenakker et al., 2008). The fact that ATP deprivation occurs in all types of cell death suggests that energy metabolism may play a critical role in the survival of cancer cells under stress. Thus, it could be possible that the A2780 cells maybe undergoing late-stage apoptosis

cell death in response to the combination 1 treatment whereas the A2780CR maybe undergoing early-stage apoptosis cell death. In our study, we found that combination 1 inhibited glycolysis in A2780 cells by depletion the level of NAD⁺. Moreover, the level of NAD⁺ was found decreased in A2780CR cells after combination 2 treatment. It appears that the combinations had more impact on oxidative phosphorylation pathway in both cell lines in comparison with melittin as a single treatment (Alonezi et al., 2016). The inhibition of nicotinamide phosphoribosyl transferase (NAMPT) leads to suppression of tumor cell growth and induction of apoptosis due to NAD⁺ depletion (Tan et al., 2015). NAMPT represents a promising therapeutic target for the development of potential novel cancer drugs (Giannetti et al., 2014; Zheng et al., 2013). In most cancer cells, poly (ADP-ribose) polymerase is activated due to DNA damage and cell death induced by oxidative stress (Yu et al., 2002; Du et al., 2003). Therefore, NAMPT inhibition leads to attenuation of glycolysis, resulting in further alteration of carbohydrate metabolism in the cells (Tan et al., 2015).

5.6 Conclusions

Based on the results presented a metabolic signature for the cisplatin and melittin combination treatment for A2780 and A2780CR ovarian cancer cells is proposed. The findings highlight the potential of metabolomic approaches to study treatment effects in order to better understand their mechanisms of action, predict associated mechanism of toxicity and metabolism. Melittin and cisplatin alone have different metabolic effects on ovarian cancer cells. It appears that melittin treatment preferentially affects amino acids and TCA cycle intermediates, while the addition of cisplatin therapy caused a strong modification of the A2780 and A2780CR metabolism as compared with the monotherapy treatments. The most affected metabolites due to melittin-cisplatin treatment in both cell lines were highly ranked in the TCA cycle, oxidative phosphorylation and the purine, pyrimidine and arginine/proline pathways. This different mechanism of action of melittin-cisplatin may provide a paradigm for overcoming chemoresistance in ovarian cancer therapy. Our results provide rationale for the ongoing study with melittin in combination with cisplatin could allow dramatically improved therapy for platinum resistance in ovarian cancer.

Chapter 6

Lipidomic Analysis of the Effects of Melittin on Ovarian Cancer Cells Using Mass Spectrometry

6 Lipidomic Analysis of the Effects of Melittin on Ovarian Cancer Cells Using Mass Spectrometry

6.1 Abstract

Lipids help to maintain the integrity of cells, which is the reason for their association with cancer. We hypothesized that the difference in lipid content of ovarian cancer cells sensitive- and resistant to cisplatin might be a useful indirect measure of a variety of functions coupled to ovarian cancer progression. To evaluate the effect of a melittin, a cytotoxic peptide from bee venom with known effects on cell membranes, on the lipid composition of ovarian cancer cell lines A2780 (cisplatin-sensitive) and A2780CR (cisplatin-resistant) a liquid chromatography-mass spectrometry (LC-MS) coupled to an Orbitrap Exactive mass spectrometer using an ACE silica gel column was employed. The A2780 and A2780CR cells were treated with 6.8 and 4.5 $\mu\text{g}/\text{mL}$ of melittin, respectively. Data extraction with MZmine 2.10 and database searching were applied to provide metabolite lists. Principal component analysis (PCA) and OPLS-DA models were used to assess the different profiles of the lipid composition obtained from the two cell lines. Both models gave clear separation between the treated and untreated samples. In our study, phosphatidylcholine (PC) was the most abundant lipid class in both cell lines, followed by phosphatidylethanolamine (PE), and sphingomyelin. We found a higher level of lipids in ovarian cancer cells sensitive to cisplatin as compared to the resistant cells. Differences in the levels of lysoPC 16:0 and 18:0 were non-significant between cell lines. The changes induced by melittin in both cell lines led mostly to decrease the level of PC and PE lipids. However, the LysoPC level was increased in both cell lines after melittin treatment. The results of the present study show that lipids were significantly altered in both A2780 and

A2780CR cells. The observed effect was much more marked in the cisplatin-sensitive cells, suggesting that the sensitive cells undergo much more extensive membrane re-modelling in response to melittin in comparison with the resistant cells.

6.2 Introduction

Lipidomics is the science of profiling lipids and forms a subset of metabolomics; it combines technological tools, and especially mass spectrometry, with the principles of analytical chemistry to map on a large scale the lipid composition of a metabolome (Han and Gross, 2003; Wenk, 2010). The contribution made by lipids in cancer pathogenesis is substantial and they have central roles to play in the invasion, migration, and proliferation of cancers (Fernandis and Wenk, 2009). Lipidomics has been studied increasingly in recent years, with particular emphasis on finding lipid indicators of use in diagnosis (Wenk, 2006), for targeting drugs (Maréchal et al., 2011), and as pharmacological mechanisms (Adibhatla et al., 2006).

Mass spectrometry has achieved value for assessing changes in lipid metabolism signalling processes mediated by lipids resulting from disease, exposure to toxic substances, gene modification, and drug therapy (Watkins et al., 2002). A number of mass spectrometry routines are now recognised as a way to elucidate lipid structure (Li et al., 2014; Pulfer and Murphy, 2003). In the matter of identifying lipid side chains, the fragmentations providing maximum information come from negative electrospray ionisation (ESI) mode, which generates negative ion fragments thanks to the lipid's fatty acid substituents. In a positive ion mode, phosphocholine (PC) lipid information generated is limited because, due to the phosphatidylcholine head group,

the foremost fragmentation mode gives an ion at m/z 184 (Pulfer and Murphy, 2003).

Lipids have three major roles in cells: they may be structural molecules used to make up membranes, they can provide an important stores of chemical energy, and they play important roles in cell signalling. Lipids are classified according to the International Lipid Classification and Nomenclature Committee into eight classes, that is, fatty acyls, glycerolipids, glycerophospholipids, sphingolipids, sterol lipids, prenol lipids, saccharolipids, and polyketides (Fahy et al., 2009). Among the lipids, the phospholipids are possibly one of the most commonly reported in relationship to cancer. During the past few years, elevations in phosphocholine metabolites have been detected in most of the cancers studied (Tania et al., 2010).

A number of lipid metabolic pathways have been linked to ovarian cancer, particularly those including phospholipids, and fatty acid biosynthesis (Tania et al., 2010). One previous study employed mass spectrometry to explore the potential of lysophospholipids, such as lysophosphatidic acid, lysophosphatidylinositol, and lysophosphatidylcholine, as biomarkers for ovarian cancer detection in women with ovarian cancer and healthy controls (Sutphen et al., 2004). Previous studies on ovarian cancer cells have shown that the ovaries are abundant in glycerophospholipids which are a potential signature of ovarian cancer (Iorio et al., 2005; Ben Sellem et al., 2011; Halama et al., 2015). Xu et al. (1998) reported that lysophosphatidic acid, which is one of the glycerophospholipids with one fatty acid chain and a phosphate group, as a potential biomarker for ovarian and other gynaecological cancers (Xu et al., 1998). A previous study showed that lysophosphatidic acid, lysophosphatidylserine and

sphingosylphosphorylcholine all induce transient increases in cytosolic free calcium $[Ca^{2+}]$ in both ovarian and breast cancer cell lines (Xu et al., 1995). There is a strong relationship between the calcium and lipid metabolism and cell death. Intracellular calcium homeostasis is extremely important for healthy cells, and the alteration in intracellular calcium homeostasis will lead to cell damage or death (Mattson and Chan, 2003; Garcia-Prieto et al., 2013).

Melittin is a major toxin component of honey bee venom that has been reported to exhibit a variety of anticancer applications (Gajski and Garaj-Vrhovac, 2013). The amphipathic property of melittin makes it pass through the phospholipid bilayers of cell membrane and it acts as a surfactant. The interaction between melittin and cell membranes leads to a disruption of the acyl groups of the phospholipids, increased susceptibility to action by phospholipase on the phospholipid, and higher rates of prostaglandin synthesis from arachidonic acid liberated from phospholipid breakdown (Mufson et al., 1979). Another study showed that FK866 treatment resulted in a significant dose-dependent increase in the glycerophosphocholine levels in A2780 cells (Tolstikov et al., 2014). Alteration in glycerophospholipids may be connected with their roles in membrane integrity and mitogenic signal transduction (Ackerstaff et al., 2003). Moreover, recent studies on metabolic alterations in cancer cells directed into apoptosis reported increased levels of mobile lipids (Milkevitch et al., 2005; Rainaldi et al., 2008).

Despite a lipidomic approach having acknowledged value in differentiating between classes and molecular species of phospholipid (PL) (Milne et al., 2006), most studies

focus on only one or a limited number of PL classes and rarely on identifying those lipid molecular species which cancer changes and which could also identify changed metabolic pathways and potential biomarkers. Chapter 3 reported metabolomic studies based on ovarian cancer cells metabolic profiling related to the effect of melittin on the A2780 and A2780CR (Alonezi et al., 2016). Therefore, the goal of the current study was to extend the metabolomics analysis to lipidomic analysis of ovarian cancer cell lines. With this approach, changes in membrane lipid composition in ovarian cancer cells were identified. The profiling of lipids was performed by LC-MS using a high performance liquid chromatography (HPLC) system coupled to an Orbitrap Exactive mass spectrometer using an ACE silica gel column. The selective MS² fragmentation of some lipids was carried out by using a HPLC system combined with a LTQ-Orbitrap mass spectrometer. The resulting data were extracted by MZMine and subsequently analysed by univariate and multivariate approaches with SIMCA-P.

6.3 Materials and Methods

6.3.1 Cell lines and cultures

As detailed in section 2.2.1, Chapter 2.

6.3.2 Cell viability assay against melittin

As detailed in section 3.3.2, Chapter 3.

6.3.3 Determination of IC₅₀

As detailed in section 2.2.2, Chapter 2.

6.3.4 Determination of effect of melittin on cell lipids metabolism

The A2780 and A2780CR cell lines were separately treated with melittin at concentrations of 6.8 and 4.5 $\mu\text{g}/\text{mL}$ respectively for 24 h (n=4). The cells were seeded at 75×10^4 cells/mL in T-25 cell culture flasks and incubated for 1 doubling time (48 h) before treatment with the melittin and incubation for an additional 24 h. After the treatment, the medium was removed and the cells were washed twice with 3 mL of phosphate-buffered saline (PBS) at 37°C before lysis. Lipids were extracted with isopropanol (4°C) (1 mL per 2×10^6 cells). The cells were scraped and cell lysates mixed on a Thermo mixer at 1440 rotations per minute (r.p.m.) for 12 min at 4°C, before being centrifuged at 13500 r.p.m. for 15 min at 0°C. The supernatants were collected and transferred into HPLC vials for LC-MS analysis. During the analysis, the temperature of the autosampler was maintained at 4 °C. The pooled quality control (QC) sample were injected in each analysis run in order to facilitate identification and to evaluate the stability and reproducibility of the analytical method, respectively. The pooled QC sample was obtained by taking equal aliquots from all the samples and placing them into the same HPLC vial.

6.3.5 Chromatographic conditions for column

As detailed in section 2.3.3, Chapter 2.

6.3.6 Liquid Chromatography–Mass Spectrometry (LC-MS) conditions

As detailed in sections 2.4.1, and 2.4.2, Chapter 2.

6.3.7 Data extraction and analysis

As detailed in section 2.5, Chapter 2.

6.4 Results

The effects of melittin on the lipid composition of ovarian cancer cells (A2780 and A2780CR) were assessed using LCMS and LCMSMS based lipidomics. Differences in the levels of lipids induced by exposure to melittin at concentrations corresponding to IC_{50} with respect to each cell line were assessed. Multivariate (PCA and OPLS-DA) analyses were used to classify the metabolic phenotypes and identify the differentiating lipids. A clear separation of melittin-treated A2780 and A2780CR cells, and their respective untreated controls, was achieved indicating unique lipid profiles for the treated and control cells with PCA and OPLS-DA models (Figure 6.1 A and B, respectively). Pooled quality control (QC) samples were injected in the analysis run in order to quantify the precision of the measurements (Figure 6.1A). The PCA model parameters were: 4 components, R^2X (cum) = 0.984; Q^2 (cum) = 0.967. The OPLS-DA model parameters and validation of the plot suggested a strong model (R^2X (cum) 0.984, R^2Y (cum) 0.994, Q^2 (cum) 0.984), three components), and the CV-ANOVA for this model was $3.29E-16$. Hierarchical clustering analysis of metabolomics data showed distinct separation between the control and treated samples (Figure 6.2).

There was a very clear separation of the treated versus untreated A2780CR cells obtained by using OPLS-DA model based on the significant metabolites (Figure 6.3 A). The OPLS-DA model parameters and validation of the plot suggested a strong model (2 components, R^2X (cum) = 0.844, R^2Y (cum) = 1, Q^2 (cum) = 0.988, CV-

ANOVA= 1.47E-5). Model validity was verified using permutation tests and receiver operating characteristic (ROC) analysis (Figure S6.1, appendix). The AUC for a ROC classification is regarded as excellent when $AUC > 0.9$. The OPLS-DA model classified the treated and untreated A2780 cells into two groups, and the AUC of the ROC for the groups were excellent to perfect classification.

In case of the A2780 cells, OPLS-DA models were also generated by comparing control and treated samples based on the significant metabolites (Figure 6.3 B). The model parameters and validation of the plot suggested a strong model (R^2X (cum) = 0.955, R^2Y (cum) = 1, Q^2 (cum) = 0.998), two components), and the CV-ANOVA for this model was 4.01E-5. Furthermore, the validity of the ROC and permutation test showed the constructed OPLS-DA model was valid (Figure S6.2, appendix).

For univariate statistical analysis of candidate specific biomarkers in OCC's after exposure to the combinations, the false discovery rate (FDR) was used to reduce the probability of false positive results. There were important differences in lipid composition between the two cell lines before and after treatment with melittin. Changes in various classes of lipids, especially glycerophosphocholines (GPC), glycerophosphoethanolamines (GPE), sphingomyelins, glycerophosphoglycerols (GPG), glycerophosphoinositols (GPI) and glycerophosphoserines (GPS). A list of the putative lipid metabolites is shown in Table 6.1.

Figure 6.4 and 6.5 shows a heat map of phosphocholines, phosphoethanolamines, phosphoinositols, sphingolipid, phosphoglycerols, phosphoserines and diradylglycerols, which are the top 67 lipids by intensity extracted from the A2780 cells in comparison with A2780CR cells. It is clear that the A2780 cell line generally contains more lipids than the A2780CR cell line. The really marked differences between the two cell lines are in several sphingolipids such as dehydrosphinganine and lactosylceramide, and in some ether lipids such as PC36:3, PC36:4, PC38:4 and PC38:6, all of which are lower in the resistant cells. The level of GPE such as PE38:5 was also found in higher abundance in A2780 cell lines. The differences in lipid composition of the two cell lines suggest that either re-modelling of the cell membrane might have occurred in order for the A2780CR cells to become resistant, or there is decreased biosynthesis and/or increased utilisation of lipids in cisplatin resistant cells as has been suggested by others (Poisson et al., 2015). Melittin appears to have some effect on lipid composition in the A2780 cells with the levels of the abundant lipid PC34:1 decreasing, but the effect on this lipid in the A2780CR cells is less marked. Moreover, it was found that treatment of the ovarian cancer cell lines with melittin caused a decrease in PE lipids such as PE34:1 and PE34:2. Overall there are many changes in lipid abundance in response to melittin but they are generally quite small and restricted to the less abundant lipids. The decrease in the lipids induced by treatment with melittin is less in the case of the A2780CR cells suggesting less membrane damage in the case of these cells.

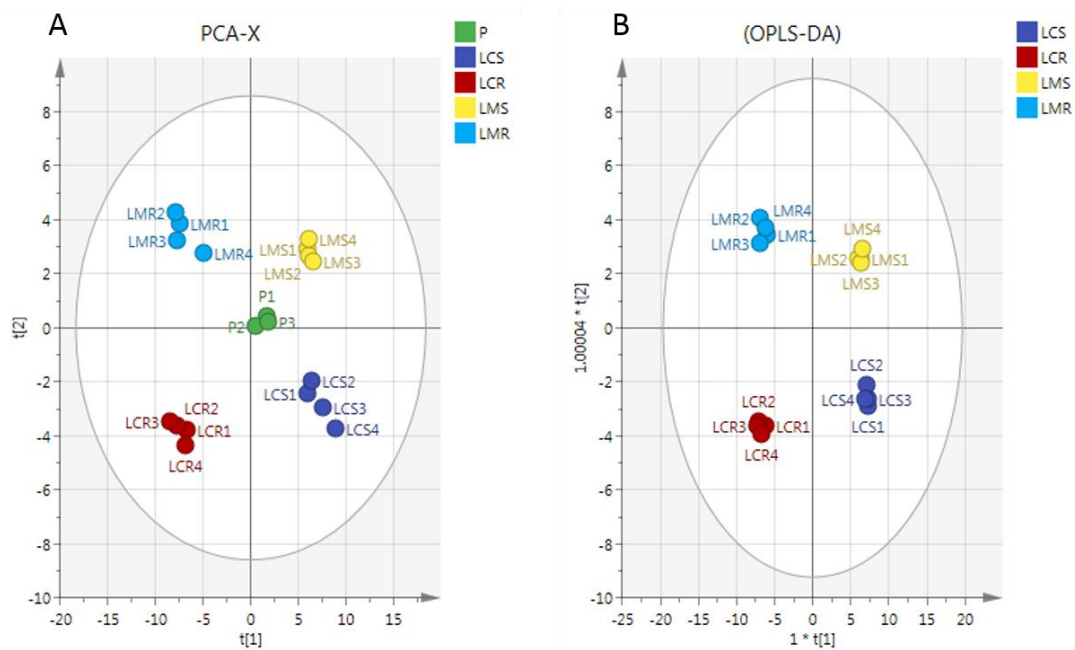


Figure 6.1. (A) PCA vs (B) OPLS-DA. PCA and OPLS-DA scores plot generated from PCA and OPLS-DA using LC-MS normalized data of cells after exposure to melittin and controls of A2780 and A2780CR cell lines. LMS circles: A2780-treated cells; LCS circles: untreated A2780 cells; LMR circles: A2780CR –treated cells; LCR circles: untreated A2780CR. P circles: Quality control (QC) samples.

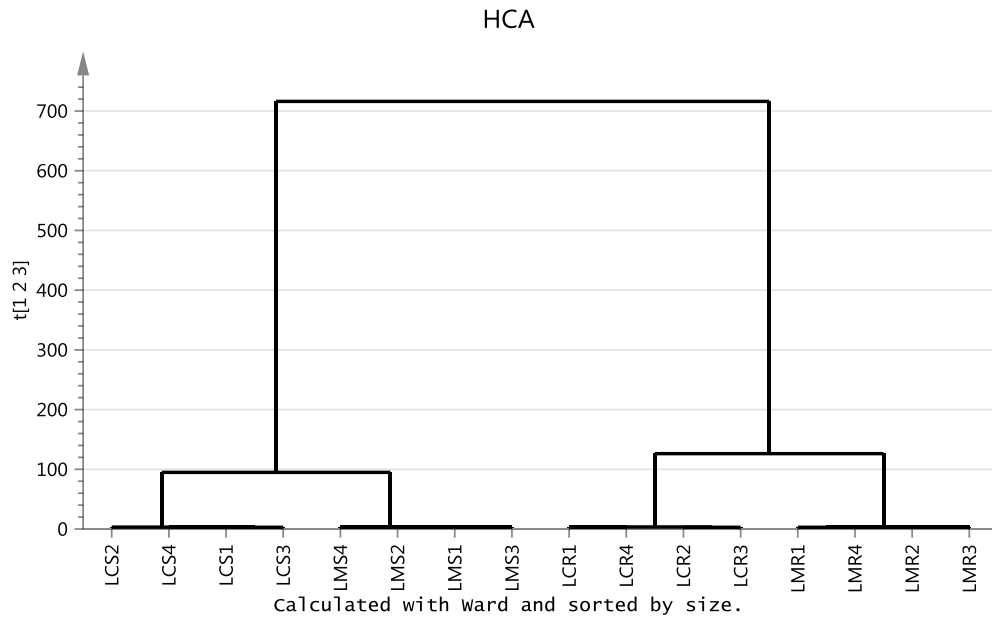


Figure 6.2. Hierarchical clustering analysis (HCA) of 16 ovarian cancer cell samples. It shows two main groups and four subgroups. The groups: LCR, control of cisplatin resistance cell lines; LMR: A2780CR after treatment with melittin; LCS, control of cisplatin sensitive cell lines; LCS, A2780 after treatment with melittin.

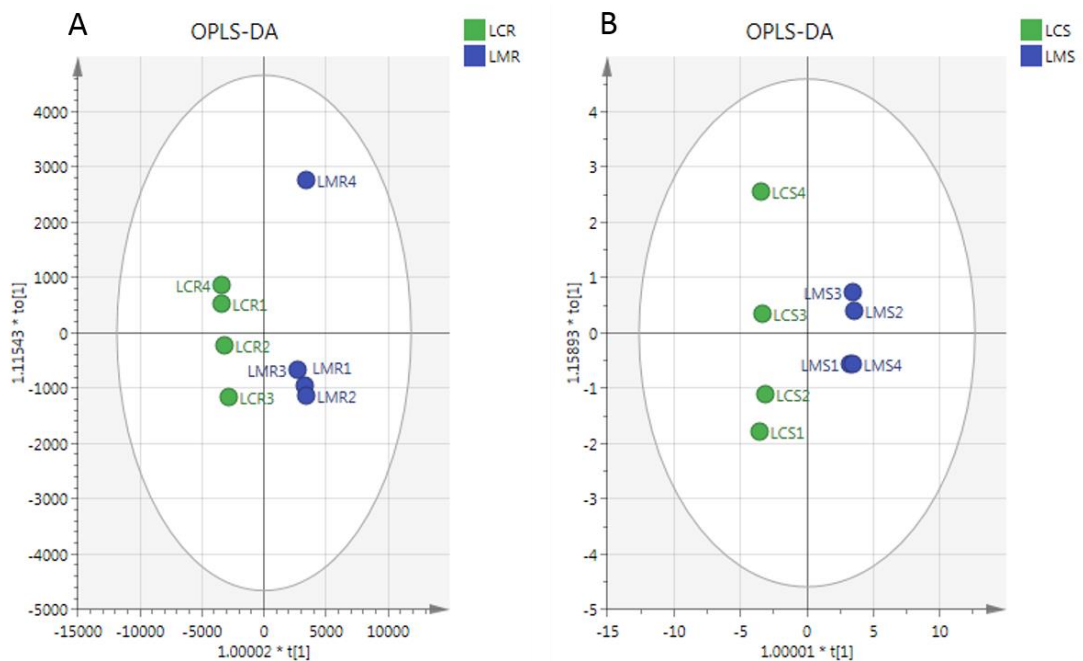


Figure 6.3. OPLS-DA score plot of (A) A2780CR cell lines before and after treatment with melittin; (B) A2780 cell lines before and after treatment with melittin.

Table 6.1. Differences in the lipids between A2780 cells and A2780CR cells before and after melittin treatment.

m/z	Rt(min)	Metabolites	S/R		LMS/LMR		LMR/R		LMS/S	
			P value	Ratio	P value	Ratio	P value	Ratio	P value	Ratio
Sphingolipid (Phosphosphingolipids; Sphingomyelins)										
703.575	14.5	SM 34:1	<0.001	1.875	<0.01	1.723	ns	1.048	ns	0.963
729.590	14.4	SM 36:2	<0.001	2.756	<0.001	2.587	ns	1.126	ns	1.057
731.606	14.5	SM 36:1	<0.001	2.969	<0.001	3.069	ns	1.067	ns	1.103
785.652	14.4	SM 40:2	<0.001	3.042	<0.001	3.099	ns	1.090	ns	1.110
787.668	14.4	SM 40:1	<0.001	3.650	<0.001	3.702	ns	1.049	ns	1.064
813.684	14.4	SM 42:2	<0.001	1.842	<0.01	1.706	ns	1.068	ns	0.989
Sphingolipid (Sphingoid bases)										
300.289	10.4	3-dehydrosphinganine (3-ketosphinganine)	<0.001	6.209	<0.001	6.634	<0.01	0.616	<0.01	0.659
Sphingolipid (Neutral glycosphingolipids)										
862.624	3.1	LacCer(d18:1/16:0)	<0.001	5.109	<0.001	3.788	ns	1.163	ns	0.862
Sphingolipid (Acidic glycosphingolipids)										
852.587	13.8	(3'-sulfo)Galbeta-Cer(d18:0/20:0(2OH))	<0.001	0.446	<0.01	0.358	ns	0.781	ns	0.626
Glycerophosphoinositols										
887.564	3.6	PI38:3	<0.001	2.321	<0.001	3.662	ns	0.963	<0.01	1.520
883.535	3.5	PI38:5	<0.001	2.469	<0.001	1.603	<0.01	1.727	ns	1.121
835.534	3.8	PI34:1	<0.001	1.751	<0.001	1.449	<0.01	1.977	<0.001	1.635
861.550	3.7	PI36:0	ns	1.026	ns	0.846	<0.01	1.750	<0.01	1.444
887.563	3.5	PI38:4	<0.05	1.169	ns	0.948	<0.01	1.386	<0.05	1.124

Table 6.1. (Contd.)

m/z	Rt(min)	Metabolites	S/R		LMS/LMR		LMR/R		LMS/S	
			P value	Ratio	P value	Ratio	P value	Ratio	P value	Ratio
Glycerophosphocholines										
706.538	14.1	PC30:0	<0.05	1.307	ns	1.063	<0.01	0.605	<0.01	0.492
704.523	13.9	PC30:1	<0.001	2.664	<0.001	3.037	<0.01	0.472	<0.01	0.538
720.555	14.0	PC31:0	<0.05	1.240	ns	0.805	ns	1.154	<0.05	0.749
732.553	14.0	PC32:1	<0.01	1.874	<0.001	1.756	<0.05	0.594	<0.01	0.557
734.569	14.0	PC32:0	<0.01	1.438	ns	1.100	ns	0.793	<0.01	0.606
730.538	13.9	PC32:2	<0.001	3.790	<0.001	4.606	<0.01	0.578	<0.01	0.703
758.569	13.9	PC34:2	<0.01	1.584	<0.001	1.677	<0.01	0.687	<0.05	0.728
746.605	14.1	PC34:0	<0.001	3.280	<0.001	2.954	ns	0.820	<0.01	0.738
760.584	13.9	PC34:1	<0.05	1.360	ns	1.054	ns	0.824	<0.01	0.639
786.600	13.9	PC36:2	ns	1.097	ns	0.972	ns	0.846	<0.05	0.749
788.615	13.9	PC36:1	ns	0.994	<0.01	0.584	ns	1.111	<0.01	0.653
784.584	13.8	PC36:3	<0.01	1.580	<0.01	1.296	ns	0.930	<0.05	0.763
782.567	13.7	PC36:4	<0.01	1.763	<0.05	1.387	ns	1.204	ns	0.948
808.583	13.7	PC38:5	<0.05	1.636	<0.05	1.411	ns	1.299	ns	1.120
810.599	13.7	PC38:4	<0.01	1.882	ns	0.925	<0.05	1.840	ns	0.905
772.585	13.9	PC35:2	<0.05	1.408	<0.05	1.453	ns	0.902	ns	0.930
814.631	13.9	PC38:2	<0.01	0.666	<0.05	0.493	ns	0.810	<0.01	0.600
774.600	13.9	PC35:1	ns	1.242	ns	0.868	ns	1.205	ns	0.842
838.631	13.7	PC40:4	<0.01	1.783	ns	0.808	ns	1.387	<0.05	0.629
840.647	13.8	PC40:3	ns	1.195	ns	0.862	ns	0.791	<0.01	0.571
842.662	13.8	PC40:2	<0.001	0.573	<0.01	0.430	<0.01	0.661	<0.01	0.496

Table 6.1. (Contd.)

m/z	Rt(min)	Metabolites	S/R		LMS/LMR		LMR/R		LMS/S	
			P value	Ratio	P value	Ratio	P value	Ratio	P value	Ratio
Glycerophosphocholines										
756.552	13.9	PC34:3	<0.001	2.162	<0.001	2.326	<0.05	0.758	<0.01	0.815
716.559	13.9	PC32:1	<0.001	2.373	<0.01	1.908	ns	1.413	<0.01	1.136
754.537	13.9	PC34:4	<0.001	1.921	<0.001	2.297	<0.01	0.667	<0.01	0.798
496.339	15.0	LysoPC 16:0	ns	1.050	<0.001	0.258	<0.001	5.991	<0.05	1.471
524.371	14.8	LysoPC 18:0	ns	0.847	<0.001	0.173	<0.01	13.157	<0.01	2.695
PC ether lipids										
744.590	13.9	PC34:1 ether lipid	<0.001	1.881	<0.001	1.492	ns	1.188	ns	0.942
794.605	13.8	PC38:5 ether lipid	<0.001	3.578	<0.001	2.011	<0.01	2.115	ns	1.188
796.620	13.8	PC38:4 ether lipid	<0.001	5.719	<0.001	3.027	<0.05	1.730	ns	0.916
770.605	13.9	PC36:2 ether lipid	<0.001	2.704	<0.01	1.585	ns	1.070	<0.01	0.627
692.558	14.2	PC30:2 ether lipid	<0.001	3.447	<0.001	2.796	<0.01	0.767	<0.01	0.622
772.621	14.0	PC36:1 ether lipid	<0.001	2.081	<0.01	1.701	ns	0.975	ns	0.797
774.636	14.1	PC36:0 ether lipid	<0.001	3.398	<0.001	3.110	<0.05	0.758	<0.01	0.694
720.589	14.2	PC32:2 ether lipid	<0.001	4.623	<0.001	5.498	<0.05	0.689	ns	0.820
718.574	14.1	PC32:0 ether lipid	<0.001	3.311	<0.001	2.353	ns	1.167	ns	0.829
768.588	13.8	PC36:3 ether lipid	<0.001	4.563	<0.001	2.746	<0.05	1.621	ns	0.975
766.574	13.7	PC36:4 ether lipid	<0.001	2.545	ns	1.236	<0.01	3.083	<0.01	1.497
792.589	13.7	PC38:6 ether lipid	<0.01	2.357	ns	1.269	<0.05	1.908	ns	1.027
PE ether lipids										
744.553	10.1	PE36:2 ether lipid	ns	0.892	ns	0.824	<0.05	0.746	<0.05	0.689
750.542	9.6	PE38:4 ether lipid	<0.01	1.779	<0.001	1.571	ns	1.044	ns	0.922
724.527	9.7	PE36:5 ether lipid	<0.05	1.510	ns	1.107	<0.05	1.407	ns	1.032
746.569	10.2	PE34:1 ether lipid	<0.01	0.688	<0.01	0.586	ns	0.777	<0.01	0.662

Table 6.1. (Contd.)

m/z	Rt(min)	Metabolites	S/R		LMS/LMR		LMR/R		LMS/S	
			P value	Ratio	P value	Ratio	P value	Ratio	P value	Ratio
Glycerophosphoethanolamines										
768.552	9.7	PE38:4	<0.001	1.871	<0.001	1.484	<0.01	1.414	ns	1.122
752.558	9.6	PE38:5	<0.001	3.199	<0.001	2.291	<0.05	1.313	ns	0.940
718.538	10.3	PE34:1	ns	1.139	ns	1.077	<0.01	0.610	<0.01	0.577
716.522	10.2	PE 34:2	<0.001	1.652	<0.001	1.861	<0.01	0.543	<0.01	0.612
676.528	10.3	PE 32:0	<0.001	6.850	<0.001	29.351	ns	0.714	<0.001	3.062
704.557	10.3	PE 34:3	<0.001	3.619	<0.001	9.955	ns	0.836	<0.001	2.299
Glycerophosphoglycerols										
721.503	3.7	PG32:0	<0.001	114.589	<0.001	49.988	ns	3.227	<0.05	1.408
775.549	3.7	PG36:1	<0.001	3.688	<0.01	1.573	ns	0.989	<0.01	0.422
773.534	3.5	PG36:2	<0.001	9.482	<0.05	2.057	<0.05	1.782	<0.01	0.387
Glycerophosphoserines										
804.575	14.0	PS37:0	ns	0.965	ns	1.111	ns	1.144	<0.01	1.317
Diacylglycerols										
603.535	3.7	DAG 34:3	<0.001	0.862	<0.01	1.290	<0.001	0.542	<0.01	0.812

PC (Phosphatidylcholine); PE (Phosphatidylethanolamine); PI (Phosphatidylinositol); PG (Phosphatidylglycerol); PS (Phosphatidylserine); DAG (Diacylglycerol); SM (Sphingomyelin); S (A2780 cells); R (A2780CR cells); LMS (melittin treated A2780 cells); LMR (melittin treated A2780CR cells).

m/z	Rt(min)	Metabolites	Mean S	Mean R	Mean LMS	Mean LMR
706.538	14.1	PC30:0	Yellow	Yellow	Yellow	Yellow
704.522	13.9	PC30:1	Red	Red	Red	Red
720.555	14.0	PC31:0	Red	Red	Red	Red
732.553	13.9	PC32:1	Yellow	Yellow	Yellow	Yellow
734.569	14.0	PC32:0	Yellow	Yellow	Yellow	Yellow
730.538	13.9	PC32:2	Yellow	Red	Yellow	Red
758.569	13.8	PC34:2	Yellow	Yellow	Yellow	Yellow
746.605	14.1	PC34:0	Yellow	Yellow	Yellow	Yellow
760.584	13.9	PC34:1	Green	Green	Green	Green
786.600	13.9	PC36:2	Yellow	Yellow	Yellow	Yellow
788.615	13.9	PC36:1	Yellow	Yellow	Yellow	Yellow
784.584	13.8	PC36:3	Yellow	Yellow	Yellow	Yellow
782.567	13.7	PC36:4	Yellow	Yellow	Yellow	Yellow
808.583	13.7	PC38:5	Yellow	Yellow	Yellow	Yellow
810.599	13.7	PC38:4	Yellow	Yellow	Yellow	Yellow
772.585	13.8	PC35:2	Yellow	Yellow	Yellow	Yellow
814.631	13.8	PC38:2	Yellow	Yellow	Yellow	Yellow
774.600	13.9	PC35:1	Yellow	Yellow	Yellow	Yellow
838.631	13.7	PC40:4	Red	Red	Red	Red
840.647	13.8	PC40:3	Red	Red	Red	Red
842.662	13.8	PC40:2	Red	Red	Red	Red
756.552	13.8	PC34:3	Yellow	Yellow	Yellow	Yellow
716.558	13.9	PC32:1	Red	Red	Red	Red
754.536	13.9	PC34:4	Red	Red	Red	Red
496.339	15.0	LysoPC16:0	Red	Red	Red	Yellow
524.370	14.9	LysoPC18:0	Red	Red	Red	Yellow
766.573	13.7	PC36:4 ether lipid	Yellow	Yellow	Yellow	Yellow
744.590	13.9	PC34:1 ether lipid	Yellow	Yellow	Yellow	Yellow
794.605	13.8	PC38:5 ether lipid	Yellow	Yellow	Yellow	Yellow
796.620	13.8	PC38:4 ether lipid	Yellow	Yellow	Yellow	Yellow
770.605	13.9	PC36:2 ether lipid	Yellow	Yellow	Yellow	Yellow
692.558	14.2	PC30:2 ether lipid	Yellow	Red	Yellow	Red
772.620	14.0	PC36:1 ether lipid	Yellow	Yellow	Yellow	Yellow
774.636	14.1	PC36:0 ether lipid	Yellow	Red	Yellow	Red
720.589	14.2	PC32:2 ether lipid	Yellow	Yellow	Yellow	Yellow
718.574	14.1	PC32:0 ether lipid	Yellow	Yellow	Yellow	Yellow
768.588	13.8	PC36:3 ether lipid	Yellow	Yellow	Yellow	Yellow
792.589	13.7	PC38:6 ether lipid	Yellow	Red	Yellow	Yellow

Figure 6.4. Heat Map showing the relative abundance of phosphocholine lipids in A2780 (S), A2780CR (R) and melittin treated (LMS and LMR) cells. Red $< 2 \times 10^5$, Yellow $> 1 \times 10^6$, Green $> 1 \times 10^7$.

m/z	Rt(min)	Metabolites	Mean S	Mean R	Mean LMS	Mean LMR
703.574	14.5	SM (d18:1/16:0)				
729.590	14.4	SM(d18:1/18:1(9Z))				
731.605	14.5	SM(d18:0/18:1(9Z))				
785.652	14.4	SM(d18:1/22:1(13Z))				
787.668	14.4	SM(d18:1/22:0)				
813.683	14.3	SM(d18:1/24:1(15Z))				
300.289	10.4	3-dehydrosphinganine				
862.624	3.1	LacCer(d18:1/16:0)				
852.587	13.8	(3'-sulfo)Galbeta-Cer(d18:0/20:0(2OH))				
768.552	9.7	PE38:4				
752.558	9.6	PE38:5				
718.538	10.3	PE34:1				
716.522	10.2	PE 34:2				
676.527	10.3	PE 32:0				
704.557	10.3	PE 34:3				
744.553	10.1	PE36:2 ether lipid				
750.542	9.6	PE38:4 ether lipid				
724.527	9.7	PE36:5 ether lipid				
746.569	10.2	PE34:1 ether lipid				
887.564	3.6	PI38:3				
883.534	3.5	PI38:5				
835.534	3.8	PI34:1				
861.550	3.7	PI36:0				
887.563	3.5	PI38:4				
721.503	3.7	PG 32:0				
775.549	3.7	PG 36:1				
773.534	3.5	PG 36:2				
804.575	13.9	PS37:0				
603.534	3.7	DAG 34:3				

Figure 6.5. Heat Map showing the relative abundance of various types of lipid in A2780 (S), A2780CR (R) and melittin treated (LMS and LMR) cells. Red $< 2 \times 10^5$, Yellow $> 1 \times 10^6$, Green $> 1 \times 10^7$.

MS/MS experiments are used to further identify lipid species or to screen for individual lipid classes. In the case of phosphocholine lipids, in order to avoid the spectrum being dominated by the phosphocholine head group the following method is used. When formate is used in the mobile phase the molecular ions of the negatively charged PC lipids appear as their negatively charged formate adducts. In order to

promote the formation of negatively charge ions derived from the acyl chains attached to the glycerol backbone an in source fragmentation energy is applied in negative ion mode. The source fragmentation results in the loss of the formic acid and one of the methyl groups from the choline moiety thus removing the fixed positive charge from the choline head group. The resulting ion is then subjected to further fragmentation by MS/MS or MS² in the mass spectrometer. Using this method the fatty acids substituted onto the glycerol backbone are observed as their negatively charged ions. LysoPCs are the phosphocholines that have lost one of the two O-acyl chains, and they generally have molecular masses in the range of 400–650 (Dutta et al., 2012). Figure 6.6 shows the MS² spectrum of Lysophosphatidylcholines (16:0) and (18:0) in negative ion mode. In this case the MS² spectrum is indicative of the palmitic acid and stearic acid within the structure with prominent ions at m/z 255 and 283, respectively. Figure 6.7 shows the MS² spectrum of 18:1 / 18:1 PC in negative ion mode. In this case the MS² spectrum is indicative of the acyl groups within the structure with prominent ions at m/z 281 due to the acyl ion C₁₇H₃₃COO⁻ and at m/z 506 which result from the loss of C₁₈H₃₃O₂⁻ from the [M-CH₃]⁻ ion at m/z 770. In contrast, in positive ion mode the main fragment ion produced is at m/z 184 due to the phosphocholine head group (Figure 6.8). The PC ether lipids gave diagnostic fragments in MS² in negative ion mode. MS² in negative ion mode was used to characterise of PC ether lipids 36:6 and 36:5 as shown in figure 6.9. From the information shown in figure 6.9 it is apparent that these two lipids both have and an alkyl chain C16:1 and acyl substitutions of C20:5 and C20:4 respectively. The spectra have a common ion at m/z 466 due to neutral loss of the acyl chains from the [M-CH₃]⁻ ion. Levels of the 36:6 and 36:5 ether lipids are lower in the resistant cells.

A lactosyl ceramide lipid is lower in the resistant cells. From previous work product ion analysis of the $(M + H)^+$ ions of ceramides reveals cleavage of the amide bond and dehydration of the sphingoid base to form highly abundant, structurally specific O^+ fragment ions (Merrill et al., 2005). These product ions yield information regarding the number of carbon atoms in the chain, degree of hydroxylation, unsaturation, or other structural modifications of the long-chain base (e.g., sphingosine, m/z 264; and sphinganine, m/z 266). With this knowledge about the sphingoid base composition and the original precursor m/z , the identity of the fatty acids can be deduced. The lipids were at low levels and the clearest result was obtained by using source induced dissociation (SID). Using ESI-SID in positive mode product ions at m/z 264 and m/z 266 can be used to identify the sphingosine and sphinganine, respectively (Figure 6.10).

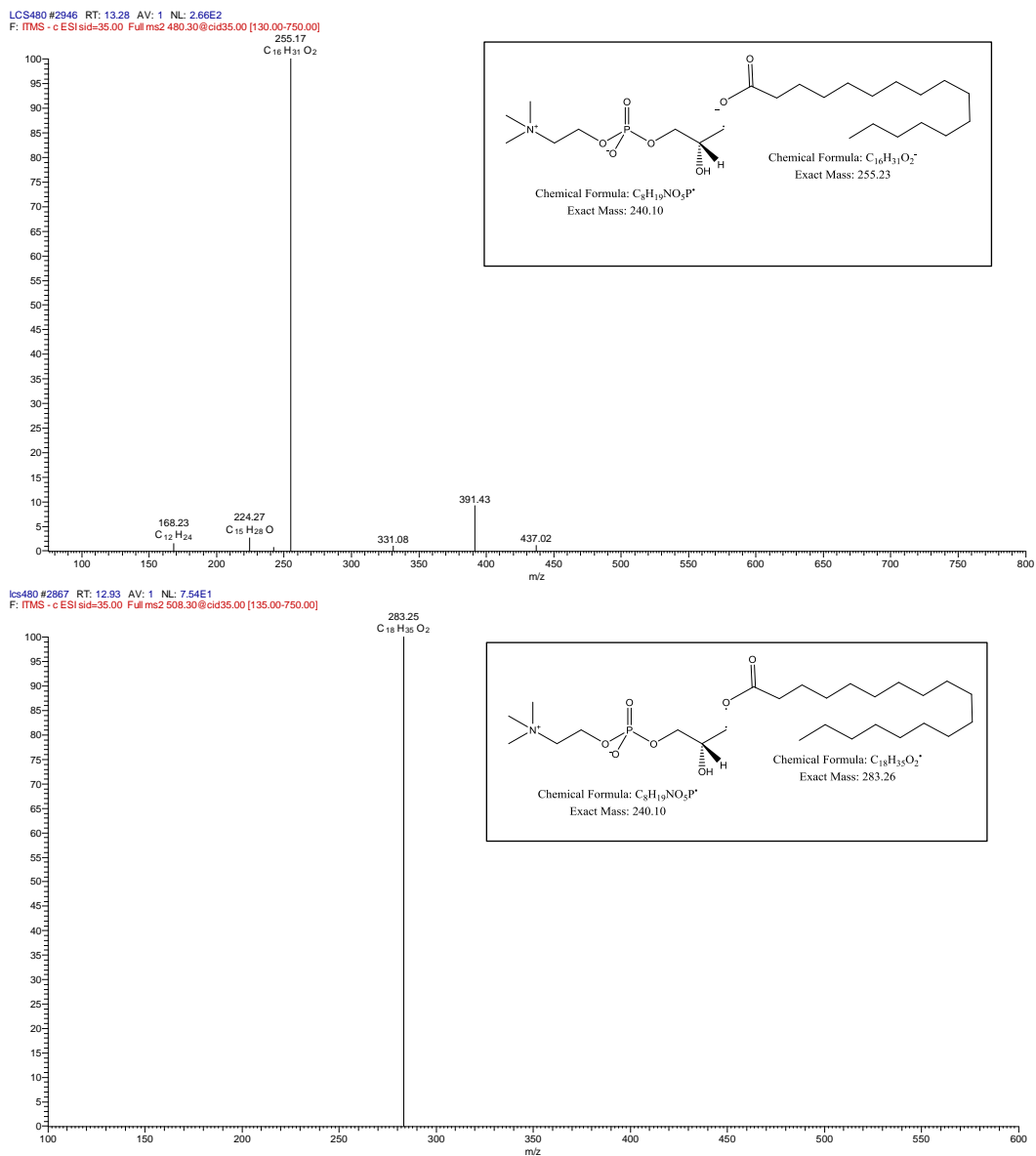


Figure 6.6. MS² spectra of (A) LysoPC 16:0 and (B) LysoPC 18:0 lipid at 35 V following application of a source fragmentation energy of 35 V.

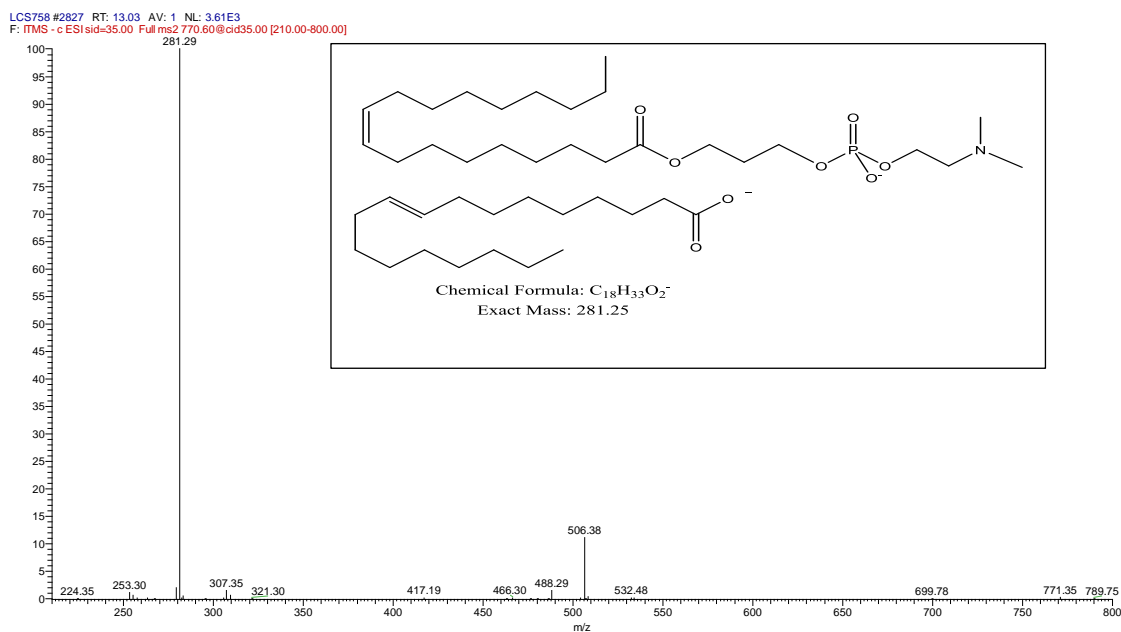


Figure 6.7. MS² spectra of 18:1/18:1 PC lipid at 35 V following application of a source fragmentation energy of 35 V.

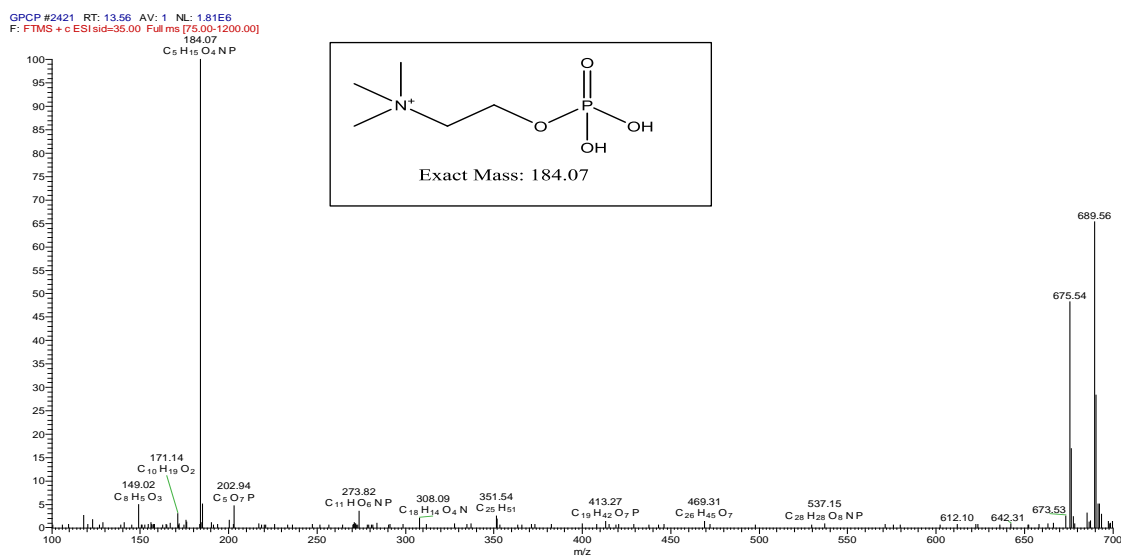


Figure 6.8. Fragmentation of PC lipids in positive ion mode resulting in m/z 184 due to the phosphocholine head group.

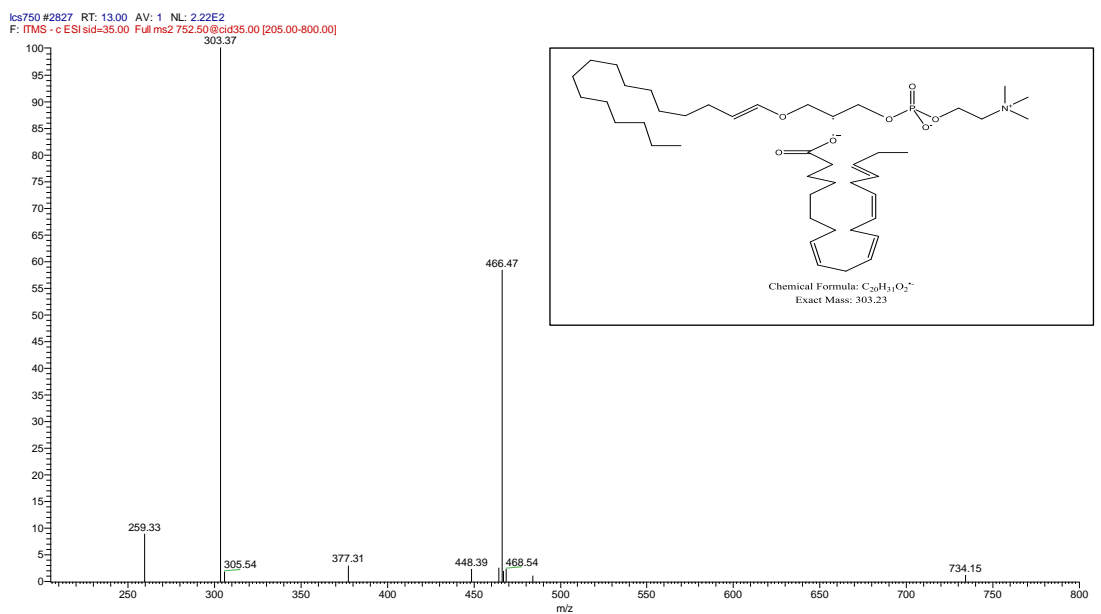
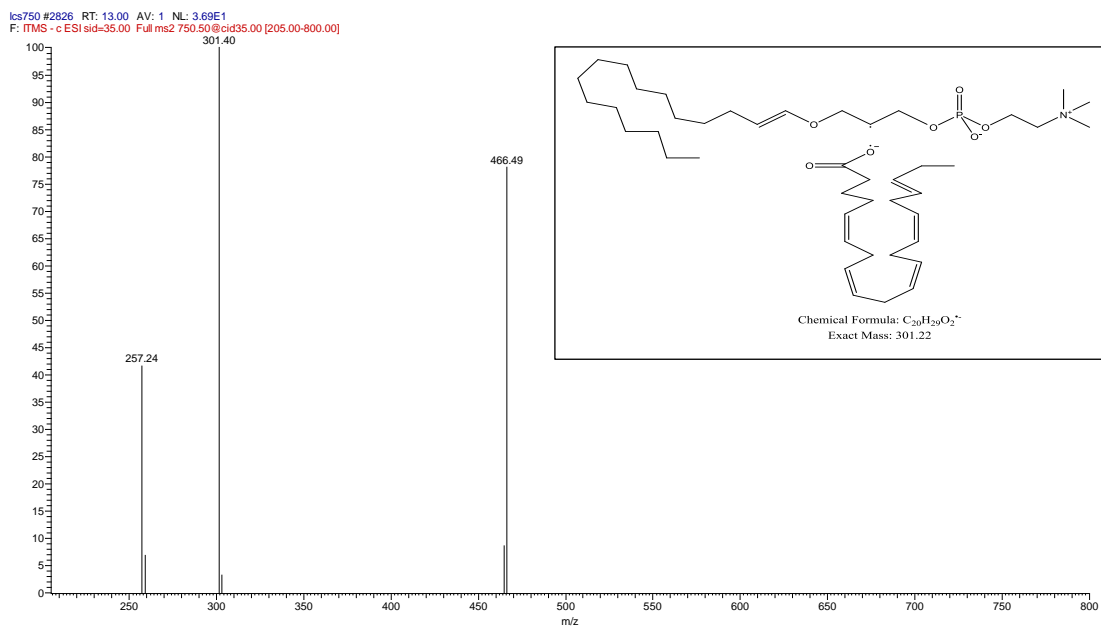


Figure 6.9. MS² spectra of PC ether lipids 36:6 and 36:5 indicate that they are acylated with 20:5 and 20:4 chains respectively.

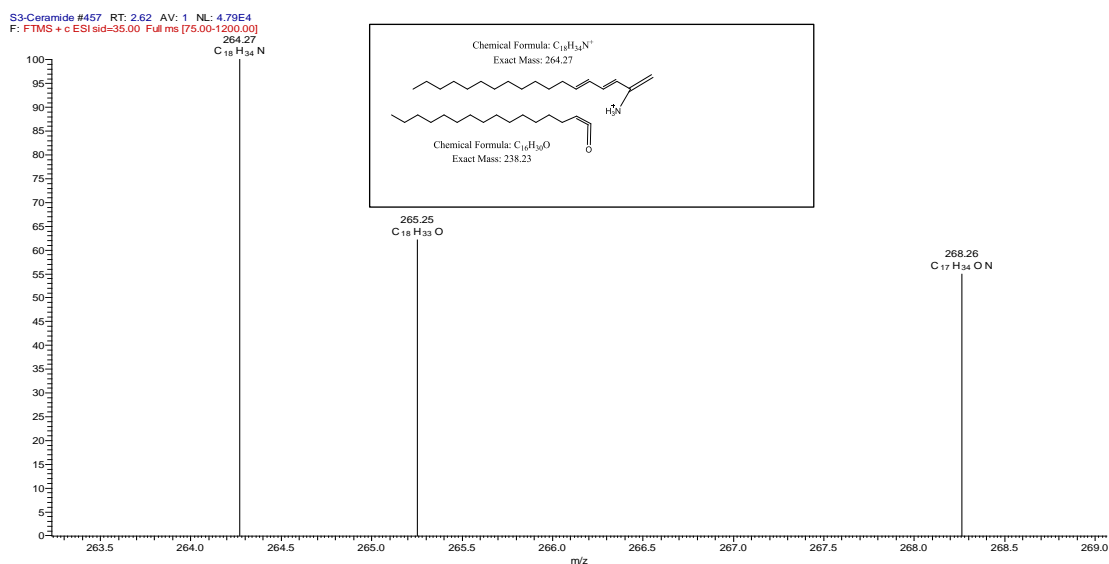


Figure 6.10. Source induced dissociation spectrum of lactosylceramide (d18:1/16:0) lipid at 35 V.

Figure 6.11 shows the MS^2 spectrum of 18:0/20:4 PE in negative ion mode. In this case the MS/MS or MS^2 spectrum is indicative of the acyl groups which appear as negatively charged fatty acids at m/z 303 due to $C_{19}H_{31}COO^-$ and at m/z 283 due to $C_{17}H_{35}COO^-$. In the example shown in figure 6.11 we can also see that there are additional minor fatty acids attached and thus the peak is a mixture of several isomers with different fatty acid chain lengths.

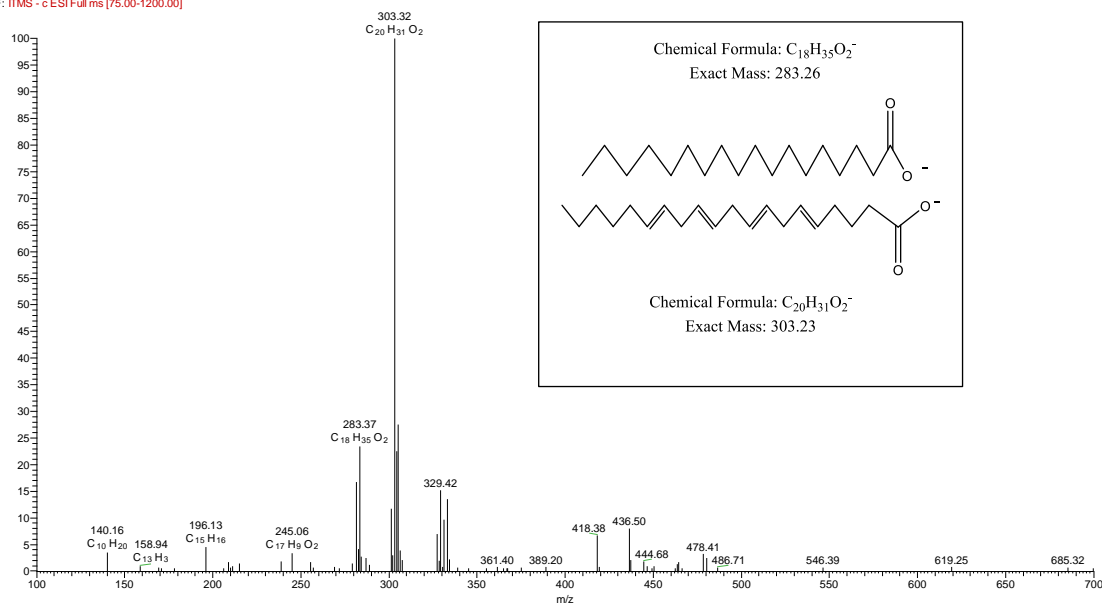


Figure 6.11. MS² spectra of 18:0/20:4 PE lipid.

6.5 Discussion

In order to evaluate alterations in the phospholipid profile of human ovarian cancer cells following melittin treatment, mass spectrometry was used to characterise the lipid profiles of A2780 (cisplatin-sensitive) and A2780CR (cisplatin-resistant) cell lines in response to their exposure to melittin. Because of mass spectrometry, we now have much greater access to detailed information concerning cellular lipid composition. ESI-MS has been shown to have an essential role in the characterization, identification, and quantification of lipids (Han and Gross, 2003; Welte and Wang, 2004). Recently, mass spectrometry has been used to determine whether lysophospholipids are useful markers for diagnosis and/or prognosis of ovarian cancer in plasma samples (Sutphen et al., 2004). We have found phosphatidylcholine was the most abundant lipid class in ovarian cancer cells, followed by phosphatidylethanolamine, phosphatidylinositol,

phosphoglycerols, sphingomyelins and phosphoserines. We have also detected a variety of lyso- and ether-linked derivatives of PC and PE.

There are some significant differences in the lipid composition between A2780 and A2780CR cells. The levels of phosphocholine lipids were higher in A2780 cells in comparison to the A2780CR cells. Previous studies also show that an increase in the levels glycerophospholipids could be a signature of ovarian cancer (Halama et al., 2015; Iorio et al., 2005; Ben Sellem et al., 2011). Other studies show that an increase of the level of glycerophosphocholine is the most common feature in a large variety of tumours demonstrating biosynthetic and/or catabolic phosphatidylcholine-cycle pathways of cell membrane turnover (Hishikawa et al., 2014; McLean et al., 2009). Following treatment with melittin, lipids were significantly altered in both A2780 and A2780CR cells. The effect on lipids is much more marked in that case of the sensitive cells and suggests that the sensitive cells undergo much more extensive membrane remodelling in response to melittin in comparison with the resistant cells.

However, the level of certain species of PC ether lipids were higher in the A2780 cells. For example, PC ether lipids 36:4 and 36:3 were elevated in these cells. The MS² spectra of these two lipids (figure 6.9) indicate that they are acylated with 20:5 and 20:4 chains respectively. The levels of lyso PCs are also elevated in both cells after exposure to melittin. For example, LPC 16:0 and LPC 18:0 were markedly increased in A2780CR cells following melittin exposure. Fragmentation patterns of these two lipids (figure 6.6) indicate of the palmitic acid and stearic acid as the acyl chains. There were no significant differences in those lyso PCs lipid compositions in the untreated

A2780 and A2780CR cells. In a previous study it was found that the levels of lysophosphatidic acids were increased in the plasma of ovarian and other gynecologic cancer patients as compared with healthy controls (Xu et al., 1998). Moreover, lysophosphatidic acid (LPA) and other lysophospholipids (LPL) such as lysophosphatidylinositol were found useful markers for diagnosis and/or prognosis of ovarian cancer in comparison with healthy control setting (Sutphen et al., 2004). Lyso PC lipids are recycled back into PC lipids via the Lands' cycle. The Lands cycle allows remodelling of acyl chains enabling modification of the fatty acid composition of phospholipids that derive from the Kennedy pathway (Wang et al., 2012). The process involves alteration of the fatty acyl composition at the sn-2-position of PC resulting in generation of varied PC species with unique fatty acids, each with a different carbon chain length and degree of saturation (Shimizu et al., 2006; Schlame et al., 2000; Lands, 2000). Thus our observations suggest that sensitive cells incorporate LPCs into their membranes faster than the resistant cells and thus remodel their membrane more quickly.

Phosphatidylethanolamine (PE) is a phospholipid found in all living organisms. Most biological membranes are made up of PE together with phosphatidylcholine (PC), phosphatidylserine (PS) and phosphatidylinositol (PI). The levels of several phosphatidylethanolamines such as PE 38:4, PE 38:5, PE 32:0 and PE 34:3 were higher in sensitive cells in comparison to the resistant cells. Furthermore, higher phosphatidylethanolamine and phosphatidylcholine levels in A2780 cells suggest increases in the *de novo* synthesis of these GPLs (Budczies et al., 2012). Our findings are resemble those from a previous study in which the level of glycerophospholipids

were increased as a signature of ovarian cancer (Iorio et al., 2005; Ben Sellem et al., 2011). Phosphatidylethanolamine can provide a substrate for phosphatidylcholines, whose extreme elevation has previously been observed in ovarian carcinomas (Halama et al., 2015; Iorio et al., 2005). There may be a connection between alteration in GPLs and the part they play in membrane integrity and transduction of mitogenic signals (Ackerstaff et al., 2003). Furthermore, an association has been seen between an increase in phosphatidylinositol and deregulation of the phosphoinositide-3 kinase (PI3K) pathway, which leads in its turn to carcinogenesis and angiogenesis (Halama et al., 2015). Phosphoethanolamine, is a substrate for many cell membrane phospholipids that has recently been shown to induce both cell cycle arrest and apoptosis in cancer cells (Ferreira et al., 2013a; Ferreira et al., 2013b). Here, intracellular phosphoethanolamine levels for PE 34:1 and PE 34:2 were decreased in both cell lines after exposure to melittin. In contrast, the level of some PE lipids such as PE 32:0 and PE 34:3 were found increased in A2780 following melittin treatment. Moreover, the levels of PE 38:4 and PE 38:5 were increased in A2780CR cells. This effect could be indicative of increased phospholipid membrane turnover or an apoptotic response to the increasing stress levels.

Several sphingomyelin (SM) lipids are higher in the A2780 cells in comparison to the A2780CR cells. This differs from previous reports of increased ceramide lipids, particularly glucosylceramides and galactosylceramides, in multidrug resistant ovarian cancer cells (Veldman et al., 2002) and breast cancer cells (Lavie et al., 1996). However, in these previous studies ceramides or glycosylceramides were measured rather than sphingomyelin lipids. Another study showed increases of

dihydroceramide, ceramide, sphingomyelin, lactosylceramide, and ganglioside species in ovarian cancer (A2780) cells that had been exposed to synthetic retinoids (Valsecchi et al., 2010). In common with Veldman et al. (Veldman et al., 2002), we have seen that resistant cells contained lower levels of lactosylceramide. Lactosylceramide was characterized by identification of the ions obtained by MS² (Figure 6.10).

That many lipids are present in lower levels in resistant cells, and especially lipids whose function includes promotion of membrane stability, indicates the possibility that resistance to cisplatin is unconventional in this cell line. Cisplatin is a polar drug which crosses cell membranes through the action of organic cation transporters (several of which have been identified) and not by passive diffusion (Yonezawa and Inui, 2011). Thus it is possible that cisplatin resistance could be mediated through mechanisms other than augmentation of membrane lipids. This possibility is supported by two of our findings which suggest that melittin, an agent known to destabilise cell membranes, was more active on the cisplatin resistant compared to cisplatin sensitive cells, and that polyamines were higher in the sensitive cells as described previously (Alonezi et al., 2016). Both observations further illustrate the fact that the A2780 cell line may have a more stable cell membrane.

Following treatment with melittin, lipids were significantly altered in both A2780 and A2780CR cells. The observed effect was much more marked in the cisplatin-sensitive cells, suggesting that the latter undergo much more extensive membrane re-modelling in response to melittin in comparison with the resistant cells.

6.6 Conclusions

It will be important to investigate the lipid metabolism as modulators of cell membrane integrity. This study shows that the cisplatin sensitive A2780 cells contain relatively higher levels of sphingolipid and phosphocholine ether lipids which might result in increased membrane stability and repair and thus resistance to the lytic action of melittin in comparison with the cisplatin resistant A2780CR cells. After exposure to melittin, the levels of most of the significantly affected lipid metabolites, particularly phosphocholines (e.g. PC34:0, PC34:1, PC36:1, PC36:2, PC36:3, PC40:3, PC40:4), were lower in A2780 compared to A2780CR cells, suggesting different metabolic responses in the two cell lines. The higher levels of glycerophosphocholine in A2780 cells may be related to higher *de novo* lipid synthesis and re-direction of cellular metabolism. Given that melittin interacts with cell membranes, the observed effect of greater toxicity of melittin to the resistant cells might suggest that the membranes are less adaptable in the cisplatin resistant cells compared to the sensitive ones. Over all, this study shows that a LC-MS based metabolomics approach for the assessment of drug effects *in vitro* provides a powerful tool for obtaining insights into the mechanism of action of potential therapeutic agents, while offering the possibility to identify key metabolite markers for *in vivo* monitoring of tumour responsiveness to standard chemotherapy. Melittin might serve as a valuable adjuvant in cancer chemotherapy for overcoming chemoresistance.

Chapter 7

General Discussion and Future Works

7 General discussion and Future Works

Discussion

Metabolomics represents a critical tool for studying phenotypic diversity at the molecular level. Metabolomics performs an important role clarifying mechanism of drug action, the molecular biology of diseases, and biomarker discovery (Dettmer et al., 2007). The focus of this thesis has been the careful study of the effects of melittin, cisplatin and melittin-cisplatin combination therapy on cisplatin resistant and cisplatin sensitive ovarian cancer cells through metabolomic profiling, taking advantage of the aforementioned benefits from metabolomics. This profiling was accomplished through the use of LCMS and biolog microarray technology. Using these profiling techniques the study focused on the A2780 and A2780CR ovarian cancer cells, identifying altered metabolites in both cells which represent several different pathways.

Chapter three revealed the effects of melittin on the metabolic pathways of A2780 and A2780CR ovarian cancer cell lines as demonstrated using mass spectrometry and biolog microarray technology. The pathways affected by melittin pertain to amino acid, carbohydrate, and energy metabolism. These findings echoed the work of Vermeersch et al. (2014) which found that docetaxel produced considerable alterations in the amino acid and carbohydrate metabolism of ovarian cancer cells (Vermeersch et al., 2014). Other studies have shown that gossypol reduces cellular levels of aspartic acid, GSH, and FAD (Wang et al., 2013). Consequently, the findings for melittin in this study confirm and add to the increasing body of literature which demonstrates the usefulness of metabolomics for determining metabolism-related changes induced in cancer cells by various agents. This study, much like several others, suggests that

melittin induces a stronger metabolism-related response in cisplatin-sensitive cells in comparison to cisplatin-resistant cells. This in turn suggests that the cisplatin-sensitive cell line has a much greater capacity than the resistant cells in terms of neutralising the impact of melittin. Several amino acids in A2780 cells were reduced in their levels following exposure to melittin. These amino acids include arginine, glutamate, glutamate-5-semialdehyde, N-acetyl-L-glutamate, proline, and pyrroline-3-hydroxy-5-carboxylate. It should be noted that the findings of the current study differ from the findings of Poisson et al. (2015) with regard to arginine. The previously mentioned study by Poisson et al. found that arginine was higher in sensitive cell lines (Poisson et al., 2015) while the current study found that arginine was higher in the resistant cell lines in both pre- and post-melittin treatment. The current study also discovered that some acyl carnitines responded to exposure to melittin, but only in the A2780 cell line and not the A2780CR cell line. Decreases in acetylcarnitine, butanoylcarnitine, and L-carnitine levels in the A2780 were dose-dependent; these decreases may be attributed to cell-specific alterations in metabolic pathways. Carnitine is critical to the regulation of energy production related to fatty acids and glucose at the cellular level; it is also involved in the conveyance of long-chain fatty acids across the inner mitochondrial membrane. Carnitine also facilitates chain-shortened acyl group transportation from where the groups are produced in peroxisomes to the mitochondria for additional energy metabolism (Zammit et al., 2009). From the findings of the current study, which reflect similar findings of prior research, it appears that A2780 cells have relatively higher levels of the polyamines which influence membrane stability and repair. This effect on membrane stability and repair seems to impair the lytic action of melittin when compared to the A2780CR cells. Melittin exposure affected the

metabolite levels, particularly with regard to amino acids and TCA cycle intermediates, much more significantly in the A2780 cells, with lower levels registered in those cells when compared to the A2780CR cells. This result suggests that the two cell lines have different metabolic responses to the melittin. It also suggests that melittin interacts with cell membranes, indicating that the membranes of sensitive cells are more adaptable than those of the resistant cells. Consequently, these findings demonstrate how a LC-MS based metabolomics approach for drug effect assessments can be a powerful tool for understanding the mechanism of action for potential therapeutic agents and the identification of key metabolic markers.

As a continuation of the previous studies, LC-MS and phenotype microarray profiling were carried out of ovarian cancer cells after the cells were exposed to cisplatin. The effects observed in this study are based on the intracellular metabolites of A2780 and A2780CR following cisplatin treatment at IC₅₀ concentrations within 24h. The findings reveal that the sensitive cells displayed a much more noteworthy response to the treatment than the resistant cells. This is attributed to the idea that the resistant cells may have developed a mechanism that either transports the cisplatin across the cell wall or otherwise deactivates the drug. However, in both cell lines most of the pathways affected by the treatment were related to amino acid metabolism, with considerable alterations to those pathways related to carbohydrate, energy, and nucleotide metabolism. The specific amino acids affected in both cell lines following cisplatin exposure include arginine, glycine, proline, serine, and threonine. A previous study by von Stechow et al. (2013) found that cisplatin produced significant metabolic changes in methionine degradation pathways; these include transmethylation and

transsulfuration/glutathione synthesis. Polyamine synthesis and catabolism, urea cycle, proline and arginine metabolism, and nucleotide metabolism of amino acid and carbohydrate metabolism in pluripotent stem cells are also affected (von Stechow et al., 2013). Other metabolomics studies focusing on cancer cells have shown that docetaxel produced major metabolic changes to amino acids and carbohydrate metabolism in those cells (Vermeersch et al., 2014). Other studies which have examined the effects of cisplatin on various kinds of cancer cells, as well as pluripotent cells and cells from organs, have documented changes in levels of arginine, GSH, and proline (Bayet-Robert et al., 2010; Doherty et al., 2014; Huang et al., 2012; Lodi and Ronen, 2011; Rainaldi et al., 2008; von Stechow et al., 2013). Depletion of GSH in particular has been implicated as a factor for cisplatin sensitivity in cancer cells (Byun et al., 2005). GSH or metallothioneins are cysteine-rich peptides which can detoxify the highly reactive aquo-complexes – but in ovarian cancer cisplatin resistance was directly proportional to increased intracellular glutathione (Lukyanova, 2010). What this contrast suggests ultimately is that oxidative damage is a significant contributing factor to the cisplatin response of A2780 cells but not A2780CR cells. Furthermore, these findings also insinuate that glutathione-related metabolic pathways are more likely to be altered in A2780 cells than A2780CR cells. Nucleotides were likewise observed to undergo changes. GTP and xanthine, which are metabolites produced by the purine pathway, were considerably changed in the sensitive cells when compared to the resistant cells. In other words, cisplatin treatment has the potential to decrease GTP in sensitive cells, likely as a result of cisplatin-induced apoptosis. Recent studies have likewise demonstrated a decrease in GTP levels in the context of anticancer treatments/agents and ischemic-induced apoptosis (Cummings and Schnellmann,

2002; Dagher, 2000; Vitale et al., 1997). This suggests that cisplatin's effect on nucleotide sugars is most likely cell-dependent (Duarte et al., 2013). Cisplatin clearly effects carbohydrate and energy metabolism in both sensitive and resistant cells following treatment but in different ways. A2780 cells appear to have lower levels of gluconic acid following treatment. Resistant cells in contrast showed lower levels of malate, 2-oxoglutarate and N-acetylneuraminate following cisplatin treatment when compared to the sensitive cells. D-sorbitol levels slightly decreased in sensitive cells following cisplatin treatment, but level changes in resistant cells were not significant. The phenotype array experiment reveals that glucose utilisation drops in the sensitive cells when compared to resistant cells after cisplatin treatment. Lower ATP and NADH levels in the sensitive cells points to lower rates of glucose metabolism; in resistant cells oxoglutarate and malate are lower, suggesting greater changes in the TCA cycle.

Given these effects on cellular metabolism it should come as no surprise that cisplatin comes with serious side effects. It is one of the most effective anticancer agents currently available for the treatment of various types of cancers; however, given its side effects, it is often given in combination therapy. Combination therapy has been the standard care, particularly in cancer treatment, since its purpose is to increase an individual's response and tolerability and to decrease resistance (Pinto et al., 2011). The work conducted for Chapter 5 assessed whether melittin enables an inhibitory effect in combination with cisplatin in both sensitive and resistant cells. It also evaluated whether melittin has a synergistic effect in combination with cisplatin. Recent studies suggest that certain components of bee venom may possess anti-tumor properties when used on human ovarian cancer as well as enhancing the cytotoxic

effect of cisplatin (Alizadehnohi et al., 2012). The respective mechanisms of melittin and cisplatin can interact to increase or decrease anticancer efficacy. This creates three possible effects, additive, antagonist, and synergism (as previously discussed in Chapter 5). In the case of melittin and cisplatin a combination index analysis demonstrated that the effect of the two agents is synergistic with regard to the A2780 cells when the concentrations were 5+2 $\mu\text{g/mL}$. In the A2780CR cells synergistic effects were observed when the concentrations of melittin+cisplatin were 2+10 $\mu\text{g/mL}$. Antagonistic effects were observed when the concentration of melittin remained fixed but the concentration of cisplatin was increased. This suggests that the A2780CR cells are resistant to cisplatin and remain unaffected by cisplatin. The current study utilised untargeted metabolomics to compare the metabolic profiles of the sensitive and resistant cells following treatment using melittin-cisplatin combination therapy; metabolomics were assessed using a LC-MS based metabolomics approach. The intracellular metabolites of A2780 and A2780CR cells both showed differential changes following combination treatment. The most altered metabolites in A2780 and A2780CR cells were related to amino acid, energy, carbohydrate, and nucleotide metabolism. However, the most affected group of metabolites were amino acids, therefore affecting the amino acid metabolism pathway. Most of the metabolites grouped associated with the arginine and proline pathways were reduced in sensitive cells after combination treatments. However, arginine and its metabolites were non-significantly altered in resistant cells.

The work carried out in Chapter 3 examined the effect of melittin on A2780 and A2780CR cells and showed that the level of arginine was downregulated in cisplatin

sensitive cells in comparison to resistant cells. A number of studies have reported that arginine deficiency enhances apoptosis in different cell lines (Gong et al., 2000; Feun et al., 2008; Szlosarek et al., 2006). Glutathione levels were likewise downregulated following combination treatment in both sensitive and resistant cells, though the A2780 cells showed a stronger response. This indicates that the combination effects of melittin and cisplatin affected the DNA damage response, with particular reference to the p53 pathway contributing to apoptosis. Separately, melittin and cisplatin have differential metabolic effects on ovarian cancer cells. Melittin therapy preferentially affects amino acids and TCA cycle intermediates. However, this effect is changed when cisplatin is added, noticeably affecting the metabolism of the A2780 and A2780CR cells in a similar manner in some areas such as purine metabolism.

The work carried out in Chapter 6 demonstrated that the sensitive A2780 cells show relatively higher levels of sphingolipid and phosphocholine ether lipids which may produce increased membrane stability and repair, in turn increasing the resistance of the cells to the lytic action of melittin when compared to the resistant A2780CR cells. Following exposure to melittin the levels of some of the most significantly affected lipid metabolites, namely phosphocholine (e.g. PC34:0, PC34:1, PC36:1, PC36:2, PC36:3, PC40:3, PC40:4), were lower in the sensitive cells when compared to the resistant cells, underlining the idea that the two types of cells have different metabolic responses. A27808 cells that experience significant increases in glycerophosphocholine may be experiencing increased *de novo* lipid synthesis as well as cellular metabolism re-direction. It has been shown that melittin interacts with cell membranes; this suggests that the observed effects point to the notion that the

membranes are less adaptable in the resistant cells as compared to the sensitive cells. This study demonstrates how a LC-MS-based metabolomics approach to assessing drug effects *in vitro* offers a remarkable tool for understanding the mechanisms of actions regarding potential therapeutic agents. It also offers the opportunity to identify key metabolite markers for *in vivo* monitoring of tumour responsiveness to standard chemotherapy. It is possible that melittin may serve as a valuable addition to cancer chemotherapy as a means of overcoming chemoresistance.

Future Works

The findings of this study, which is the first of its kind, may offer more evidence and insight regarding many facets of metabolomics, cisplatin, ovarian cancer, and metabolomic profiling resources. This includes their use in profiling the effects of melittin on cisplatin sensitive and cisplatin resistant ovarian cancer cells; profiling the responses of ovarian cancer cells to cisplatin exposure; and comparing metabolomic profiles of the effects of melittin in combination with cisplatin on ovarian cancer cells. It also demonstrates how a lipidomic analysis using LC-MS was able to clarify the effects of melittin on ovarian cancer cells. But despite the not-insignificant amounts of information and evidence generated by the study, there remains a need for further research and work in the future. There are several areas which emerged as the research unfolded which would clarify where and how such work may be accomplished.

The most interesting area for further exploration would be to examine in greater depth the differences between mechanisms of action resulting from the combination therapy of melittin-cisplatin which may offer a paradigm for battling chemoresistance that

emerges in the course of ovarian cancer therapy. The results of this study demonstrate a rationale for the ongoing examination of melittin-cisplatin combination therapy since the combination had a very different effect on the cell metabolome in comparison to melittin and cisplatin on their own. It would seem as if the effects of melittin on the cells whether resistant or sensitive affects the ability of the cell to defend itself against cisplatin. We carried out preliminary work (not reported here) which indicated that melittin increased the kill rate for cisplatin over time so that small amounts of melittin in the presence of cisplatin lead to an increase in the cytotoxic effect of cisplatin during a 48 hour incubation. This work was carried out at the end of the study and is the obvious next step for study both in terms of looking at cell death mechanism (apoptosis vs necrosis) and examining the metabolomic effects. Aside from further exploring the synergy between melittin and cisplatin, it would be interesting to explore synergy between melittin and other drugs and also to look at different cell lines. Combinations of melittin at subtoxic levels in combination with cisplatin could improve therapy across a wide range of chemoresistant ovarian cancers. An extension of the current work could involve the labelling of the metabolome of ovarian cancer cells with stable isotopes (e.g. ^{13}C -glucose, and ^{15}N labelled arginine) to track the dynamic response of cancer cells in three different scenarios: treatment with melittin alone, cisplatin alone, and melittin-cisplatin combination therapy. This would give further insight into the therapeutic potential of melittin. In addition further work could be carried with different Biolog array plates to assess the importance of other substrates such as amino acids to the ovarian cancer cell lines.

Appendix

8 Appendix

Chapter 2

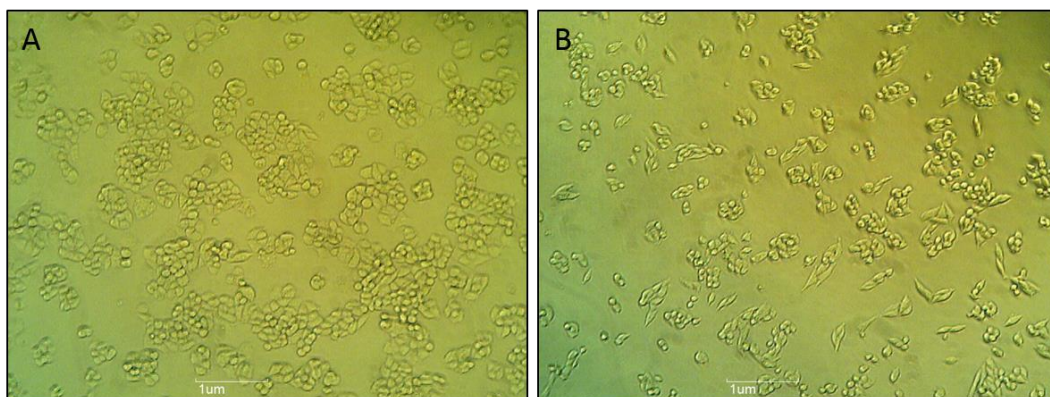


Figure S2.1. Morphology of A2780 and A2780CR cells. Cells visualized under 10 \times magnification. Cisplatin sensitive cells (A2780) (a) have round morphology and grow in tight clusters with substantial cellular cohesion. Comparatively, the cisplatin resistant cells (A2780CR) (b) have a spindle-like morphology.

Chapter 3

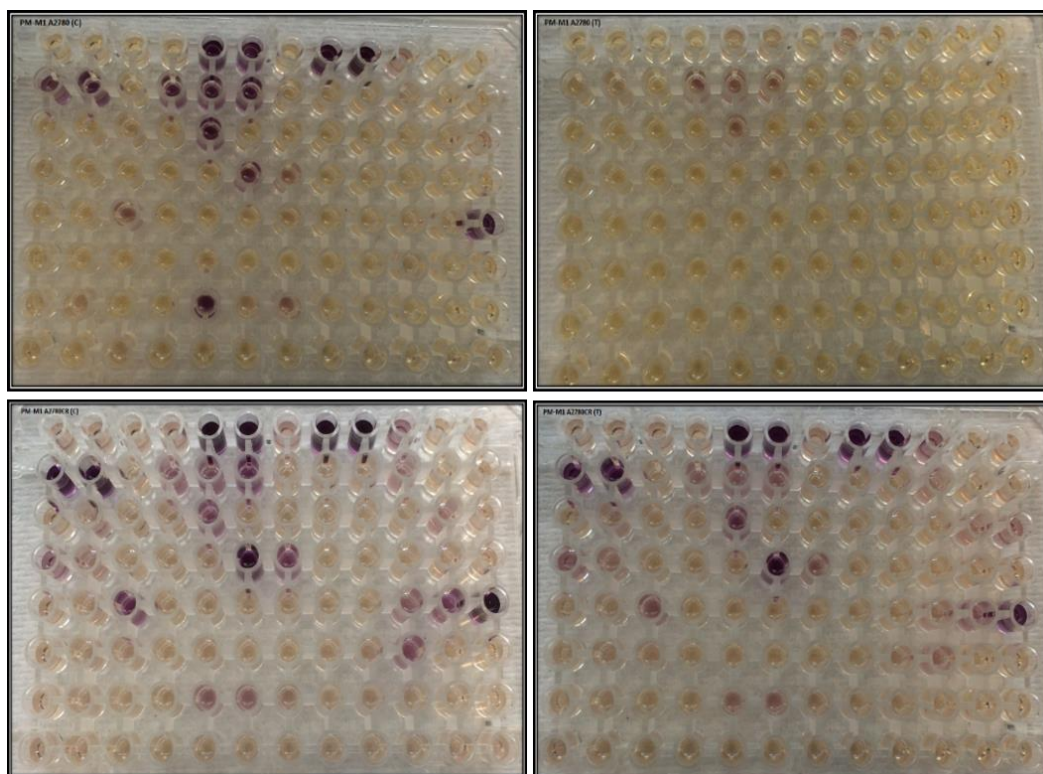


Figure S3.1. Changes in the metabolism of ovarian cancer A2780 and A2780CR cells. (a) Top left was A2780 without treatment; (b) Top right was A2780 after exposure to melittin; (c) Bottom left was A2780CR without treatment; (d) Bottom right was A2780CR after exposure to melittin.

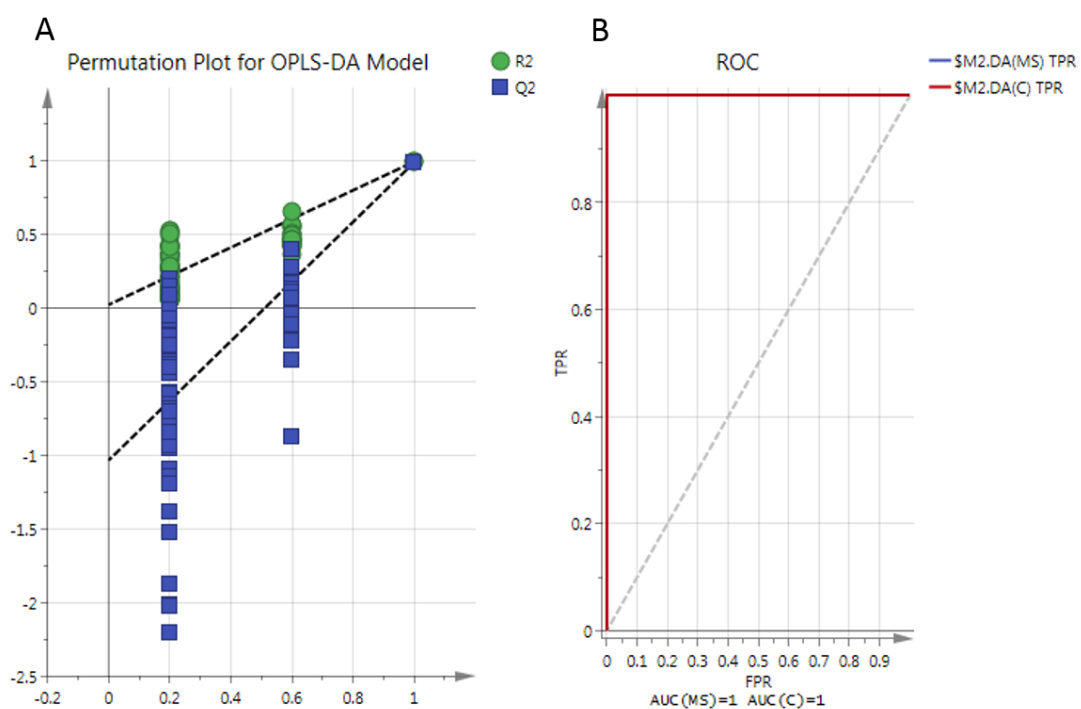


Figure S3.2. (A) Permutation analysis of OPLS-DA model derived from A2780 cells treated with melittin and control cells. Statistical validation of the OPLS-DA model by permutation analysis using 100 different model permutations. The goodness of fit (R2) and predictive capability (Q2) of the original model are indicated on the far right and remain higher than those of the 100 permuted models to the left. OPLS-DA, orthogonal partial least squares discriminant analysis. **(B)** Receiver Operating Characteristics (ROC) curve shows sensitivity (true positive rate (TPR)) on the y-axis versus (false positive rate (FPR = 1 - Specificity)) on the x-axis. The area under ROC curve (AUROCC) =1 for MS and C groups.

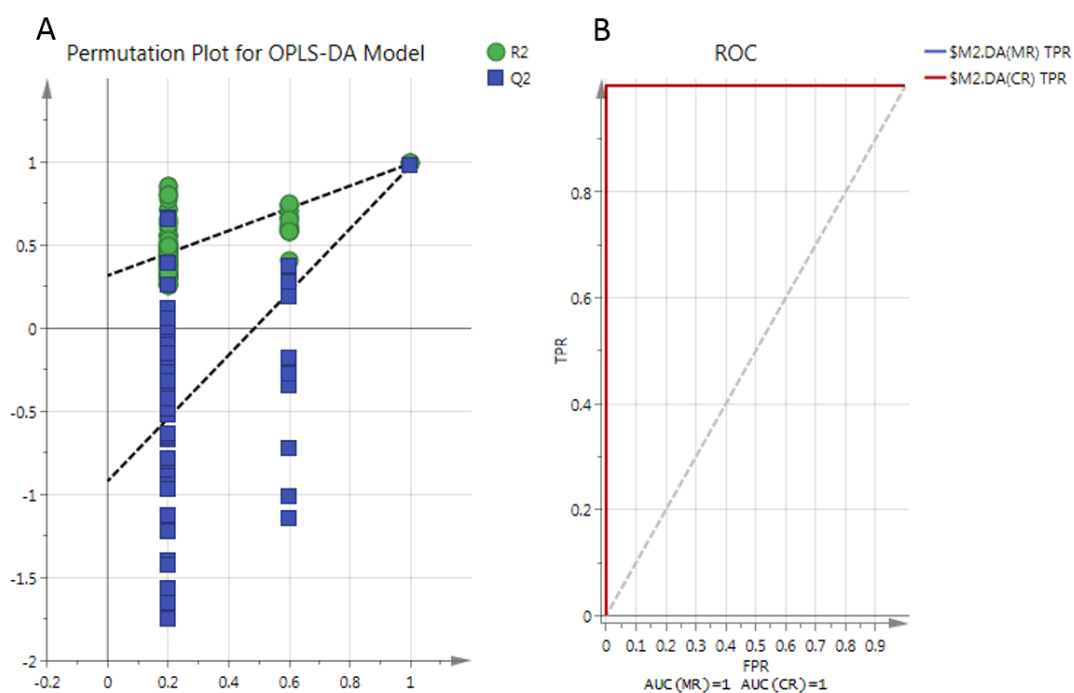


Figure S3.3. (A) Permutation analysis of OPLS-DA model derived from A2780CR cells treated with melittin and controls cells. Statistical validation of the OPLS-DA model by permutation analysis using 100 different model permutations. The goodness of fit (R2) and predictive capability (Q2) of the original model are indicated on the far right and remain higher than those of the 100 permuted models to the left. OPLS-DA, orthogonal partial least squares discriminant analysis. (B) Receiver Operating Characteristics (ROC) curve shows sensitivity (true positive rate (TPR)) on the y-axis versus (false positive rate (FPR = 1 - Specificity)) on the x-axis. The area under ROC curve (AUROCC) =1 for MR and CR groups.

Chapter 4

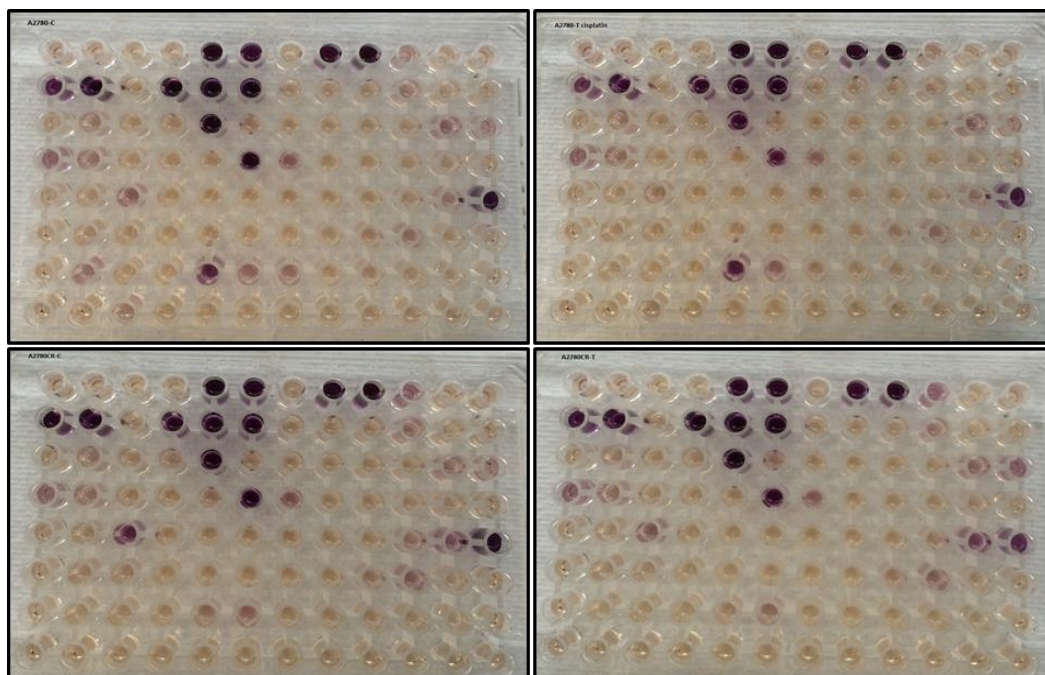


Figure S4.1. Changes in the metabolism of ovarian cancer A2780 and A2780CR cells after treatment with cisplatin at IC_{50} values. Top left was A2780 without treatment. Top right was A2780 after exposure to cisplatin. Bottom left was A2780CR without treatment. Bottom right was A2780CR after exposure to cisplatin.

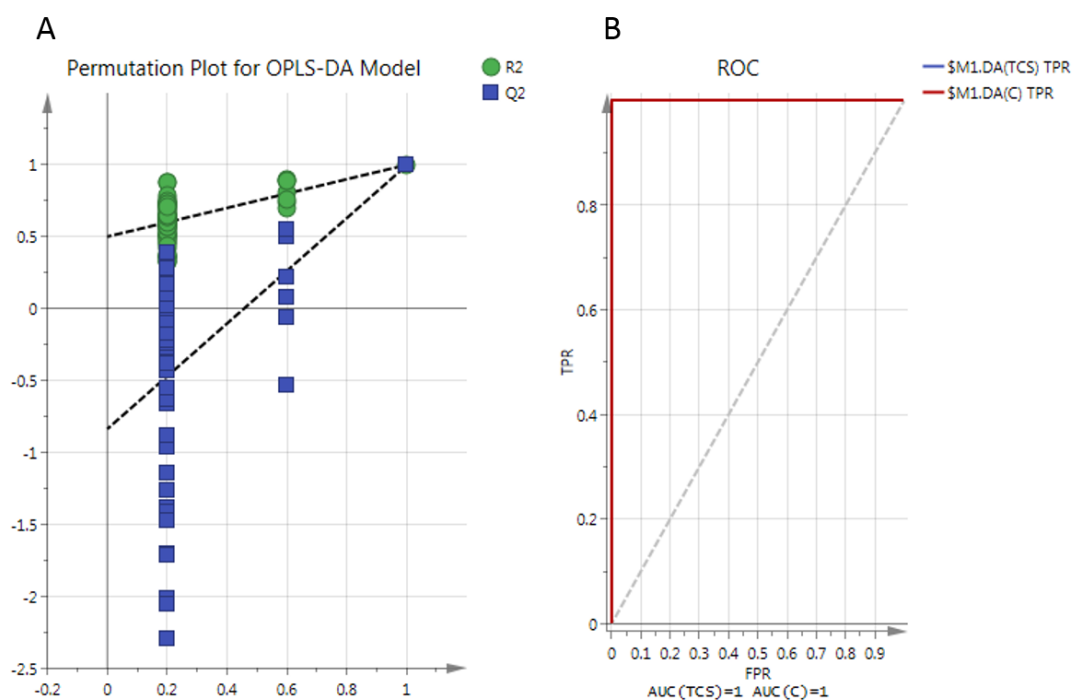


Figure S4.2. (A) Permutation analysis of OPLS-DA model derived from A2780 cells treated with cisplatin and controls cells. Statistical validation of the OPLS-DA model by permutation analysis using 100 different model permutations. The goodness of fit (R²) and predictive capability (Q²) of the original model are indicated on the far right and remain higher than those of the 100 permuted models to the left. OPLS-DA, orthogonal partial least squares discriminant analysis. (B) Receiver Operating Characteristics (ROC) curve shows sensitivity (true positive rate (TPR)) on the y-axis versus (false positive rate (FPR = 1 - Specificity)) on the x-axis. The area under ROC curve (AUROCC) =1 for TCS and C groups.

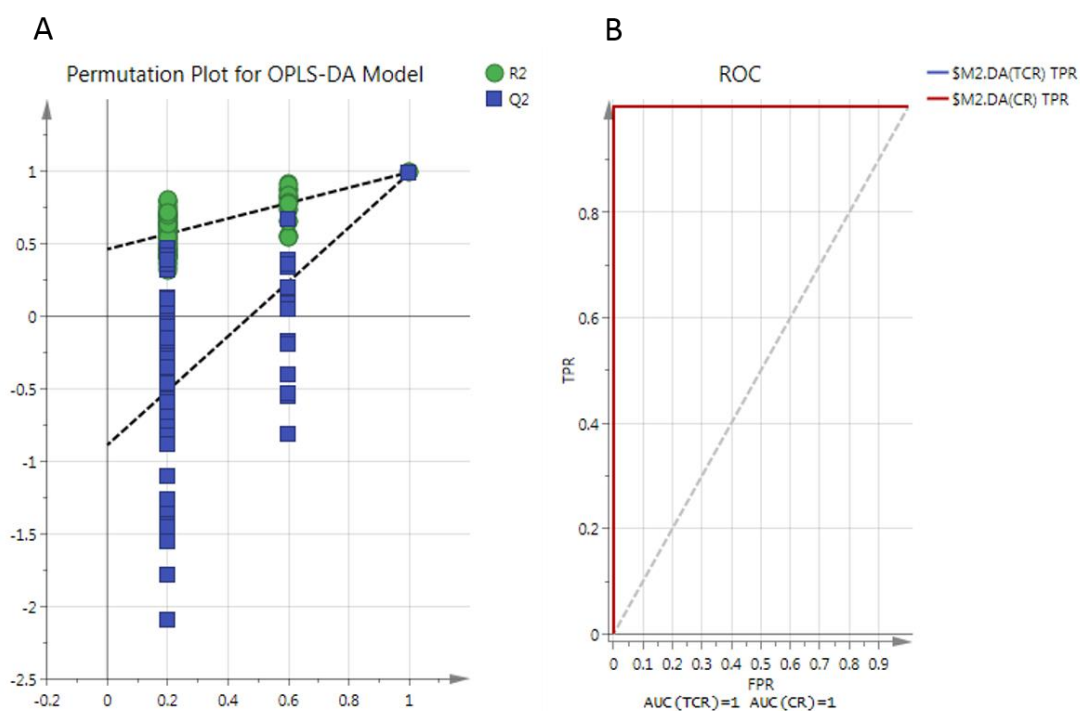


Figure S4.3. (A) Permutation analysis of OPLS-DA model derived from A2780CR cells treated with cisplatin and controls cells. Statistical validation of the OPLS-DA model by permutation analysis using 100 different model permutations. The goodness of fit (R2) and predictive capability (Q2) of the original model are indicated on the far right and remain higher than those of the 100 permuted models to the left. OPLS-DA, orthogonal partial least squares discriminant analysis. (B) Receiver Operating Characteristics (ROC) curve shows sensitivity (true positive rate (TPR)) on the y-axis versus (false positive rate (FPR = 1 - Specificity)) on the x-axis. The area under ROC curve (AUROCC) =1 for TCR and CR groups.

Chapter 5

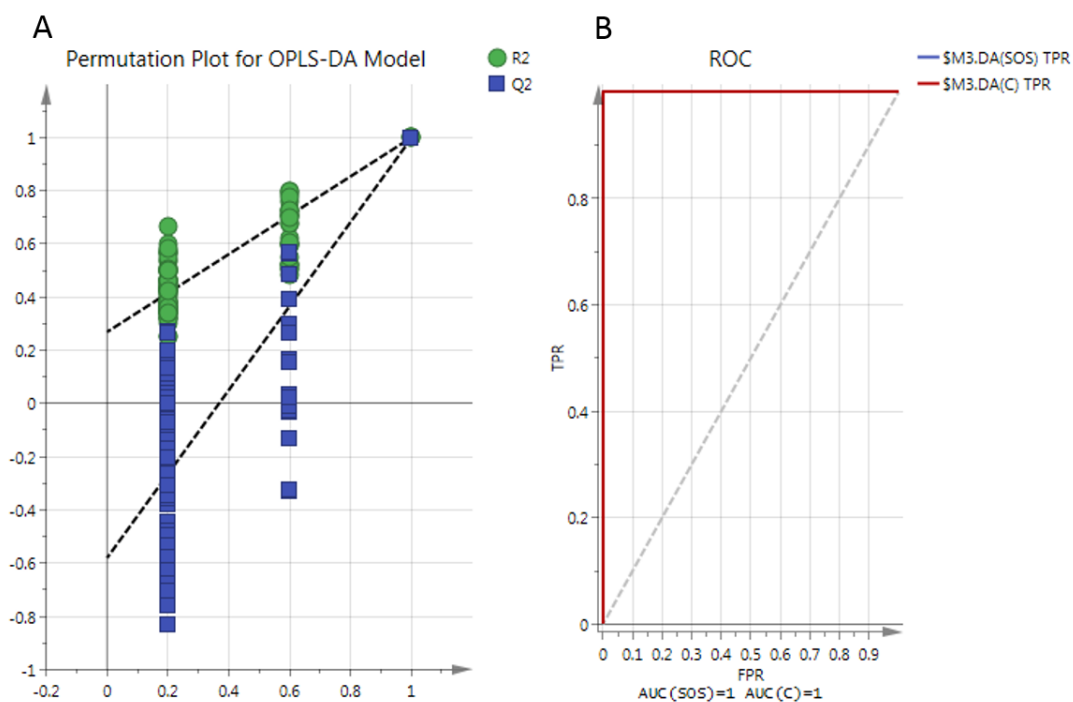


Figure S5.1. (A) Permutation analysis of OPLS-DA model derived from A2780 cells treated with melittin/cisplatin and controls cells. Statistical validation of the OPLS-DA model by permutation analysis using 100 different model permutations. The goodness of fit (R2) and predictive capability (Q2) of the original model are indicated on the far right and remain higher than those of the 100 permuted models to the left. OPLS-DA, orthogonal partial least squares discriminant analysis. (B) Receiver Operating Characteristics (ROC) curve shows sensitivity (true positive rate (TPR)) on the y-axis versus (false positive rate (FPR = 1 - Specificity)) on the x-axis. The area under ROC curve (AUROCC) =1 for SOS and C groups.

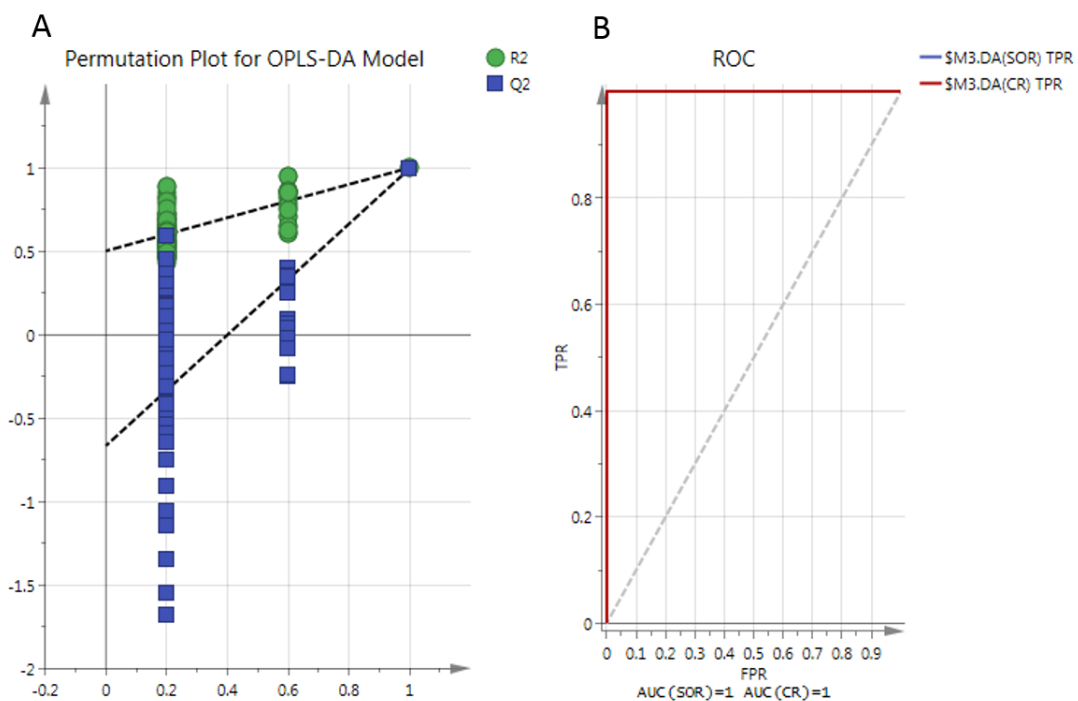


Figure S5.2. (A) Permutation analysis of OPLS-DA model derived from A2780CR cells treated with melittin/cisplatin and controls cells. Statistical validation of the OPLS-DA model by permutation analysis using 100 different model permutations. The goodness of fit (R2) and predictive capability (Q2) of the original model are indicated on the far right and remain higher than those of the 100 permuted models to the left. OPLS-DA, orthogonal partial least squares discriminant analysis. **(B)** Receiver Operating Characteristics (ROC) curve shows sensitivity (true positive rate (TPR)) on the y-axis versus (false positive rate (FPR = 1 - Specificity)) on the x-axis. The area under ROC curve (AUROCC) =1 for SOR and CR groups.

Chapter 6

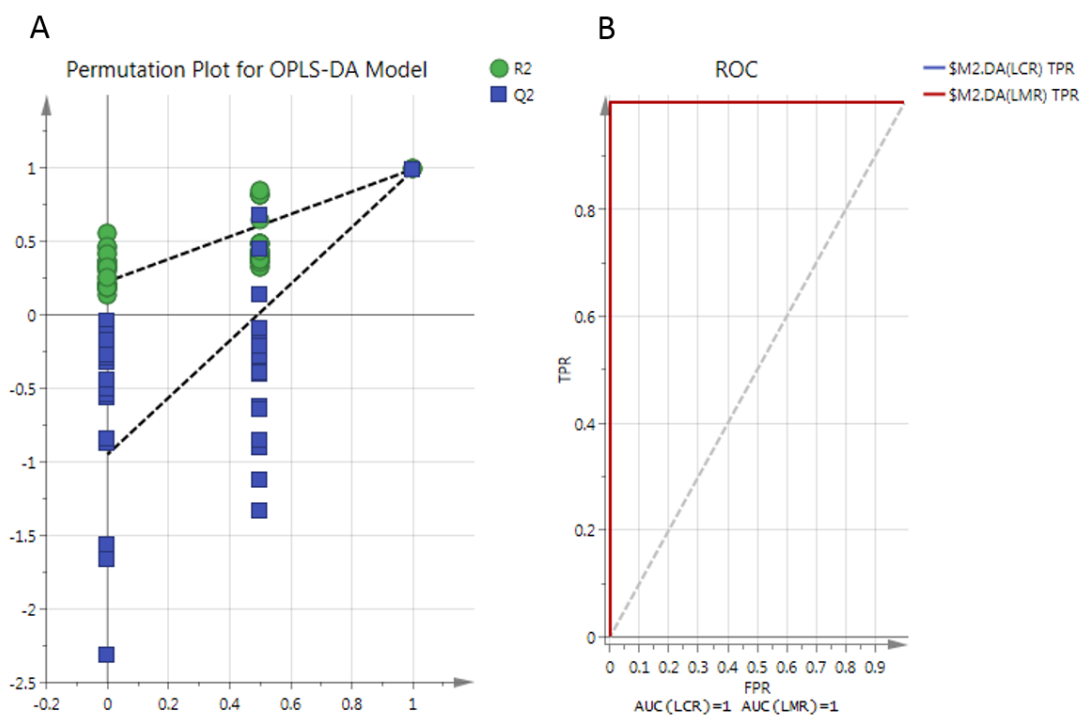


Figure S6.1. (A) Permutation analysis of OPLS-DA model derived from A2780CR cells treated with melittin and controls. Statistical validation of the OPLS-DA model by permutation analysis using 100 different model permutations. The goodness of fit (R²) and predictive capability (Q²) of the original model are indicated on the far right and remain higher than those of the 100 permuted models to the left. OPLS-DA, orthogonal partial least squares discriminant analysis. (B) Receiver Operating Characteristics (ROC) curve shows sensitivity (true positive rate (TPR)) on the y-axis versus (false positive rate (FPR = 1 - Specificity)) on the x-axis. The area under ROC curve (AUROC) = 1 for LCR and LMR groups.

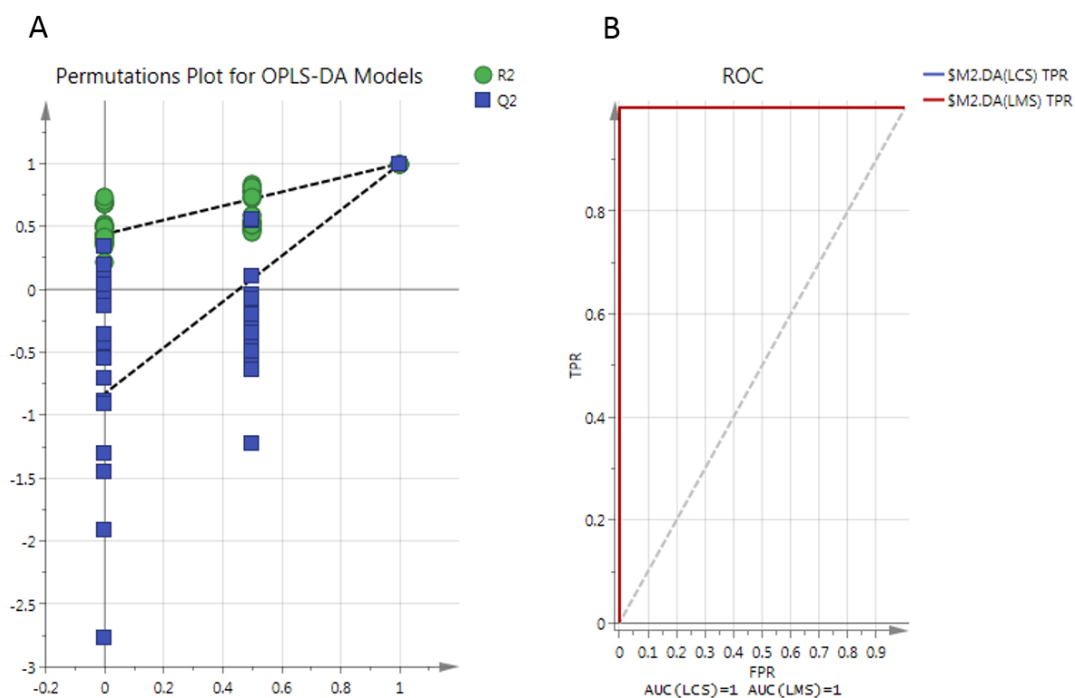


Figure S6.2. (A) Permutation analysis of OPLS-DA model derived from A2780 cells treated with melittin and controls. Statistical validation of the OPLS-DA model by permutation analysis using 100 different model permutations. The goodness of fit (R2) and predictive capability (Q2) of the original model are indicated on the far right and remain higher than those of the 100 permuted models to the left. OPLS-DA, orthogonal partial least squares discriminant analysis. (B) Receiver Operating Characteristics (ROC) curve shows sensitivity (true positive rate (TPR)) on the y-axis versus (false positive rate (FPR = 1 - Specificity)) on the x-axis. The area under ROC curve (AUROCC) =1 for LCS and LMS groups.

9 References

- ACKERSTAFF, E., GLUNDE, K. & BHUJWALLA, Z. M. 2003. Choline phospholipid metabolism: a target in cancer cells? *Journal of cellular biochemistry*, 90, 525-533.
- ADIBHATLA, R. M., HATCHER, J. & DEMPSEY, R. 2006. Lipids and lipidomics in brain injury and diseases. *The AAPS journal*, 8, E314-E321.
- AGARWAL, R. & KAYE, S. B. 2003. Ovarian cancer: strategies for overcoming resistance to chemotherapy. *Nature Reviews Cancer*, 3, 502-516.
- ALIZADEHNOHI, M., NABIUNI, M., NAZARI, Z., SAFAEINEJAD, Z. & IRIAN, S. 2012. The synergistic cytotoxic effect of cisplatin and honey bee venom on human ovarian cancer cell line A2780cp. *Journal of venom research*, 3, 22.
- ALONEZI, S., TUSIIMIRE, J., WALLACE, J., DUFTON, M., PARKINSON, J., YOUNG, L., CLEMENTS, C., PARK, J., JEON, J., FERRO, V. & WATSON, D. 2016. Metabolomic Profiling of the Effects of Melittin on Cisplatin Resistant and Cisplatin Sensitive Ovarian Cancer Cells Using Mass Spectrometry and Biolog Microarray Technology. *Metabolites*, 6, 35.
- AMELIO, I., CUTRUZZOLA, F., ANTONOV, A., AGOSTINI, M. & MELINO, G. 2014. Serine and glycine metabolism in cancer. *Trends in biochemical sciences*, 39, 191-198.
- ATHERTON, H. J., BAILEY, N. J., ZHANG, W., TAYLOR, J., MAJOR, H., SHOCKCOR, J., CLARKE, K. & GRIFFIN, J. L. 2006. A combined ¹H-NMR spectroscopy-and mass spectrometry-based metabolomic study of the PPAR- α null mutant mouse defines profound systemic changes in metabolism linked to the metabolic syndrome. *Physiological genomics*, 27, 178-186.
- BAE, J., LEE, B., HAN, E., AHN, I., LIM, S., KWON, M., KIM, S. & KIM, H. 2011. Urinary biomarkers for cisplatin-induced nephrotoxicity using metabolomic approach in vivo. *Toxicology Letters*, 205, S217.
- BAO, L., JARAMILLO, M. C., ZHANG, Z., ZHENG, Y., YAO, M., ZHANG, D. D. & YI, X. 2015. Induction of autophagy contributes to cisplatin resistance in human ovarian cancer cells. *Molecular medicine reports*, 11, 91-98.
- BAST, R. C., HENNESSY, B. & MILLS, G. B. 2009. The biology of ovarian cancer: new opportunities for translation. *Nature Reviews Cancer*, 9, 415-428.
- BAWAZEER, S., SUTCLIFFE, O. B., EUERBY, M. R., BAWAZEER, S. & WATSON, D. G. 2012. A comparison of the chromatographic properties of silica gel and silicon hydride modified silica gels. *Journal of Chromatography A*, 1263, 61-67.
- BAYET-ROBERT, M., MORVAN, D., CHOLLET, P. & BARTHOMEUF, C. 2010. Pharmacometabolomics of docetaxel-treated human MCF7 breast cancer cells provides evidence of varying cellular responses at high and low doses. *Breast cancer research and treatment*, 120, 613-626.
- BEDAIR, M. & SUMNER, L. W. 2008. Current and emerging mass-spectrometry technologies for metabolomics. *TrAC Trends in Analytical Chemistry*, 27, 238-250.
- BEGER, R. D. 2013. A review of applications of metabolomics in cancer. *Metabolites*, 3, 552-574.

- BEN SELLEM, D., ELBAYED, K., NEUVILLE, A., MOUSSALLIEH, F. M., LANG-AVEROUS, G., PIOTTO, M., BELLOCQ, J. P. & NAMER, I. J. 2011. Metabolomic Characterization of Ovarian Epithelial Carcinomas by HRMAS-NMR Spectroscopy. *J Oncol*, 2011, 174019.
- BIBLE, K. C. & KAUFMANN, S. H. 1997. Cytotoxic synergy between flavopiridol (NSC 649890, L86-8275) and various antineoplastic agents: the importance of sequence of administration. *Cancer research*, 57, 3375-3380.
- BOCCARD, J., VEUTHEY, J. L. & RUDAZ, S. 2010. Knowledge discovery in metabolomics: an overview of MS data handling. *Journal of separation science*, 33, 290-304.
- BOCHNER, B. R., SIRI, M., HUANG, R. H., NOBLE, S., LEI, X. H., CLEMONS, P. A. & WAGNER, B. K. 2011. Assay of the multiple energy-producing pathways of mammalian cells. *PLoS One*, 6, e18147.
- BOOKMAN, M. 2005. Standard treatment in advanced ovarian cancer in 2005: the state of the art. *International Journal of Gynecological Cancer*, 15, 212-220.
- BRADY, H. R., KONE, B. C., STROMSKI, M. E., ZEIDEL, M. L., GIEBISCH, G. & GULLANS, S. R. 1990. Mitochondrial injury: an early event in cisplatin toxicity to renal proximal tubules. *American Journal of Physiology-Renal Physiology*, 258, F1181-F1187.
- BUCKENDAHL, A.-C., BUDCZIES, J., FIEHN, O., DARB-ESFAHANI, S., KIND, T., NOSKE, A., WEICHERT, W., SEHOULI, J., BRAICU, E. & DIETEL, M. 2011. Prognostic impact of AMP-activated protein kinase expression in ovarian carcinoma: correlation of protein expression and GC/TOF-MS-based metabolomics. *Oncology reports*, 25, 1005-1012.
- BUDCZIES, J., DENKERT, C., MÜLLER, B. M., BROCKMÖLLER, S. F., KLAUSCHEN, F., GYÖRFFY, B., DIETEL, M., RICHTER-EHRENSTEIN, C., MARTEN, U. & SALEK, R. M. 2012. Remodeling of central metabolism in invasive breast cancer compared to normal breast tissue—a GC-TOFMS based metabolomics study. *BMC genomics*, 13, 334.
- BUSZEWSKI, B. & NOGA, S. 2012. Hydrophilic interaction liquid chromatography (HILIC)—a powerful separation technique. *Analytical and bioanalytical chemistry*, 402, 231-247.
- BYUN, S. S., KIM, S. W., CHOI, H., LEE, C. & LEE, E. 2005. Augmentation of cisplatin sensitivity in cisplatin - resistant human bladder cancer cells by modulating glutathione concentrations and glutathione - related enzyme activities. *BJU international*, 95, 1086-1090.
- CANCERRESEARCHUK. 2016 *Stages of ovarian cancer* [Online]. Available: <http://www.cancerresearchuk.org> [Accessed 24 December 2016].
- CAO, X., FANG, L., GIBBS, S., HUANG, Y., DAI, Z., WEN, P., ZHENG, X., SADEE, W. & SUN, D. 2007. Glucose uptake inhibitor sensitizes cancer cells to daunorubicin and overcomes drug resistance in hypoxia. *Cancer chemotherapy and pharmacology*, 59, 495-505.
- CARRASCO, R. A., STAMM, N. B. & PATEL, B. K. 2003. One-step cellular caspase-3/7 assay. *Biotechniques*, 34, 1064-1067.
- CAZES, J. 2005. *Encyclopedia of Chromatography*, New York, Taylor & Francis.
- CHAN, E. C. Y., MAL, M. & PASIKANTI, K. K. 2012. Metabonomics. In: POOLE, C.

- (ed.) *Gas Chromatography*. Oxford: Elsevier
- CHAN, M. M. & FONG, D. 2007. Overcoming Ovarian Cancer Drug Resistance with Phytochemicals and other Compounds. *In: PARSONS, R. A. (ed.) Progress in Cancer Drug Resistance Research*. New York: Nova Science
- CHANEY, S. G., CAMPBELL, S. L., BASSETT, E. & WU, Y. 2005. Recognition and processing of cisplatin-and oxaliplatin-DNA adducts. *Critical reviews in oncology/hematology*, 53, 3-11.
- CHANG, T., GULATI, S., CHOU, T., VEGA, R., GANDOLA, L., IBRAHIM, S. E., YOPP, J., COLVIN, M. & CLARKSON, B. 1985. Synergistic effect of 4-hydroperoxycyclophosphamide and etoposide on a human promyelocytic leukemia cell line (HL-60) demonstrated by computer analysis. *Cancer research*, 45, 2434-2439.
- CHEN, J. & LARIVIERE, W. R. 2010. The nociceptive and anti-nociceptive effects of bee venom injection and therapy: a double-edged sword. *Progress in neurobiology*, 92, 151-183.
- CHEN, J., ZHOU, L., ZHANG, X., LU, X., CAO, R., XU, C. & XU, G. 2012. Urinary hydrophilic and hydrophobic metabolic profiling based on liquid chromatography - mass spectrometry methods: Differential metabolite discovery specific to ovarian cancer. *Electrophoresis*, 33, 3361-3369.
- CHEN, V. J., BEWLEY, J. R., ANDIS, S. L., SCHULTZ, R. M., IVERSEN, P. W., SHIH, C., MENDELSON, L. G., SEITZ, D. E. & TONKINSON, J. L. Cellular pharmacology of MTA: a correlation of MTA-induced cellular toxicity and in vitro enzyme inhibition with its effect on intracellular folate and nucleoside triphosphate pools in CCRF-CEM cells. *Seminars in oncology*, 1999, 48-54.
- CHOI, K. E., HWANG, C. J., GU, S. M., PARK, M. H., KIM, J. H., PARK, J. H., AHN, Y. J., KIM, J. Y., SONG, M. J. & SONG, H. S. 2014. Cancer cell growth inhibitory effect of bee venom via increase of death receptor 3 expression and inactivation of NF-kappa B in NSCLC cells. *Toxins*, 6, 2210-2228.
- CHONG, I.-G. & JUN, C.-H. 2005. Performance of some variable selection methods when multicollinearity is present. *Chemometrics and Intelligent Laboratory Systems*, 78, 103-112.
- CHOU, T.-C., MOTZER, R. J., TONG, Y. & BOSL, G. J. 1994. Computerized quantitation of synergism and antagonism of taxol, topotecan, and cisplatin against human teratocarcinoma cell growth: a rational approach to clinical protocol design. *Journal of the National Cancer Institute*, 86, 1517-1524.
- CHOU, T.-C. & TALALAY, P. 1983. Analysis of combined drug effects: a new look at a very old problem. *Trends in Pharmacological Sciences*, 4, 450-454.
- CHOU, T.-C. & TALALAY, P. 1984. Quantitative analysis of dose-effect relationships: the combined effects of multiple drugs or enzyme inhibitors. *Advances in enzyme regulation*, 22, 27-55.
- CHOU, T. & MARTIN, N. 2005. CompuSyn for drug combinations: PC Software and user's guide: a computer program for quantitation of synergism and antagonism in drug combinations, and the determination of IC50 and ED50 and LD50 values. *ComboSyn, Paramus, NJ*.
- CHVETZOFF, G., BONNOTTE, B. & CHAUFFERT, B. 1998. [Anticancer

- chemotherapy. Prevention of toxicity]. *Presse medicale (Paris, France: 1983)*, 27, 2106-2112.
- COLOMBO, N. 2014. Optimising the treatment of the partially platinum-sensitive relapsed ovarian cancer patient. *European Journal of Cancer Supplements*, 12, 7-12.
- CREEK, D. J., JANKEVICS, A., BURGESS, K. E., BREITLING, R. & BARRETT, M. P. 2012. IDEOM: an Excel interface for analysis of LC-MS-based metabolomics data. *Bioinformatics*, 28, 1048-1049.
- CUI, Q., LEWIS, I. A., HEGEMAN, A. D., ANDERSON, M. E., LI, J., SCHULTE, C. F., WESTLER, W. M., EGHBALNIA, H. R., SUSSMAN, M. R. & MARKLEY, J. L. 2008. Metabolite identification via the madison metabolomics consortium database. *Nature biotechnology*, 26, 162-164.
- CUMMINGS, B. S. & SCHNELLMANN, R. G. 2002. Cisplatin-induced renal cell apoptosis: caspase 3-dependent and-independent pathways. *Journal of Pharmacology and Experimental Therapeutics*, 302, 8-17.
- ČUPERLOVIĆ-CULF, M., BARNETT, D. A., CULF, A. S. & CHUTE, I. 2010. Cell culture metabolomics: applications and future directions. *Drug discovery today*, 15, 610-621.
- DAGHER, P. C. 2000. Modeling ischemia in vitro: selective depletion of adenine and guanine nucleotide pools. *American Journal of Physiology-Cell Physiology*, 279, C1270-C1277.
- DAVIS, J. L., FALLON, H. J. & MORRIS, H. P. 1970. Two enzymes of serine metabolism in rat liver and hepatomas. *Cancer research*, 30, 2917-2920.
- DENKERT, C., BUDCZIES, J., KIND, T., WEICHERT, W., TABLACK, P., SEHOULI, J., NIESPOREK, S., KÖNSGEN, D., DIETEL, M. & FIEHN, O. 2006. Mass spectrometry-based metabolic profiling reveals different metabolite patterns in invasive ovarian carcinomas and ovarian borderline tumors. *Cancer research*, 66, 10795-10804.
- DETTMER, K., ARONOV, P. A. & HAMMOCK, B. D. 2007. Mass spectrometry - based metabolomics. *Mass spectrometry reviews*, 26, 51-78.
- DI GANGI, I. M., VRHOVSEK, U., PAZIENZA, V. & MATTIVI, F. 2014. Analytical metabolomics-based approaches to pancreatic cancer. *TrAC Trends in Analytical Chemistry*, 55, 94-116.
- DOHERTY, B., LAWLOR, D., GILLET, J.-P., GOTTESMAN, M., O'LEARY, J. J. & STORDAL, B. 2014. Collateral sensitivity to cisplatin in KB-8-5-11 drug-resistant cancer cells. *Anticancer research*, 34, 503-507.
- DRÖGE, W., SCHULZE-OSTHOFF, K., MIHM, S., GALTER, D., SCHENK, H. E., ECK, H., ROTH, S. & GMÜNDER, H. 1994. Functions of glutathione and glutathione disulfide in immunology and immunopathology. *The FASEB journal*, 8, 1131-1138.
- DU, L., ZHANG, X., HAN, Y. Y., BURKE, N. A., KOCHANNEK, P. M., WATKINS, S. C., GRAHAM, S. H., CARCILLO, J. A., SZABÓ, C. & CLARK, R. S. 2003. Intra-mitochondrial poly (ADP-ribosylation) contributes to NAD⁺ depletion and cell death induced by oxidative stress. *Journal of Biological Chemistry*, 278, 18426-18433.
- DUARTE, I., LADEIRINHA, A., LAMEGO, I., GIL, A., CARVALHO, L., CARREIRA, I. & MELO, J. 2013. Potential markers of cisplatin treatment response unveiled

- by NMR metabolomics of human lung cells. *Molecular pharmaceutics*, 10, 4242-4251.
- DUDLEY, E., YOUSEF, M., WANG, Y. & GRIFFITHS, W. 2010. Targeted metabolomics and mass spectrometry. *Adv Protein Chem Struct Biol*, 80, 45-83.
- DUNN, W. B., BAILEY, N. J. & JOHNSON, H. E. 2005. Measuring the metabolome: current analytical technologies. *Analyst*, 130, 606-625.
- DUNN, W. B. & ELLIS, D. I. 2005. Metabolomics: current analytical platforms and methodologies. *TrAC Trends in Analytical Chemistry*, 24, 285-294.
- DUTTA, A., SHETTY, P., BHAT, S., RAMACHANDRA, Y. & HEGDE, S. 2012. A mass spectrometric study for comparative analysis and evaluation of metabolite recovery from plasma by various solvent systems. *Journal of biomolecular techniques: JBT*, 23, 128.
- ECKSTEIN, N. 2011. Platinum resistance in breast and ovarian cancer cell lines. *J Exp Clin Cancer Res*, 30, 91.
- ENSOR, C. M., HOLTSBERG, F. W., BOMALASKI, J. S. & CLARK, M. A. 2002. Pegylated arginine deiminase (ADI-SS PEG20, 000 mw) inhibits human melanomas and hepatocellular carcinomas in vitro and in vivo. *Cancer research*, 62, 5443-5450.
- ERIKSSON, L., BYRNE, T., JOHANSSON, E., TRYGG, J. & VIKSTROM, C. 2013. *Multi- and Megavariate Data Analysis: Basic Principles and Application*, Sweden, MKS Umetrics AB.
- ERIKSSON, L., TRYGG, J. & WOLD, S. 2008. CV - ANOVA for significance testing of PLS and OPLS® models. *Journal of Chemometrics*, 22, 594-600.
- FAHY, E., SUBRAMANIAM, S., MURPHY, R. C., NISHIJIMA, M., RAETZ, C. R., SHIMIZU, T., SPENER, F., VAN MEER, G., WAKELAM, M. J. & DENNIS, E. A. 2009. Update of the LIPID MAPS comprehensive classification system for lipids. *Journal of lipid research*, 50, S9-S14.
- FAN, L., ZHANG, W., YIN, M., ZHANG, T., WU, X., ZHANG, H., SUN, M., LI, Z., HOU, Y. & ZHOU, X. 2012. Identification of metabolic biomarkers to diagnose epithelial ovarian cancer using a UPLC/QTOF/MS platform. *Acta Oncologica*, 51, 473-479.
- FERNANDIS, A. Z. & WENK, M. R. 2009. Lipid-based biomarkers for cancer. *Journal of Chromatography B*, 877, 2830-2835.
- FERRARA, M. & SEBEDIO, J. L. 2014. Challenges in nutritional metabolomics: from experimental design to interpretation of data sets. In: SEBEDIO, J. L. & BRENNAN, L. (eds.) *Metabolomics as a Tool in Nutrition Research*. Cambridge: Elsevier Science.
- FERREIRA, A. K., FREITAS, V. M., LEVY, D., RUIZ, J. L. M., BYDLOWSKI, S. P., RICI, R. E. G., R FILHO, O. M., CHIERICE, G. O. & MARIA, D. A. 2013a. Anti-angiogenic and anti-metastatic activity of synthetic phosphoethanolamine. *PloS one*, 8, e57937.
- FERREIRA, A. K., MENEGUELO, R., PEREIRA, A., R FILHO, O. M., CHIERICE, G. O. & MARIA, D. A. 2013b. Synthetic phosphoethanolamine induces cell cycle arrest and apoptosis in human breast cancer MCF-7 cells through the mitochondrial pathway. *Biomedicine & Pharmacotherapy*, 67, 481-487.
- FEUN, L., YOU, M., WU, C., KUO, M., WANGPAICHITR, M., SPECTOR, S. & SAVARAJ,

- N. 2008. Arginine deprivation as a targeted therapy for cancer. *Current pharmaceutical design*, 14, 1049-1057.
- FONG, M. Y., MCDUNN, J. & KAKAR, S. S. 2011. Identification of metabolites in the normal ovary and their transformation in primary and metastatic ovarian cancer. *PLoS One*, 6, e19963.
- FONTAINE, F., OVERMAN, J. & FRANÇOIS, M. 2015. Pharmacological manipulation of transcription factor protein-protein interactions: opportunities and obstacles. *Cell Regeneration*, 4, 1.
- FREZZA, C., ZHENG, L., TENNANT, D. A., PAPKOVSKY, D. B., HEDLEY, B. A., KALNA, G., WATSON, D. G. & GOTTLIEB, E. 2011. Metabolic profiling of hypoxic cells revealed a catabolic signature required for cell survival. *PLoS One*, 6, e24411.
- FURUYA, M. 2012. Ovarian Cancer Stroma: Pathophysiology and the Roles in Cancer Development. *Cancers*, 4, 701.
- GAJSKI, G., ČIMBORA-ZOVKO, T., RAK, S., OSMAK, M. & GARAJ-VRHOVAC, V. 2015. Antitumour action on human glioblastoma A1235 cells through cooperation of bee venom and cisplatin. *Cytotechnology*, 1-9.
- GAJSKI, G., ČIMBORA - ZOVKO, T., RAK, S., ROŽMAN, M., OSMAK, M. & GARAJ - VRHOVAC, V. 2014. Combined antitumor effects of bee venom and cisplatin on human cervical and laryngeal carcinoma cells and their drug resistant sublines. *Journal of Applied Toxicology*, 34, 1332-1341.
- GAJSKI, G. & GARAJ-VRHOVAC, V. 2013. Melittin: a lytic peptide with anticancer properties. *Environmental toxicology and pharmacology*, 36, 697-705.
- GALLUZZI, L., SENOVILLA, L., VITALE, I., MICHELS, J., MARTINS, I., KEPP, O., CASTEDO, M. & KROEMER, G. 2012. Molecular mechanisms of cisplatin resistance. *Oncogene*, 31, 1869-1883.
- GARCIA-PRIETO, C., AHMED, K. B. R., CHEN, Z., ZHOU, Y., HAMMOUDI, N., KANG, Y., LOU, C., MEI, Y., JIN, Z. & HUANG, P. 2013. Effective killing of leukemia cells by the natural product OSW-1 through disruption of cellular calcium homeostasis. *Journal of Biological Chemistry*, 288, 3240-3250.
- GIANNETTI, A. M., ZHENG, X., SKELTON, N. J., WANG, W., BRAVO, B. J., BAIR, K. W., BAUMEISTER, T., CHENG, E., CROCKER, L. & FENG, Y. 2014. Fragment-based identification of amides derived from trans-2-(pyridin-3-yl) cyclopropanecarboxylic acid as potent inhibitors of human nicotinamide phosphoribosyltransferase (NAMPT). *Journal of medicinal chemistry*, 57, 770-792.
- GOFF, B. A., MANDEL, L. S., DRESCHER, C. W., URBAN, N., GOUGH, S., SCHURMAN, K. M., PATRAS, J., MAHONY, B. S. & ANDERSEN, M. R. 2007. Development of an ovarian cancer symptom index. *Cancer*, 109, 221-227.
- GONG, H., ZÖLZER, F., VON RECKLINGHAUSEN, G., HAVERS, W. & SCHWEIGERER, L. 2000. Arginine deiminase inhibits proliferation of human leukemia cells more potently than asparaginase by inducing cell cycle arrest and apoptosis. *Leukemia (08876924)*, 14.
- GONZALEZ, V. M., FUERTES, M. A., ALONSO, C. & PEREZ, J. M. 2001. Is cisplatin-induced cell death always produced by apoptosis? *Molecular pharmacology*, 59, 657-663.
- GRIFFIN, J. L. & SHOCKCOR, J. P. 2004. Metabolic profiles of cancer cells. *Nat Rev*

- Cancer*, 4, 551-561.
- GUO, Y. & GAIKI, S. 2005. Retention behavior of small polar compounds on polar stationary phases in hydrophilic interaction chromatography. *Journal of Chromatography A*, 1074, 71-80.
- GUOYAO, W. & MORRIS, S. M. 1998. Arginine metabolism: nitric oxide and beyond. *Biochemical Journal*, 336, 1-17.
- HALAMA, A., GUERROUAHEN, B. S., PASQUIER, J., DIBOUN, I., KAROLY, E. D., SUHRE, K. & RAFII, A. 2015. Metabolic signatures differentiate ovarian from colon cancer cell lines. *Journal of translational medicine*, 13, 223.
- HAN, X. & GROSS, R. W. 2003. Global analyses of cellular lipidomes directly from crude extracts of biological samples by ESI mass spectrometry a bridge to lipidomics. *Journal of lipid research*, 44, 1071-1079.
- HARRIS, D. C. 2010. *Quantitative Chemical Analysis*, New York, W. H. Freeman.
- HEINTZ, A. P. M., ODICINO, F., MAISONNEUVE, P., QUINN, M. A., BENEDET, J. L., CREASMAN, W. T., NGAN, H. Y. S., PECORELLI, S. & BELLER, U. 2006. Carcinoma of the Ovary. FIGO 6th Annual Report on the Results of Treatment in Gynecological Cancer. *International Journal of Gynecology and Obstetrics*, 95, S161-S192.
- HISHIKAWA, D., HASHIDATE, T., SHIMIZU, T. & SHINDOU, H. 2014. Diversity and function of membrane glycerophospholipids generated by the remodeling pathway in mammalian cells. *Journal of lipid research*, 55, 799-807.
- HOLČAPEK, M., JIRÁSKO, R. & LÍSA, M. 2012. Recent developments in liquid chromatography-mass spectrometry and related techniques. *Journal of Chromatography A*, 1259, 3-15.
- HORAI, H., ARITA, M., KANAYA, S., NIHEI, Y., IKEDA, T., SUWA, K., OJIMA, Y., TANAKA, K., TANAKA, S. & AOSHIMA, K. 2010. MassBank: a public repository for sharing mass spectral data for life sciences. *Journal of mass spectrometry*, 45, 703-714.
- HOWLADER, N., NOONE, A. M., KRAPCHO, M., MILLER, D., BISHOP, K., ALTEKRUSE, S. F., KOSARY, C. L., YU, M., RUHL, J., TATALOVICH, Z., MARIOTTO, A., LEWIS, D. R., CHEN, H. S., FEUER, E. J. & CRONIN, K. A. 2016. *Cancer Stat Facts: Ovarian Cancer* [Online]. Available: <http://seer.cancer.gov/statfacts/html/ovary.html> [Accessed 12 December 2016].
- HU, C., YU, J., LIN, W.-W., DONALD, S. P., SUN, X.-Y., ALMASHANU, S., STEEL, G., PHANG, J. M., VOGELSTEIN, B. & VALLE, D. Overexpression of proline oxidase, a p53 induced gene (PIG6) induces reactive oxygen species generation and apoptosis in cancer cells. *Proc Am Assoc Cancer Res*, 2001. 225.
- HU, Q., NOLL, R. J., LI, H., MAKAROV, A., HARDMAN, M. & GRAHAM COOKS, R. 2005. The Orbitrap: a new mass spectrometer. *Journal of mass spectrometry*, 40, 430-443.
- HUANG, W., ZHOU, Q., YUAN, X., GE, Z.-M., RAN, F.-X., YANG, H.-Y., QIANG, G.-L., LI, R.-T. & CUI, J.-R. 2016. Proteasome Inhibitor YSY01A Enhances Cisplatin Cytotoxicity in Cisplatin-Resistant Human Ovarian Cancer Cells. *Journal of Cancer*, 7, 1133-1141.
- HUANG, Y., BELL, L. N., OKAMURA, J., KIM, M. S., MOHNEY, R. P., GUERRERO-

- PRESTON, R. & RATOVITSKI, E. A. 2012. Phospho- Δ Np63 α /SREBF1 protein interactions: bridging cell metabolism and cisplatin chemoresistance. *Cell Cycle*, 11, 3810-3827.
- HUI, L., LEUNG, K. & CHEN, H. 2001. The combined effects of antibacterial peptide cecropin A and anti-cancer agents on leukemia cells. *Anticancer research*, 22, 2811-2816.
- IORIO, E., MEZZANZANICA, D., ALBERTI, P., SPADARO, F., RAMONI, C., D'ASCENZO, S., MILLIMAGGI, D., PAVAN, A., DOLO, V. & CANEVARI, S. 2005. Alterations of choline phospholipid metabolism in ovarian tumor progression. *Cancer research*, 65, 9369-9376.
- IVOSEV, G., BURTON, L. & BONNER, R. 2008. Dimensionality reduction and visualization in principal component analysis. *Analytical chemistry*, 80, 4933-4944.
- JANDERA, P. 2008. Stationary phases for hydrophilic interaction chromatography, their characterization and implementation into multidimensional chromatography concepts. *Journal of separation science*, 31, 1421-1437.
- JANDERA, P. 2011. Stationary and mobile phases in hydrophilic interaction chromatography: a review. *Analytica chimica acta*, 692, 1-25.
- JEONG, Y.-J., CHOI, Y., SHIN, J.-M., CHO, H.-J., KANG, J.-H., PARK, K.-K., CHOE, J.-Y., BAE, Y.-S., HAN, S.-M. & KIM, C.-H. 2014. Melittin suppresses EGF-induced cell motility and invasion by inhibiting PI3K/Akt/mTOR signaling pathway in breast cancer cells. *Food and Chemical Toxicology*, 68, 218-225.
- JO, M., PARK, M. H., KOLLIPARA, P. S., AN, B. J., SONG, H. S., HAN, S. B., KIM, J. H., SONG, M. J. & HONG, J. T. 2012. Anti-cancer effect of bee venom toxin and melittin in ovarian cancer cells through induction of death receptors and inhibition of JAK2/STAT3 pathway. *Toxicology and applied pharmacology*, 258, 72-81.
- JOHNSON, H. E., BROADHURST, D., GOODACRE, R. & SMITH, A. R. 2003. Metabolic fingerprinting of salt-stressed tomatoes. *Phytochemistry*, 62, 919-928.
- KADERBHAI, N. N., BROADHURST, D. I., ELLIS, D. I., GOODACRE, R. & KELL, D. B. 2003. Functional genomics via metabolic footprinting: monitoring metabolite secretion by *Escherichia coli* tryptophan metabolism mutants using FT-IR and direct injection electrospray mass spectrometry. *Comparative and functional genomics*, 4, 376-391.
- KAMLEH, M. A., DOW, J. A. & WATSON, D. G. 2009. Applications of mass spectrometry in metabolomic studies of animal model and invertebrate systems. *Brief Funct Genomic Proteomic*, 8, 28-48.
- KATAJAMAA, M., MIETTINEN, J. & OREŠIČ, M. 2006. MZmine: toolbox for processing and visualization of mass spectrometry based molecular profile data. *Bioinformatics*, 22, 634-636.
- KATAJAMAA, M. & OREŠIČ, M. 2007. Data processing for mass spectrometry-based metabolomics. *Journal of chromatography A*, 1158, 318-328.
- KATRAGADDA, U., FAN, W., WANG, Y., TENG, Q. & TAN, C. 2013. Combined delivery of paclitaxel and tanespimycin via micellar nanocarriers: pharmacokinetics, efficacy and metabolomic analysis. *PloS one*, 8, e58619.
- KE, C., HOU, Y., ZHANG, H., FAN, L., GE, T., GUO, B., ZHANG, F., YANG, K., WANG, J.

- & LOU, G. 2015. Large - scale profiling of metabolic dysregulation in ovarian cancer. *International Journal of Cancer*, 136, 516-526.
- KIM, H., LEE, G., PARK, S., CHUNG, H.-S., LEE, H., KIM, J.-Y., NAM, S., KIM, S. K. & BAE, H. 2013. Bee Venom Mitigates Cisplatin-Induced Nephrotoxicity by Regulating CD4. *Evidence-Based Complementary and Alternative Medicine*, 2013.
- KIM, H., LEE, H., LEE, G., JANG, H., KIM, S.-S., YOON, H., KANG, G.-H., HWANG, D.-S., KIM, S. K. & CHUNG, H.-S. 2015. Phospholipase A2 inhibits cisplatin-induced acute kidney injury by modulating regulatory T cells by the CD206 mannose receptor. *Kidney international*.
- KINSEY, G. R. & OKUSA, M. D. 2014. Expanding role of T cells in acute kidney injury. *Current opinion in nephrology and hypertension*, 23, 9.
- KIRWAN, G. M., JOHANSSON, E., KLEEMANN, R., VERHEIJ, E. R., WHEELOCK, Å. M., GOTO, S., TRYGG, J. & WHEELOCK, C. E. 2012. Building multivariate systems biology models. *Analytical chemistry*, 84, 7064-7071.
- KOHNO, M., HORIBE, T., OHARA, K., ITO, S. & KAWAKAMI, K. 2014. The Membrane-Lytic Peptides K8L9 and Melittin Enter Cancer Cells via Receptor Endocytosis following Subcytotoxic Exposure. *Chemistry & biology*, 21, 1522-1532.
- KOMATSU, N., NAKAGAWA, M., ODA, T. & MURAMATSU, T. 2000. Depletion of intracellular NAD⁺ and ATP levels during ricin-induced apoptosis through the specific ribosomal inactivation results in the cytolysis of U 937 cells. *The Journal of Biochemistry*, 128, 463-470.
- KOPKA, J. 2006. Current challenges and developments in GC-MS based metabolite profiling technology. *Journal of biotechnology*, 124, 312-322.
- KRAJ, A., DESIDERIO, D. M. & NIBBERING, N. M. 2008. *Mass spectrometry: instrumentation, interpretation, and applications*, John Wiley & Sons.
- KRASTANOV, A. 2010. Metabolomics—The state of art. *Biotechnology & Biotechnological Equipment*, 24, 1537-1543.
- KRUIDERING, M., VAN DE WATER, B., DE HEER, E., MULDER, G. J. & NAGELKERKE, J. F. 1997. Cisplatin-induced nephrotoxicity in porcine proximal tubular cells: mitochondrial dysfunction by inhibition of complexes I to IV of the respiratory chain. *Journal of Pharmacology and Experimental Therapeutics*, 280, 638-649.
- KUHN, S., EGERT, B., NEUMANN, S. & STEINBECK, C. 2008. Building blocks for automated elucidation of metabolites: Machine learning methods for NMR prediction. *BMC bioinformatics*, 9, 1.
- LANDS, W. E. 2000. Stories about acyl chains. *Biochimica et Biophysica Acta (BBA)-Molecular and Cell Biology of Lipids*, 1483, 1-14.
- LAU, A. H. 1999. Apoptosis induced by cisplatin nephrotoxic injury. *Kidney international*, 56, 1295-1298.
- LAU, S. K., LAM, C.-W., CURREEM, S. O., LEE, K.-C., LAU, C. C., CHOW, W.-N., NGAN, A. H., TO, K. K., CHAN, J. F. & HUNG, I. F. 2015. Identification of specific metabolites in culture supernatant of Mycobacterium tuberculosis using metabolomics: exploration of potential biomarkers. *Emerging microbes & infections*, 4, e6.
- LAVIE, Y., CAO, H.-T., BURSTEN, S. L., GIULIANO, A. E. & CABOT, M. C. 1996.

- Accumulation of Glucosylceramides in Multidrug-resistant Cancer Cells. *Journal of Biological Chemistry*, 271, 19530-19536.
- LEE, G. & BAE, H. 2016. Bee venom phospholipase A2: Yesterday's enemy becomes today's friend. *Toxins*, 8, 48.
- LEMASTERS, J. J., QIAN, T., HE, L., KIM, J.-S., ELMORE, S. P., CASCIO, W. E. & BRENNER, D. A. 2002. Role of mitochondrial inner membrane permeabilization in necrotic cell death, apoptosis, and autophagy. *Antioxidants and Redox Signaling*, 4, 769-781.
- LI, L., HAN, J., WANG, Z., LIU, J. A., WEI, J., XIONG, S. & ZHAO, Z. 2014. Mass spectrometry methodology in lipid analysis. *International journal of molecular sciences*, 15, 10492-10507.
- LI, R. & HUANG, J. 2004. Chromatographic behavior of epirubicin and its analogues on high-purity silica in hydrophilic interaction chromatography. *Journal of chromatography A*, 1041, 163-169.
- LIEBERTHAL, W., TRIACA, V. & LEVINE, J. 1996. Mechanisms of death induced by cisplatin in proximal tubular epithelial cells: apoptosis vs. necrosis. *American Journal of Physiology-Renal Physiology*, 270, F700-F708.
- LIM, B.-S., MOON, H. J., LI, D. X., GIL, M., MIN, J. K., LEE, G., BAE, H., KIM, S. K. & MIN, B.-I. 2013. Effect of bee venom acupuncture on oxaliplatin-induced cold allodynia in rats. *Evidence-based complementary and alternative medicine*, 2013.
- LIND, D. S. 2004. Arginine and cancer. *The Journal of nutrition*, 134, 2837S-2841S.
- LIU, M., ZONG, J., LIU, Z., LI, L., ZHENG, X., WANG, B. & SUN, G. 2013. A novel melittin-MhIL-2 fusion protein inhibits the growth of human ovarian cancer SKOV3 cells in vitro and in vivo tumor growth. *Cancer Immunology, Immunotherapy*, 62, 889-895.
- LIU, S., WANG, W., ZHOU, X., GU, R. & DING, Z. 2014. Dose responsive effects of cisplatin in L02 cells using NMR-based metabolomics. *Environmental toxicology and pharmacology*, 37, 150-157.
- LIU, Y., BORCHERT, G. L., DONALD, S. P., SURAZYNSKI, A., HU, C.-A., WEYDERT, C. J., OBERLEY, L. W. & PHANG, J. M. 2005. MnSOD inhibits proline oxidase-induced apoptosis in colorectal cancer cells. *Carcinogenesis*, 26, 1335-1342.
- LOCASALE, J. W. 2013. Serine, glycine and one-carbon units: cancer metabolism in full circle. *Nature Reviews Cancer*, 13, 572-583.
- LODI, A. & RONEN, S. M. 2011. Magnetic resonance spectroscopy detectable metabolomic fingerprint of response to antineoplastic treatment. *PloS one*, 6, e26155.
- LUKYANOVA, N. Y. 2010. Characteristics of homocysteine-induced multidrug resistance of human MCF-7 breast cancer cells and human A2780 ovarian cancer cells. *Exp Oncol*, 32, 10-4.
- MACINTYRE, L., ZHANG, T., VIEGELMANN, C., MARTINEZ, I. J., CHENG, C., DOWDELLS, C., ABDELMOHSEN, U. R., GERNERT, C., HENTSCHEL, U. & EDRADE-EBEL, R. 2014. Metabolomic tools for secondary metabolite discovery from marine microbial symbionts. *Marine drugs*, 12, 3416-3448.
- MADDOCKS, O. D., BERKERS, C. R., MASON, S. M., ZHENG, L., BLYTH, K., GOTTLIEB, E. & VOUSDEN, K. H. 2013. Serine starvation induces stress and p53-

- dependent metabolic remodelling in cancer cells. *Nature*, 493, 542-546.
- MAGUIRE, M. L. 2014. An introduction to metabolomics and systems biology. In: JONES, O. A. H. (ed.) *Metabolomics and Systems Biology in Human Health and Medicine*. Wallingford: CABI.
- MAHADEVAN, S., SHAH, S. L., MARRIE, T. J. & SLUPSKY, C. M. 2008. Analysis of metabolomic data using support vector machines. *Analytical Chemistry*, 80, 7562-7570.
- MAHMOODZADEH, A., MORADY, A., ZARRINNAHAD, H., GHASEMI-DEHKORDI, P., MAHDAVI, M., SHAHBAZZADEH, D. & SHAHMORADY, H. 2013. Isolation of melittin from bee venom and evaluation of its effect on proliferation of gastric cancer cells. *Tehran University of Medical Sciences*, 70.
- MAHMOODZADEH, A., ZARRINNAHAD, H., BAGHERI, K. P., MORADIA, A. & SHAHBAZZADEH, D. 2015. First report on the isolation of melittin from Iranian honey bee venom and evaluation of its toxicity on gastric cancer AGS cells. *Journal of the Chinese Medical Association*, 78, 574-583.
- MAKAROV, A. & SCIGELOVA, M. 2010. Coupling liquid chromatography to Orbitrap mass spectrometry. *Journal of Chromatography A*, 1217, 3938-3945.
- MANDIC, A., HANSSON, J., LINDER, S. & SHOSHAN, M. C. 2003. Cisplatin induces endoplasmic reticulum stress and nucleus-independent apoptotic signaling. *Journal of Biological Chemistry*, 278, 9100-9106.
- MARÉCHAL, E., RIOU, M., KERBOEUF, D., BEUGNET, F., CHAMINADE, P. & LOISEAU, P. M. 2011. Membrane lipidomics for the discovery of new antiparasitic drug targets. *Trends in parasitology*, 27, 496-504.
- MARKMAN, M., MARKMAN, J., WEBSTER, K., ZANOTTI, K., KULP, B., PETERSON, G. & BELINSON, J. 2004. Duration of response to second-line, platinum-based chemotherapy for ovarian cancer: implications for patient management and clinical trial design. *Journal of clinical oncology*, 22, 3120-3125.
- MARTÍN, M. 2001. Platinum compounds in the treatment of advanced breast cancer. *Clinical breast cancer*, 2, 190-208.
- MATSUO, K., ENO, M. L., IM, D. D., ROSENSHEIN, N. B. & SOOD, A. K. 2010. Clinical relevance of extent of extreme drug resistance in epithelial ovarian carcinoma. *Gynecologic oncology*, 116, 61-65.
- MATTAINI, K. R., SULLIVAN, M. R. & VANDER HEIDEN, M. G. 2016. The importance of serine metabolism in cancer. *The Journal of Cell Biology*, 214, 249-257.
- MATTSON, M. P. & CHAN, S. L. 2003. Calcium orchestrates apoptosis. *Nature cell biology*, 5, 1041-1043.
- MAXWELL, S. A. & RIVERA, A. 2003. Proline oxidase induces apoptosis in tumor cells, and its expression is frequently absent or reduced in renal carcinomas. *Journal of Biological Chemistry*, 278, 9784-9789.
- MCLEAN, M. A., PRIEST, A. N., JOUBERT, I., LOMAS, D. J., KATAOKA, M. Y., EARL, H., CRAWFORD, R., BRENTON, J. D., GRIFFITHS, J. R. & SALA, E. 2009. Metabolic characterization of primary and metastatic ovarian cancer by ¹H - MRS in vivo at 3T. *Magnetic Resonance in Medicine*, 62, 855-861.
- MENENDEZ, J. A., LUPU, R. & COLOMER, R. 2004. Inhibition of tumor-associated

- fatty acid synthase hyperactivity induces synergistic chemosensitization of HER-2/neu-overexpressing human breast cancer cells to docetaxel (taxotere). *Breast cancer research and treatment*, 84, 183-195.
- MERRILL, A. H., SULLARDS, M. C., ALLEGOOD, J. C., KELLY, S. & WANG, E. 2005. Sphingolipidomics: high-throughput, structure-specific, and quantitative analysis of sphingolipids by liquid chromatography tandem mass spectrometry. *Methods*, 36, 207-224.
- MICHALSKI, A., DAMOC, E., HAUSCHILD, J.-P., LANGE, O., WIEGHAUS, A., MAKAROV, A., NAGARAJ, N., COX, J., MANN, M. & HORNING, S. 2011. Mass spectrometry-based proteomics using Q Exactive, a high-performance benchtop quadrupole Orbitrap mass spectrometer. *Mol Cell Proteomics*, 10, 1-11.
- MICHALSKI, A., DAMOC, E., LANGE, O., DENISOV, E., NOLTING, D., MÜLLER, M., VINER, R., SCHWARTZ, J., REMES, P. & BELFORD, M. 2012. Ultra high resolution linear ion trap Orbitrap mass spectrometer (Orbitrap Elite) facilitates top down LC MS/MS and versatile peptide fragmentation modes. *Molecular & Cellular Proteomics*, 11, 0111. 013698.
- MILKEVITCH, M., SHIM, H., PILATUS, U., PICKUP, S., WEHRLE, J. P., SAMID, D., POPTANI, H., GLICKSON, J. D. & DELIKATNY, E. J. 2005. Increases in NMR-visible lipid and glycerophosphocholine during phenylbutyrate-induced apoptosis in human prostate cancer cells. *Biochimica et Biophysica Acta (BBA)-Molecular and Cell Biology of Lipids*, 1734, 1-12.
- MILNE, S., IVANOVA, P., FORRESTER, J. & BROWN, H. A. 2006. Lipidomics: an analysis of cellular lipids by ESI-MS. *Methods*, 39, 92-103.
- MOGHIMI, S. M., SYMONDS, P., MURRAY, J. C., HUNTER, A. C., DEBSKA, G. & SZEWCZYK, A. 2005. A two-stage poly (ethylenimine)-mediated cytotoxicity: implications for gene transfer/therapy. *Molecular Therapy*, 11, 990-995.
- MOHELL, N., ALFREDSSON, J., FRANSSON, A., UUSTALU, M., BYSTROM, S., GULLBO, J., HALLBERG, A., BYKOV, V. J., BJORKLUND, U. & WIMAN, K. G. 2015. APR-246 overcomes resistance to cisplatin and doxorubicin in ovarian cancer cells. *Cell Death Dis*, 6, e1794.
- MOINARD, C., CYNOBER, L. & DE BANDT, J.-P. 2005. Polyamines: metabolism and implications in human diseases. *Clinical Nutrition*, 24, 184-197.
- MOLDOVEANU, S. C. & DAVID, V. 2016. *Selection of the HPLC Method in Chemical Analysis*, Amsterdam, Elsevier
- MONK, B. J., HERZOG, T. J., KAYE, S. B., KRASNER, C. N., VERMORKEN, J. B., MUGGIA, F. M., PUJADE-LAURINE, E., LISYANSKAYA, A. S., MAKHSON, A. N. & ROLSKI, J. 2010. Trabectedin plus pegylated liposomal doxorubicin in recurrent ovarian cancer. *Journal of clinical oncology*, 28, 3107-3114.
- MOORE, Z. & BOOTHMAN, D. A. 2014. Tumor-specific targeting of the NAD metabolome with β -lapachone and NamPT inhibition. *Cancer Research*, 74, 1760-1760.
- MORRÉ, D. J., KARTENBECK, J. & FRANKE, W. W. 1979. Membrane flow and interconversions among endomembranes. *Biochimica et Biophysica Acta (BBA)-Reviews on Biomembranes*, 559, 71-152.
- MORRIS, S. M. 2004. Enzymes of arginine metabolism. *The Journal of nutrition*,

134, 2743S-2747S.

- MUFSON, R., LASKIN, J., FISHER, P. & WEINSTEIN, I. 1979. Melittin shares certain cellular effects with phorbol ester tumour promoters.
- MURATA, T., HIBASAMI, H., MAEKAWA, S., TAGAWA, T. & NAKASHIMA, K. 1989. Preferential binding of cisplatin to mitochondrial DNA and suppression of ATP generation in human malignant melanoma cells. *Biochemistry international*, 20, 949-955.
- NEVEDOMSKAYA, E., PERRYMAN, R., SOLANKI, S., SYED, N., MAYBORODA, O. A. & KEUN, H. C. 2015. A systems oncology approach identifies NT5E as a key metabolic regulator in tumor cells and modulator of platinum sensitivity. *Journal of proteome research*, 15, 280-290.
- NGUYEN, T. 2008. Paclitaxel; The Billion Dollar Natural Product. *Chemistry*.
- NHS. 2015. *Ovarian Cancer* [Online]. Available: <http://www.nhs.uk/> [Accessed 12 December 2016].
- NICHOLSON, L. J., SMITH, P. R., HILLER, L., SZLOSAREK, P. W., KIMBERLEY, C., SEHOULI, J., KOENSGEN, D., MUSTEA, A., SCHMID, P. & CROOK, T. 2009. Epigenetic silencing of argininosuccinate synthetase confers resistance to platinum - induced cell death but collateral sensitivity to arginine auxotrophy in ovarian cancer. *International journal of cancer*, 125, 1454-1463.
- ODUNSI, K., WOLLMAN, R. M., AMBROSONE, C. B., HUTSON, A., MCCANN, S. E., TAMMELA, J., GEISLER, J. P., MILLER, G., SELLERS, T. & CLIBY, W. 2005. Detection of epithelial ovarian cancer using ¹H - NMR - based metabonomics. *International journal of cancer*, 113, 782-788.
- OH, S.-B., HWANG, C. J., SONG, S.-Y., JUNG, Y. Y., YUN, H.-M., SOK, C. H., SUNG, H. C., YI, J.-M., PARK, D. H. & HAM, Y. W. 2014. Anti-cancer effect of tectochrysin in NSCLC cells through overexpression of death receptor and inactivation of STAT3. *Cancer letters*, 353, 95-103.
- OLIVER, S. G., WINSON, M. K., KELL, D. B. & BAGANZ, F. 1998. Systematic functional analysis of the yeast genome. *Trends in biotechnology*, 16, 373-378.
- OLIVERO, O. A., CHANG, P. K., LOPEZ-LARRAZA, D. M., SEMINO-MORA, M. C. & POIRIER, M. C. 1997. Preferential formation and decreased removal of cisplatin-DNA adducts in Chinese hamster ovary cell mitochondrial DNA as compared to nuclear DNA. *Mutation Research/Genetic Toxicology and Environmental Mutagenesis*, 391, 79-86.
- OZOLS, R. 2006. Challenges for chemotherapy in ovarian cancer. *Annals of Oncology*, 17, v181-v187.
- PALMNAS, M. S. & VOGEL, H. J. 2013. The future of NMR metabolomics in cancer therapy: towards personalizing treatment and developing targeted drugs? *Metabolites*, 3, 373-396.
- PAN, X., WILSON, M., MCCONVILLE, C., ARVANITIS, T. N., GRIFFIN, J. L., KAUPPINEN, R. A. & PEET, A. C. 2013. Increased unsaturation of lipids in cytoplasmic lipid droplets in DAOY cancer cells in response to cisplatin treatment. *Metabolomics*, 9, 722-729.
- PARKER, R. J., EASTMAN, A., BOSTICK-BRUTON, F. & REED, E. 1991. Acquired cisplatin resistance in human ovarian cancer cells is associated with

- enhanced repair of cisplatin-DNA lesions and reduced drug accumulation. *J Clin Invest*, 87, 772-7.
- PARSONS, H. M., LUDWIG, C., GUNTHER, U. L. & VIANT, M. R. 2007. Improved classification accuracy in 1- and 2-dimensional NMR metabolomics data using the variance stabilising generalised logarithm transformation. *BMC Bioinformatics*, 8, 234.
- PASIKANTI, K. K., ESUVARANATHAN, K., HO, P. C., MAHENDRAN, R., KAMARAJ, R., WU, Q. H., CHIONG, E. & CHAN, E. C. Y. 2010. Noninvasive urinary metabonomic diagnosis of human bladder cancer. *Journal of proteome research*, 9, 2988-2995.
- PATRICK REYNOLDS, C. & MAURER, B. J. 2005. Evaluating response to antineoplastic drug combinations in tissue culture models. *Chemosensitivity: Volume 1 In Vitro Assays*, 173-183.
- PIKE, N. 2011. Using false discovery rates for multiple comparisons in ecology and evolution. *Methods in Ecology and Evolution*, 2, 278-282.
- PINTO, A. C., MOREIRA, J. N. & SIMÕES, S. 2011. *Combination chemotherapy in cancer: principles, evaluation and drug delivery strategies*, INTECH Open Access Publisher.
- PLUSKAL, T., CASTILLO, S., VILLAR-BRIONES, A. & OREŠIČ, M. 2010. MZmine 2: modular framework for processing, visualizing, and analyzing mass spectrometry-based molecular profile data. *BMC bioinformatics*, 11, 1.
- PODDER, B., KIM, Y.-S. & SONG, H.-Y. 2013. Cytoprotective effect of bioactive sea buckthorn extract on paraquat-exposed A549 cells via induction of Nrf2 and its downstream genes. *Molecular medicine reports*, 8, 1852-1860.
- POISSON, L. M., MUNKARAH, A., MADI, H., DATTA, I., HENSLEY-ALFORD, S., TEBBE, C., BUEKERS, T., GIRI, S. & RATTAN, R. 2015. A metabolomic approach to identifying platinum resistance in ovarian cancer. *Journal of ovarian research*, 8, 1-14.
- PORTILLA, D., LI, S., NAGOTHU, K., MEGYESI, J., KAISLING, B., SCHNACKENBERG, L., SAFIRSTEIN, R. & BEGER, R. 2006. Metabolomic study of cisplatin-induced nephrotoxicity. *Kidney international*, 69, 2194-2204.
- PULFER, M. & MURPHY, R. C. 2003. Electrospray mass spectrometry of phospholipids. *Mass spectrometry reviews*, 22, 332-364.
- PURWAHA, P., LORENZI, P. L., SILVA, L. P., HAWKE, D. H. & WEINSTEIN, J. N. 2014. Targeted metabolomic analysis of amino acid response to L-asparaginase in adherent cells. *Metabolomics*, 10, 909-919.
- QIAN, C.-Y., WANG, K.-L., FANG, F.-F., GU, W., HUANG, F., WANG, F.-Z., LI, B. & WANG, L.-N. 2015. Triple-controlled oncolytic adenovirus expressing melittin to exert inhibitory efficacy on hepatocellular carcinoma. *International Journal of Clinical and Experimental Pathology*, 8, 10403.
- RABIK, C. A. & DOLAN, M. E. 2007. Molecular mechanisms of resistance and toxicity associated with platinating agents. *Cancer Treatment Reviews*, 33, 9-23.
- RAINALDI, G., ROMANO, R., INDOVINA, P., FERRANTE, A., MOTTA, A., INDOVINA, P. L. & SANTINI, M. T. 2008. Metabolomics using ¹H-NMR of apoptosis and Necrosis in HL60 leukemia cells: differences between the two types of cell death and independence from the stimulus of apoptosis used. *Radiation*

- research*, 169, 170-180.
- ROESSNER, U., WAGNER, C., KOPKA, J., TRETHERWEY, R. N. & WILLMITZER, L. 2000. Simultaneous analysis of metabolites in potato tuber by gas chromatography–mass spectrometry. *The Plant Journal*, 23, 131-142.
- ROJO, D., BARBAS, C. & RUPÉREZ, F. J. 2012. LC-MS metabolomics of polar compounds. *Bioanalysis*, 4, 1235-1243.
- SANTALI, E. Y., EDWARDS, D., SUTCLIFFE, O. B., BAILES, S., EUERBY, M. R. & WATSON, D. G. 2014. A comparison of Silica C and silica gel in HILIC mode: the effect of stationary phase surface area. *Chromatographia*, 77, 873-881.
- SASADA, S., MIYATA, Y., TSUTANI, Y., TSUYAMA, N., MASUJIMA, T., HIHARA, J. & OKADA, M. 2013. Metabolomic analysis of dynamic response and drug resistance of gastric cancer cells to 5-fluorouracil. *Oncology reports*, 29, 925-931.
- SAYQAL, A., XU, Y., TRIVEDI, D. K., ALMASOUD, N., ELLIS, D. I., MUHAMADALI, H., RATTRAY, N. J., WEBB, C. & GOODACRE, R. 2016. Metabolic analysis of the response of *Pseudomonas putida*. *Metabolomics*, 12, 1-12.
- SCHAUER, N., STEINHAUSER, D., STRELKOV, S., SCHOMBURG, D., ALLISON, G., MORITZ, T., LUNDGREN, K., ROESSNER-TUNALI, U., FORBES, M. G. & WILLMITZER, L. 2005. GC–MS libraries for the rapid identification of metabolites in complex biological samples. *FEBS letters*, 579, 1332-1337.
- SCHLAME, M., RUA, D. & GREENBERG, M. L. 2000. The biosynthesis and functional role of cardiolipin. *Progress in lipid research*, 39, 257-288.
- SCHUBER, F. 1989. Influence of polyamines on membrane functions. *Biochemical Journal*, 260, 1.
- SCOVASSI, A. I. & POIRIER, G. G. 1999. Poly (ADP-ribosylation) and apoptosis. *Molecular and cellular biochemistry*, 199, 125-137.
- SEILER, N. & RAUL, F. 2005. Polyamines and apoptosis. *Journal of cellular and molecular medicine*, 9, 623-642.
- SERKOVA, N., FULLER, T. F., KLAWITTER, J., FREISE, C. E. & NIEMANN, C. U. 2005. ¹H-NMR–based metabolic signatures of mild and severe ischemia/reperfusion injury in rat kidney transplants. *Kidney international*, 67, 1142-1151.
- SHIMIZU, T., OHTO, T. & KITA, Y. 2006. Cytosolic phospholipase A2: biochemical properties and physiological roles. *IUBMB life*, 58, 328-333.
- SHUVAYEVA, G., BOBAK, Y., IGUMENTSEVA, N., TITONE, R., MORANI, F., STASYK, O. & ISIDORO, C. 2014. Single Amino Acid Arginine Deprivation Triggers Prosurvival Autophagic Response in Ovarian Carcinoma SKOV3. *BioMed research international*, 2014.
- SIDDIK, Z. H. 2003. Cisplatin: mode of cytotoxic action and molecular basis of resistance. *Oncogene*, 22, 7265-7279.
- SIMMLER, C., NAPOLITANO, J. G., MCALPINE, J. B., CHEN, S.-N. & PAULI, G. F. 2014. Universal quantitative NMR analysis of complex natural samples. *Current opinion in biotechnology*, 25, 51-59.
- SINGH, M., CHAUDHRY, P., FABÍ, F. & ASSELIN, E. 2013. Cisplatin-induced caspase activation mediates PTEN cleavage in ovarian cancer cells: a potential mechanism of chemoresistance. *BMC cancer*, 13, 1.
- SKULACHEV, V. 2006. Bioenergetic aspects of apoptosis, necrosis and mitoptosis.

- Apoptosis*, 11, 473-485.
- SLUPSKY, C. M., STEED, H., WELLS, T. H., DABBS, K., SCHEPANSKY, A., CAPSTICK, V., FAUGHT, W. & SAWYER, M. B. 2010. Urine metabolite analysis offers potential early diagnosis of ovarian and breast cancers. *Clinical Cancer Research*, 16, 5835-5841.
- SNELL, K. 1984. Enzymes of serine metabolism in normal, developing and neoplastic rat tissues. *Advances in enzyme regulation*, 22, 325-400.
- SPRATLIN, J. L., SERKOVA, N. J. & ECKHARDT, S. G. 2009. Clinical applications of metabolomics in oncology: a review. *Clinical Cancer Research*, 15, 431-440.
- STIPETIC, L. H., DALBY, M. J., DAVIES, R. L., MORTON, F. R., RAMAGE, G. & BURGESS, K. E. 2016. A novel metabolomic approach used for the comparison of *Staphylococcus aureus* planktonic cells and biofilm samples. *Metabolomics*, 12, 1-11.
- SUMNER, L. W., AMBERG, A., BARRETT, D., BEALE, M. H., BEGER, R., DAYKIN, C. A., FAN, T. W.-M., FIEHN, O., GOODACRE, R. & GRIFFIN, J. L. 2007. Proposed minimum reporting standards for chemical analysis. *Metabolomics*, 3, 211-221.
- SUTPHEN, R., XU, Y., WILBANKS, G. D., FIORICA, J., GRENDYS, E. C., LAPOLLA, J. P., ARANGO, H., HOFFMAN, M. S., MARTINO, M. & WAKELEY, K. 2004. Lysophospholipids are potential biomarkers of ovarian cancer. *Cancer Epidemiology Biomarkers & Prevention*, 13, 1185-1191.
- SZLOSAREK, P. W., KLABATSA, A., PALLASKA, A., SHEAFF, M., SMITH, P., CROOK, T., GRIMSHAW, M. J., STEELE, J. P., RUDD, R. M. & BALKWILL, F. R. 2006. In vivo loss of expression of argininosuccinate synthetase in malignant pleural mesothelioma is a biomarker for susceptibility to arginine depletion. *Clinical Cancer Research*, 12, 7126-7131.
- TAKAHASHI, H., MORIMOTO, T., OGASAWARA, N. & KANAYA, S. 2011. AMDORAP: Non-targeted metabolic profiling based on high-resolution LC-MS. *BMC Bioinformatics*, 12, 259.
- TAKAKURA, M., NAKAMURA, M., KYO, S., HASHIMOTO, M., MORI, N., IKOMA, T., MIZUMOTO, Y., FUJIWARA, T., URATA, Y. & INOUE, M. 2010. Intraperitoneal administration of telomerase-specific oncolytic adenovirus sensitizes ovarian cancer cells to cisplatin and affects survival in a xenograft model with peritoneal dissemination. *Cancer gene therapy*, 17, 11-19.
- TAN, B., DONG, S., SHEPARD, R. L., KAYS, L., ROTH, K. D., GEEGANAGE, S., KUO, M.-S. & ZHAO, G. 2015. Inhibition of nicotinamide phosphoribosyltransferase (NAMPT), an enzyme essential for NAD⁺ biosynthesis, leads to altered carbohydrate metabolism in cancer cells. *Journal of Biological Chemistry*, 290, 15812-15824.
- TANG, D. Q., ZOU, L., YIN, X. X. & ONG, C. N. 2014. HILIC-MS for metabolomics: An attractive and complementary approach to RPLC-MS. *Mass Spectrom Rev doi*, 10.
- TANIA, M., KHAN, M. & SONG, Y. 2010. Association of lipid metabolism with ovarian cancer. *Current Oncology*, 17, 6.
- TERWILLIGER, T. C. & EISENBERG, D. 1982. The structure of melittin. II.

- Interpretation of the structure. *Journal of Biological Chemistry*, 257, 6016-6022.
- TIZIANI, S., LODI, A., KHANIM, F. L., VIANT, M. R., BUNCE, C. M. & GUNTHER, U. L. 2009. Metabolomic profiling of drug responses in acute myeloid leukaemia cell lines. *PloS one*, 4, e4251.
- TOLSTIKOV, V., NIKOLAYEV, A., DONG, S., ZHAO, G. & KUO, M.-S. 2014. Metabolomics Analysis of Metabolic Effects of Nicotinamide Phosphoribosyltransferase (NAMPT) Inhibition on Human Cancer Cells. *PloS one*, 9, e114019.
- TOMITA, R., TODOROKI, K., MACHIDA, K., NISHIDA, S., MARUOKA, H., YOSHIDA, H., FUJIOKA, T., NAKASHIMA, M., YAMAGUCHI, M. & NOHTA, H. 2014. Assessment of the efficacy of anticancer drugs by amino acid metabolomics using fluorescence derivatization-HPLC. *Analytical Sciences*, 30, 751-758.
- TOSS, A., TOMASELLO, C., RAZZABONI, E., CONTU, G., GRANDI, G., CAGNACCI, A., SCHILDER, R. J. & CORTESI, L. 2015. Hereditary ovarian cancer: not only BRCA 1 and 2 genes. *BioMed research international*, 2015.
- TRIBA, M. N., LE MOYEC, L., AMATHIEU, R., GOOSSENS, C., BOUCHEMAL, N., NAHON, P., RUTLEDGE, D. N. & SAVARIN, P. 2015. PLS/OPLS models in metabolomics: the impact of permutation of dataset rows on the K-fold cross-validation quality parameters. *Molecular BioSystems*, 11, 13-19.
- TROCHINE, A., CREEK, D. J., FARAL-TELLO, P., BARRETT, M. P. & ROBELLO, C. 2014. Benznidazole biotransformation and multiple targets in *Trypanosoma cruzi* revealed by metabolomics. *PLoS Negl Trop Dis*, 8, e2844.
- TSUGAWA, H. & BAMBA, T. 2014. Statistical Analysis. In: PUTRI, S. P. & FUKUSAKI, E. (eds.) *Mass Spectrometry-Based Metabolomics: A Practical Guide*. Florida: CRC Press.
- TUSHIMIRE, J., WALLACE, J., DUFTON, M., PARKINSON, J., CLEMENTS, C. J., YOUNG, L., PARK, J. K., JEON, J. W. & WATSON, D. G. 2015. An LCMS method for the assay of melittin in cosmetic formulations containing bee venom. *Analytical and bioanalytical chemistry*, 407, 3627-3635.
- UBHI, B. K., RILEY, J. H., SHAW, P. A., LOMAS, D. A., TAL-SINGER, R., MACNEE, W., GRIFFIN, J. L. & CONNOR, S. C. 2012. Metabolic profiling detects biomarkers of protein degradation in COPD patients. *European Respiratory Journal*, 40, 345-355.
- UETAKI, M., TABATA, S., NAKASUKA, F., SOGA, T. & TOMITA, M. 2015. Metabolomic alterations in human cancer cells by vitamin C-induced oxidative stress. *Scientific reports*, 5.
- VALSECCHI, M., AURELI, M., MAURI, L., ILLUZZI, G., CHIGORNO, V., PRINETTI, A. & SONNINO, S. 2010. Sphingolipidomics of A2780 human ovarian carcinoma cells treated with synthetic retinoids. *Journal of lipid research*, 51, 1832-1840.
- VAN DEN BERG, R. A., HOEFSLOOT, H. C., WESTERHUIS, J. A., SMILDE, A. K. & VAN DER WERF, M. J. 2006. Centering, scaling, and transformations: improving the biological information content of metabolomics data. *BMC genomics*, 7, 142.

- VANDER HEIDEN, M. G., CANTLEY, L. C. & THOMPSON, C. B. 2009. Understanding the Warburg effect: the metabolic requirements of cell proliferation. *science*, 324, 1029-1033.
- VANLANGENAKKER, N., BERGHE, T. V., KRYSKO, D. V., FESTJENS, N. & VANDENABEELE, P. 2008. Molecular mechanisms and pathophysiology of necrotic cell death. *Current molecular medicine*, 8, 207-220.
- VELDMAN, R. J., KLAPPE, K., HINRICHS, J., HUMMEL, I., VAN DER SCHAAF, G., SIETSMA, H. & KOK, J. W. 2002. Altered sphingolipid metabolism in multidrug-resistant ovarian cancer cells is due to uncoupling of glycolipid biosynthesis in the Golgi apparatus. *FASEBJ*, 16, 1111-3.
- VERMEERSCH, K. A. & STYCZYNSKI, M. P. 2013. Applications of metabolomics in cancer research. *Journal of carcinogenesis*, 12, 9.
- VERMEERSCH, K. A., WANG, L., MCDONALD, J. F. & STYCZYNSKI, M. P. 2014. Distinct metabolic responses of an ovarian cancer stem cell line. *BMC systems biology*, 8, 134.
- VIEIRA, H., HAOUZI, D., EL HAMEL, C., JACOTOT, E., BELZACQ, A., BRENNER, C. & KROEMER, G. 2000. Permeabilization of the mitochondrial inner membrane during apoptosis: impact of the adenine nucleotide translocator. *Cell death and differentiation*, 7, 1146-1154.
- VITALE, M., ZAMAI, L., FALCIERI, E., ZAULI, G., GOBBI, P., SANTI, S., CINTI, C. & WEBER, G. 1997. IMP dehydrogenase inhibitor, tiazofurin, induces apoptosis in K562 human erythroleukemia cells. *Cytometry*, 30, 61-66.
- VOGELZANG, N. J., RUSTHOVEN, J. J., SYMANOWSKI, J., DENHAM, C., KAUKEL, E., RUFFIE, P., GATZEMEIER, U., BOYER, M., EMRI, S. & MANEGOLD, C. 2003. Phase III study of pemetrexed in combination with cisplatin versus cisplatin alone in patients with malignant pleural mesothelioma. *Journal of clinical oncology*, 21, 2636-2644.
- VON STECHOW, L., RUIZ-ARACAMA, A., VAN DE WATER, B., PEIJNENBURG, A., DANEN, E. & LOMMEN, A. 2013. Identification of cisplatin-regulated metabolic pathways in pluripotent stem cells. *PloS one*, 8, e76476.
- VOUSDEN, K. H. & PRIVES, C. 2009. Blinded by the light: the growing complexity of p53. *Cell*, 137, 413-431.
- WADE, K. L., GARRARD, I. J. & FAHEY, J. W. 2007. Improved hydrophilic interaction chromatography method for the identification and quantification of glucosinolates. *Journal of chromatography A*, 1154, 469-472.
- WALL, M. E. & WANI, M. C. 1995. Camptothecin and taxol: discovery to clinic—thirteenth Bruce F. Cain Memorial Award Lecture. *Cancer research*, 55, 753-760.
- WANG, D. & LIPPARD, S. J. 2005. Cellular processing of platinum anticancer drugs. *Nature reviews Drug discovery*, 4, 307-320.
- WANG, J., JIN, L., LI, X., DENG, H., CHEN, Y., LIAN, Q., GE, R. & DENG, H. 2013. Gossypol induces apoptosis in ovarian cancer cells through oxidative stress. *Molecular BioSystems*, 9, 1489-1497.
- WANG, L., SHEN, W., KAZACHKOV, M., CHEN, G., CHEN, Q., CARLSSON, A. S., STYMNE, S., WESELAKE, R. J. & ZOU, J. 2012. Metabolic interactions between the Lands cycle and the Kennedy pathway of glycerolipid

- synthesis in Arabidopsis developing seeds. *The Plant Cell*, 24, 4652-4669.
- WANI, M. C., TAYLOR, H. L., WALL, M. E., COGGON, P. & MCPHAIL, A. T. 1971. Plant antitumor agents. VI. Isolation and structure of taxol, a novel antileukemic and antitumor agent from *Taxus brevifolia*. *Journal of the American Chemical Society*, 93, 2325-2327.
- WATKINS, S. M., REIFSNYDER, P. R., PAN, H.-J., GERMAN, J. B. & LEITER, E. H. 2002. Lipid metabolome-wide effects of the PPAR γ agonist rosiglitazone. *Journal of Lipid Research*, 43, 1809-1817.
- WATSON, D. G. 2012. *Pharmaceutical Analysis A Textbook for Pharmacy Students and Pharmaceutical Chemists*, London, Elsevier Churchill Livingstone.
- WATSON, D. G., TONELLI, F., ALOSSAIMI, M., WILLIAMSON, L., CHAN, E., GORSHKOVA, I., BERDYSHEV, E., BITTMAN, R., PYNE, N. J. & PYNE, S. 2013. The roles of sphingosine kinases 1 and 2 in regulating the Warburg effect in prostate cancer cells. *Cellular signalling*, 25, 1011-1017.
- WATSON, J. T. & SPARKMAN, O. D. 2007. *Introduction to mass spectrometry: instrumentation, applications, and strategies for data interpretation*, Chichester, John Wiley & Sons.
- WEDGE, D. C., ALLWOOD, J. W., DUNN, W., VAUGHAN, A. A., SIMPSON, K., BROWN, M., PRIEST, L., BLACKHALL, F. H., WHETTON, A. D. & DIVE, C. 2011. Is serum or plasma more appropriate for intersubject comparisons in metabolomic studies? An assessment in patients with small-cell lung cancer. *Analytical chemistry*, 83, 6689-6697.
- WELTI, R. & WANG, X. 2004. Lipid species profiling: a high-throughput approach to identify lipid compositional changes and determine the function of genes involved in lipid metabolism and signaling. *Current opinion in plant biology*, 7, 337-344.
- WEN, H., YANG, H.-J., CHOI, M.-J., KWON, H.-N., KIM, M.-A., HONG, S.-S. & PARK, S.-H. 2011. Identification of urinary biomarkers related to cisplatin-induced acute renal toxicity using NMR-based metabolomics. *Biomolecules and Therapeutics*, 19, 38-44.
- WENK, M. R. 2006. Lipidomics in drug and biomarker development. *Expert opinion on drug discovery*, 1, 723-736.
- WENK, M. R. 2010. Lipidomics: new tools and applications. *Cell*, 143, 888-895.
- WIKLUND, S., JOHANSSON, E., SJOESTROEM, L., MELLEROWICZ, E. J., EDLUND, U., SHOCKCOR, J. P., GOTTFRIES, J., MORITZ, T. & TRYGG, J. 2008. Visualization of GC/TOF-MS-based metabolomics data for identification of biochemically interesting compounds using OPLS class models. *Analytical chemistry*, 80, 115-122.
- WIKLUND, S., NILSSON, D., ERIKSSON, L., SJÖSTRÖM, M., WOLD, S. & FABER, K. 2007. A randomization test for PLS component selection. *Journal of Chemometrics*, 21, 427-439.
- WOO, H. M., KIM, K. M., CHOI, M. H., JUNG, B. H., LEE, J., KONG, G., NAM, S. J., KIM, S., BAI, S. W. & CHUNG, B. C. 2009. Mass spectrometry based metabolomic approaches in urinary biomarker study of women's cancers. *Clinica Chimica Acta*, 400, 63-69.
- WU, X., ZHAO, B., CHENG, Y., YANG, Y., HUANG, C., MENG, X., WU, B., ZHANG, L., LV, X. & LI, J. 2015. Melittin induces PTCH1 expression by down-regulating

- MeCP2 in human hepatocellular carcinoma SMMC-7721 cells. *Toxicology and applied pharmacology*, 288, 74-83.
- XI, Y., DE ROPP, J. S., VIANT, M. R., WOODRUFF, D. L. & YU, P. 2008. Improved identification of metabolites in complex mixtures using HSQC NMR spectroscopy. *Anal Chim Acta*, 614, 127-33.
- XIA, J., BROADHURST, D. I., WILSON, M. & WISHART, D. S. 2013. Translational biomarker discovery in clinical metabolomics: an introductory tutorial. *Metabolomics*, 9, 280-299.
- XIA, J., SINELNIKOV, I. V., HAN, B. & WISHART, D. S. 2015. MetaboAnalyst 3.0--making metabolomics more meaningful. *Nucleic Acids Res*, 43, W251-7.
- XU, Y., FANG, X., CASEY, G. & MILLS, G. 1995. Lysophospholipids activate ovarian and breast cancer cells. *Biochemical Journal*, 309, 933-940.
- XU, Y., SHEN, Z., WIPER, D. W., WU, M., MORTON, R. E., ELSON, P., KENNEDY, A. W., BELINSON, J., MARKMAN, M. & CASEY, G. 1998. Lysophosphatidic acid as a potential biomarker for ovarian and other gynecologic cancers. *Jama*, 280, 719-723.
- YAMAGUCHI, R., JANSSEN, E., PERKINS, G., ELLISMAN, M., KITADA, S. & REED, J. C. 2011. Efficient elimination of cancer cells by deoxyglucose-ABT-263/737 combination therapy. *PLoS one*, 6, e24102.
- YANG, F., LONG, W., XUECHUAN, H., XUEQIN, L., HONGYUN, M. & YONGHUI, D. 2015a. Upregulation of Fas in epithelial ovarian cancer reverses the development of resistance to Cisplatin. *BMB Rep*, 48, 30-35.
- YANG, J., ZHAO, X., LU, X., LIN, X. & XU, G. 2015b. A data preprocessing strategy for metabolomics to reduce the mask effect in data analysis. *Frontiers in molecular biosciences*, 2, 4.
- YONEZAWA, A. & INUI, K.-I. 2011. Organic cation transporter OCT/SLC22A and H⁺/organic cation antiporter MATE/SLC47A are key molecules for nephrotoxicity of platinum agents. *Biochemical pharmacology*, 81, 563-568.
- YOON, J., JEON, J.-H., LEE, Y.-W., CHO, C.-K., KWON, K.-R., SHIN, J.-E., SAGAR, S., WONG, R. & YOO, H.-S. 2012. Sweet bee venom pharmacopuncture for chemotherapy-induced peripheral neuropathy. *Journal of acupuncture and meridian studies*, 5, 156-165.
- YOUNG, S. P., KAPOOR, S. R., VIANT, M. R., BYRNE, J. J., FILER, A., BUCKLEY, C. D., KITAS, G. D. & RAZA, K. 2013. The impact of inflammation on metabolomic profiles in patients with arthritis. *Arthritis Rheum*, 65, 2015-23.
- YU, S.-W., WANG, H., POITRAS, M. F., COOMBS, C., BOWERS, W. J., FEDEROFF, H. J., POIRIER, G. G., DAWSON, T. M. & DAWSON, V. L. 2002. Mediation of poly (ADP-ribose) polymerase-1-dependent cell death by apoptosis-inducing factor. *Science*, 297, 259-263.
- ZAMMIT, V. A., RAMSAY, R. R., BONOMINI, M. & ARDUINI, A. 2009. Carnitine, mitochondrial function and therapy. *Advanced drug delivery reviews*, 61, 1353-1362.
- ZAMZAMI, N. & KROEMER, G. 2001. The mitochondrion in apoptosis: how Pandora's box opens. *Nature Reviews Molecular Cell Biology*, 2, 67-71.
- ZHANG, H., GE, T., CUI, X., HOU, Y., KE, C., YANG, M., YANG, K., WANG, J., GUO, B. & ZHANG, F. 2015. Prediction of advanced ovarian cancer recurrence by

- plasma metabolic profiling. *Molecular BioSystems*, 11, 516-521.
- ZHANG, P., CHEN, J., WANG, Y., HUANG, Y., TIAN, Y., ZHANG, Z. & XU, F. 2016a. Discovery of Potential Biomarkers with Dose-and Time-Dependence in Cisplatin-Induced Nephrotoxicity Using Metabolomics Integrated with a Principal Component-Based Area Calculation Strategy. *Chemical research in toxicology*, 29, 776-783.
- ZHANG, R., WATSON, D. G., WANG, L., WESTROP, G. D., COOMBS, G. H. & ZHANG, T. 2014. Evaluation of mobile phase characteristics on three zwitterionic columns in hydrophilic interaction liquid chromatography mode for liquid chromatography-high resolution mass spectrometry based untargeted metabolite profiling of Leishmania parasites. *J Chromatogr A*, 1362, 168-79.
- ZHANG, R., ZHANG, T., ALI, A. M., AL WASHIH, M., PICKARD, B. & WATSON, D. G. 2016b. Metabolomic Profiling of Post-Mortem Brain Reveals Changes in Amino Acid and Glucose Metabolism in Mental Illness Compared with Controls. *Comput Struct Biotechnol J*, 14, 106-16.
- ZHANG, T. & WATSON, D. G. 2015. A short review of applications of liquid chromatography mass spectrometry based metabolomics techniques to the analysis of human urine. *Analyst*, 140, 2907-15.
- ZHANG, T., WATSON, D. G., WANG, L., ABBAS, M., MURDOCH, L., BASHFORD, L., AHMAD, I., LAM, N. Y., NG, A. C. & LEUNG, H. Y. 2013. Application of Holistic Liquid Chromatography-High Resolution Mass Spectrometry Based Urinary Metabolomics for Prostate Cancer Detection and Biomarker Discovery. *PLoS One*, 8, e65880.
- ZHANG, T., WU, X., KE, C., YIN, M., LI, Z., FAN, L., ZHANG, W., ZHANG, H., ZHAO, F. & ZHOU, X. 2012a. Identification of potential biomarkers for ovarian cancer by urinary metabolomic profiling. *Journal of proteome research*, 12, 505-512.
- ZHANG, T., WU, X., YIN, M., FAN, L., ZHANG, H., ZHAO, F., ZHANG, W., KE, C., ZHANG, G. & HOU, Y. 2012b. Discrimination between malignant and benign ovarian tumors by plasma metabolomic profiling using ultra performance liquid chromatography/mass spectrometry. *Clinica Chimica Acta*, 413, 861-868.
- ZHENG, J. F., LU, J., WANG, X. Z., GUO, W. H. & ZHANG, J. X. 2015. Comparative Metabolomic Profiling of Hepatocellular Carcinoma Cells Treated with Sorafenib Monotherapy vs. Sorafenib-Everolimus Combination Therapy. *Med Sci Monit*, 21, 1781-91.
- ZHENG, L., T'KIND, R., DECUYPERE, S., VON FREYEND, S. J., COOMBS, G. H. & WATSON, D. G. 2010. Profiling of lipids in Leishmania donovani using hydrophilic interaction chromatography in combination with Fourier transform mass spectrometry. *Rapid Communications in Mass Spectrometry*, 24, 2074-2082.
- ZHENG, X., BAUER, P., BAUMEISTER, T., BUCKMELTER, A. J., CALIGIURI, M., CLODFELTER, K. H., HAN, B., HO, Y.-C., KLEY, N. & LIN, J. 2013. Structure-based discovery of novel amide-containing nicotinamide phosphoribosyltransferase (nampt) inhibitors. *Journal of medicinal chemistry*, 56, 6413-6433.

- ZHOU, S. & LUO, R. 2013. Metabolomic response to sorafenib treatment in human hepatocellular carcinoma cells. *The FASEB Journal*, 27, 663.7-663.7.
- ZHU, W., SMITH, J. W. & HUANG, C.-M. 2009. Mass spectrometry-based label-free quantitative proteomics. *BioMed Research International*, 2010.
- ZWELLING, L. A. & KOHN, K. W. 1978. Mechanism of action of cis-dichlorodiammineplatinum (II). *Cancer treatment reports*, 63, 1439-1444.
- ZWELLING, L. A. & KOHN, K. W. 1979. Mechanism of action of cis-dichlorodiammineplatinum(II). *Cancer Treat Rep*, 63, 1439-44.